MASS TRANSFER WITH SIMULTANEOUS CHEMICAL REACTION IN DROPS FOR LIQUID-LIQUID SYSTEMS

MASS TRANSFER WITH SIMULTANEOUS CHEMICAL REACTION IN DROPS FOR LIQUID-LIQUID SYSTEMS

by

Hideki Watada, B.A.Sc., M.A.Sc.

A Thesis

Submitted to the Faculty of Graduate Studies in

Partial Fulfilment of the Requirements for the Degree

Doctor of Philosophy

McMaster University

October, 1968

DOCTOR OF PHILOSOPHY (1968) MCMASTER UNIVERSITY, Hamilton, Ontario

TITLE: Mass Transfer With Simultaneous Chemical Reaction in Drops for Liquid-Liquid Systems

AUTHOR: Hideki Watada, B.A.Sc. (University of Toronto)
M.A.Sc. (University of Toronto)

SUPERVISOR: Professor A.I. Johnson

ASSOCIATE SUPERVISOR: Associate Professor A.E. Hamielec

NUMBER OF PAGES: xvi, 249.

SCOPE AND CONTENT

This dissertation is divided into three major self-contained sections. The first one contains a review of previous work in the field of mass transfer in drops for liquid-liquid systems.

The second section outlines the numerical solutions of the continuity equation for forced convection with simultaneous chemical reaction in the dispersed phase. The solutions are compared with those predicted by existing theoretical models for mass transfer in the dispersed phase.

The third section describes the experimental equipment and method of operation. Physical mass transfer in drops is studied initially. This established a basis for evaluating the effect of chemical reaction on the rate of mass transfer in a later study. The results from these experimental studies are used to test the ability of existing models to predict mass transfer with simultaneous chemical reaction in drops.

TABLE OF CONTENTS

MASS TRANSFER WITH SIMULTANEOUS CHEMICAL REACTION IN DROPS FOR LIQUID-LIQUID SYSTEMS

Table Index

Figure Index

I General Introduction and Scope of Work

This thesis is concerned with a theoretical and an experimental study of mass transfer with chemical reaction in single drops by forced convection. Resistance to mass transfer was confined in the dispersed phase.

Theoretical models have been developed to describe mass transfer into stagnant, circulating and turbulent drops by Vermeulen, Kronig and Brink, and Handlos and Baron, respectively. These equations were extended to include the effects of simultaneous chemical reaction by Danckwerts.

Recently, solutions for a model describing mass transfer from a viscous, circulating drop were presented by Johns and Beckmann, for drop Reynolds Numbers in the Stokes flow regime.

The present study generalized the model to include the effects of simultaneous chemical reaction on the transfer rate into drops. The circulation rates inside the drop varied from stagnant to fully circulating, for Reynolds Numbers up to 80.

Experimental studies were carried out to test the reliability of these models. Initially, the effects of concentration driving forces on the rates of physical mass transfer into aqueous drops were examined. These results served as a basis for later comparisons with data from reaction mass transfer studies into aqueous sodium hydroxide drops.

Thus, this thesis is separated into three main sections.

1) A literature survey section to summarize previous studies in the field covered in this thesis.

2) A section to describe the development of a theoretical equation

to predict mass transfer with reaction into single drops by forced convection.

3) A section to show the results of experimental study of mass transfer with and without reaction into single drops.

Each section is complete with its own introduction, main body and conclusions.

II Literature Survey

II-A Introduction

This survey is concerned with mass transfer with or without simultaneous chemical reaction involving only liquid drops moving through a liquid. Transfer processes for gas bubbles or solid drops will be discussed only in cases which are useful in evaluating liquid-liquid transfer processes.

Many general surveys, such as by Harriott (48) and Kintner (74), have been published on mass transfer to and from dispersed fluids. Recently, a comprehensive text on this subject was published by Treybal (10). The fluid dynamics required to describe the motion and the convective mass transfer to and from dispersed phases, in many cases, have been thoroughly reviewed by Levich (39).

II-B Mass Transfer Periods

Whitman et al (1) showed that there were at least three periods in the life of a drop during which mass transfer occurred.

1) During drop formation in the continuous phase. In this case, the mass transferred during the drop formation, the break-off from the nozzle and the acceleration or the deceleration to its terminal velocity, was included in this period.
2) During free rise or fall of the drop through this continuous phase.
3) During coalescence of the drop at the end of the free rise or fall period.

Since then, this concept has been developed and analyzed by several

workers (2-11). Periods (1) and (3) are usually combined together and expressed as combined end-effect corrections in mass transfer studies. End-effect corrections and mass transfer phenomena in period (2) will be discussed separately in the following sections.

II-C End Effect Corrections

The two important papers on the calculation of end-effect corrections have been written by Hamielec (7) and Popovich (15). Hamielec was interested in defining a method for calculating the overall end-effect corrections. Popovich was interested in the formation end-effects.

II-C-1 Overall End Effect Corrections

The important papers on this study were reviewed by Hamielec (7). Since most of the early investigations involved extraction from drops in spray towers (1,2,3,5,9), they are not pertinent to this study. However, it was concluded by Licht and Pansing (5) that much of the formation end effects were due largely to oscillations of the drops, just after breaking off the nozzle and before reaching their terminal velocity.

A graphical technique was developed by Hamielec (7) to calculate the end effect corrections.

The various transfer regions were defined in terms of efficiencies as follows:-

$$E_{f1} = \frac{C_1 - C_2}{C_1 - C_\phi} \qquad E_{f2} = \frac{C_3 - C_4}{C_3 - C_\phi} \qquad \text{(II- 1)}$$

$$E_M = \frac{C_2 - C_3}{C_2 - C_\phi} \qquad E_T = \frac{C_1 - C_4}{C_1 - C_\phi} \qquad \text{(II- 2)}$$

where C_ϕ is the saturation concentration of the solute in the dispersed phase. The other concentrations are as shown in Figure II-1.

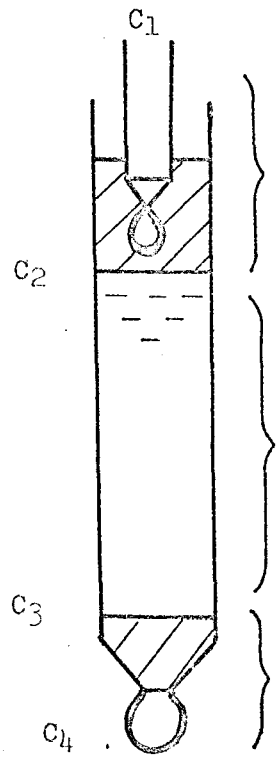

Figure II-1

Period of formation, initial oscillation and drop acceleration or deceleration.

Steady fall period of drop.

Period of coalescence and contact of settled dispersed phase with continuous phase.

E_M is the fractional approach to equilibrium during steady fall or rise period. Various mechanisms are tested in this period.

E_T is the fractional approach to equilibrium, calculated by measuring the concentration of entering and leaving dispersed phases.

E_{f1} is the formation end effect, which included mass transfer during drop formation and during the unsteady period following detachment from the nozzle.

E_{f2} is the coalescence end-effect, which includes mass transfer during drop coalescence and may include transfer to the coalesced phase.

This follows from the assumption that the end effects are independent of the concentration driving forces of the solute between the dispersed and continuous phases. For continuous drop sizes and formation rates, the end effects are normally assumed to be independent of column height.

From the definitions:-

$$E_M = \frac{E_T - E_F}{1 - E_F} \qquad (II-3)$$

where $$E_F = E_{f1} + E_{f2} - E_{f1} \times E_{f2} \qquad (II-4)$$

E_T, the combined end effect, may be found by extrapolating a graph of total mass transferred against column height to zero height.

Wellek (22) claimed that Hamielec's technique was valid only for cases where the plot of the data was a straight line. Instead, the coalescence end effect was minimized by reducing the interfacial area of the coalesced layer to a minimum. Since the exit concentration of the drop was now approximately equal to the concentration just before coalescence, the formation end-effect was the exit concentration from the shortest column height. Hence, the average drop concentration during free fall from any column height was considered to vary from the exit concentration of the shortest column C_E, to the exit concentration from any longer column C_L.

$$E_M = \frac{C_L - C_E}{C_\rho - C_E} \qquad (II-5)$$

However, it can be shown that

$$\frac{C_L - C_E}{C_\phi - C_E} = \frac{C_2 - C_3}{C_2 - C_\phi} \qquad \text{(II- 6)}$$

i.e., the methods of finding the end effect corrections for mass transfer studies by Hamielec and Wellek were equivalent.

I-C-2 Formation End Effects

A survey of the important papers on mass transfer during drop formation only, was given by Popovich (15). Early models predicting this, were based on the Higbie penetration theory (19). The theory assumed that the depth of penetration of the diffusing substance was small compared to the drop radius. Licht (5) developed a model in which the whole drop area became older according to Higbie's theory. The growth of the whole drop surface area with time only, was considered.

Heertjes (18) studied the transfer between isobutanol and water in a spray column. A model was developed based on the Higbie (19) theory, in which the velocity of diffusion was small compared to the drop growth rate. Coulson and Skinner (16) developed an apparatus which formed drops on the end of a capillary and then withdrew them before breaking away. Organic acids were extracted from water with benzene drops which were formed at a constant rate and then pushed back into the nozzle at the same rate. The total mass transferred was measured and the amount transferred to a single drop was calculated.

Groothius and Kramers (17) measured the absorption of sulfur dioxide by growing water drops. It was assumed that as the drop formed,

fresh surface areas were continuously exposed to the transfer medium. No mixing was allowed between areas of different ages. With these assumptions, a model was developed, again based on the Higbie (19) theory. Baird (12) correlated the results of Coulson (16), and of Groothius (17) with the equation proposed by Ilkovic (13) and derived by MacGillovry (14). The model was based on the assumption that the interface movement influenced the diffusion layer thickness, stretching it evenly around the sphere. Comparison of results with the Ilkovic equation showed a deviation of $\pm$ 18%, probably due to the heat of absorption of sulfur dioxide in water (Groothius (17)), the non-spherical shape of drops (Coulson (16)) and to circulation in the drop.

Popovich (15) studied the extraction of radio-active sodium iodide ($N_a\ ^{131}I$) from single water drops into isobutanol, using an experimental apparatus similar to that developed by Coulson (16). Drop formation and withdrawal times were varied independently and mass transfer during formation time was found by extrapolation to zero time. The variation of drop area with time was defined as:-

$$A_D = K_A t^n \qquad \text{(II-7)}$$

where the constants K_A and n accounted for the variation of area A_D with time involved in the mechanisms of Licht (5), Groothius (17), Ilkovic (13), and Heertjes (18). Coupled with the Higbie penetration theory, the rate of mass transfer N_A across the drop area A_D, at time t after drop formation was given as:-

$$N_A = (C_\phi - C_i)\ A_D\ (D_L/\pi t)^{\frac{1}{2}} \qquad \text{(II-8)}$$

The resultant correlation for the mass transferred by the different mechanisms was as follows:-

$$M_A = \text{Const } (C_\phi - C_i)(D_L \pi)^{\frac{1}{2}}(d_f)^2(t_f)^{-2/3}(t)^{7/6} \qquad \text{(II- 9)}$$

where M_A is the mass transferred from the drop in time t, and d_f is the final drop diameter at the end of the formation period t_f. The constants varied with the proposed mechanism. It was found that the experimental data were best correlated by the Ilkovic mechanism (13).

The dynamic situation present during drop formation was not reproduced when the method of drop withdrawal after formation was used by Coulson (16) and later by Popovich (15). Heertjes (70) overcame this problem by maintaining the column effect and the coalescence effect as small as possible in order to measure the formation effect. By this method, it was found that the mass transfer to growing drops was best described by assuming that drops grew by formation of fresh surface elements. The mass transfer efficiency at formation E_{f1} was given by:-

$$E_{f1} = \left\{ 2 \frac{A_R}{V_{DR}} + \frac{4}{3} B \right\} \left\{ \frac{D_L t_f}{\pi} \right\} \qquad \text{(II- 10)}$$

It is very difficult to measure the mass transfer rate from a dispersed phase during the fall period immediately following drop formations. Any method which involved physical contact with the dispersed phase produced errors due to coalescence end-effects. To overcome this difficulty, a photographic technique was recently described by Marsh and Heidiger (69). The rate of transfer was determined by the rate of change in the drop diameter as recorded on a movie film. This method is limited to those cases where the change in diameter is large enough to be accurately measured.

IIC-3 Coalescence End Effects

Most of the study of this phenomenon has been directed towards the definition of the conditions for coalescence to occur. Johnson and Bliss (9) found that drops coalesced more easily when solute transfer was from the dispersed phase to the continuous phase. Groothius and Zuiderweg (20) observed that when acetic acid was extracted from a dispersed phase of benzene into water, coalescence of the drop was promoted. This was due to the composition dependence of the interfacial tension for the benzene-water-acetic acid system. Smith et al (21) showed that ease of coalescence may be predicted from the ternary solubility diagram. If the mutual solubility of the main component in the dispersed and the continuous phase was increased by the solute, then if the transfer was from the dispersed to the continuous phase, coalescence of the drops was promoted. For the opposite direction of transfer, coalescence was inhibited. No similar mechanisms are available for binary systems. MacKay and Mason (31) studied the rate of thinning of the liquid film trapped between the drop and liquid interface and the subsequent coalescence of the drop. The effect of coalescence on mass transfer was not studied.

Hamielec (7) suggested that coalescence end effects may be described by the Higbie approach (19) where each drop coalesced and spread a layer of initial, uniform concentration C_3, across the previously settled phase. Transient mass transfer then occurred, until the next drop arrived to cover the surface. Thus the coalescence end effect E_{f2} is as follows:

$$Ef_2 = \frac{2A_i}{Vd}\left\{\frac{D_L \Delta t}{\pi}\right\}^{0.5} \qquad \text{(II- 11)}$$

A film presented by G.V. Jeffreys (University of Manchester, Manchester, England) and J.L. Hawksley (ICI, Billingham, England) at the AIChE conference in Pittsburgh on May 17, 1964, showed that as drops coalesced, it seemed to jet into the coalesced phase. Hence, the hydrodynamic and mass transfer phenomena during coalescence are very complex. Considerable experimental and theoretical study in this field are still required.

II-D Dispersed Phase - Physical Mass Transfer

During the steady fall or rise period of a drop, heat or mass is transferred in or out by a transient process. Most of the theoretical and experimental investigations have been directed toward the study of this process.

Equations describing this have been summarized by Sideman et al (51), Wellek (52,53) and Hamielec et al (7,8).

The basic assumptions were as follows:-

1) the drops were spherical.
2) the systems were so dilute that physical properties were unaffected by the solute (or average values were used).
3) the fluids were incompressible and Newtonian. Except where noted, the continuous phase resistance was assumed to be negligible.

II-D-1 Mass Transfer into Stagnant Drops

For stagnant drops with no internal circulation, mass was transferred by molecular diffusion only. Using as a model, the drying rates in porous, solid spheres, Newman (54) defined the following equation, based on Fick's second law of diffusion.

$$\frac{\partial C}{\partial t} = \frac{D_L}{r^2} \frac{\partial}{\partial r} \left\{ r^2 \frac{\partial C}{\partial r} \right\} \qquad \text{(II- 12)}$$

This assumed a constant diffusion coefficient, with spherical symmetry for solute concentrations.

The boundary conditions were:-

$$C = C_2 \qquad o \leq r \leq a \qquad t = o \qquad \text{(II- 13)}$$

$$C = \text{finite} \qquad r = o \qquad t = t \qquad \text{(II- 14)}$$

$$C = C_\phi \qquad r = a \qquad t > o \qquad \text{(II- 15)}$$

Boundary condition II- 15 implied that the continuous phase resistance was negligible. The concentration at the center was kept at some finite value. The solution in terms of extraction efficiency was in the form of an infinite series:-

$$E_M = \frac{C_2 - C_3}{C_2 - C_\phi} = 1.0 - \frac{6}{\pi^2} \sum_{n=1}^{\infty} \frac{1}{n^2} \exp\left[-n^2 \pi^2 \frac{D_L t}{a^2} \right] \qquad \text{(II- 16)}$$

The boundary condition II- 15 was modified by Groeber (55) to account for finite resistance in the continuous phase. The resultant solution of Equation II- 12 was shown to be:-

$$E_M = 1 - 6 \sum_{n=1}^{\infty} A_n \exp\left\{ -\lambda_n^2 \frac{D_L t}{a^2} \right\} \qquad \text{(II- 17)}$$

An outline of the derivation of Equation II- 17 was given by Jakob (56). A table of A_n and λ_n values as functions of the continuous phase Nusselt

Number, was calculated by Elzinga and Banchero (47) for heat transfer situations.

Nusselt Number is defined as:-

$$N_u = \frac{hL}{K_H} \qquad (II-18)$$

where h = film coefficient, BTU/(sec.)(cm.^{2})(deg.F)

K_H = conductivity, BTU/(sec.)(cm.)(deg.F)

L = characteristic length of heat transfer path, cm

In order to relate the heat transfer solution to the case of mass transfer, Wellek (52) suggested including the equilibrium constant into Jakob's derivations (56). Thus, the Nusselt Number in Elzinga's table (47) should be replaced by the Sherwood Number when using the values of A_n and λ_n for mass transfer applications.

Sherwood Number is defined as:-

$$Sh = \frac{K_L L}{mD_L} \qquad (II-19)$$

where m is the distribution coefficient for solute between phases at equilibrium (II-20)

$$C = m\overline{C_B}$$

$\overline{C_B}$ is the bulk concentration of solute B in the continuous phase.

An empirical equation closely approximating the Newman Equation III-16 was suggested by Vermeulen (57) as follows:-

$$E_M = \left\{1 - \exp\left[\frac{-D_L \pi^2 t}{a^2}\right]\right\}^{0.5}$$

$$\text{or} - \ln(1 - E_M^2) = \frac{D_L \pi^2 t}{a^2} \qquad (II-21)$$

By expanding exp $\left(- \frac{D_L \pi^2 t}{a^2} \right)$ in the right hand side, this equation may be simplified to:

$$E_M = \left\{ \frac{\pi^2 D_L t}{a^2} \right\}^{0.5} \qquad \text{(II- 22)}$$

It was shown by Hamielec (7) that this equation showed close agreement with the Newman equation for $E_M < 0.5$.

II-D-2 Mass Transfer into Circulating Drops

The Navier-Stokes equation for the motion of dispersed and continuous phases in the Stokes flow region ($0.0 < Re < 1.0$) was solved by Hadamard (37) and Rybczynski (38). The equation for the concentration distribution inside a drop, with internal circulation rates as described by the Hadamard equation, was derived by Kronig and Brink (58). Since the circulation time was assumed to be small, compared to the solute diffusion rate, the concentration profiles were identical to the internal circulation profile. This limited their solution to systems with low viscosity ratios of approximately zero. Here, viscosity ratio was defined as:-

$$X = \frac{\mu_i}{\mu_o} = \frac{\text{viscosity of drop}}{\text{viscosity of continuous phase}} \qquad \text{(II- 23)}$$

Kronig and Brink modified the stream functions of Hadamard by translating the origin of the co-ordinate system to the center of the drop, with the radius a of the drop, as the unit in which the distance from the origin is measured.

ψ_i, the internal streamline for the drop is:-

$$\psi_i = - \frac{g (\rho_i - \rho_o) a^4 R^2 (1 - R^2) \sin^2\theta}{6 (3\mu_i + 2\mu_o)} \qquad \text{(II-24)}$$

The velocity components V_R and V_θ were derived from the following definitions:-

$$V_R = \frac{1}{R^2 \sin\theta} \frac{\partial \psi_i}{\partial \theta} \qquad \text{(II-25)}$$

$$V_\theta = -\frac{1}{R \sin\theta} \frac{\partial \psi_i}{\partial R} \qquad \text{(II-26)}$$

The co-ordinate system was expressed in terms of

$$\xi = 4R^2 (1 - R^2) \sin^2\theta \qquad \text{(II-27)}$$

which represented the streamlines ψ_i and

$$\zeta = \frac{R^4 \cos^4\theta}{2R^2 - 1} \qquad \text{(II-28)}$$

which represented lines orthogonal to ξ.

Thus $\xi = 0$ at $R = 1$, $0 < \theta < \pi$

(on the drop boundary and the polar axis)

$$\xi = 1 \text{ at } R = \tfrac{1}{2}\sqrt{2}, \ \theta = \frac{\pi}{2} \qquad \text{(II-29)}$$

The two sets of curves are as shown in Figure II-2, the upper quadrant of the vertical cross-section. Axial symmetry was assumed for the other half of the drop.

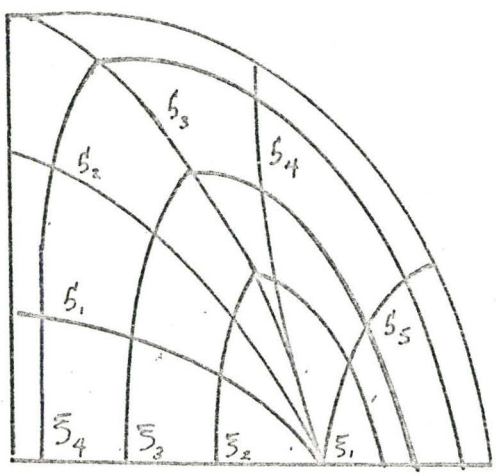

Figure II-2

The resulting partial differential equation for the mass transfer mechanism was

$$\frac{\partial}{\partial \xi}\left[P(\xi) \frac{\partial c}{\partial \xi} \right] = \frac{a^2}{16 D_L} q(\xi) \frac{\partial c}{\partial t} \qquad \text{(II-30)}$$

where $$P(\xi) = \int \frac{(2R^2 - 1)^2 \sin^2\theta}{R\cos^3\theta} d\xi \qquad \text{(II-31)}$$

$$q(\xi) = \int \frac{(2R^2 - 1)^2 \, d\xi}{4R^3\cos^3\theta \; (1 - R^2)^2\cos^2\theta + (2R^2 - 1)^2\sin^2\theta} \qquad \text{(II-32)}$$

The boundary conditions for transfer into the drop were:-

$$C = C_\phi \qquad \xi = 0, \qquad t > 0 \qquad \text{(II- 33)}$$

$$C = C_2 \qquad \xi = \xi, \qquad t = 0 \qquad \text{(II- 34)}$$

Condition II- 33 stated that there was no resistance to mass transfer in the continuous phase. The surface concentration of the drop always equaled the equilibrium concentration of the solute in the bulk phase.

The solution of the equation was:-

$$E_M = 1 - 3/8 \sum_{n=1}^{\infty} A_n^2 \exp\left[-\lambda_n \frac{16 D_L t}{a^2}\right] \qquad \text{(II- 35)}$$

Values for A_n and λ_n for n = 1 and 2 were obtained. This was shown by Heertjes et al (18) to be inaccurate at short time durations. Hence the values of A_n and λ_n were found for n = 1 to 7 as shown in Table II-1.

Table II-1

Values for A_n and λ_n for Kronig and Brink Eqn. by Heertjes et al (18)

n	1	2	3	4	5	6	7
A_n	1.33	0.60	0.36	0.35	0.28	0.22	0.16
λ_n	1.678	8.48	21.10	38.5	63.0	89.8	123.8

Danckwerts (59) has shown that Equation II- 35 may be used at drop Reynolds Number > 1 as long as the internal conditions did not depart too

far from the postulated behavior. In practice, the Kronig and Brink equation was probably valid up to drop Reynolds Number = 10.

Drop Reynolds Number was defined as:-

$$\text{Re. No.} = \frac{dV_D \rho_o}{\mu_o} \qquad \text{(II- 36)}$$

where ρ_o and μ_o are the density and viscosity of the continuous phase.

d and V_D are the diameter and velocity of the drop.

A modification of the Vermeulen Equation II- 21 was shown by Korchinski (46) to represent the Kronig and Brink Equation II- 35 well:-

$$E_M = \left\{ 1 - \exp \left(\frac{- \dot{R} \pi^2 D_L t}{a^2} \right) \right\}^{0.5} \qquad \text{(II- 37)}$$

where $\dot{R}$ = enhancement factor for the molecular diffusivity, produced by the circulation in the drop

$$\dot{R} = \frac{\text{effective diffusivity}}{\text{molecular diffusivity}} \qquad \text{(II- 38)}$$

A value of $\dot{R} = 2.25$ was used by Korchinski to correlate his results. It was shown by Wellek (52) that $\dot{R}$ varied from 5.97 to 2.70 for E_M values of .0916 to 1.0. Hence instead of $\dot{R} = 2.25$, a value of $\dot{R} = 2.5$ was suggested as the best average value for use over the normal range of extraction efficiencies. However since $\dot{R}$ is a variable, accurate results are obtained only by the use of the exact equation.

In their study of heat transfer to liquid drops, Elzinga and Banchero (47) extended the Kronig and Brink solution to the case of finite continuous phase resistances. Although the form of their solution was the same as Kronig and Brink's, the values of A_n and λ_n were now functions of the continuous phase resistance to transfer. Values of A_n and λ_n for n = 1 to 3 were calculated.

Hamielec (7) modified the Grocber Equation II- 17 to define the factor $\dot{R}$ as follows:-

$$E_M = 1 - 6 \sum_{n=1}^{\infty} A_n \exp \left\{ - \frac{\lambda_n^2 \dot{R} D_L t}{a^2} \right\} \qquad (II-39)$$

It was also shown that for $E_M \leqslant 0.5$, Equation II- 39 was approximated by the following empirical equation:-

$$E_M = 0.905 \left\{ \frac{\pi^2 \dot{R} D_L t}{a^2} \right\}^{0.5} + 0.0189 . \qquad (II-40)$$

This equation was introduced as an improvement over the modified Vermeulen Equation II- 21 , for zero resistance in the continuous phase. Wellek (52) showed that for $E_M = 0.1$ to 0.5, Equation II- 40 correlated experiment data better than the Vermeulen equation. For $E_M < 0.1$, the Vermeulen equation was better.

II-D-3 Mass Transfer into Turbulent Drops

Handlos and Baron (60) proposed another model for higher ranges of Reynolds Numbers (about 1000). They assumed that mass transfer was due entirely to the eddy diffusion effects of a turbulence caused by random radial motion superimposed upon the circulatory pattern. These patterns were assumed to take the shape of a torus, rather than the Hadamard circulation pattern in the Kronig and Brink model (58). The entire transfer process was assumed to occur within the outer surface of the torus. A probability function for the location of a particle in a given position was developed. The average circulation time was defined by an equation developed by Kronig and Brink (58). The eddy diffusion was described as a function of the torus radius. Since mass transfer in the torus was only in the radial direction, the partial

differential equation was:-

$$\frac{128\ d^2}{D_L\ Pe^1}\ \frac{\partial c}{\partial t} = \frac{1}{1-y}\ \frac{\partial}{\partial y}\left\{(1 - 5y + 10y^2 - 6y^3)\ \frac{\partial C}{\partial y}\right\} \qquad \text{(II- 41)}$$

where Pe^1 = modified Peclet Number

$$= \frac{Pe}{1+\mu_i/\mu_o} \qquad \text{(II- 42)}$$

$$Pe = \frac{dV_D}{D_L} \qquad \text{(II- 43)}$$

$$y = 1 - r_T = 1 - \frac{4W}{d} \qquad \text{(II- 44)}$$

where W = radial distance from the centre of the circulation torus.

The boundary conditions for transfer into the drop were:-

$$C = C_2 \qquad 0 \leqslant y \leqslant 1 \qquad t = 0 \qquad \text{(II- 45)}$$

$$C = C_\phi \qquad y = 0 \qquad t > 0 \qquad \text{(II- 46)}$$

Again, as for the Kronig and Brink model, condition II- 45 indicated no resistance to transfer in the continuous phase. The surface concentration of the torus remained equal to the equilibrium concentration of the solute in the bulk phase.

The solution was given as:-

$$E_M = 1 - 2\sum_{n=1}^{\infty} B_n^2 \exp\left\{-\frac{\gamma_n D_L t\ Pe^1}{128 d^2}\right\} \qquad \text{(II- 47)}$$

Handlos and Baron claimed that only the first eigenvalue, $\gamma_1 = 2.88$ was required. B_1 was set equal to unity.

Wellek (52,77) extended the Handlos and Baron model to the case of finite continuous phase resistance. The resultant solution was:-

$$E_M = 1 - \sum_{n=1}^{\infty} B_n^2 \exp(-\gamma_n bt) \qquad \text{(II- 48)}$$

where $$b = \frac{V_D}{128\ (1+\mu_i/\mu_o)\ d} \qquad \text{(II- 49)}$$

A list of B_n and γ_n as calculated by Wellek for n = 1 to 4, is given in Table II-2.

Table II-2

Values for B_n and γ_n for Handlos and Baron Eqn. by Wellek et al (52,77)

n	1	2	3	4
B_n	0.225	0.421	0.479	0.071
γ_n	2.868	24.56	75.60	367.0

By solving Equation II- 41 numerically, Olander (76) showed that at short contact times, the analytical results of Handlos and Baron grossly underestimated the amount transferred. At dimensionless time

$$\frac{D_L t}{a^2} > 0.1$$

the numerical solutions by Olander was approximately

$$E_M = 1 - 0.64 \exp\left\{ - \frac{2.80\ D_L t\ Pe^1}{128\ d^2} \right\} \qquad \text{(II- 50)}$$

Again, the Handlos and Baron model was solved numerically by Patel and Wellek (78) for transfer with finite continuous phase resistances. This work confirmed the inaccuracy of the analytical solutions for the Handlos and Baron model at short contact times.

II-D-4 Mass Transfer into Oscillating Drops

The Handlos and Baron model was described as applying to turbulent and/or oscillating drops (52,53,75,77). However Rose and Kintner (73) showed photographically that within oscillating drops, fluid motion was in the order of random mixing, with only a slight

tendency towards internal circulation. Hence it was concluded that the Handlos and Baron model applied only for drops at high Reynolds Number in the non-oscillating region.

Based on their observations, Rose and Kintner (73) developed a highly complicated extraction model for fully oscillating drops, which considered the effect of interfacial stretch. All resistance was confined to a thin zone near the interface. The core of the drop was assumed to be well-mixed. Similarily, Angelo et al (79) have developed a generalization of the penetration theory for surface stretch to predict mass transfer to oscillating drops. Both models required estimates of the amplitude and frequency of oscillation. Although these models more accurately represented the physical situation, comparisons with experimental data showed no significant differences with the predictions by the Handlos and Baron model. This was due to poor and scanty data in the high Reynolds Number region.

II-E Dispersed Phase Mass Transfer Accompanied by Chemical Reaction

Very few studies have been reported in the literature on the subject of dispersed phase mass transfer accompanied by chemical reaction for liquid-liquid systems.

A qualitative study of extraction of organic acids from benzene drops into aqueous potassium hydroxide solutions was made by Fujinawa (61). In all cases, at a critical concentration of the alkali, the extraction rate of the solute decreased. No explanations were given for this phenomenon. This may have been due to the salt effect of the alkali which reduced the solubility and hence the diffusion rate of the

solute in the continuous phase. However, neither this effect, nor the possible influence of interfacial turbulence was considered. This mechanism is caused by localized interfacial tension lowering by solutes (which may be present or produced by the reaction) which induced spontaneous convection currents at the interface. Current studies by the author have shown that these two phenomena had very important influences on the transfer rates.

A method for analyzing the mass transfer process by simultaneous diffusion and first order chemical reaction into falling drops was given by Danckwerts (59). The method described the transient concentration - distribution and the rate of absorption by transformation of expressions for diffusion without reaction. Since these expressions exist for stagnant, circulating and turbulent drops, reaction mass transfer into them may be analyzed by this method.

The transformation was:-

$$C = K_R \int_0^t \left[\exp\left(-K_R t\right)\right] C^1 dt + C^1 \left[\exp\left(-K_R t\right)\right] \qquad \text{(II- 51)}$$

where C^1 = solution for diffusion without chemical reaction.
The initial solute concentration in the absorbent was zero.

Danckwerts solved the Kronig and Brink Equation II- 35 and the Newman Equation II-16 for mass transfer into circulating and stagnant drops with simultaneous first order reaction using this method.

Equation II- 51 was found empirically by Danckwerts. Recently, Lightfoot (62) developed a method for unsteady state mass transfer in systems where the velocity profile and concentration boundary conditions were time dependent, and the density and mass diffusivity were constant. By a Laplace transform of the diffusion equation, the following equation

was found:-

$$C(r,t) = g \exp(K_R t) + f(r,t) \exp(K_R t) - K_R \int_0^t f(r,t) \exp(K_R t)\, dt \qquad \text{(II- 52)}$$

The first term on the right hand side extended Danckwerts' solution to systems of finite initial concentration in the absorbent. The second and third terms were the same as those in Danckwerts' solution.

The application of the Danckwerts' modifications to mass transfer models to account for first-order equations are shown in Table IV-3 in the Experimental Section IV of this thesis.

II-F General Model for Mass Transfer into Drops

Until the advent of computers, models describing mass transfer into drops rapidly became too complicated to solve analytically. Hence the models described in Sections II-D and E, all contained simplifying assumptions which enabled them to be solved.

Johns and Beckmann (86) were the first to show numerical solutions for mass transfer into a viscous, circulating drop. Further discussions of their work will be given in the theoretical section of this report since their results are compared with those obtained by the author.

II-G Effects of Interfacial Turbulence on Mass Transfer to Drops

It has long been known that Marangoni forces have a large effect on mass transfer across liquid-liquid interfaces. Whenever interfacial tensions were strongly affected by solute concentrations, interfacial

instability can be produced to significantly enhance the mass transfer rates.

Interfacial turbulence have been observed by many workers (23,24,25). This phenomenon was recently reviewed by Davies (71,72). A qualitative investigation of this phenomenon was made by Wei (23,27). They observed that no activity occurred unless either phase contained a component which was soluble in the other.

II-G-1 Sternling and Scriven Model for Prediction of Interfacial Turbulence

Sternling and Scriven (28) were the first to define the conditions to formulate a quantitative mechanism under which instability caused by Marangoni effect occurred on a flat interface. Their model was limited to consideration of two-dimensional, rather than three-dimensional solutions.

It was asserted that small fluctuations of concentration or temperature about the interface may be amplified into fully developed flows under favourable conditions, by the Marangoni effect. Variations in the interfacial concentrations would cause corresponding changes in the interfacial tension. Thus, the interface tended to seek a state of lower free energy through expansion of regions of low interfacial tension, at the expense of adjacent regions of higher energy (the Marangoni effect). Due to the continuity of velocity at the interface, flow was induced in one phase by fluid motion in the other. Depending on the direction of the induced flow, the original flow may be dampened or amplified.

Such flows may be the highly irregular, interfacial turbulence, or the ordered, laminar flows which may arrange themselves into regular cellular pattern. In both cases, the flows decayed as the concentration driving forces also diminished.

The model consisted of two-dimensional roll cells formed in two semi-infinite liquid phases in contact along a plane interface. A single component was transferred between the two planes. The resultant problem of hydrodynamic stability in the presence of small perturbation due to diffusion and interfacial movements, was solved by the method of linearized stability (80). The theory decomposed the motion into a mean flow (whose stability is under study) and into a disturbance superimposed on it. The stability criteria was expressed in terms of wave numbers (or frequency of roll-cell disturbances) and amplification factors. When both their signs are the same, the system became unstable and interfacial turbulence occurred. These conditions depended on the viscosity ratio of the two phases, the diffusivity ratio of the solute in both phases and a function relating them to the disturbance.

Orell and Westwater (29) presented a comprehensive survey of experimental and theoretical investigations of interfacial turbulence phenomena up to that time (1962). Orell had studied photographically the interfacial cellular convections accompanying the extraction of acetic acid out of ethylene glycol with ethyl acetate. The cells were found to consist of 3-dimensional roll cells with additional flow rising in the center. Thus, it was concluded that the Sternling-Scriven model must be modified greatly before the phenomena could be accurately defined.

A qualitative study of the phenomenon was made by Goltz (32) for the case of solute transfer from a drop suspended in a stagnant liquid-liquid system.

Depending on the concentration driving force of the solute between the two phases, three different transfer regimes were observed:-

1) At a subcritical driving force or decrease in interfacial tension forces, transfer occurred by molecular diffusion only.

2) At a critical driving force or decrease in interfacial tension, eruption of solute-rich material occurred. It was postulated that as a small area of low interfacial tension appeared, liquid was pulled away tangentially by the surrounding areas of higher interfacial tension. Due to continuity of velocity at the interface, fresh material was brought from the drop interior to the interface. The resultant rapid, initial transfer rate at the new interface was believed to be responsible for the eruption.

3) Above the critical concentration driving force or interfacial tension decrease, the drop interface was in a state of constant turbulence.

II-G-2 Ruckenstein Model for Prediction of Interfacial Turbulence

Ruckenstein (33) noted that when interfacial activity became well-developed, cellular structures were present not only for flat interfaces between phases, but also for curved interfaces. He extended the Sternling and Scriven model for the appearance of interfacial turbulence, when diffusion in one of the phases was accompanied by first order chemical

reaction. The characteristic equation was derived in a manner similiar to the Sternling and Scriven theory. Again, the instability condition was examined in terms of wave number and amplification factors. It was noted that since the wave number must be a real quantity, it must be greater or equal to zero. Hence the system was unstable when both the wave number and amplification factors were positive.

The following conclusions were drawn by Ruckenstein regarding the stability of systems where diffusion was accompanied by chemical reaction.

1) The occurrence of instability was determined by many physical-chemical parameters. The criteria of instability were so different from the case of diffusion only, that even small values of the reaction rate constant changed the conditions in which instability occurred. Thus, a system may be stable when diffusion was not accompanied by chemical reaction and unstable when a reaction occurred.

2) Instability always occurred when the reaction product diffused through only one phase, if not in one direction, then in the other, at steady state. Cases in which the system was unstable with transfer in either direction were also possible. When the product diffused through both phases, the system may remain stable.

3) For very small cell sizes (due to viscous shear forces) and for very large cell sizes (due to inertia of the fluid mass), the amount of amplification was reduced. Hence between these two extremes, there must be a cell of a size such that the perturbation was amplified to a maximum and finally became dominant in the system.

These models of Sternling and Scriven and of Ruckenstein were applicable only for situations where the system was stagnant and all mass transfer was by diffusive forces (molecular diffusion or interfacial turbulence). However, in the case of extraction from a drop moving in a fluid, a boundary layer type of concentration gradient was set up around the drop by the viscous drag forces of the continuous phase. This concentration gradient may cause interfacial turbulence to occur. Ruckenstein (34) has extended the Hadamard (37), Rybczynski (38) and Levich (39) solution for transfer from a rising bubble, to include Marangoni effect at the interface. His results indicated that the drop velocity and the mass transfer coefficients were affected by the Marangoni effect only in small drops. The mass transfer coefficient was influenced by the direction of transfer, due to the concentration gradient around a moving drop. This has been observed experimentally (35,36) for gas-liquid systems. The transfer coefficient may be increased if the interfacial tension diminished as transfer continued during the motion of the drop.

II-G-3 Effects of Interfacial Turbulence on Mass Transfer Rates

The effects of concentration driving force on mass transfer coefficients for three component systems have been studied by Sawistowski et al (30), Olander et al (66) and Blokker et al (67,68). In all cases, the overall coefficients increased sharply with concentration driving forces. This increase was caused entirely by interfacial turbulence.

It was shown by Olander (66) that even at low concentration driving forces, interfacial turbulence could occur. In fact, the activity

did not have to be visually apparent to affect the transfer mechanism. Thus, at least three components were required to produce interfacial turbulence .

Several workers (23,26) have shown that when mass transfer was accompanied by simultaneous chemical reaction, interfacial turbulence occurred in many cases. This resulted in a transfer rate enhanced beyond that produced by the chemical reaction alone.

II-H Effect of Surface-Active Impurities

Mass transfer rates into drops are enhanced by interfacial turbulence and circulation currents in them. When these phenomena are reduced by surface active impurities, the transfer rates are also reduced. Studies of the retardation mechanisms are given in this section.

It was shown by Treybal (40) that interfacial turbulence is dampened by surface-active impurities which reduced the interfacial tension imbalances causing the convection currents.

A large amount of work on the action of surface-active agents has been done by Terjesen, et al (41 - 45). Surface-active agents soluble only in the aqueous phase reduced the rate of transfer from the aqueous solution to organic drops to such an extent that the mass transfer coefficients became equal to those for solid bodies.

Drops moving through a fluid tends to circulate, due to external viscous shear forces at the interface. As surface-active agents are swept to the rear of the drop, a surface tension gradient opposing the external shear (48) may be established. Hence internal circulation

currents are reduced at the rear of the drop. If enough material is present, the entire drop may become stagnant. For drops with a high surface tension, an appreciable tension gradient may be produced by only a trace of impurity (48). Garner and Skelland (49) had noted the large dampening effect of trace impurity on the internal circulation of drops. They observed that as interfacial tension increased, the circulations in drops decreased. This observation was later confirmed by Linton and Sutherland (50).

For a given system, the effect of surface tension gradient increased inversely with the drop size. Drops below a certain size did not circulate (48). The critical Reynolds Number required for circulation was correlated by Garner and Skelland (49) as:-

$$\text{Re No} = 100\ (\mu_o)^{-4/3} \qquad \text{(II- 53)}$$

II-I Conclusions

This survey has shown that the broad field of mass transfer into drops have been studied. However, several areas which require further investigation have also been indicated:

1) general model predicting convective mass transfer rate into drops with simultaneous chemical reaction
2) the effect of concentration driving forces on mass transfer rates for binary systems
3) more experimental data for mass transfer with simultaneous chemical reaction into drops, to test the various models predicting this phenomenon
4) more experimental and theoretical studies on the interfacial

turbulence phenomenon

5) more work on formation end-effects for drops to include the mass transfer rates after breaking off the nozzle and before reaching terminal velocity

6) more work on coalescence end effects for drops

Points (1) to (3) are included in the scope of this thesis.

II-J Nomenclature

a = radius at the surface of a drop, cm

A_D = surface area of a drop, cm^2

A_i = interfacial area at coalescence, cm^2

A_n, λ_n = constants for n'th term in series solution by Elzinga and Banchero (47), and by Heertjes (18).

A_R = surface area of rest drop, cm^2

B = ratio of drop surface to volume, cm^{-1}

B_n, γ_n = constants for n'th term in series solution for Handlos and Baron Equation II-47

C = concentration, gm/cc

$\overline{C_B}$ = average concentration of solute B in a continuous phase, gm/cc

C_1 = initial concentration, gm/cc

C_ϕ = equilibrium concentration, gm/cc

d = diameter at surface of drop, cm

D_e = effective diffusivity, cm^2/sec

d_f = final drop diameter, cm

D_L = molecular diffusivity, cm^2/sec

h = heat transfer coefficient, BTU/(sec)(sq cm)(deg F)

K_A = coefficient for variation of surface area with time

K_H = thermal conductivity, BTU/(sec)(cm)(deg F)

K_L = mass transfer coefficient, cm/sec

K_R = first order chemical reaction rate constant, sec^{-1}

L = characteristic length, cm

m = distribution coefficient for solute between two phases at equilibrium, ie. $C = m\overline{C_B}$

M_A = mass transferred across drop of area A_D, gm

N_A = rate of mass transfer across drop of area A_D, gm/sec

N_{Sh} = Sherwood Number

$$= \frac{K_L d}{D_L}$$

Nu = Nusselt Number

$$= \frac{hd}{K_H}$$

Pe = Peclet Number

$$= \frac{dV_D}{D_L}$$

Pe^1 = modified Peclet Number

$$= \frac{Pe}{1 + X}$$

Re = drop Reynolds Number

$$= \frac{dV_D \rho_o}{\mu_o}$$

R = enhancement factor

$$= \frac{D_e}{D_L}$$

r_D = drop radius, cm

r_T = dimensionless radius of torus

$$= \frac{4W}{d}$$

t = time, sec

t_f = drop formation time, sec

V = drop volume, cc

V_D = drop velocity, cm/sec

V_{DR} = volume of released drop, cc

V_R, V_Θ = velocity components of streamlines in the R and Θ directions, respectively, cm/sec

W = radial distance from center of circulation torus, cm

X = viscosity ratio

$= \frac{\mu_i}{\mu_o}$

y = $(1 - r_T)$, dimensionless

Efficiency Terms

E_T = overall mass transfer efficiency

E_M = mass transfer efficiency during steady rise or fall of drop

E_F = overall end effect

E_{f_1} = formation end effect

E_{f_2} = coalescence end effect

Greek Letters

γ, λ = eigenvalue for n'th term in a series

ψ = streamline, cc/sec

μ = viscosity, centipoise

ρ = density, gm/cc

Subscripts

O = continuous phase

D,i = dispersed phase

L = condition for long column

E = condition for shortest column

1 = at initial state of drop

2 = at start of free fall period of drop

3 = at end of free fall period of drop before coalescence

4 = at final state of drop after coalescence

III Theoretical Study of Forced Convection With Simultaneous Chemical Reactions in Drops

III-A Introduction

This section is concerned with development of a model to predict mass transfer by forced convection in drops with simultaneous first-order chemical reaction. The resistance to transfer was confined to the dispersed phase. Predictions by the model were compared with results from currently existing models. The accuracy of these models were examined in the experimental section of this thesis.

Drops may move through fluids either as stagnant drops or as circulating drops, due to the viscous shear forces at the interface. A graphical representation of a drop with internal circulation patterns or streamlines formed by the continuity of the velocity profile at the interface, is shown in Figure III-1, for creeping flow.

In stagnant drops with no internal circulation, mass is transferred by molecular diffusion. This system has been solved by Newman (54) and is shown in Equation II-16.

Before a solution of the forced-convection equation may be attempted, a knowledge of the velocity distribution in fluid particles moving under the influence of gravity is required. This information is available for the Stokes flow regime and to a limited extent, for the intermediate Reynolds Number range. Hadamard (37) and Rybczynski (38) have solved the linearized equations of motion for flow in and around fluid spheres. This solution applies in the Reynolds Number range, $0 \leq Re \leq 1$. Satapathy and Smith (81) solved the linearized equations for flow in and around fluid spheres following Hadamard and Rybczynski, but set the disturbance to parallel flow caused by the sphere to be zero on

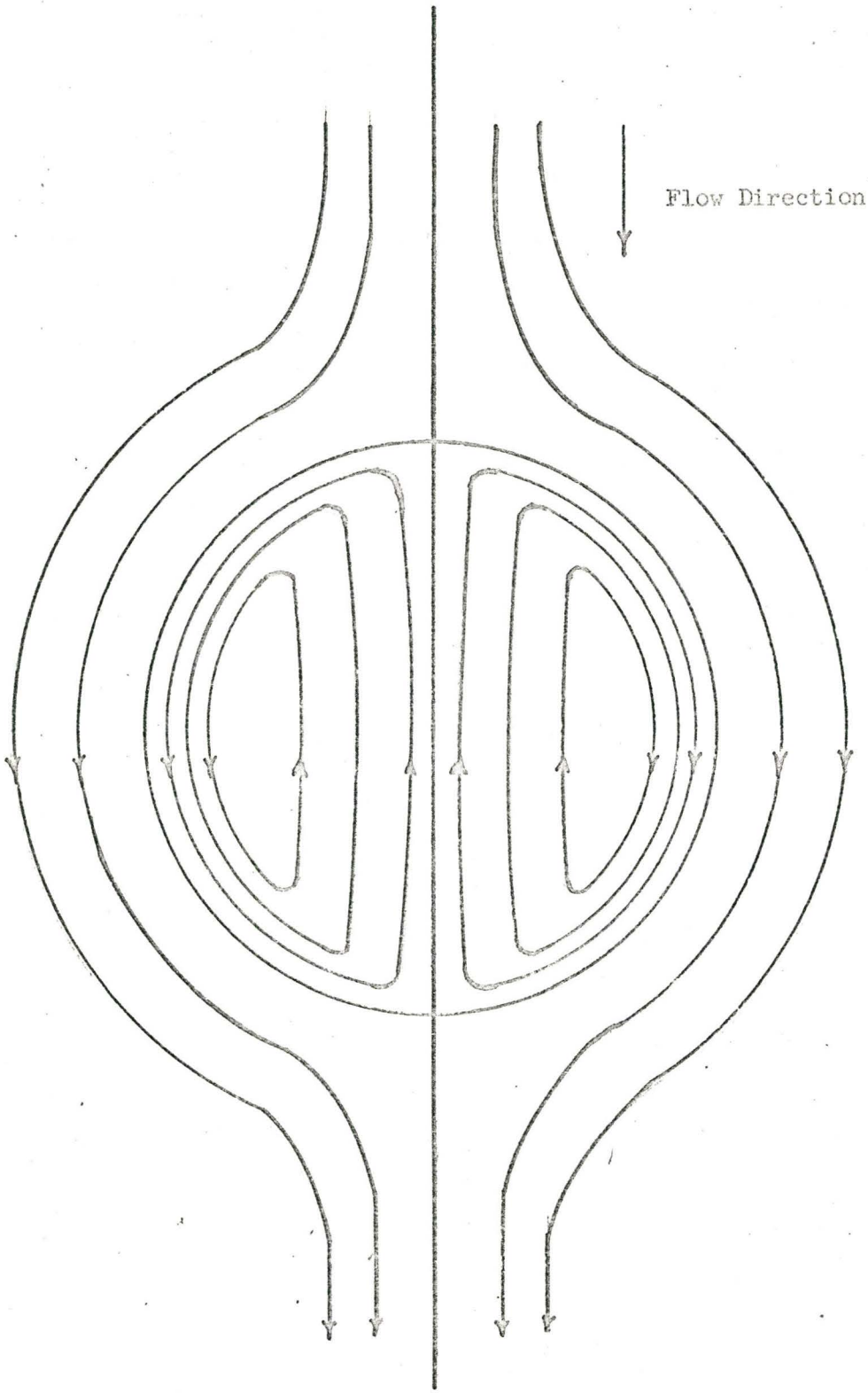

Figure III-1 : Circulation Pattern in a Moving Drop at Creeping Flow

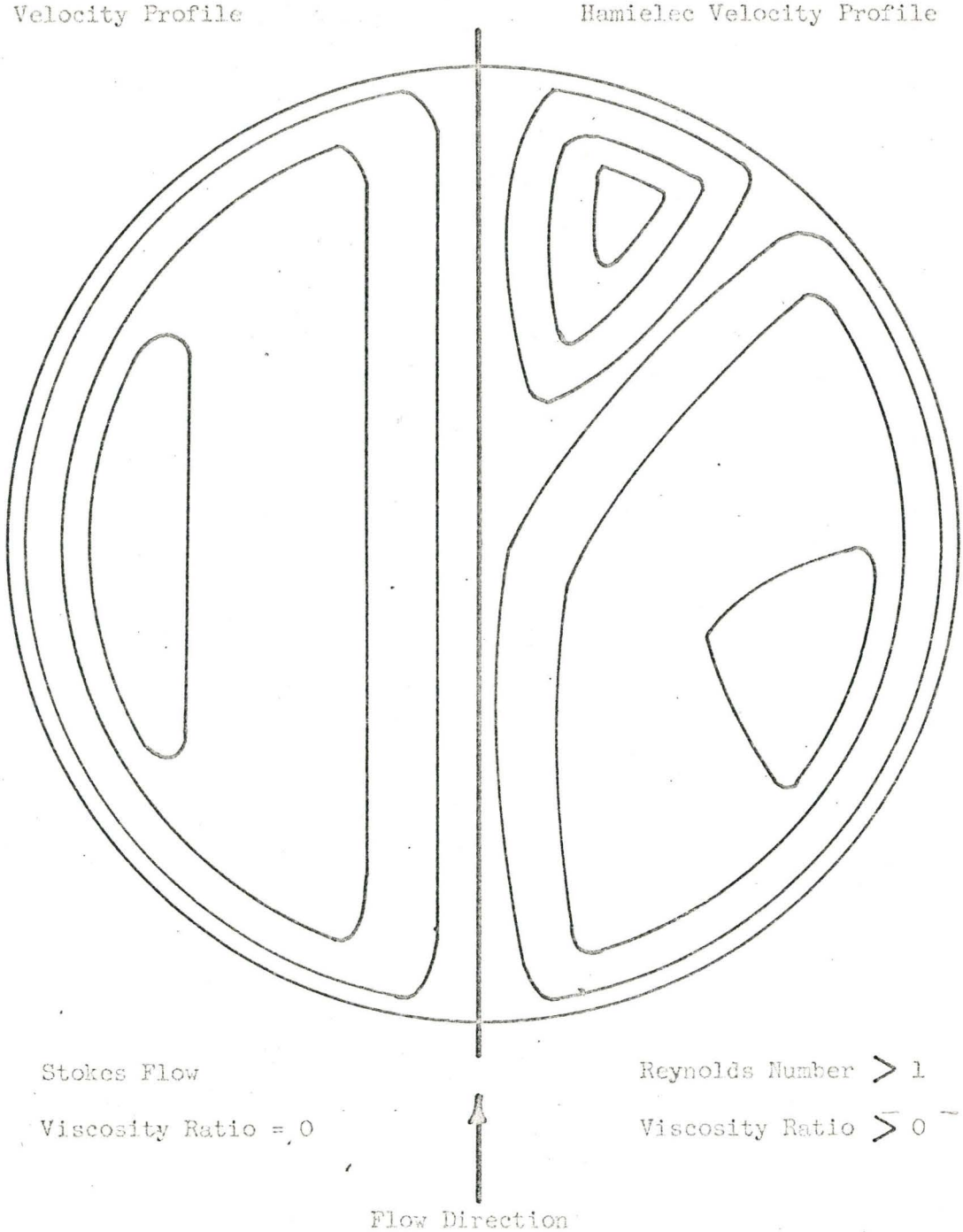

Figure III-2 : Hadamard-Rybczynski and Hamielec Velocity Profiles at Low and Intermediate Reynolds Numbers Regions

a finite, concentric, spherical boundary. In this manner, a wall effect has been allowed for. These solutions indicated that as the wall proximity increased, the circulation velocities in the fluid spheres also increased. Hamielec and Johnson (82,83), using an error-distribution method, have predicted velocity distributions for the Reynolds Number range, $5 \leq Re \leq 90$. Solutions of the potential flow equations closely approximated the profiles around and in fluid spheres of low viscosity ratio, $\frac{\mu_i}{\mu_o} = 0$ with the continuous phase at Reynold Numbers greater than 100 (7).

The Hadamard and the Hamielec profiles are shown in a composite diagram in Figure III-2. At low Reynolds Numbers, the circulation profile in the drop is described by the Hadamard and Rybczynski profile. As the Reynolds Numbers increased, an almost stagnant cap formed in the rear of the fluid sphere. Finally, when the exterior flow separated, the surface velocity changed direction and a second vortex ring formed in the rear portion of the sphere. This effect as shown in Figure III-2, has been described by the Hamielec and Johnson (82) solution of the momentum equation. Experimentally, circulation patterns similar to Hadamard's have been photographed by such people as Kintner (85). However, the profile predicted by Hamielec and Johnson has not so far been observed. Due to their small size, the small vortex rings at the rear of the drops may be hidden by the refraction of light around the moving drop. Drop deformation may also reduce the size of the second vortex ring and reduce velocities within it.

Recently, a more accurate velocity profile has been obtained by

Nakano and Tien (84) by modifying Hamielec's solution for flow inside fluid spheres. By the retention of the inertia terms of the interior fluid in the solution, circulation velocity within the drop was found to increase with the increase of internal Reynolds Number, which is defined as:-

$$Re_i = \frac{d V_D \rho_i}{\mu_i} \qquad \text{(III-1)}$$

where V_D is the relative velocity between the particle and the field fluid. The external flow characteristics such as drag coefficients were unaffected by the internal Reynolds Number. The solution of Nakano and Tien approached Hamielec's at internal Reynolds Number, $Re_i = 0$. Unfortunately, since this new velocity profile became available only recently, it was not used in this work.

The forced-convection equation has so far proved insoluble by any analytical method. Kronig and Brink (58), using the Hadamard-Rybczynski velocity profile , modified the forced-convection equation using an approximation. Their model assumed that lines of constant concentration and the stream lines were coincidental. This required that circulation velocities be much greater than diffusion velocities, limiting the applicability of the model to systems of low viscosity ratio and long diffusion times. This model was shown in Equation II-52 .

Recently, Johns and Beckmann (86) solved the forced-convection equation using finite difference methods and the Hadamard-Rybczynski velocity profile. Using spherical coordinates, they were unable to find a stable solution near the center of the fluid sphere. Thus, a rectangular mesh with a circular boundary was used to obtain stable solutions.

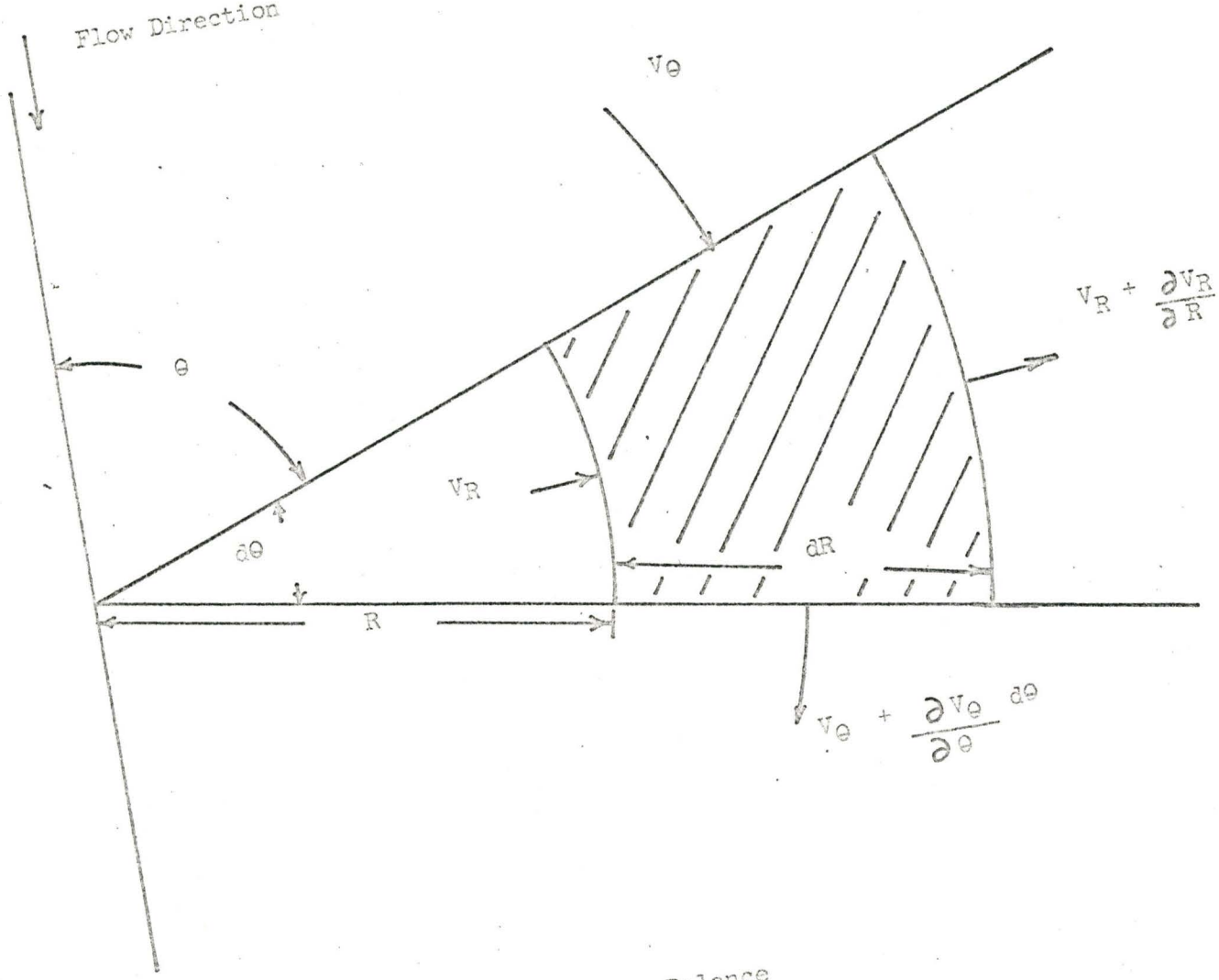

Figure III-3 : Spherical Element for Mass Balance

The present study, which is also concerned with solving the forced convection equation, using finite difference methods was initiated before the results of Johns and Beckmann were available. However, stable solutions were found using spherical polar co-ordinates. The present study is also concerned with simultaneous chemical reaction and the intermediate Reynolds Number range. In this sense, it is an extension of the work of Johns and Beckmann to a far less limiting condition.

III-B Theory

The solution of the forced-convection equation by finite difference methods which follows makes use of the following basic assumptions:-

1) Spherical, circulating drops or bubbles moving under influence of gravity at constant velocity.
2) Physical properties are independent of solute concentration, viz, molecular diffusion coefficient, viscosity and density are independent of concentration.
3) Fluids are incompressible and Newtonian.
4) Axial symmetry is assumed for the concentration profile. Hence the profile for only half of the sphere is required.

The spherical element for mass balance is shown in Figure III-3. The solute transfer in the volume is due to a sum of:-

1) Convective flux due to tangential and radial velocity components, V_Θ and V_R of the streamlines.

2) Molecular diffusion flux, described by Fick's first law:-

$$N_A = - D_L \frac{\partial C^1}{\partial x^1} \qquad \text{(III-2)}$$

i.e. mass flux N_A is due to the concentration gradient $\frac{\partial C^1}{\partial x^1}$ of the solute.

3) The chemical reaction which acts as a sink.

The dimensionless forced convection equation which describes this transfer of matter is:-

$$\frac{\partial C}{\partial T} = \frac{\partial^2 C}{\partial R^2} + \frac{2}{R}\frac{\partial C}{\partial R} + \frac{\cot\theta}{R^2}\frac{\partial C}{\partial \theta} + \frac{1}{R^2}\frac{\partial^2 C}{\partial \theta^2}$$

$$- RK\, C - \frac{Pe}{2}\left\{ \frac{V_\theta}{R}\frac{\partial C}{\partial \theta} + V_R \frac{\partial C}{\partial R} \right\} \qquad \text{(III-3)}$$

where V_θ, V_R = velocity profile components (III-4)
and the following dimensionless terms were used.

$$C = \frac{C^1}{C_\phi} = \text{concentration} \qquad \text{(III-5a)}$$

$$R = \frac{r^1}{a} = \text{radius} \qquad \text{(III-5b)}$$

$$T = \frac{D_L t}{a^2} = \text{time} \qquad \text{(III-5c)}$$

$$RK = \frac{RK^1 a^2}{D_L} = \text{reaction constant} \qquad \text{(III-5d)}$$

$$Pe = \frac{2aV_D}{D_L} = \text{Peclet number} \qquad \text{(III-5e)}$$

Boundary and Initial Conditions

$$R = 1 \quad C = 1 \quad T \geq 0 \qquad \text{(III-6)}$$

$$0 \leq R \leq 1 \quad C = 0 \quad T = 0$$

III-C Mass Transfer Coefficient, K_L

The mass transfer coefficient and the dimensional surface flux $\frac{dM^1}{dt^1}$ are defined by the mass balance equation:-

$$\frac{dM^1}{dt^1} = - D_L \left\{ \frac{\partial C^1}{\partial r} \right\}_{r = a} dA \qquad \text{(III-7)}$$

where $$K_L = - \frac{D_L}{C\phi} \left\{ \frac{\partial C^1}{\partial r} \right\}_{r = a} \qquad \text{(III-8)}$$

and A = drop surface area, cm^2

In dimensionless terms, local mass transfer coefficients are expressed as local Sherwood Numbers:-

$$Sh_{Local} = \frac{2aK_L(local)}{D_L} = -2 \left. \frac{\partial C}{\partial R} \right| R = 1 \qquad \text{(III-9)}$$

at the surface of the drop.

The overall Sherwood Number is:-

$$Sh = \tfrac{1}{2} \int_0^{\pi} Sh_{Local} \sin \theta d\theta \qquad \text{(III-10)}$$

III-D Mass Transferred

The average concentration, $\bar{C}$, of the solute in the fluid sphere was calculated from the sum of the concentration in each elemental volume dV, as shown:-

$$\bar{C} = \frac{\int^V C dV}{\int^V dV} \qquad \text{(III-11)}$$

When the reaction constant is zero, the mass transferred during $\triangle t$ is the change in the average concentration of the mass in the drop. This is not true when reaction is present. Instead, Equation III-8 must be solved. The total mass transferred M^1 is:-

$$M^1 = \int^{A} D_L \left\{ \frac{\partial C^1}{\partial r} \right\}_{r = a} dA \int^{t} dt$$

$$= \int^{\pi} D_L \left\{ \frac{\partial C^1}{\partial r} \right\}_{r = a} 2\pi a^2 \sin\theta \, d\theta \int^{t} dt \qquad \text{(III-12)}$$

or in dimensionless terms

$$M = \int^{\pi} Sh_{Loc} \, \pi \sin\theta d\theta \int^{T} dT \qquad \text{(III-13)}$$

where $$M = \frac{M^1}{C_\rho a^3} \qquad \text{(III-14)}$$

III-E Circulation Time Around Hadamard-Rybczynski Streamline in a Drop

The circulation time of a particle on a Hadamard-Rybczynski streamline was given by Kronig and Brink (8) as:-

$$t = \frac{6 (3\mu_i + 2\mu_o) q(\xi)}{g (\rho_i - \rho_o) a} \qquad \text{(III-15)}$$

where $q(\xi)$ was a function defined by Kronig and Brink, to describe the position along a dimensionless streamline ξ, defined as:-

$$\xi = 4R^2(1 - R^2) \sin^2\theta \qquad \text{(III-15a)}$$

Values of ξ and $q(\xi)$ are shown in Table III-1

Table III-1

Values of $q(\xi)$ at Streamline ξ

ξ	0.0	0.1	0.2	0.3	0.4	0.5	0.6	0.7	0.8	0.9	1.0
$q(\xi)$	∞	3.26	2.93	2.75	2.62	2.52	2.44	2.37	2.32	2.27	2.22

Using the definition for dimensionless time t from Equation III-5C and the definitions for drag coefficient C_D:-

$$C_D = \frac{8 (\rho_i - \rho_o) ga}{3 \rho_o V_D^2} \quad \text{(from gravitational force balance)} \qquad \text{(III-16)}$$

and $$C_D = \frac{4\mu_o}{aV_D\rho_o} \left\{ \frac{3X + 2}{X + 1} \right\} \qquad \text{(III-16a)}$$

for drops with Hadamard-Rybczynski velocity profiles (82),

Equation III-15 is redefined in terms of dimensionless time as:-

$$T = \frac{8\,(X+1)\,q\,(\xi)}{Pe} \qquad \text{(III-17)}$$

where X = viscosity ratio $= \frac{\mu_i}{\mu_o}$ (III-18)

This expression for circulation time is used later in examining the variations of the Sherwood Number with time.

III-F Method of Solution of the General Equation III-3

An explicit, forward difference method was used to solve Equation III-3. In this method, the derivatives were represented by finite difference approximations. Then, based on the concentration profile at time T, the new concentration profile at time $(T + \Delta T)$ was calculated.

The finite difference equation which replaced Equation III-3, for the region $0 < R \leq 1$ and $0 \leq \theta \leq \pi$ is:-

$$\begin{aligned}
CONC(I,J,2) = {} & CONC(I,J,1)\left[1 - \frac{2\Delta T}{\Delta R^2} - \frac{2\Delta T}{R^2\Delta\theta^2} - RK^*\Delta T\right] \\
& + CONC(I+1,J,1)\left[\frac{\Delta T}{\Delta R^2} + \frac{\Delta T}{R\Delta R} - \frac{PeV_R\Delta T}{4\Delta R}\right] \\
& + CONC(I-1,J,1)\left[\frac{\Delta T}{\Delta R^2} - \frac{\Delta T}{R\Delta R} + \frac{PeV_R\Delta T}{4\Delta R}\right] \\
& + CONC(I,J+1,1)\left[\frac{\cot\theta\,\Delta T}{2R^2\Delta\theta} + \frac{\Delta T}{R^2\Delta\theta^2} - \frac{PeV_\theta\Delta T}{4R\Delta\theta}\right] \\
& + CONC(I,J-1,1)\left[-\frac{\cot\theta\,\Delta T}{2R^2\Delta\theta} + \frac{\Delta T}{R^2\Delta\theta^2} + \frac{PeV_\theta\Delta T}{4R\Delta\theta}\right] \qquad \text{(III-19)}
\end{aligned}$$

where I and J defined the radial and angular increment, respectively. The circular mesh system used is shown in Figure III-4. CONC (I,J,1) is

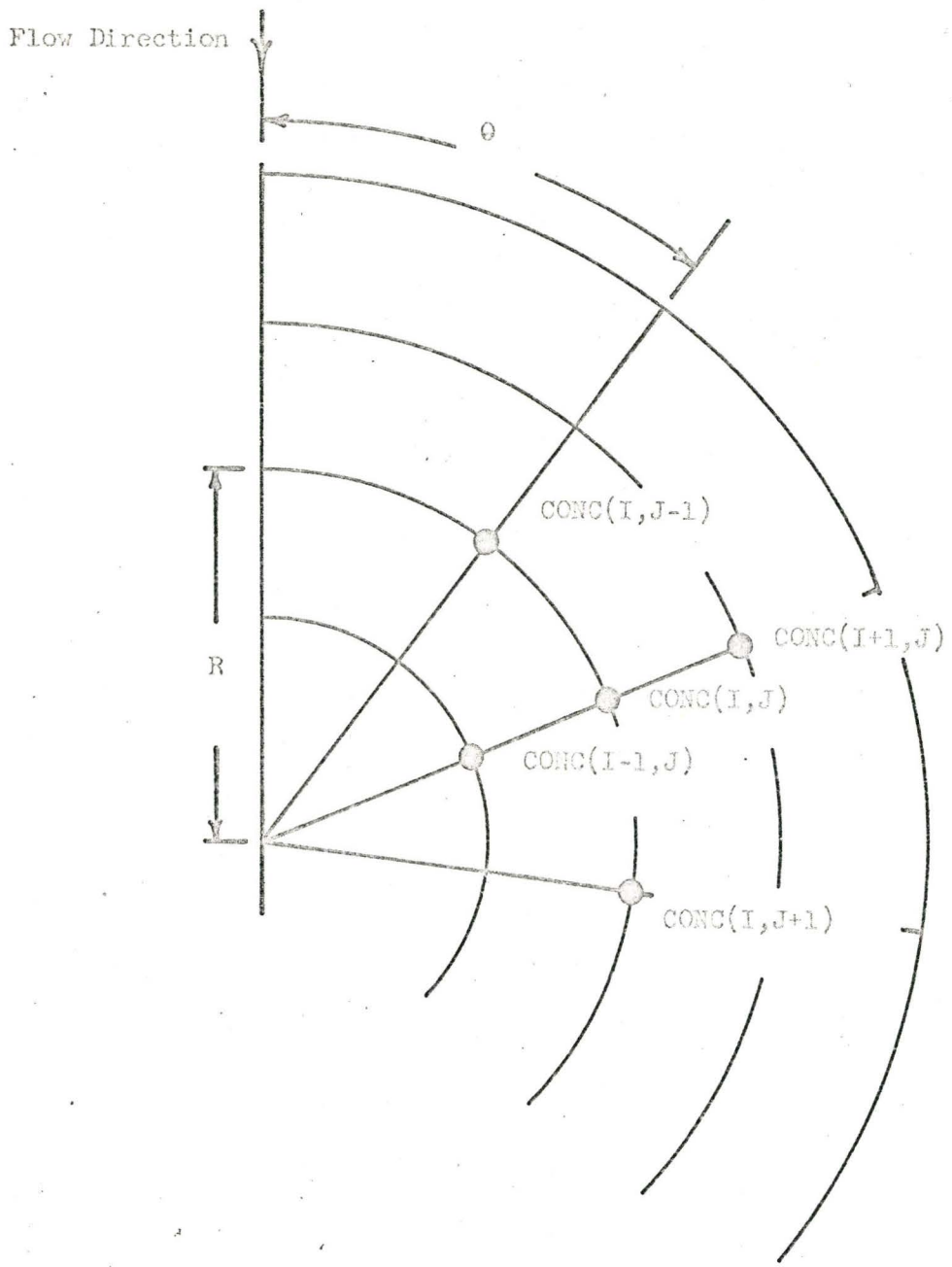

Figure III-4 : Circular Mesh System Used in Numerical Solution of Mass Transfer Equation

the concentration at point (I,J) at time (1) and CONC (I,J,2), the concentration at a time ΔT later. After a complete march through the mesh, CONC (I,J,2) is set equal to CONC (I,J,1) and the process is repeated. The concentration at the centre, R = 0, is defined to be:-

$$\text{CONC}(1,J,2) = \frac{\text{CONC}(2,1,2) + \text{CONC}(2,\text{NAINC},2)}{2} \qquad \text{(III-20)}$$

where J = NAINC at $\theta = \pi$, i.e. $\frac{\partial C}{\partial R}$ = constant on the axis of symmetry at the centre of the drop. Also, since $\frac{\partial C}{\partial \theta} = 0$ along the axis of symmetry,

$$\text{CONC}(I,1,2) = \text{CONC}(I,2,2)$$

$$\text{CONC}(I,\text{NAINC},2) = \text{CONC}(I,\text{NAINC}-1,2) \qquad \text{(III-21)}$$

where $R \neq 0$ and $R \neq 1$

A copy of the program is enclosed in Appendix VIII-1.

III-G Stokes' Flow Regime

Translated into a system of spherical co-ordinates (R,θ,ϕ) with the origin at the centre of the fluid sphere, the dimensionless Hadamard-Rybczynski stream function ψ_i is given by:

$$\psi_i = \frac{HR^2(1 - R^2)}{\frac{\mu_i}{\mu_o} + 1} \sin^2\theta$$

where H is a function of the position of the outer spherical boundary. R_{max} values for H are tabulated in Table III-2 for various viscosity ratios $X = \frac{\mu_i}{\mu_o}$.

Table III-2

Wall Proximity Factors by Satapathy and Smith (81)

R_{max}	X=0	X=1	X=2
1.1	-5.3510	-5.3450	-3.5505
1.3	-2.0115	-1.9081	-1.1154
1.5	-1.2776	-1.0418	-0.6555
1.6	-1.0749	-0.8210	-0.5453
1.7	-0.9293	-0.6777	-0.4685
1.9	-0.7456	-0.5134	-0.3693
2	-0.6864	-0.4632	-0.3357
4	-0.3845	-0.2187	-0.1527
6	-0.3295	-0.1783	-0.1222
8	-0.3062	-0.1620	-0.1101
10	-0.2934	-0.1532	-0.1037
20	-0.2702	-0.1379	-0.0925
∞	-0.2500	-0.2500	-0.2500

The dimensionless velocity components are given by:

$$V_R = \frac{1}{R^2 \sin\theta} \frac{\partial \psi_i}{\partial \theta} \qquad \text{(III-23)}$$

$$= -\frac{2H(1-R^2)\cos\theta}{(1+X)} \qquad \text{(III-23a)}$$

$$V_\theta = -\frac{1}{R \sin\theta} \frac{\partial \psi_i}{\partial R} \qquad \text{(III-24)}$$

$$= \frac{2H(1-2R^2)\sin\theta}{(1+X)} \qquad \text{(III-24a)}$$

$$V_\phi = 0 \qquad \text{(III-25)}$$

III-H Intermediate Reynolds Number Flow Regime

The approximate solutions of Hamielec (82) may be expressed as:-

$$\psi_i = E_1 (R^2 - R^4)\sin^2\theta - F_1(R^2 - R^4)\sin^2\theta\cos\theta \qquad \text{(III-26)}$$

$$V_\theta = 2E_1(1 - 2R^2)\sin\theta - 2F_1(1 - 2R^2)\sin\theta\cos\theta \qquad \text{(III-27)}$$

$$V_R = -2E_1(1 - R^2)\cos\theta + F_1(1 - R^2)(3\cos^2\theta - 1) \qquad \text{(III-28)}$$

Values of E_1 and F_1 are tabulated in Table III-3

Table III-3

Coefficients for Hamielec (82) Velocity Profiles

Reynolds Number	Viscosity Ratio	E_1	F_1
20	0	-0.426	0.069
40	0	-0.457	0.141
60	0	-0.525	0.226
20	2	0.160	0.087
40	2	0.573	0.185
60	2	-0.309	0.466

III-I Models for Comparisons

Results from the numerical solution of Equation III-19, were compared with those obtained by Danckwerts' (59) modifications of the Newman (54) and the Kronig and Brink (58) equations for transfer with first-order reaction into stagnant and fully circulating drops respectively. Results were also compared with those obtained by Johns and Beckmann (86) for physical mass transfer into viscous drops.

III-I-1 Danckwerts' Modification of the Newman Equation for Mass Transfer with Reaction into Stagnant Drops

The dimensionless average concentration in a stagnant drop in which mass is transferred and reacted with a reaction rate constant RK, is:-

$$\bar{C} = 1.0 - \sum_{n=1}^{\infty} \frac{6}{\pi^2} \frac{1}{n^2} \left\{ \frac{RK + n^2\pi^2/\exp\left[T(RK + n^2\pi^2)\right]}{RK + n^2\pi^2} \right\} \quad \text{-- (III-29)}$$

The rate of transfer and the mass transfer coefficient are functions of the concentration gradient at the surface of the absorbent.

The dimensionless concentration gradient $\frac{\partial C}{\partial R}$ was calculated from

$$\left.\frac{\partial C}{\partial R}\right]_{R=1} = 2 \sum_{n=1}^{\infty} \frac{RK + n^2\pi^2/\exp\left[T(RK + n^2\pi^2)\right]}{RK + n^2\pi^2} \quad \text{(III-30)}$$

and the dimensionless rate of transfer N, from:-

$$N = 3 \left.\frac{\partial C}{\partial R}\right]_{R=1} \quad \text{(III-31)}$$

The Sherwood Number, or dimensionless mass transfer coefficient was calculated as shown in Equation III-9.

M, the total dimensionless mass transferred per unit drop volume was given as:-

$$M = \int_0^{T=T} N \, dT = 6 \sum_{n=1}^{\infty} RK \, \frac{(RK + n^2\pi^2)T - n^2\pi^2\left[\exp\left(-T(RK+n^2\pi^2)\right)-1\right]}{(RK + n^2\pi^2)^2} \quad \text{-- (III-32)}$$

A computer program giving these calculations is shown in Appendix VIII-2.

III-I-2 Danckwerts' Modification of the Kronig and Brink Equation for Mass Transfer with Reaction into Fully Circulating Drops

The dimensionless average concentration inside the drop for reacting systems was given as:-

$$\bar{C} = 1 - \frac{3}{8}\sum_{n=1}^{\infty} \frac{A_n^2 \left[RK + 16\lambda_n / \exp\left[T\,(RK + 16\lambda_n)\right]\right]}{RK + 16\lambda_n} \qquad \text{(III-33)}$$

where A_n and λ_n values are given in Table II-1.

The dimensionless concentration gradient was given as:-

$$\left.\frac{\partial C}{\partial R}\right]_{R=1} = 2\sum_{n=1}^{\infty} \frac{A_n^2 \lambda_n \left(RK + 16\lambda_n / \exp\left[T\{RK + 16\lambda_n\}\right]\right)}{RK + 16\lambda_n} \qquad \text{(III-34)}$$

The rate of transfer was calculated as shown in Equation III-31. The Sherwood Number was calculated as shown in Equation III-9.

The total mass transferred per unit drop volume was given as:-

$$M = 6.0 \sum_{n=1}^{\infty} \frac{A_n^2 \lambda_n \left(RK\,(RK + 16\lambda_n)T - 16\lambda_n\left[\exp\left(-T\{RK+16\lambda_n\}\right) - 1\right]\right)}{(RK + 16\lambda_n)^2} \qquad \text{--(III-35)}$$

A program giving these calculations is shown in Appendix VIII-3.

III-I-3 Johns and Beckmann Model for Physical Mass Transfer into Viscous Drops

The Johns and Beckmann model for mass transfer into viscous drops was similar to the model proposed in this thesis as given in Equation III-3.

Using the Hadamard-Rybczynski velocity profile, their equation was given as:-

$$\frac{\partial C}{\partial T} = \frac{\partial^2 C}{\partial R^2} + \frac{2}{R}\frac{\partial C}{\partial R} + \frac{\cot\theta}{R^2}\frac{\partial C}{\partial \theta} + \frac{1}{R^2}\frac{\partial C^2}{\partial \theta^2} + \frac{Pe}{2}\left[\frac{(1-R^2)\cos\theta}{2(1+X)}\frac{\partial C}{\partial R} + \frac{(2R^2 - 1)\sin\theta}{2R\,(1+X)}\frac{\partial C}{\partial \theta}\right] \qquad \text{(III-36)}$$

where $C = \dfrac{C^1 - C_\phi}{\overline{C}_1 - C_\phi}$ (III-37)

Since a sign convention reverse to that used in the present work was employed by Johns, all the velocity components are negative to those shown in Equations III-24 and III-25.

A modified Peclet Number Pe_J,

$$Pe_J = \frac{Pe}{4(1+X)} \qquad \text{(III-38)}$$

was used to correct for the effects of the viscosity ratio X ($= \dfrac{\mu_i}{\mu_o}$), as defined by the denominator of the Hadamard-Rybczynski velocity components, viz:-

$$V_R = -\frac{(1 - R^2)\cos\theta}{2(1+X)} \text{ and } V_\theta = \frac{(1 - 2R^2)\sin\theta}{2(1+X)}$$

The common denominator (2(1+X)) was removed from inside the brackets in Equation III-36 and combined with $\dfrac{Pe}{2}$ to give the modified Peclet Number, Pe_J. Thus, this modification of the Peclet Number for viscosity effects, must be changed with the velocity profile used.

The mass transfer coefficient K_L, was defined by Johns and Beckmann as:-

$$K_L = \frac{D_L}{(C_\phi - \overline{C}^1)} \frac{\partial C^1}{\partial r}\bigg|_{r=a} \qquad \text{(III-39)}$$

and as before, the Sherwood Number Sh_J is:-

$$Sh_J = -2 \frac{\partial C}{\partial R}\bigg|_{R=1} \qquad \text{(III-39a)}$$

However, comparing the definition for the mass transfer coefficient K_L, in Equation III-9 and in Equation III-8 :-

$$Sh_J = \frac{Sh}{1 - \overline{C}} \qquad \text{(III-40)}$$

It was later decided to use Johns' definition of Sherwood Number since it has the advantage of giving an asymptotic value, which is not zero, as time tends to infinity.

III-J Discussion of Results for Physical Mass Transfer Calculations

The results for physical mass transfer calculations including the comparison with Johns and Beckmann data are shown first, for drops with the Hadamard-Rybczynski velocity profile. This is followed by results for mass transfer into drops in the intermediate Reynolds Number range. In the graphs, the calculated points are shown inorder to identify the various curves.

III-J-1 Step Sizes

The effect of the step sizes on the predicted mass transfer was initially investigated. The following step sizes were studied:-

1) Radial step sizes - 0.05, 0.025, 0.0125
2) Angular step sizes - 6^{o}, 3^{o}
3) Time step sizes - 1×10^{-5}, 2.5×10^{-6}, 6.25×10^{-7}

Step sizes in time were chosen as large as possible for a particular choice of radial and angular step sizes. Above this maximum ΔT, the solution diverged. It was found that the mass transfer predicted by a mesh size of (41,31) were identical to (81,31) where 41 and 81 are the number of radial increments and 31, the number of angular increments. The results for (41,31) were also identical with (41,61).

Finite difference solutions for mesh sizes (41,31) and (81,31)

Figure III-5 : Computed Results Showing Effects of Mesh Size on Calculated Mass Transferred

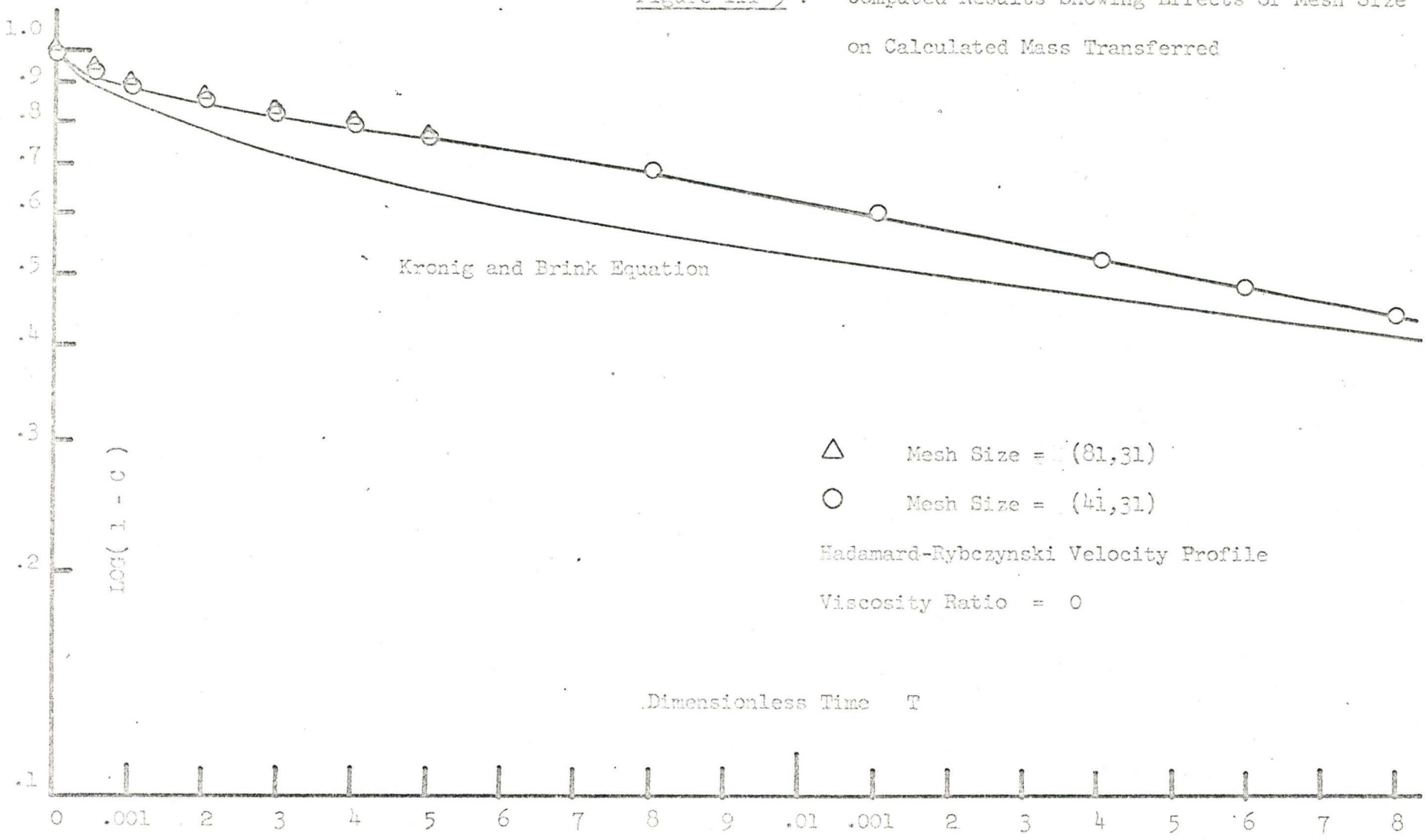

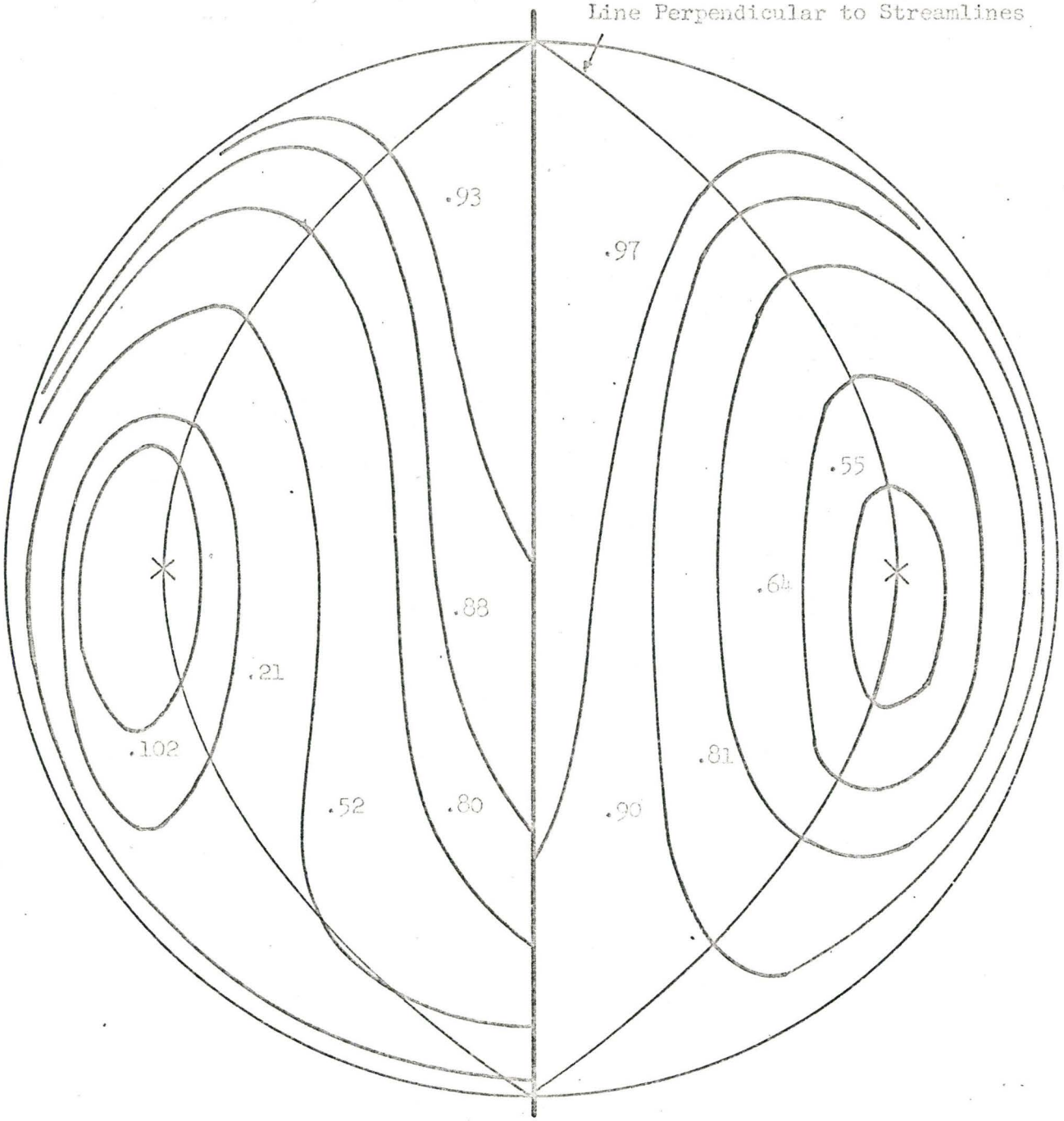

Mesh Size = (41,3,)

T = .015

Average Concentration = 0.49

RK = 0.0

Pe_J = 250

Mesh Size = (41,31)

T = .045

Average Concentration = 0.794

RK = 0.0

Pe_J = 250

Figure III-6 : Lines of Constant Concentrations Developed During Mass Transfer into Drops with Hadamard-Rybczynski Velocity Profiles

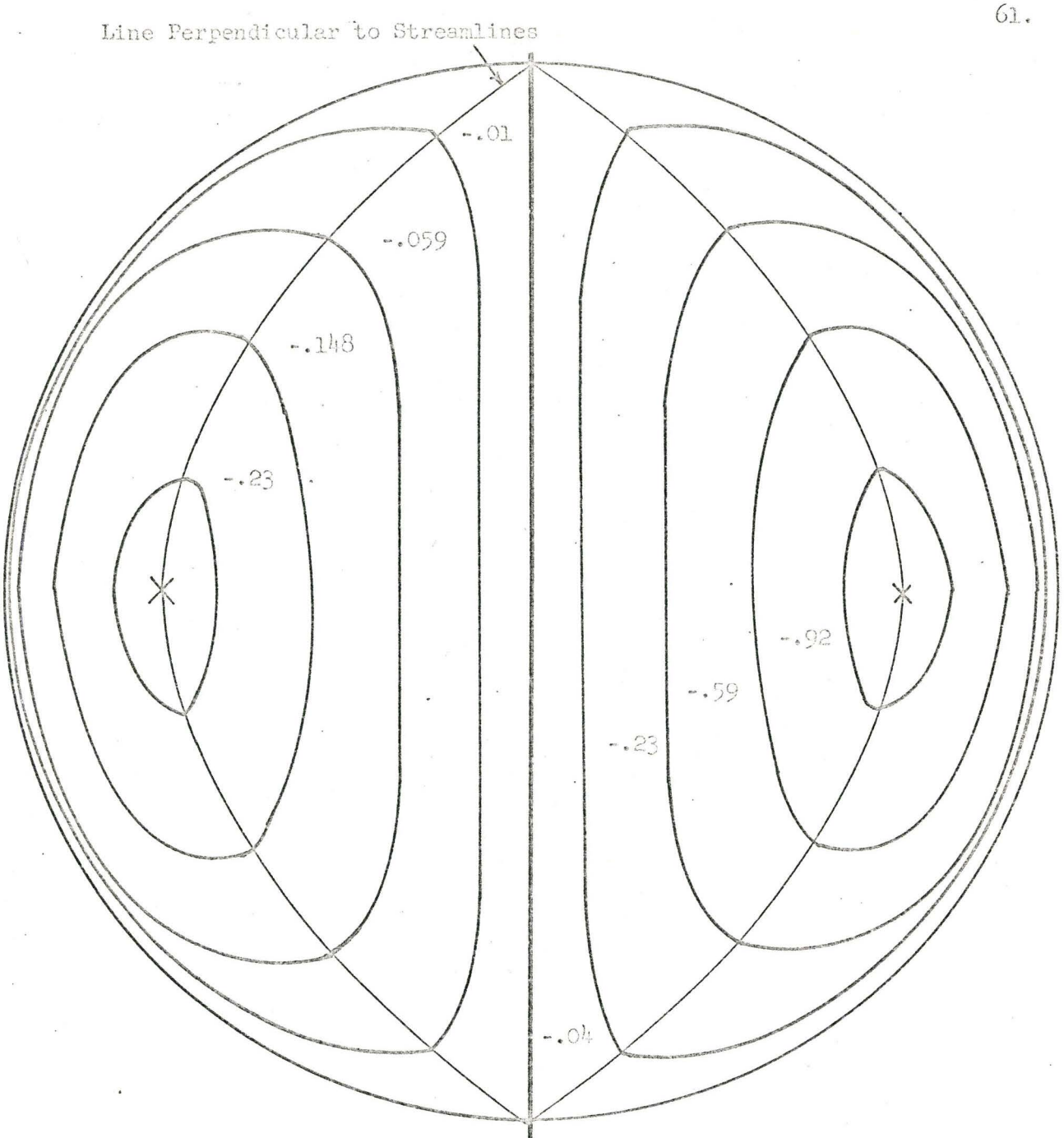

Figure III-7 : Values of Internal Streamlines for Drops with Hadamard-Rybczynski Velocity Profiles

are compared with the Kronig and Brink solution in Figure III-5, as tabulated in Appendix VIII-4. These results are given at $Pe_J = 250$ and viscosity ratio = 0, with Hadamard-Rybczynski velocity profiles. As time increased, the agreement between the finite difference method and the Kronig and Brink model improved.

The reasons for the disagreement at short diffusion time was due to the assumptions of the Kronig and Brink model. It was assumed that at all times, the lines of constant concentration and the stream lines were coincidental. This assumption breaks down at short diffusion times since a finite time is required for the solute to be distributed evenly along a stream line. The finite difference model allows for this to occur, resulting in a slower initial buildup of solute in the sphere. At large diffusion times, the lines of constant concentration and streamlines become coincidental and the two solutions, finite difference and analytical, approach each other. This is shown in Figure III-6. Lines of constant concentrations are plotted and shown to be similar to the velocity profile defined by the Hadamard-Rybczynski streamlines, as time increased. The streamlines are shown in Figure III-7.

The agreement can never be exact because of the initial slow solute buildup in the sphere.

In order to obtain accurate results at minimum computer times, a mesh size of (41,31) and a time step size, $\Delta T = 2.5 \times 10^{-6}$ were chosen for further computations in flow regimes, where the Kronig and Brink model did not apply.

Figure III-8 : Effects of Wall Proximity on Calculated Mass Transferred

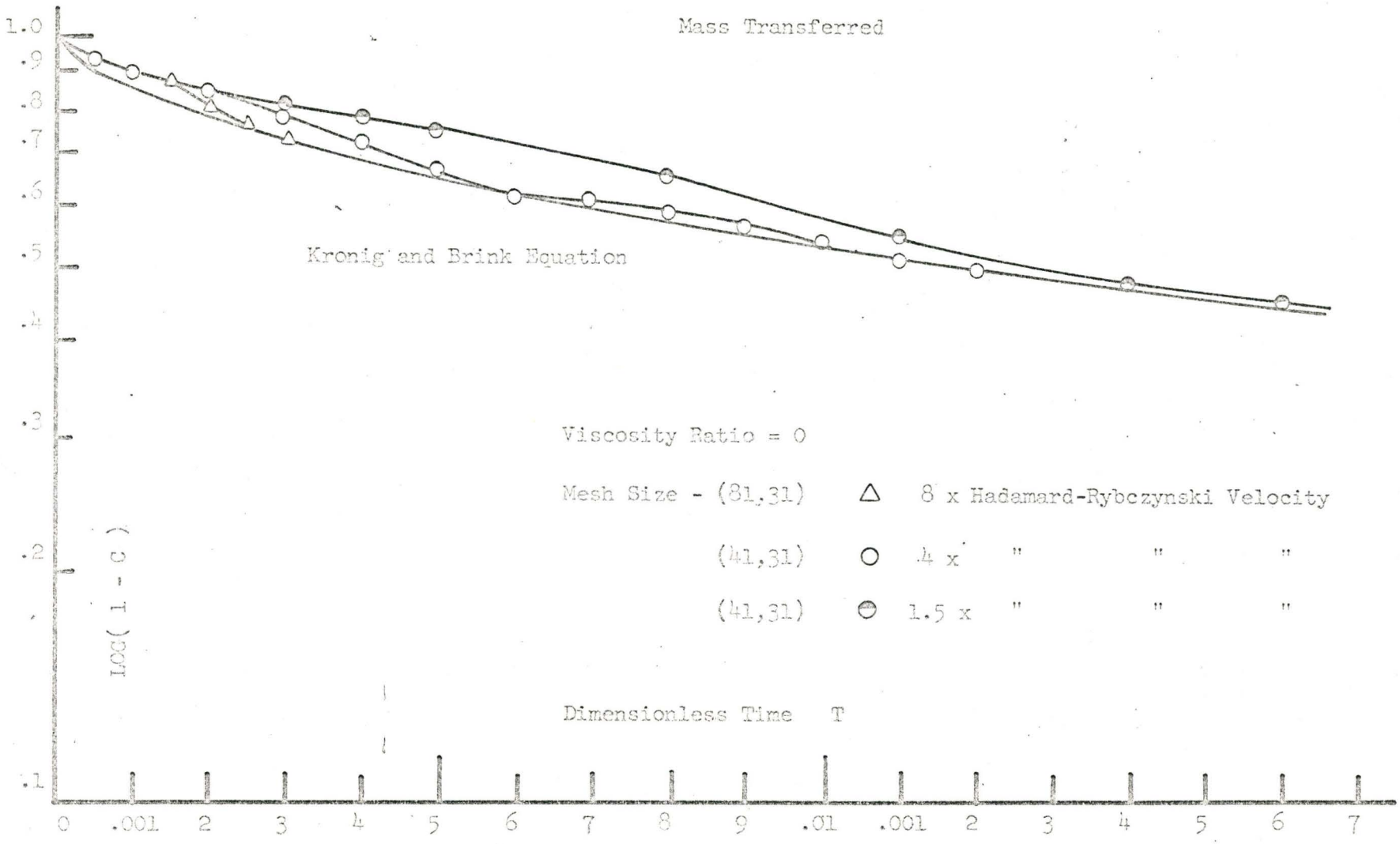

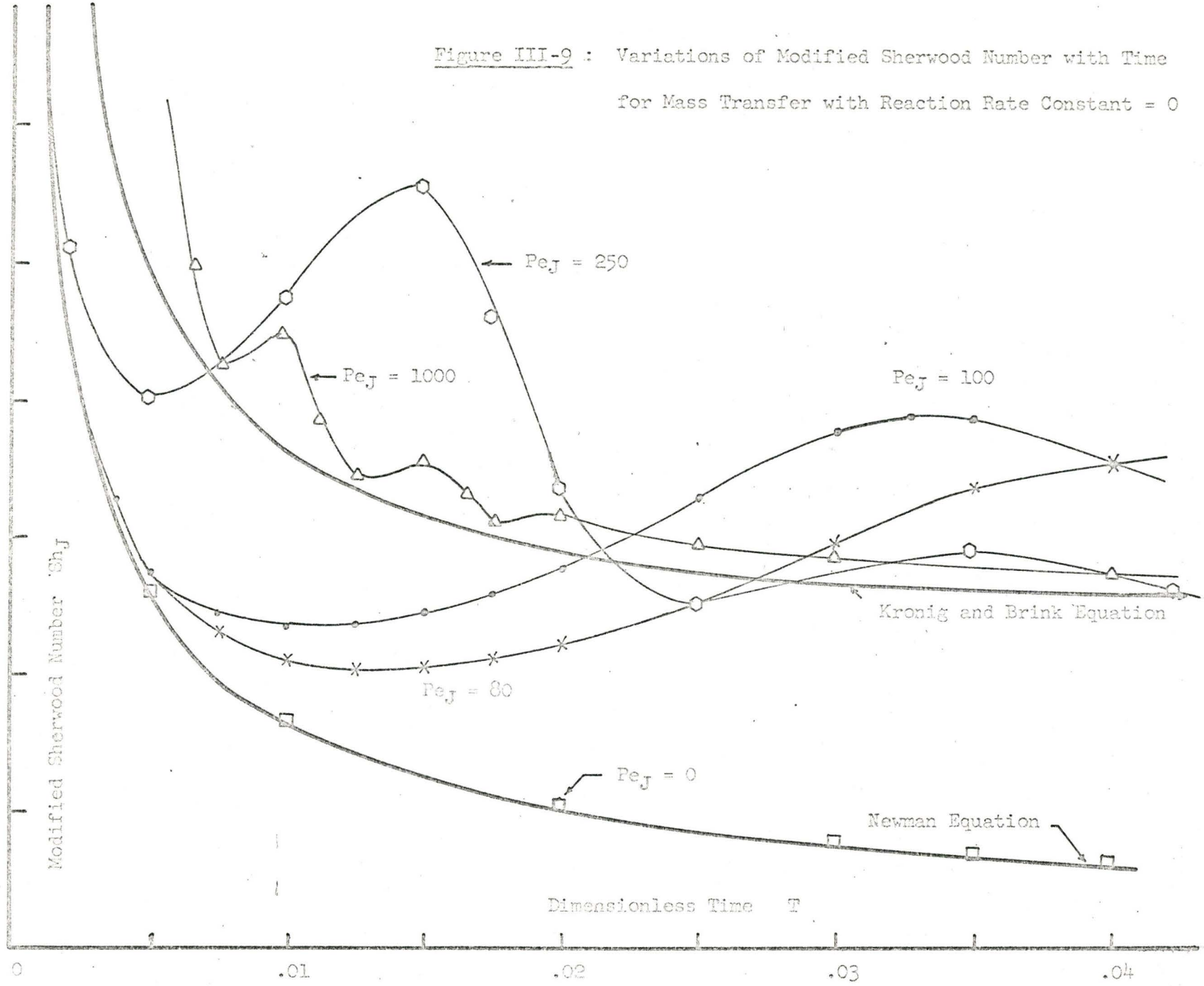

Figure III-9 : Variations of Modified Sherwood Number with Time for Mass Transfer with Reaction Rate Constant = 0

III-J-2 Stokes' Flow Regime

Referring to Table III-2 and Equations III-23and III-24, it can be seen that increasing the wall proximity merely increased the radial and tangential velocity components by a constant factor H, times the Hadamard-Rybczynski velocity components. H constants of -0.25, -0.375, -1.0 and -2.0 were used. These values correspond to 1, 1.5, 4 and 8 times the Hadamard-Rybczynski velocity profiles, respectively. The results for 1.5, 4 and 8 times are compared with the Kronig and Brink solution in Figure III-8 and in Appendix VIII-4.

Since all these computations were run at Peclet Number of 1000, the modified Peclet Number Pe_J = 250 at viscosity ratio = 0 for the Hadamard-Rybczynski velocity profile.

Thus, at 1.5, 4 and 8 times the Hadamard-Rybczynski velocity profiles, the corresponding values of the modified Peclet Numbers Pe_J are 375, 1000 and 2000, respectively.

Increasing the wall proximity and hence the modified Peclet Number, increased the circulation velocities. This resulted in a faster initial solute build up, and the Kronig and Brink model is approached in a shorter time. Hence, as the wall proximity is increased, the range of applicability of the Kronig and Brink model is increased.

III-J-3 Variations of Sherwood Number with Peclet Number

Variations of the modified Sherwood Number Sh_J with the modified Peclet Number Pe_J are shown in Figure III-9 and in Appendix VIII-5.

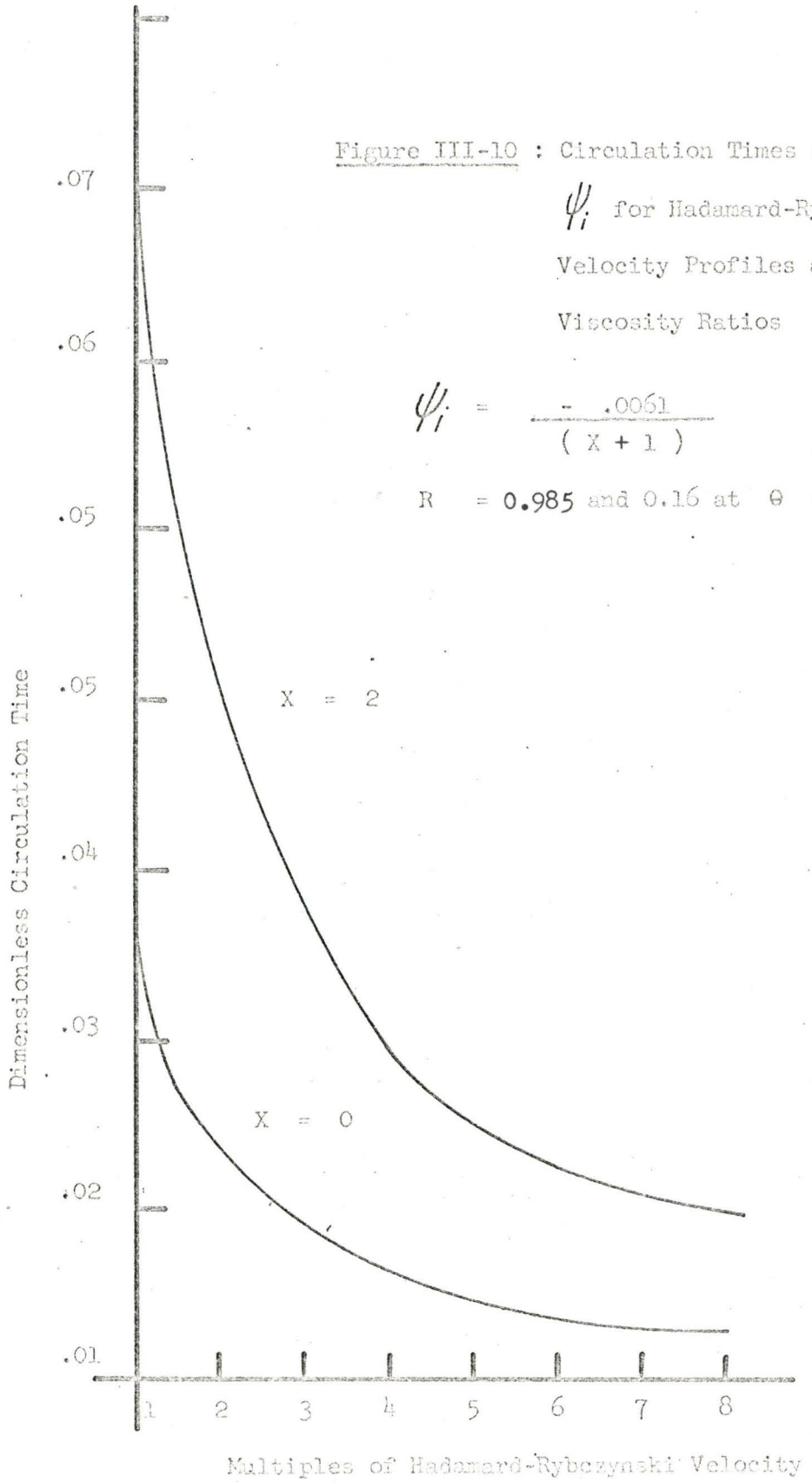

Figure III-10 : Circulation Times Around Streamline ψ_i for Hadamard-Rybczynski Velocity Profiles at Various Viscosity Ratios

$$\psi_i = \frac{-.0061}{(X+1)}$$

$R = 0.985$ and 0.16 at $\theta = \frac{\pi}{2}$

As the modified Peclet Numbers increased, all the solutions tended to oscillate about the Kronig and Brink line. As the Peclet Numbers decreased, the solutions approached the Newman line, until they merged. This agreement with Newman's equation was used to check the accuracy of the program.

The initial oscillations of the Sherwood Number are believed to be due to the velocity profiles affecting the component profile in the drop. In Figure III-10, the circulation times on a streamline $\psi_i = \frac{-.0061}{(X+1)}$ and $\xi = .01$ are shown for different multiples of the Hadamard velocity profiles at viscosity ratios of 0 and 2. The streamline cuts the drop radius at R = 0.16 in the interior and at R = 0.985 at the exterior, at $\theta = 90^\circ$. These times are also tabulated in Appendix VIII-7. By examining the circulation times for a streamline near the surface of the drop, it is seen that the oscillation periods of the Sherwood Number versus time curves correspond to the circulation times at each Peclet Number. The Sherwood Number is a function of the concentration gradient at the surface. As mass is transferred, it is circulated around the streamlines in the drop. The concentration gradient is set up in half the circulation time at the surface of the drop. This gradient is maintained as the solute is swept around into the interior, to complete the circuit. Then on the next cycle, more mass is added to the streamlines and the concentration gradient is further decreased. Hence, the period of oscillation of the Sherwood Numbers corresponds to the circulation time of the streamlines near the surface of the drop.

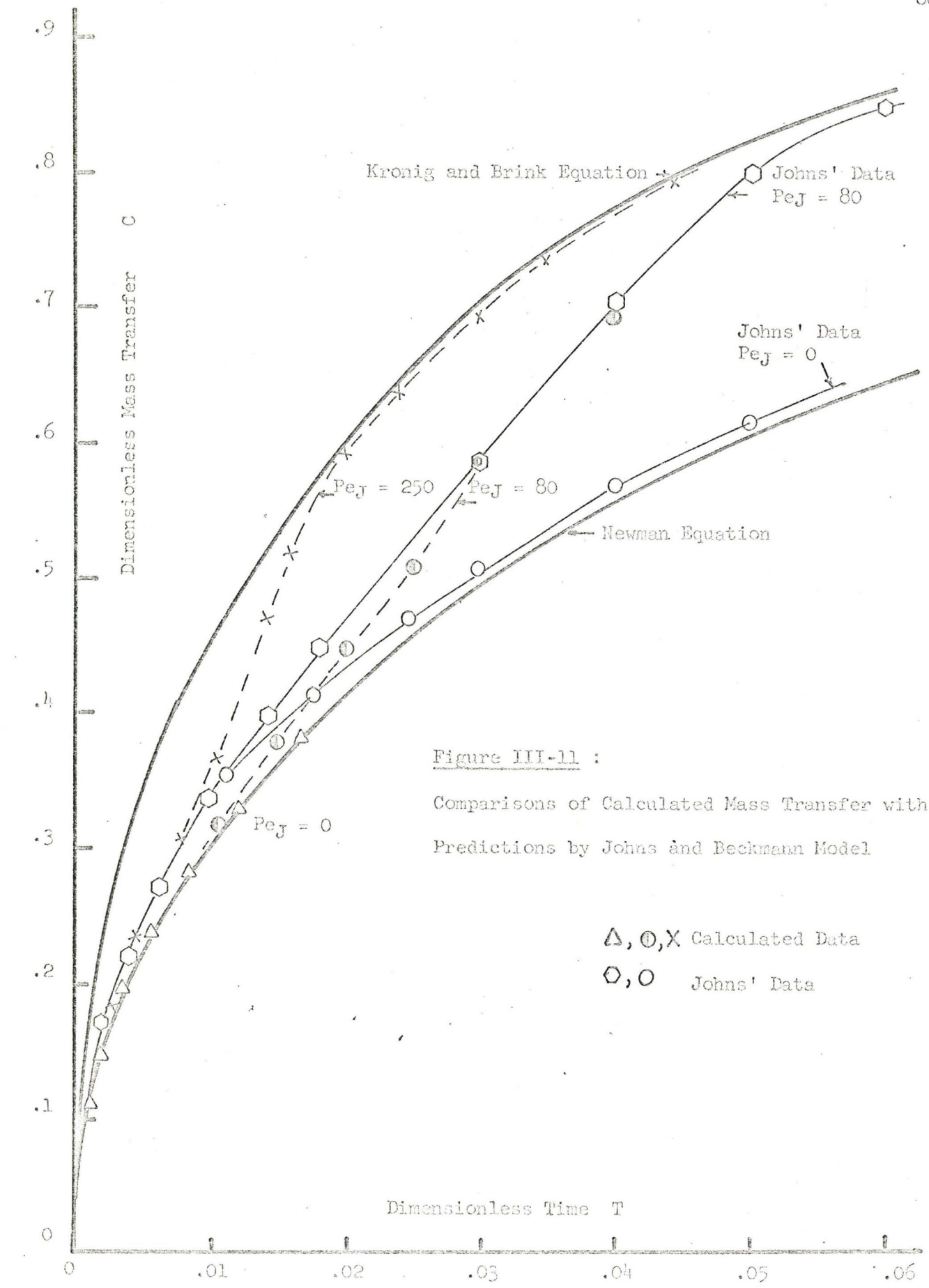

Figure III-11 :

Comparisons of Calculated Mass Transfer with Predictions by Johns and Beckmann Model

Figure III-12 : Comparisons of Calculated Sherwood Number Sh_J with Predictions by Johns and Beckmann Model

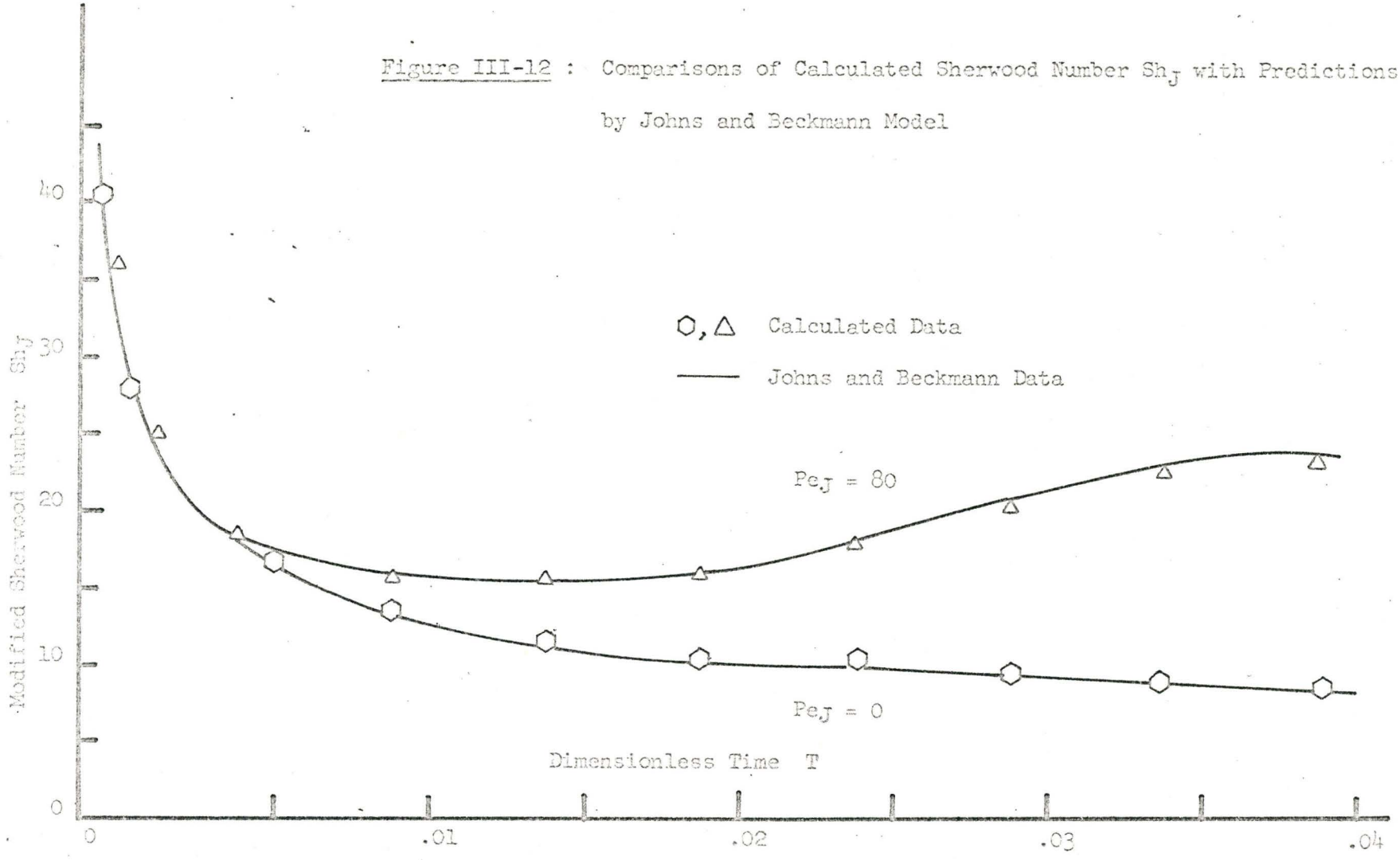

Figure III-13 : Effects of Viscosity Ratio on Calculated Mass Transfer at Low and Intermediate Reynolds Numbers

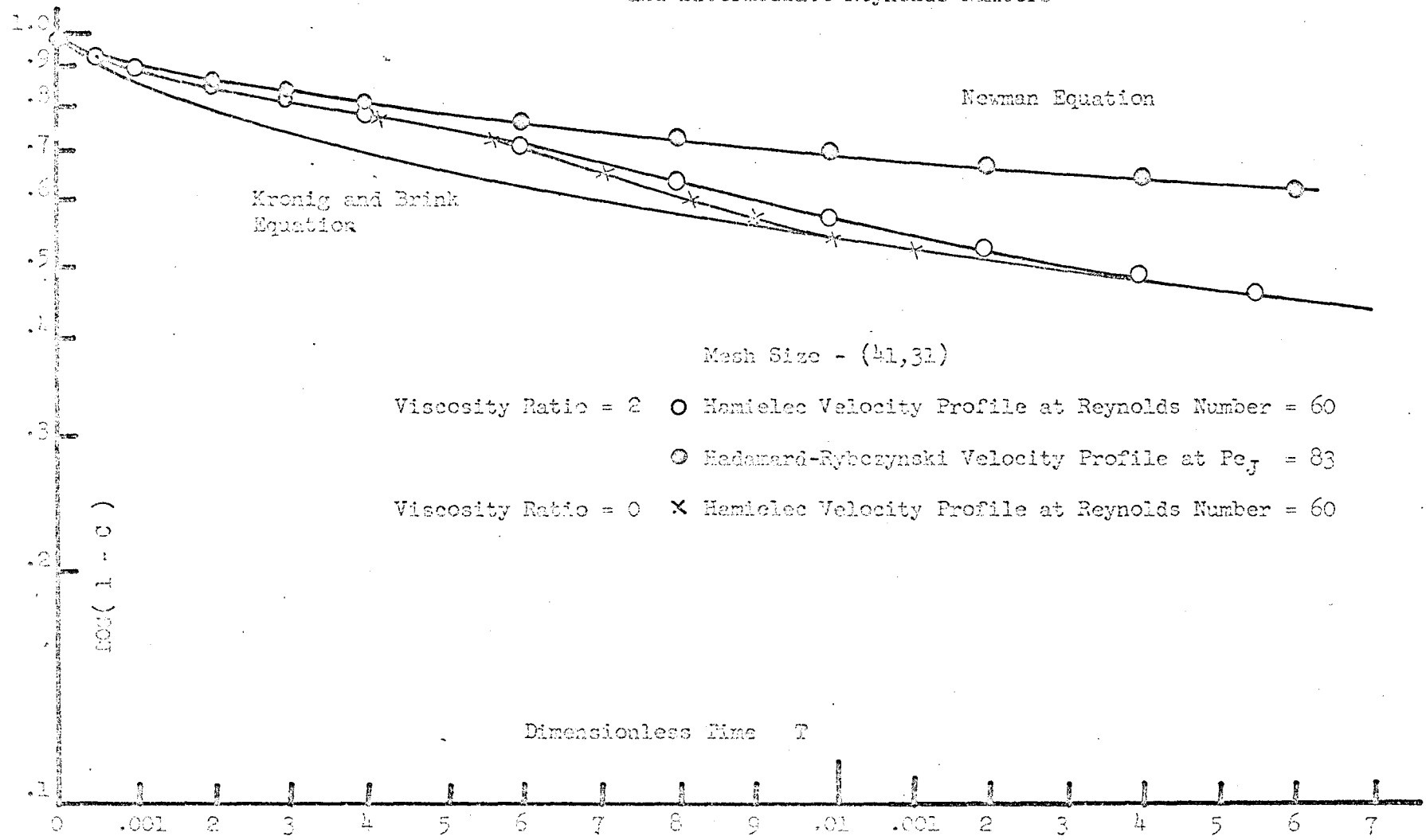

III-J-4 Comparison with Johns and Beckmann Results for Physical Mass Transfer into Viscous Drops

In Figure III-11, the variations of concentrations with time for different modified Peclet Numbers are shown, along with predictions by Kronig and Brink and the Newman equations. The results of Johns and Beckmann do not agree very well with the Newman model. At modified Peclet Number=80, the concentration results do not agree with those predicted by this study at short times. However, this may have been due to differences in the mesh sizes used in the two methods of calculation.

In Figure III-12, the variations of the modified Sherwood Numbers with time are shown graphically for modified Peclet Numbers = 0 and 80. Superimposed points from this study agree very closely with those by Johns. As shown previously, the same oscillation of the Sherwood Number with time is observed in this work also.

III-J-5 Mass Transfer at Intermediate Reynolds Number Flow Regime

Mass transfer results into a drop with a Reynolds Number of 60 are shown in Figure III-13 and are tabulated in Appendix VIII-6. Hamielec's velocity profiles given in Equations III-27 and III-28 were used at viscosity ratios of 0 and 2. Due to the way the velocity components were found, modified Peclet Numbers could not be used as a variable. Hence the Reynolds Number and the viscosity ratios for the drop with Peclet Number of 1000 are given. Mass transfer results were compared with those predicted by the Newman equation, the Kronig and

Brink equation and by the model with a Hadamard Rybczynski velocity profile and a viscosity ratio of 2.

The solution for the Hadamard-Rybczynski model agreed with the Newman equation. At this low drop velocity, drops with a viscosity ratio of 2 behaved essentially as a stagnant drop. However at Reynolds Number of 60, the transfer rate was increased markedly by the circulation rate. In fact, referring to Figure III-8, the concentration results for viscosity ratio of 2, agreed very closely with those predicted for modified Peclet Number of 375 and a Hadamard Rybczynski velocity profile. At Reynolds Number of 60 the inviscid solution was close to that for modified Peclet Number of 1000.

However even at intermediate Reynolds Numbers, the Kronig and Brink equation defined the upper limit to the rate of mass transfer into circulating drops for physical mass transfer into drops.

Figure III-14 : Variations of Modified Sherwood Number with Time for Mass Transfer with Reaction Rate Constant = 10

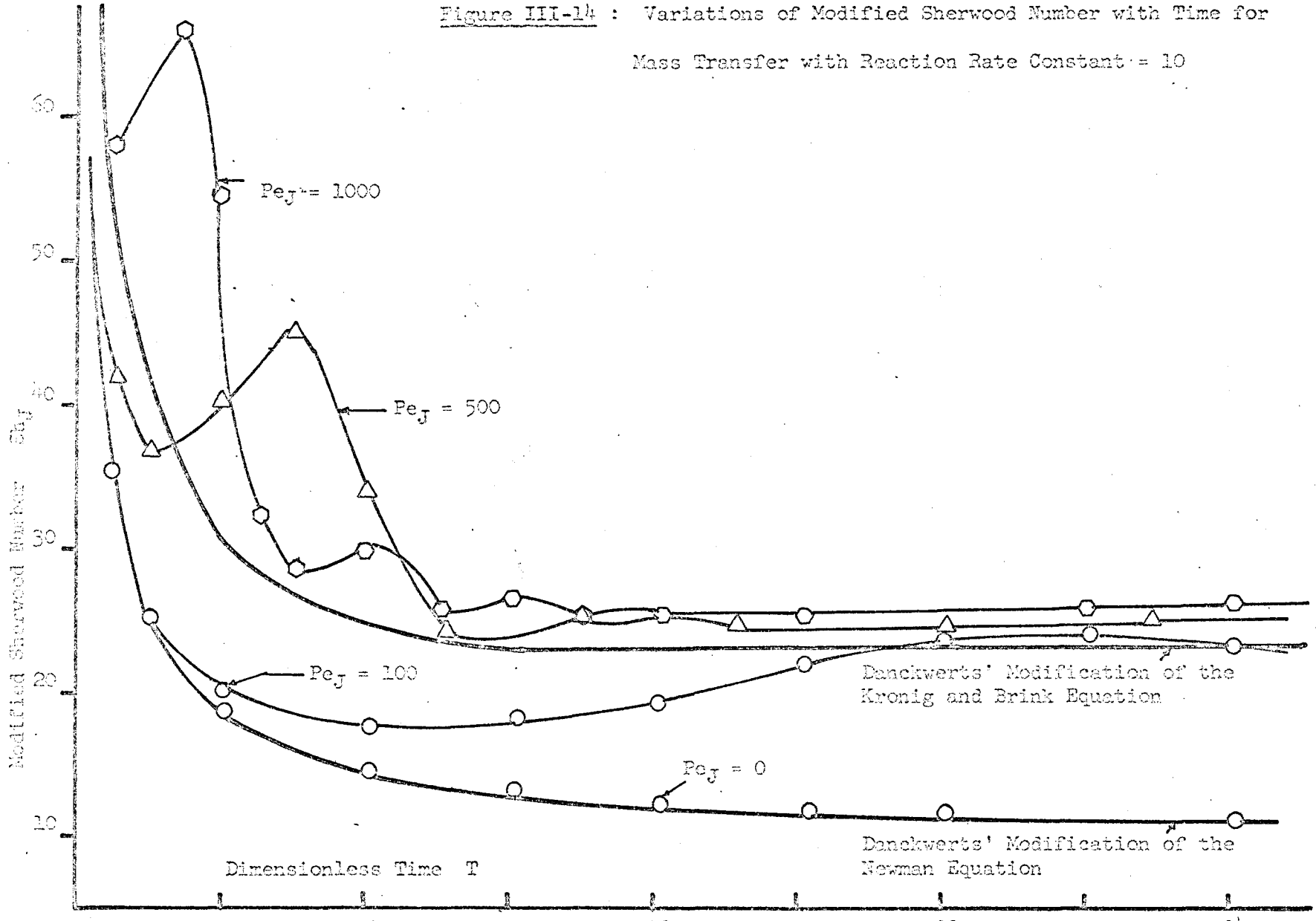

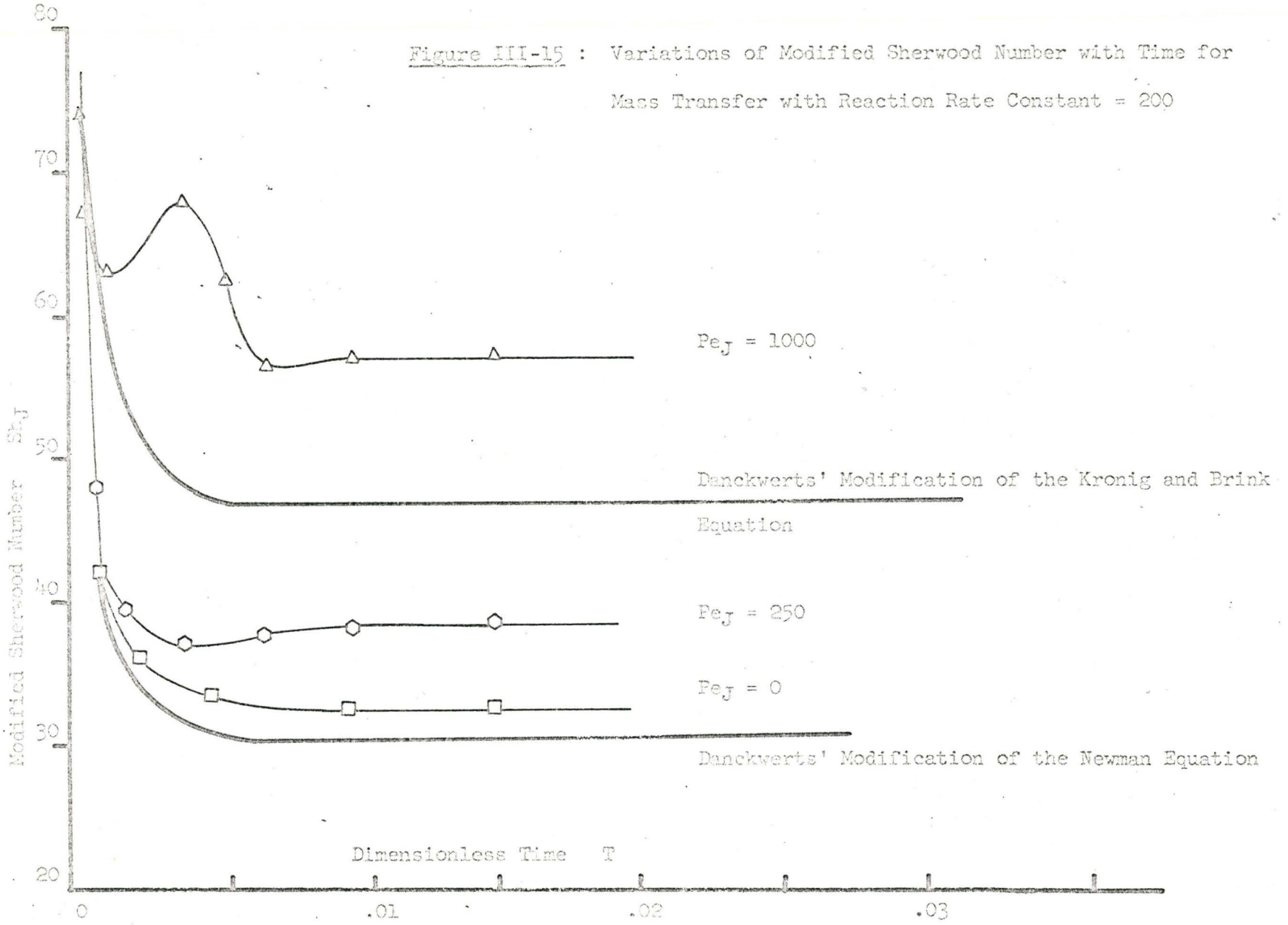

Figure III-15 : Variations of Modified Sherwood Number with Time for Mass Transfer with Reaction Rate Constant = 200

III-K Mass Transfer into Drops with Simultaneous Chemical Reaction

When mass is transferred with chemical reaction, a steady state concentration is soon reached. Thus it is more meaningful to study the variations of Sherwood Numbers with time at various Peclet Numbers.

Cases were run with a dimensionless reaction constant of 10, at modified Peclet Numbers of 0, 100, 500 and 1000. The results are tabulated in Appendix VIII-9 and plotted in Figure III-14. These results are compared with those predicted by Danckwerts' modifications of the Kronig and Brink and the Newman equation.

At low Peclet Numbers, the results tended towards the results predicted by Newman. At higher Peclet Numbers, the results tended to merge around those predicted by the Kronig and Brink model.

The differences with the predictions by the Kronig and Brink model at high Peclet Numbers are very noticeable in Figure III-15 for variations of Sherwood Numbers with time for reaction constant of 200. These variations are also tabulated in Appendix VIII-10.

As shown in Figure III-15, even the predictions by the Newman equation did not agree with those by the numerical solution. However, this is due to errors in the Newman equation which is solved by a series solution. The variations of the modified Sherwood Number with the number of terms in the series is shown below:-

Table III-4

Variations of Modified Sherwood Numbers with Number of Terms in Series Solution for Danckwerts' Modifications of the Newman Equation

Number of terms	10	30	43
Modified Sherwood Number	23.75	29.46	30.43

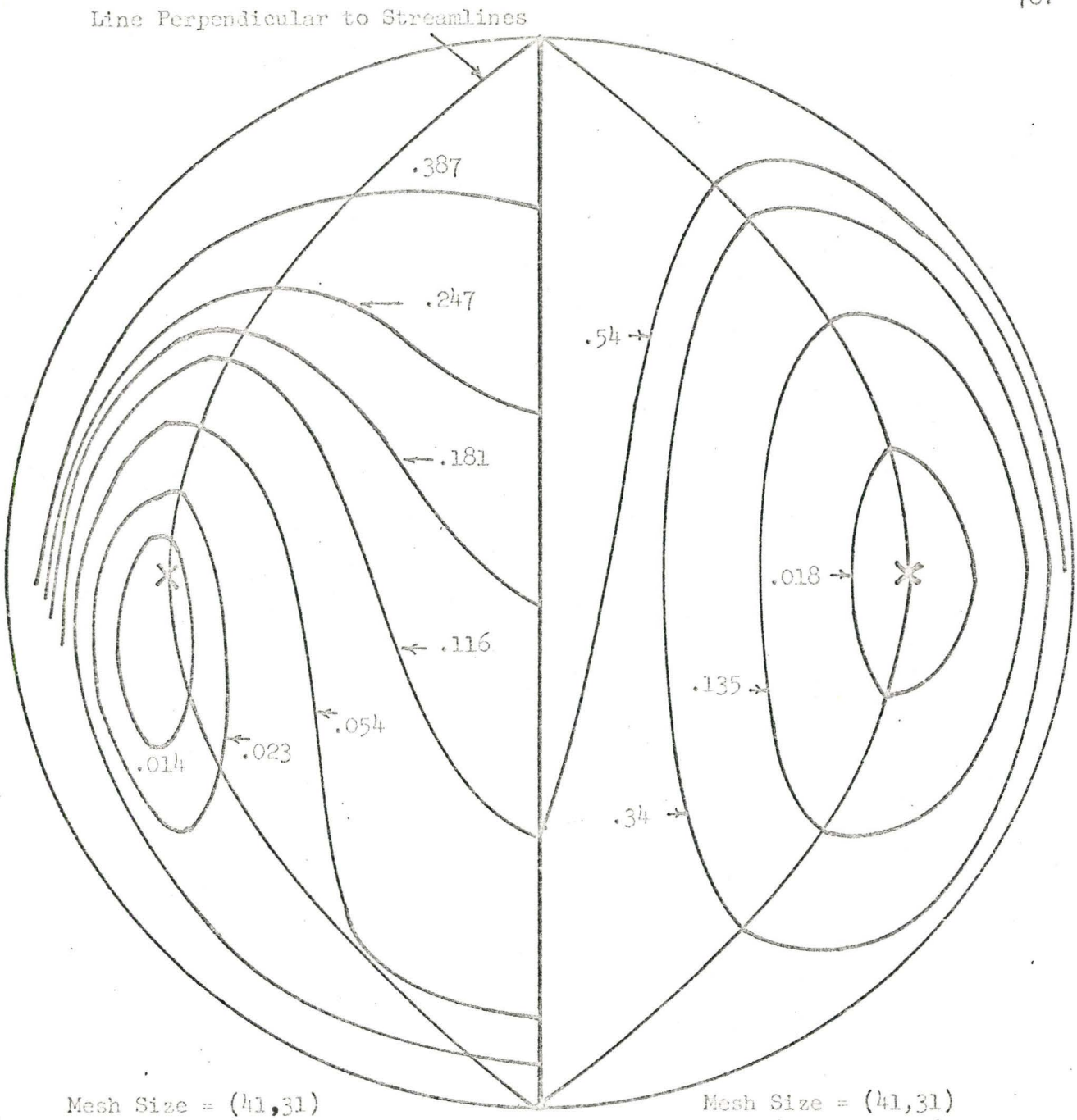

Mesh Size = (41,31)

Hadamard-Rybczynski Velocity

RK = 200 Pej = 250

T = .0148 Viscosity Ratio = 0

Average Concentration = .21

Mesh Size = (41,31)

4 x Hadamard-Rybczynski Velocity

RK = 200 Pej = 1000

T = .0148 Viscosity Ratio = 0

Average Concentration = .26

Figure III-16 : Effects of Circulation Rates on Lines of Constant Concentrations for Mass Transfer with Simultaneous Chemical Reactions into Drops

This was correlated by the following equation for the modified Sherwood Number Sh_J, where n = number of terms in the series solution,

$$Sh_J = 32.31 - 85.6\left(\frac{1}{n}\right) \qquad \text{(III-41)}$$

at time = .04. The intercept value of 32.31 corresponds to the Sherwood Number predicted by the model in this study.

The Kronig and Brink model is also solved by a series solution. However, since only seven eigenvalues were available for the model, only seven terms were used in the solution. Thus, the errors in the Kronig and Brink solution of mass transfer with reaction were probably caused by the small number of terms in the series solution.

However, as the modified Peclet Numbers increased, the lines of constant concentrations became coincident with the streamlines, as predicted by the Kronig and Brink model. This is shown in Figure III-16. Lines of constant concentrations are shown for mass transfer with reaction, at reaction constant = 200 for drops with modified Peclet Numbers of 250 and 1000. At Peclet Number of 1000, lines of constant concentrations formed inside the drop, which approached the velocity profiles. Thus, as in the case for physical mass transfer, the Newman and Kronig and Brink equations modified by Danckwerts for chemical reaction, again defined the lower and upper limits for the predictions by the model developed in this study, for mass transfer with reaction into drops.

III-L Conclusions and Contributions

A finite difference method has been developed to predict mass transfer with simultaneous chemical reaction into circulating drops in the Stokes flow and the intermediate Reynolds Number flow regimes.

Accuracy of the model was shown by the close agreements with mass transfer and Sherwood Numbers predicted by Johns and Beckmann for physical mass transfer.

The Kronig and Brink equation and the Newman equation defined the upper and lower limits of the mass transfer and Sherwood Numbers predicted by the model. As the circulation rate increased, due to increasing proximity of a concentric spherical wall surrounding the drop, or to increasing values of the modified Peclet Number, the results tended to approach the predictions by the Kronig and Brink equation.

For mass transfer into drops with simultaneous chemical reaction, similar agreements with Danckwerts' modifications of the Newman and the Kronig and Brink model for reaction transfer were found at low and high values of the modified Peclet Numbers.

It has also been shown, that as the reaction rates increased, accuracy of the Danckwerts' modifications of the Newman and the Kronig and Brink solutions suffered, unless an increasing number of terms in their series solutions were used.

III-M Recommendations

Further work at different velocity profiles are required. This can be easily done by simply changing the velocity profiles used in the program.

More work at higher chemical reaction rates are required. At these high reaction rates, Danckwerts' modifications of the Newman and the Kronig and Brink equations may no longer be accurate enough and numerical methods may be required to solve them.

At high Peclet Numbers and reaction rates the explicit forward difference method of solution of the mass transfer equation became impractical for use. Such small ΔT time steps were required that too much computer time was required to solve the model. Hence another method of solution is desirable for use in these studies.

III-N Nomenclature

a = drop radius, cm

A = surface area of drop, cm^2

A_n, λ_n = coefficients for Kronig and Brink Equation by Heertjes et al (18)

C^1 = drop concentration, gm/cc

$\overline{C}^1$ = average concentration, gm/cc

$C = \dfrac{C^1}{C_\phi}$

= dimensionless concentration

C_ϕ = equilibrium concentration in the dispersed phase, gm/cc

C_1 = initial concentration in the dispersed phase, gm/cc

$C_D = \dfrac{8\,(\rho_i - \rho_o)\,g\,a}{3\,\rho_o\,V_D^2}$

= drag coefficient

D_L = molecular diffusion coefficient, cm^2/sec

E_1,F_1 = coefficients for Hamielec (82) velocity profiles

H = wall proximity factors by Satapathy and Smith (81)

K_L = mass transfer coefficient, cm/sec

M^1 = mass transferred/unit volume, gm/cc

$M = \dfrac{M^1}{C_\phi\,a^3}$

= dimensionless mass transferred/unit volume

N_A = rate of transfer, gm/sec

N = dimensionless rate of transfer, mass/unit time

$Pe = \dfrac{2aV_D}{D_L}$

= Peclet Number

Pe_J = $\frac{Pe}{4(1+X)}$

= modified Peclet Number

Re_i = $\frac{dV_D \rho_i}{\mu_i}$

= internal Reynolds Number

Re = $\frac{dV_D \rho_o}{\mu_o}$

= drop Reynolds Number

r = radial distance, cm

R = $\frac{r}{a}$

= dimensionless radial distance, cm

RK^1 = first-order reaction constants, sec^{-1}

RK = $\frac{RK^1 a^2}{D_L}$

= dimensionless reaction constant

Sh = $\frac{2aK_L}{D_L}$

= Sherwood Number

Sh_J = $\frac{Sh}{1-\bar{C}}$

= modified Sherwood Number

t = time, sec

T = $\frac{D_L t}{a^2}$

= dimensionless time

V = volume, cc

V_D = drop velocity, cm/sec

V_R = dimensionless radial velocity component

V_Θ = dimensionless angular velocity component

V_ϕ = dimensionless axial velocity component

x^1 = distance, cm

$X = \frac{\mu_i}{\mu_o}$

= viscosity ratio

Greek Letters

ρ = density, gm/cc

μ = viscosity, centipoise

ψ = dimensionless streamline

Θ = polar angle, spherical co-ordinate

Subscripts

i = dispersed phase

o = continuous phase

IV Experimental Study of Mass Transfer With Simultaneous Chemical Reaction in Drops

IV-A Introduction

Results of the experimental study of mass transfer by forced convection into drops are presented in this section.

The areas of study were as follows:-

1) Physical mass transfer into drops to examine the effect of concentration driving forces on the transfer rates for binary systems.
2) Mass transfer accompanied by simultaneous chemical reaction into drops.
3) Examination of the ability of existing models, including the general model developed in the theoretical section, to predict mass transfer by forced convections into drops with or without simultaneous chemical reaction.

In all cases, the drops were spherical, non-oscillating and falling with Reynolds Numbers in the laminar region. Resistance to mass transfer was confined entirely to the inside of the dispersed phase.

The physical mass transfer studies were carried out with the following systems:-

1) Ethyl acetate transferring into aqueous dispersed solutions.
2) Butyl lactate transferring into aqueous dispersed solutions.
3) Paraldehyde transferring into aqueous dispersed solutions.
4) Cyclohexanol transferring into aqueous dispersed solutions.

Mass transfer studies accompanied by simultaneous chemical reactions were carried out with the following systems:-

1) Butyl lactate transferring into aqueous NaOH dispersed solutions.
2) Ethyl acetate transferring into aqueous NaOH dispersed solutions.

IV-B Discussion of Theory

The many theoretical models which have been developed to describe the transient mass transfer inside the drop, during the steady fall or rise period, have already been reviewed in the literature survey. They are tabulated in Tables IV-1 and IV-2 for reference. The model which was used depended upon whether the drop was moving as a stagnant, fully circulating or turbulent or oscillating drop. Calculation of the drag coefficient of the moving drop indicated whether it was stagnant or circulating.

Knowing the terminal velocity and hence the Reynolds Number, the drag coefficients for a solid sphere moving relative to a fluid could be found in several references (11,80).

The actual drag coefficient was calculated from (11),

$$C_D = \frac{4}{3} \frac{g\, d}{V_D^2} \left\{ \frac{\rho_i - \rho_o}{\rho_o} \right\} \qquad \text{(IV-1)}$$

where d = drop diameter, cm

V_D = drop velocity, cm/sec

g = acceleration due to gravity, cm/sec^2

ρ_i, ρ_o = density of drop and continuous phase respectively

If the drag coefficient was less than for a solid sphere, the drop was circulating. The drag coefficient - Reynolds Number curve (11) does not show a well-defined laminar-turbulent transition for solid spheres. But, since fluid drops falling in the turbulent region tend to oscillate, this can be confirmed by observation.

Table IV-1

Expressions for Mass Transfer Efficiencies E_M, E_T into Drops

Eqn	Source	Correlation	Condition
IV-2	Newman (54)	$E_M = 1 - \frac{6}{\pi^2} \sum_{n=1}^{\infty} \frac{1}{n^2} \exp\left\{ - \frac{D_L n^2 \pi^2 t}{a^2} \right\}$	stagnant drop
IV-3	Kronig and Brink (58)	$E_M = 1 - \frac{3}{8} \sum_{n=1}^{\infty} A_n^2 \exp\left\{ - \frac{\lambda_n 16 D_L t}{a^2} \right\}$	fully circulating drop for $0 \leq Re \leq 10$
IV-4	Korchinski's approx of Eqn IV-3 (46)	$E_M = \sqrt{\frac{\dot{R} \pi^2 D_L t}{a^2}}$	for $E_M < 0.5$
IV-5	Hamielec (8)	$E_T = (1 - E_F)\sqrt{\frac{\dot{R} \pi^2 D_L t}{a^2}} + E_F$	for $E_M < 0.5$
IV-6	Handlos and Baron (60)	$E_M = 1 - 2 \sum_{k=1}^{\infty} B_n^2 \exp\left\{ - \frac{\gamma_n t V_D'}{256a} \right\}$	for turbulent drop
IV-7	Well-mixed Drop	$\ln (1-E_T) = - \frac{3 K_L t}{a}$	

IV-B-1 Models for Mass Transfer into Drops

Expressions for E_M, the fractional approach to equilibrium inside drops during their steady rise or fall periods are listed in Table IV-1. These models predicted the physical mass transferred into drops under the conditions indicated.

The constants A_n and λ_n in the Kronig and Brink Equation IV-3 are tabulated in Table II-1 in the literature survey section.

Equation IV-5 was defined by Hamielec (8) by combining Equation IV-4 and the definition for E_M,

$$E_M = \frac{E_T - E_F}{1 - E_F} \qquad \text{(IV-8)}$$

in order to find E_F from the intercept of the plot of E_T versus $t^{\frac{1}{2}}$, where t = drop time in seconds.

The constants B_n and γ_n in the Handlos and Baron Equation IV-5 are tabulated in Table II-2 in the literature survey section.

For well-mixed drops, the mass transfer rate is due solely to the concentration driving forces, i.e., the difference between the solute concentration outside and inside the drop. Thus Equation IV-7 was derived from the following relation for mass transfer rate $V \frac{dC_A'}{dt}$ as a function of concentration driving force $(C\phi - C_1)$

$$V \frac{dC_A'}{dt} = - A_D K_L (C\phi - C_1) \qquad \text{(IV-9)}$$

where $C\phi$ = equilibrium concentration, gm/cc

C_1 = initial concentration, gm/cc

K_L = mass transfer coefficient, cm/sec

V = drop volume, cc

A_D = surface area of drop, cm^2

with boundary conditions

$$C_i = 0 \qquad 0 \leqslant r < a \qquad t = o \qquad \text{(IV-10)}$$

$$C = C_\phi \qquad r = a \qquad t = t \qquad \text{(IV-11)}$$

IV-B-2 Reaction Mass Transfer into Drops

Equations for physical mass transfer into drops were modified by Danckwerts (59), to account for the effect of simultaneous first-order chemical reaction on the transfer rate.

These equations are tabulated in Table IV-2.

The general analytical model describing mass transfer with simultaneous reaction into circulating drops was shown in the previous section of the thesis. In dimensionless form, it was:-

$$\frac{\partial C_A}{\partial T} = \left\{ \frac{\partial^2 C_A}{\partial R^2} + \frac{2}{R} \frac{\partial C_A}{\partial R} + \frac{\cot \theta}{R^2} \frac{\partial C_A}{\partial \theta} + \frac{1}{R^2} \frac{\partial^2 C_A}{\partial \theta^2} - RK\, C_A \right\} - \frac{Pe}{2} \left\{ \frac{V_\theta}{R} \frac{\partial C_A}{\partial \theta} + V_R \frac{\partial C_A}{\partial R} \right\} \qquad \text{(IV-15)}$$

Table IV-2

Danckwerts' Generalized Models for Mass Transferred into Drops with Simultaneous First-order Chemical Reaction, at Time t.

Eqn	Model	
IV-12	Newman	Mass transfer into stagnant drops

$$M' = 8a\pi C_\phi D_L \sum_{n=1}^{\infty} \frac{RK'\left(RK' + \frac{D_L n^2 \pi^2}{a^2}\right) t - \frac{D_L n^2 \pi^2}{a^2}\left(\exp\left\{-t\left(RK' + \frac{D_L n^2 \pi^2}{a^2}\right)\right\} - 1\right)}{\left(RK' + \frac{D_L n^2 \pi^2}{a^2}\right)^2}$$

IV-13	Kronig and Brink	Mass transfer into fully circulating drops

$$M' = 8a\pi C_\phi D_L \sum_{n=1}^{\infty} A_n^2 \lambda_n \left\{ \frac{RK'\left(RK' + \frac{16 D_L \lambda_n}{a^2}\right) t - \frac{16 D_L \lambda_n}{a^2}\left(\exp\left\{-t\left(RK' + 16 D_L \lambda_n\right)\right\} - 1\right)}{\left(RK' + \frac{16 D_L \lambda_n}{a^2}\right)^2} \right\}$$

IV-14	Handlos and Baron	Mass transfer into turbulent drops

$$M' = \frac{a^2 C_\phi V_D'}{96} \sum_{n=1}^{\infty} B_n^2 \gamma_n \left\{ \frac{RK'\left(RK' + \frac{\gamma_n V_D'}{256a}\right) t - \frac{\gamma_n V_D'}{256a}\left(\exp\left\{-t\left(RK' + \frac{\gamma_n V_D'}{256a}\right)\right\} - 1\right)}{\left(RK' + \frac{\gamma_n V_D'}{256a}\right)^2} \right\}$$

Figure IV-1 : Apparatus

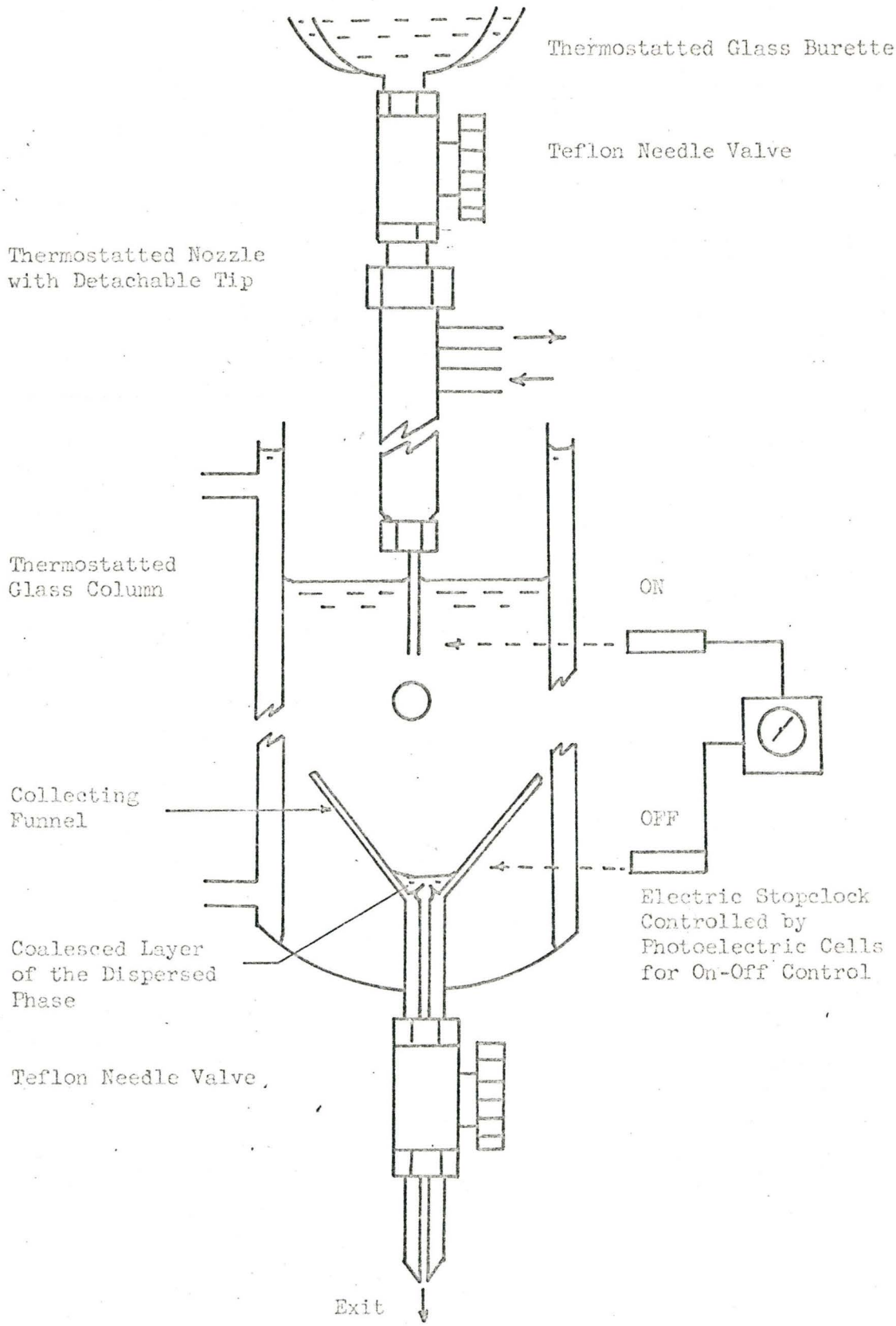

Figure IV-2 : Thermostatted Burette

Material : Glass

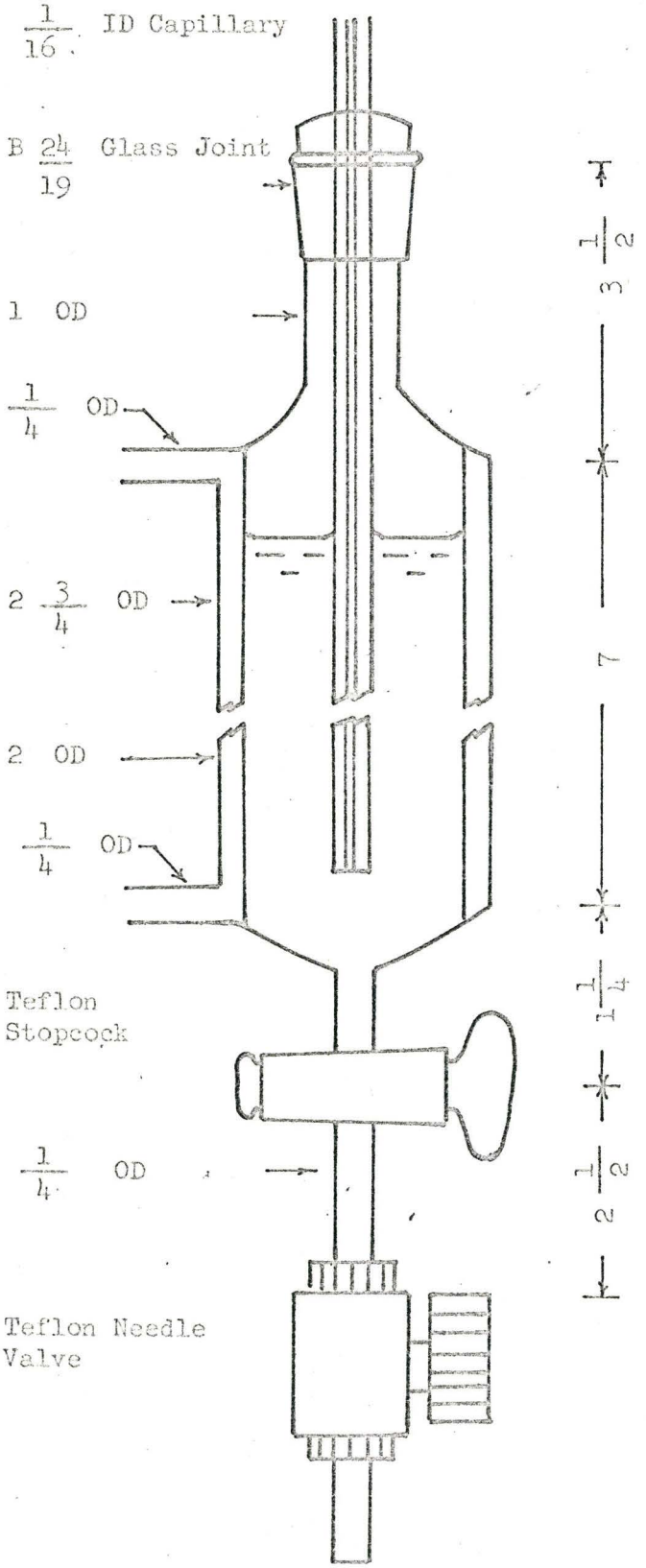

Figure IV-3 : Thermostatted Nozzle

Material : 316 Stainless Steel

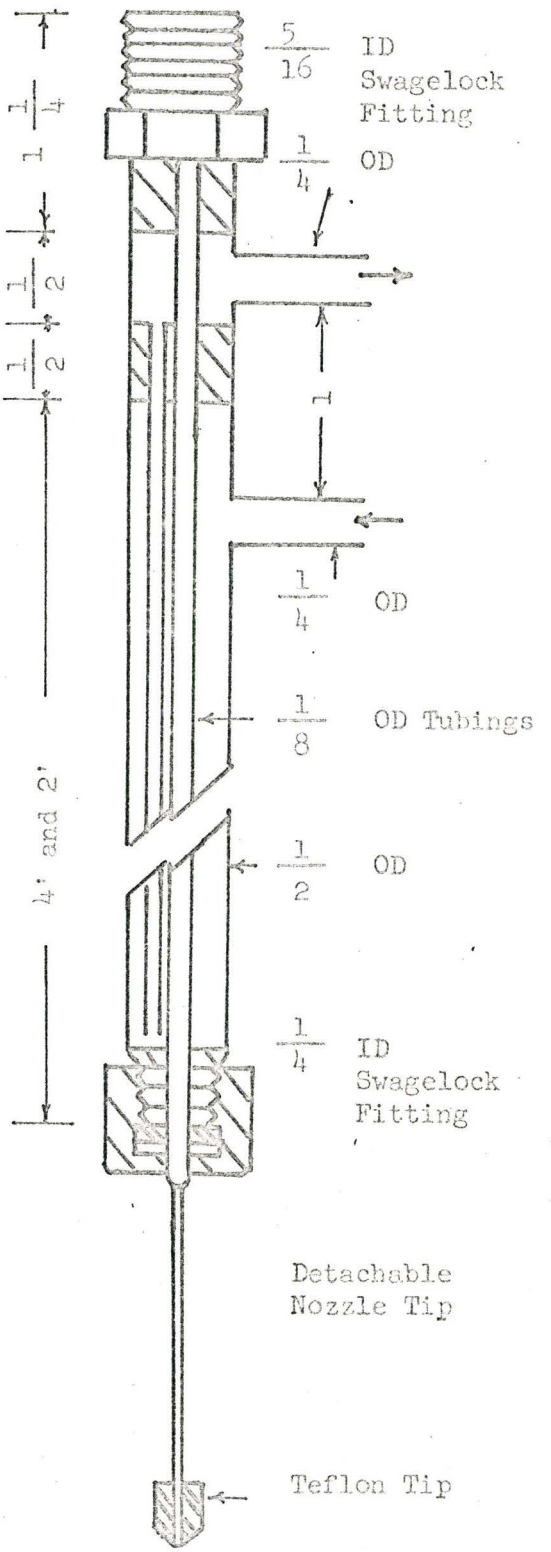

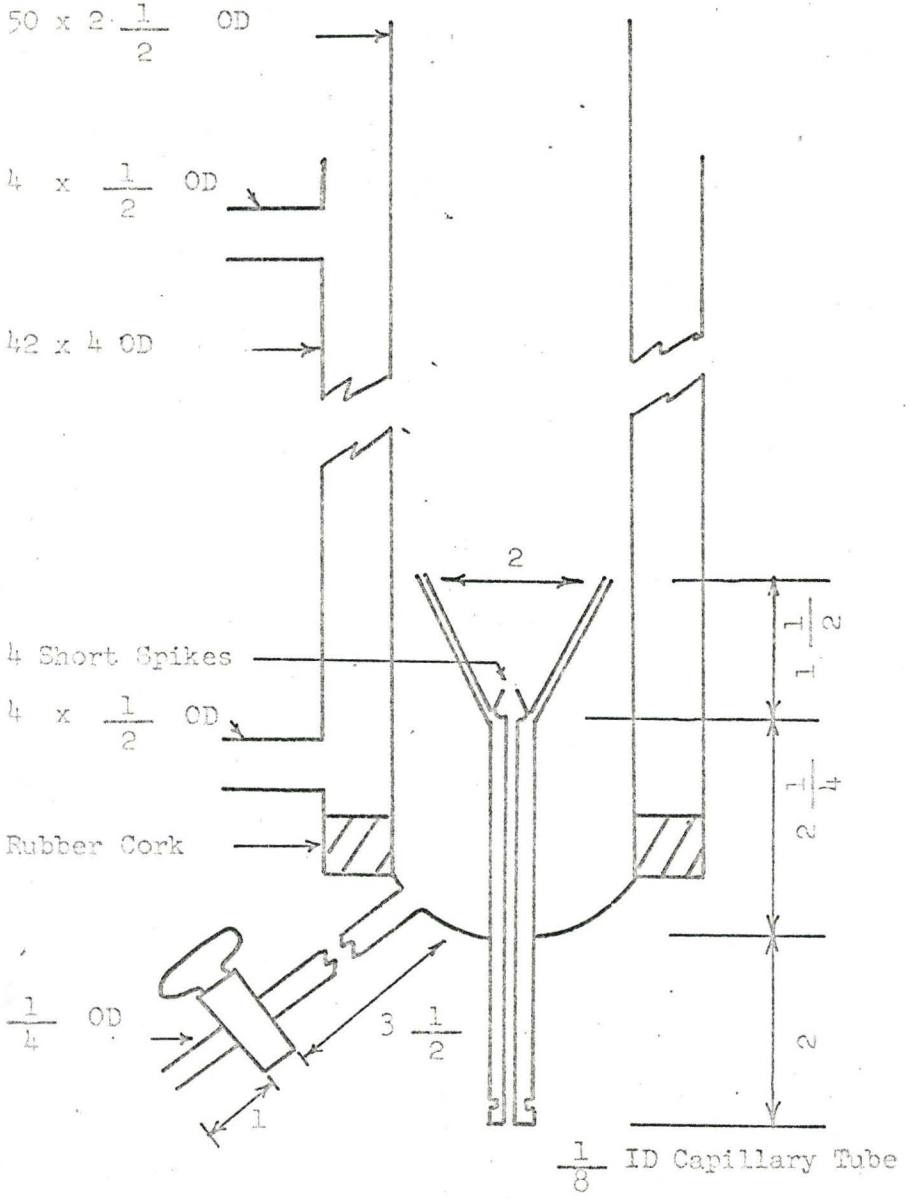

Figure IV-4 : Main Glass Column

Nozzle A : 316 Stainless Steel

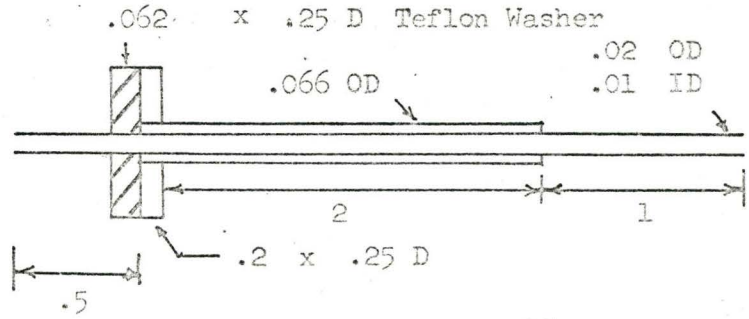

Teflon Tip

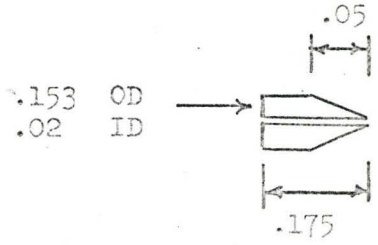

Nozzle B : 316 Stainless Steel

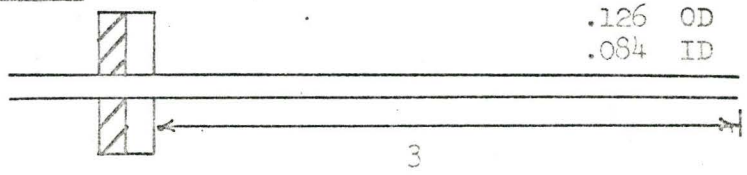

Teflon Tip

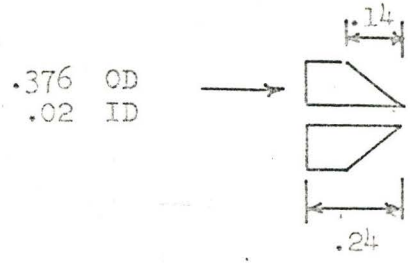

Figure IV-5 : Detachable Nozzle

IV-C Experimental Apparatus

The experimental apparatus is shown in Figure IV-1. Details of each section are shown in subsequent Figures IV-2 to IV-5. The apparatus is similar to those used by other workers in the field, such as Hamielec (82). Only glass, Teflon or stainless steel 316, were used in the apparatus to prevent contamination of the solutions used.

The column, main nozzle and the solution burette were all thermostatted to maintain a constant temperature ($\pm$ 0.5 C).

The flow of dispersed phase from the glass burette through the nozzle was controlled by a Teflon needle valve. Constant flow rate was maintained by a constant head device in the burette. This is a glass tube pierced through an air-tight plug and immersed in the liquid held in storage. A constant head was maintained throughout this depth of immersion since the solution pressure at the bottom of the tube was exactly balanced by the atmospheric pressure.

In order to produce spherical drops which fell with no oscillations, drop sizes were kept as small as practical. This limit was dictated by the fact that end effects and sampling times increased as the drop sizes decreased. Interchangeable tips were used on the thermostatted nozzle to control the drop sizes for each system studied. However, due to the small size of the nozzle required for some systems, the dispersed phase, tended to wet and cling to the tips, causing large fluctuations in the drop formation rate. This was stopped by attaching a piece of Teflon to the end of the nozzles. The dimension of these nozzles labelled A and B, and their Teflon tips are shown in Figure IV-5.

The continuous phase was kept in the main glass column. Constant holdup of the coalesced dispersed phase in the collecting funnel was maintained by another Teflon needle valve at the bottom of the column. Glass needles were required in the bottom of the collecting funnel to aid in the coalescence of the dispersed phase. Otherwise, coalescence was very difficult.

The time required for the drops to fall from the nozzle to the collecting funnel was measured by the use of photoelectric cells connected to an electric stop clock, calibrated to $\pm$ 0.01 sec. The drop height was measured by a cathetometer to the nearest .001 cm.

Terminal velocity of the dispersed phase was measured photographically with a Strobotac, as described in Appendix IX-1. Terminal velocity cannot be measured accurately from the total drop times, since the drops do not fall in a straight line. This was caused by many factors. A major cause was the disruption of the streamlines around the falling drop, caused by mass transfer effects such as interfacial turbulence. The slight departure from sphericity of the falling drops also contributed to this departure from a straight line. However, once terminal velocity was reached, measurements showed that this velocity was constant until the drop coalesced at the bottom of the column. Thus drop time and drop velocity must be measured separately.

IV-D Purifications of Systems Used

The following systems were used in the experimental study. To insure consistant results, all systems were first purified by re-distillation.

Table IV-3 Materials Used in Experimental Studies

Material	Purity	Press mm Hg	Boiling Point Range of Cuts Taken-deg. C.
Ethyl Acetate	Certified Grade	Atmos. Press.	76-78
Butyl Lactate	Practical Grade (97%+)	15 mm Hg	64-66
Paraldehyde	Certified Grade	10 mm Hg	25-26.5
Cyclohexanol	Certified Grade	5 mm Hg	58-60

Distillates for all systems except Paraldehyde were analyzed by gas chromatograph for impurity. Paraldehyde was analyzed for acetaldehyde by a titration method given in Appendix IX-2. No impurities were detected in ethyl acetate and cyclohexanol distillates. Butyl lactate contained 1.2% by weight butanol in the distillate. Paraldehyde contained .03% by weight acetaldehyde in the distillate.

IV-E Preparation of the Continuous Phase and the Apparatus

Great care was taken to prevent introduction of surface-active impurities which may affect the results. All glass and Teflon parts were cleaned with chromic acid before each new series of experiments. The stainless steel nozzles were cleaned with chromic acid and acetone. Fresh continuous phase was used for each new dispersed phase system, to reduce any possible build-up of contaminants.

In all cases, the continuous phase was saturated with water, to insure that resistance to mass transfer rested solely in the dispersed phase. The continuous phase was saturated with water by first mixing it

with as much water as possible at 5°C above the experimental temperature for 24 hours. Then the solution was poured into the main column and cooled to the required temperature. As more water was sprayed in, the supersaturated system broke down and the column became filled with tiny water drops. This generally took about 12 to 24 hours to settle out. The clear solution was now saturated at the required experimental temperature.

IV-F Experimental Procedures for Studying Physical Mass Transfer into Drops

Physical mass transfer was studied with the systems tabulated in Table IV-4. The initial concentrations of the solute in the dispersed phase were varied as shown.

Table IV-4 Experimental Conditions for Physical Mass Transfer Studies

Continuous Phase (sat'd with H_2O)	Nozzle Size	Initial Aqueous Solution Conc. % by Wt	Temp deg.C	Drop Rate Min/Drop
Ethyl Acetate	A	0.0 1.6 3.7 5.4	20	.038 - .045
Butyl Lactate	A	0.0 1.7 4.2	20	.115 - .126
Paraldehyde	A	0.0 2.85 5.75 9.4	20	.24 - .30
Cyclohexanol	B	0.0 0.9 1.78 2.65	30	.076 - .088

The physical properties of the system are tabulated in the Appendix IX-4.

All systems except cyclohexanol were run at 20°C. Due to the high freezing temperature of the latter, experiments were run at 30°C.

Duplicate runs were made on each system. The mass transferred was measured for drop heights of 90,70,50,30 and 7 cm. At each drop height, the height of the continuous phase was kept 2 cm higher, in order to keep a constant resistance to the drop forming at the nozzle.

After the nozzle height and the drop rates were adjusted, the exit flow rate from the column was adjusted to maintain a constant level in the collecting funnel. The drop rate was found by measuring the time required for 10 drops to form, with a stopwatch. The coalesced layer interface was kept to a minimum to reduce the coalescence end effects as discussed by Hamielec (7).

The photoelectric cells connected to a stopclock were adjusted at the nozzle and the collecting funnel, to measure the drop times.

About twenty minutes were allowed for the system to come to a steady state. This time was checked by measurements on occasional samples from the exit flow. Once steady state was reached, two ten minutes samples were taken from the exit flows.

During each run, the drop formation rate was checked every two minutes and kept constant by adjusting the feed rate from the dispersed phase burette. Hence, knowing the sample time and the drop formation rate, the average drop radii were calculated from the sample weight collected.

The extraction samples were analyzed with a Bausch and Lomb Dipping Refractometer which can measure refractive index to 0.74×10^{-5}.

The refractometer was used with Prism A and calibrated with known solutions. The calibration curves are shown in Appendix IX-3.

Finally, the terminal velocity of the drops was measured photographically using the Strobotac.

IV-G Mass Transfer with Simultaneous Chemical Reaction into Drops

The experimental procedure was the same as for physical mass transfer only, except in the analysis of the samples. The systems used and the conditions followed were as shown in Table IV-5.

Table IV-5 Experimental Conditions for Reaction Mass Transfer Studies

Continuous Phase (sat'd with H_2O)	Nozzle size	Normality of Aqueous NaOH Drops	Temp deg.C	Drop Rate Min/Drop
Butyl Lactate	B	0.0 0.506 1.545	20	.09 - .12
Ethyl Acetate	B	0.0 0.506 0.998 1.975	20	.03 - .039

The physical properties of the system are tabulated in Appendix X-1

Two analytical methods were used to measure the amount of esters transferred to the aqueous drops.

IV-G-1 Alkali Method

Five ml of 1N sodium hydroxide solution was added to the extraction samples to insure complete reaction of the esters. The mass transferred was found by back titration with 0.1N sulfuric acid solution.

IV-G-2 Acid Method

The sample was reacted with 5 ml of 1N sulfuric acid solution. The mass transferred was found by back titrating with 0.1 N sodium hydroxide solution.

The two analytical methods were used to obtain two different types of data. The acid method was used to stop the saponification reaction of the esters in the NaOH drops. It was hoped to obtain transient reaction data by back calculating to determine the amount of unreacted ester in the drop at the coalescence layer. The alkali method was used to calculate the total mass of esters transferred into the drops.

Both methods of analysis were used with the butyl lactate-sodium hydroxide-water system.

The alkali method was used for the ethyl acetate-sodium hydroxide-water system with 0.5 N sodium hydroxide. For higher sodium hydroxide concentrations, the acid method was used. The reasons for using these methods are given in the discussion of results.

IV-H Operation of the Equipment

In general, the equipment was simple and easy to operate. The main difficulty lay in maintaining a constant drop rate. Due to the large pressure drop at the nozzle, the drop rate fluctuated badly under atmospheric pressure conditions. This fluctuation was overcome to a certain extent by maintaining a nitrogen pressure in the burette. However, close check on the flow rate was still required during a run.

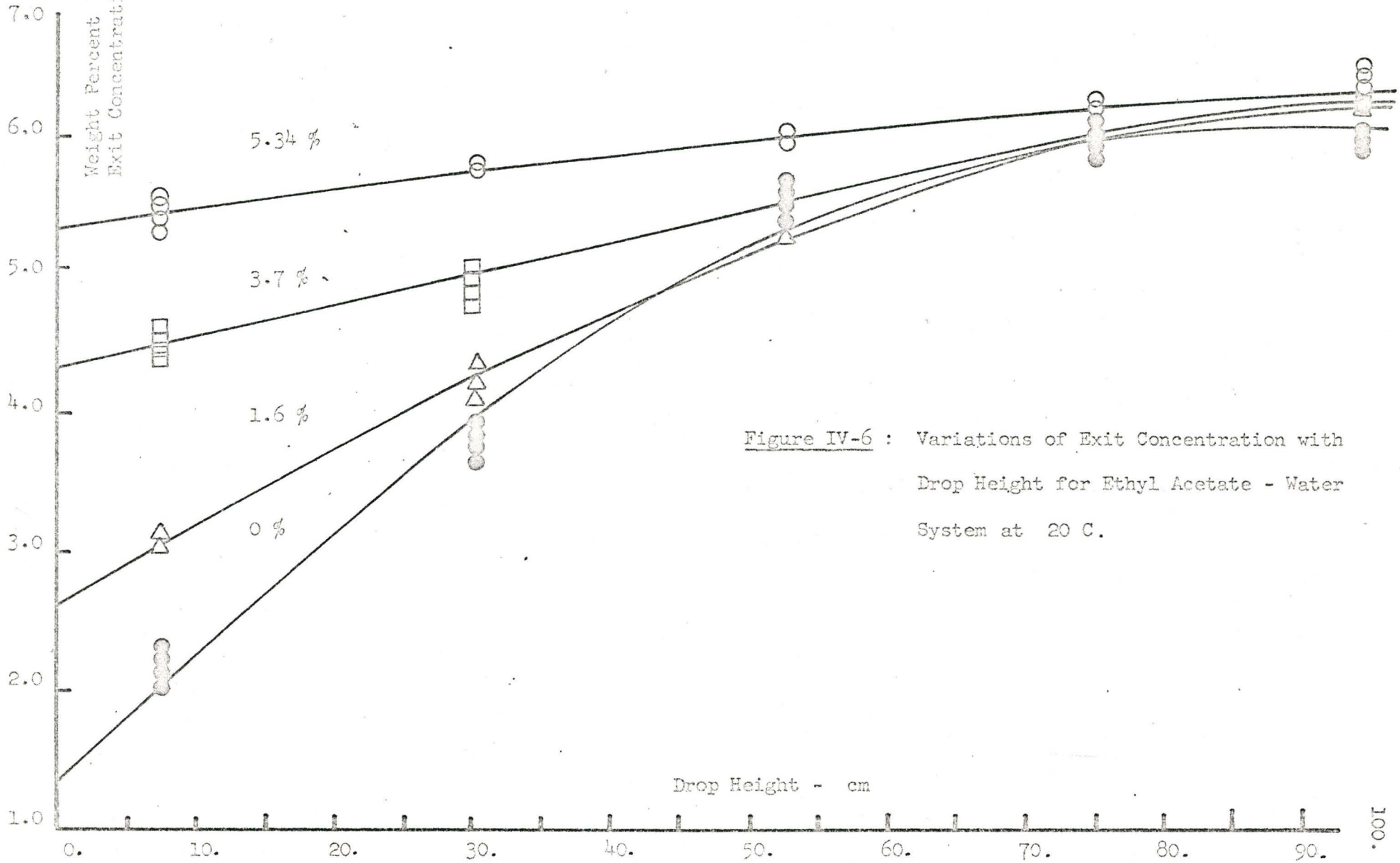

Figure IV-6 : Variations of Exit Concentration with Drop Height for Ethyl Acetate - Water System at 20 C.

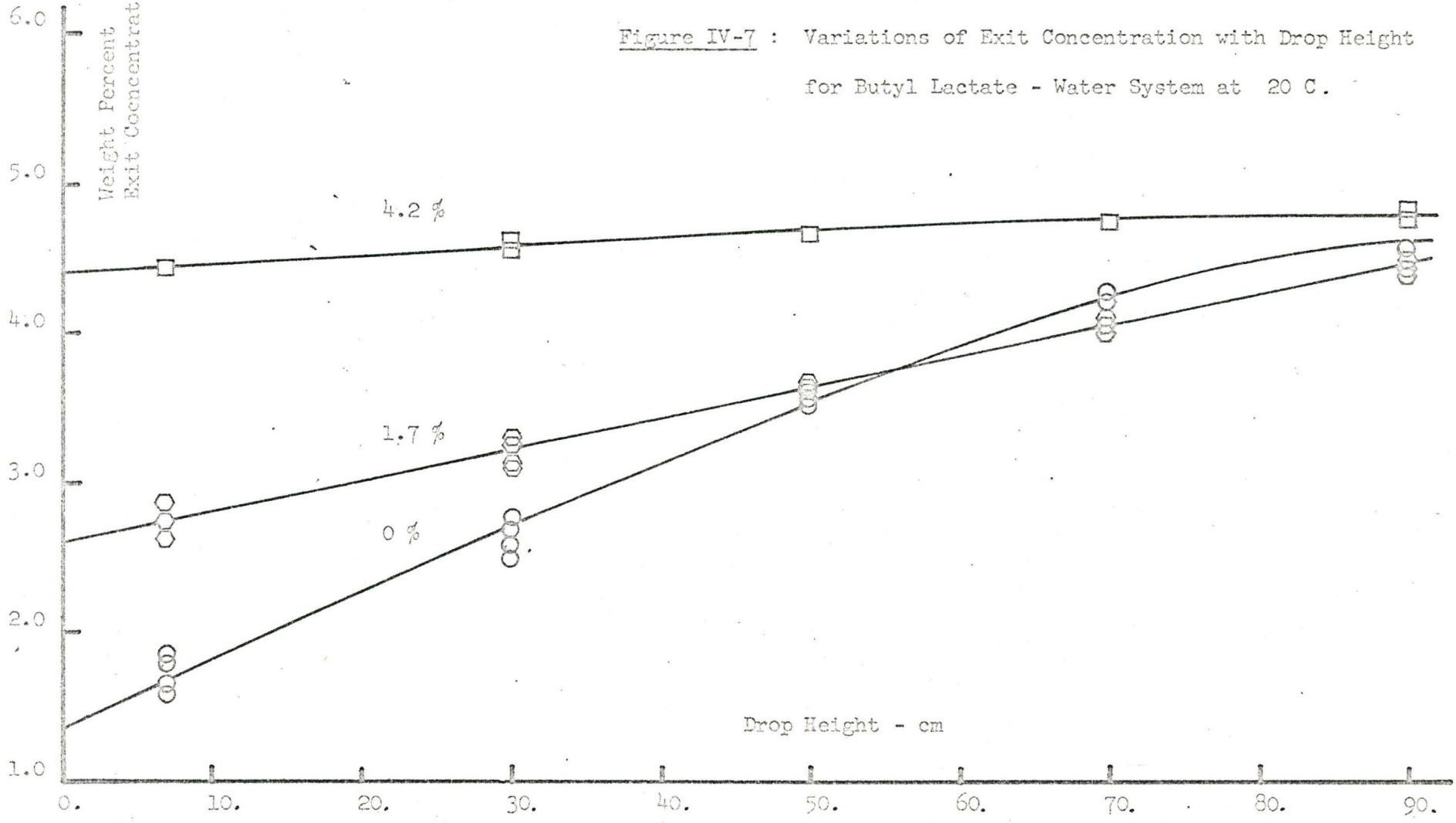

Figure IV-7 : Variations of Exit Concentration with Drop Height for Butyl Lactate - Water System at 20 C.

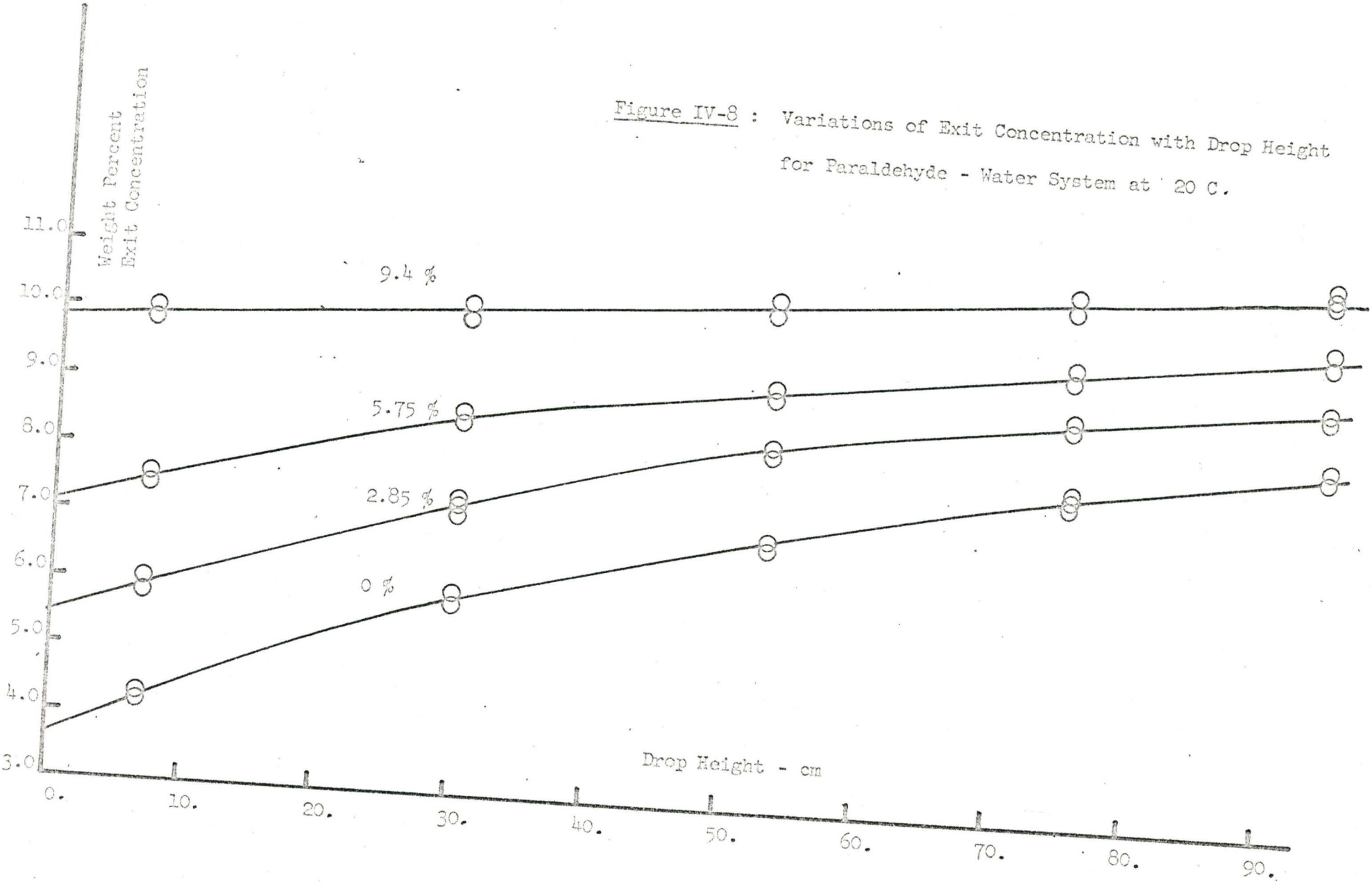

Figure IV-8 : Variations of Exit Concentration with Drop Height for Paraldehyde - Water System at 20 C.

Figure IV-9 : Variations of Exit Concentration with Drop Height for Cyclohexanol - Water System at 30 C.

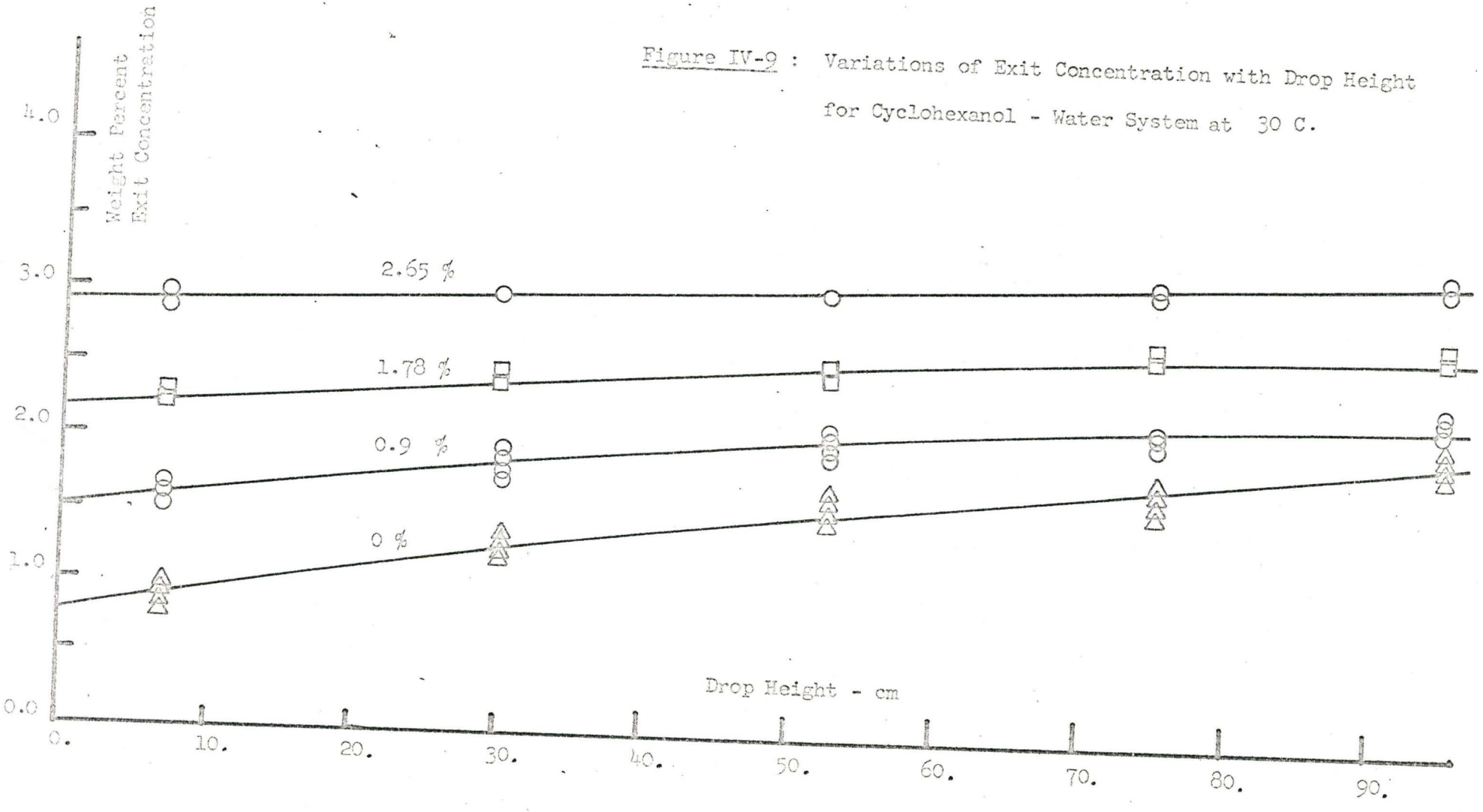

Another difficulty lay in the use of the photoelectric cells to measure drop times. Since the drops did not all fall in a straight line, the photoelectric cell at the top only was triggered by the drop. The bottom cell was triggered manually by using a knife blade to interrupt the light beam to the photoelectric cell. This was still more accurate than using a manual stopwatch, which required human reaction to both activate and stop the watch.

Hence a drop counter would be very useful to give a very accurate count of the total number of drops collected in the extraction sample. A much more sophisticated system of photoelectric cells would also be required to measure the drop time more accurately.

IV-I Presentation of Experimental Data for Physical Mass Transfer Studies

All data were initially correlated by the multiple regression analysis (MLTRG) program, supplied by the McMaster computer department.

IV-I-1 Tabulation of Experimental Data in Appendix IX-5

Physical mass transfer results are tabulated as functions of drop heights. The contributions to the scatter of the data were studied by the analysis of variance. These results are also shown in Figures IV-6 to IV-9.

IV-I-2 t - test

t was defined as the difference between the mean of a sample $\bar{x}$, and μ, the true mean of the population from which the sample was drawn, divided by S $(\bar{x})$, the estimated standard deviation of the mean.

Thus, t was written as:-

$$t = \left| \frac{\bar{x} - \mu}{S(\bar{x})} \right| \qquad \text{(IV-16)}$$

Since the t - function gave the distribution of deviations of $\bar{x}$ from μ in terms of relative frequencies or probabilities, the true mean was expressed from Equation IV-6 as follows:-

$$\mu = \bar{x} \pm t \cdot S(\bar{x}) \qquad \text{(IV-17)}$$

The term $t \cdot S(\bar{x})$ is an estimate of the precision of the measurement of $\bar{x}$; 95% of similar measurements of $\bar{x}$ would fall within the range of $\bar{x} \pm t.S(\bar{x})$ if t was taken at the 0.05 significance level from a standard t table for a given degree of freedom. The degrees of freedom were defined as the number of independent measurements which were available for the calculation. Since the determination of the mean involved fixing the sum of (n) measurements, only (n - 1) of them could be independently varied without changing the sum. Hence, there were (n - 1) degrees of freedom available for estimating the variance or standard deviation.

Here S (x) was designated as the estimate of the population standard deviation from the sample $x_1, x_2, \cdots x_n$. This estimated standard deviation was given as:-

$$S(x) = \sqrt{\frac{\Sigma (x - \bar{x})^2}{n - 1}} \qquad \text{(IV-18)}$$

$S(\bar{x})$ was the estimated standard deviation of the means of samples of size (n), drawn from the population, which were estimated to have a standard deviation of S (x). These two quantities were related by:-

$$S(\bar{x}) = \frac{S(x)}{\sqrt{n}} \qquad \text{(IV-19)}$$

Hence, the confidence limit of duplicate runs were found by these calculations.

Following this procedure, the standard deviations for replication of data were found for each system and drop height and tabulated in Appendix IX-8. The 95% probability range of experimental data for a normal distribution was also calculated. These show that replication of data for physical mass transfer was very good.

IV-I-3 Analysis of Variance

Normally, S (x) the standard deviation, was used to measure the scatter of the data and to set the confidence to a mean or a single determination. However, if the precision and hence the standard deviation of a single measurement was desired from a process in which several factors contributed to the variation of the measurements, the total variance must be first analyzed for its specific components. Then, the desired standard deviation was calculated. The estimated variance, $S^2(x)$ was the square of the standard deviation. The variance was defined as the sum of the squares of the deviations from the mean, divided by (n - 1) degrees of freedom, as shown:-

$$S^2(x) = \frac{\Sigma(x - \bar{x})^2}{n - 1} = \frac{\Sigma x^2 - \bar{x} \Sigma x}{n - 1} \qquad \text{(IV-20)}$$

Thus, the variance and the analysis of variance were very important in the statistical interpretation of data.

. The t test was used to determine if the estimated means for the samples fell within a desired distribution range about the actual population mean. Similarly, the F test provided a method to determine whether the ratio of two variances was larger than might be expected by

chance, if they had been drawn from the same population. F test charts are available at various probability or significance levels for the ratios of the variances.

In the two-factor type of experiment with replicate observations at each condition of the experiment, the comparison of the replicates provided a measure of the error. A sum of squares was calculated for all the replicates by pooling the sum of squares for each set. This sum of squares, plus the sum of squares for the main classifications, subtracted from the total sum of squares gave a remainder called the interaction sum of squares. This remainder represented a measure of the different effect of one factor at different levels of the other.

Calculation methods for analysis of variance can be found in any standard statistics text book (87,88). In the analysis, the interaction mean square was tested against the error mean square by the F test. If it was significant, each combination of the two factors behaved differently. If the interaction mean square was insignificant, the significance of each factor was tested against the error mean square. If either or both were found significant, the means for that factor were examined to determine which one differed significantly, in terms of the error variance, from the others.

In this study, the variables were:-

1) Initial concentration of solute in the dispersed phase.

2) Drop height.

3) Interaction of drop heights and initial concentrations.

Although these facts may have been self-evident, the analysis

Curves for Equation IV-5 : $E_T = (1 - E_F)\sqrt{\frac{\dot{R}\, D_L \pi^2 t}{a^2}} + E_F$

Figure IV-10 : Ethyl Acetate - Water System at 20 C.

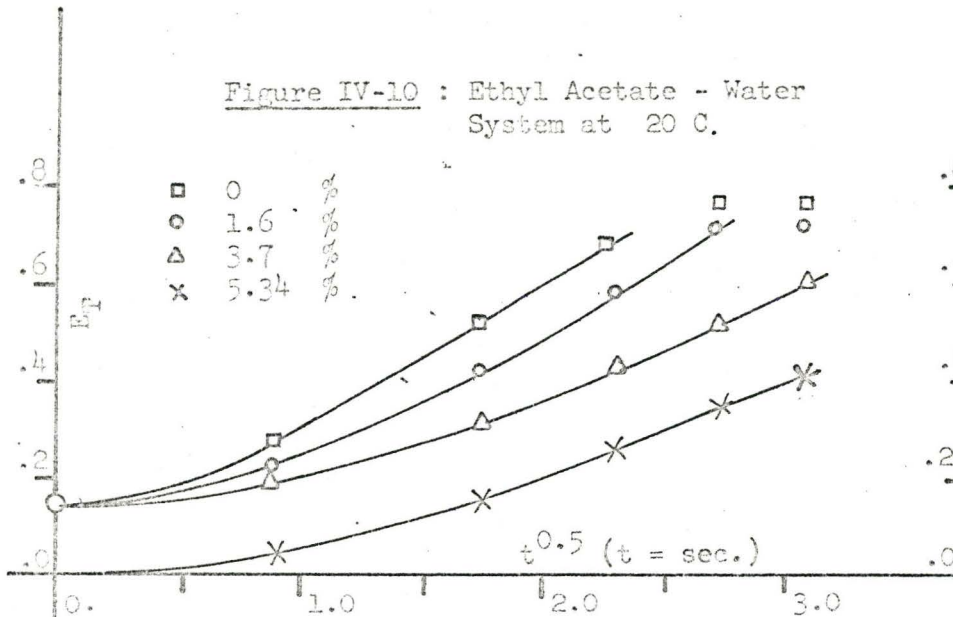

Figure IV-12 : Paraldehyde - Water System at 20 C.

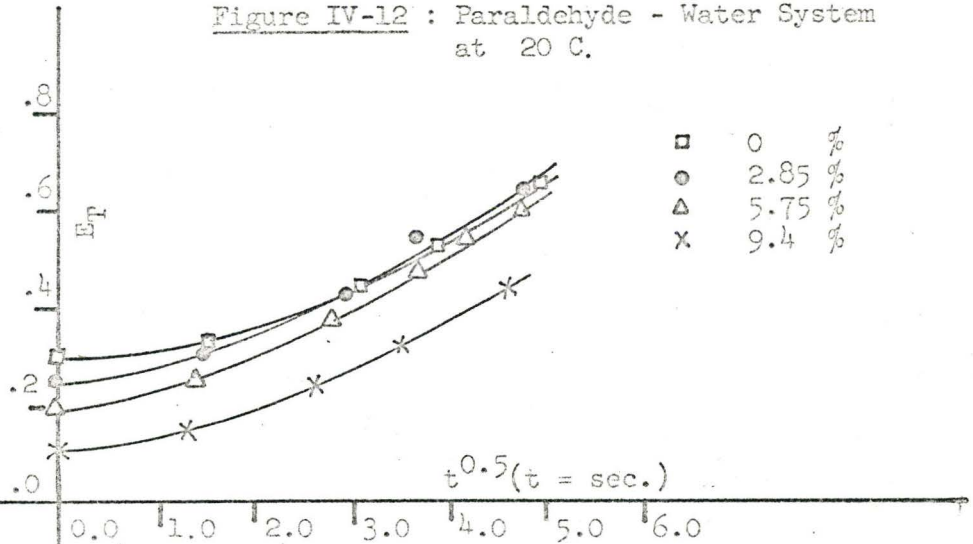

Figure IV-11 : Cyclohexanol - Water System at 30 C.

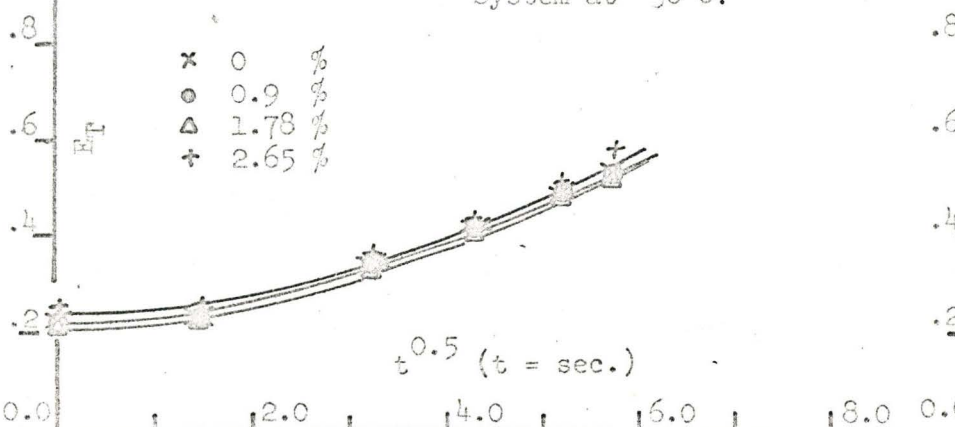

Figure IV-13 : Butyl Lactate - Water System at 20 C.

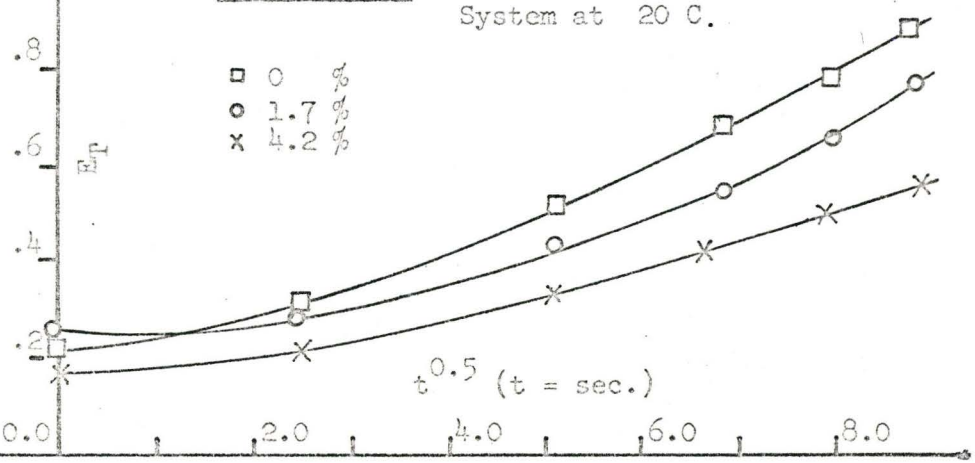

of variance actually showed the effects of these variables. The analysis shown in Appendix IX-9, indicated that the effects of all these variables were significant. The concentration effects showed that the regressed curves were in fact separate and distinct. The drop height effects showed that the data were not necessarily regressed by a straight line. The interaction effects showed that the regression lines were dissimilar in slope, i.e., mass transfer rates varied for each drop concentration at each drop height.

IV-J Models for Analysis of Data for Physical Mass Transfer into Drops

Results of drag coefficient studies tabulated in Table IV-6, showed that the drops for all systems studied were circulating.

Thus, experimental data were analyzed by equations describing transfer into circulating drops and well-mixed drops.

IV-J-1 Mass Transfer into Circulating Drops

The intercept method to find overall end effects E_F by Equation IV-5, is invalid if the mass transfer rates are affected by concentration effects. These effects were present in all systems except the cyclohexanol system, since the slopes of E_T versus $t^{\frac{1}{2}}$ plots in Figures IV-10 to IV-13 (where t = drop time), all varied with initial drop concentrations. E_T values were calculated from regressed concentration data in order to

Table IV-6

Comparison of Spherical Drag Coefficients for Systems Used in Physical Mass Transfer Studies

Continuous System (Saturated with water)	Initial Drop Solute Conc Wt Percent	Terminal Velocity cm/sec (± 1%)	Average Drop Radius -cm	Drop Re No	Drag Coefficient Actual	Drag Coefficient Solid Sphere
Ethyl Acetate	0.0	10.30	0.134 ± .0009	473	0.32	0.465
	1.6	10.24	0.135 ± .0011	474	0.34	0.465
	3.7	10.01	0.136 ± .0012	465	0.35	0.465
	5.4	9.93	0.134 ± .0011	455	0.35	0.465
Butyl Lactate	0.0	1.16	0.234 ± .0047	11.15	2.55	4.35
	1.7	1.16	0.208 ± .0025	9.94	3.59	4.65
	4.2	1.12	0.203 ± .0039	9.35	4.05	4.84
Paraldehyde	0.0	3.05	0.300 ± .0059	12.80	0.18	4.00
	2.85	3.35	0.265 ± .0077	12.45	0.84	3.96
	5.75	3.53	0.243 ± .0080	12.00	0.84	4.17
	9.4	4.29	0.230 ± .0055	13.80	0.61	3.83
Cyclohexanol	0.0	2.67	0.156 ± .0020	6.19	2.70	6.18
	0.9	2.97	0.153 ± .0016	6.75	2.33	5.70
	1.78	3.02	0.158 ± .0017	7.09	2.22	5.71
	2.65	3.26	0.156 ± .0009	7.56	1.96	5.50

Curves for Equation IV-4 : $E_M = \sqrt{\frac{\dot{R}\, D_L\, \pi^2\, t}{a^2}}$

Figure IV-14 : Ethyl Acetate - Water System at 20 C.

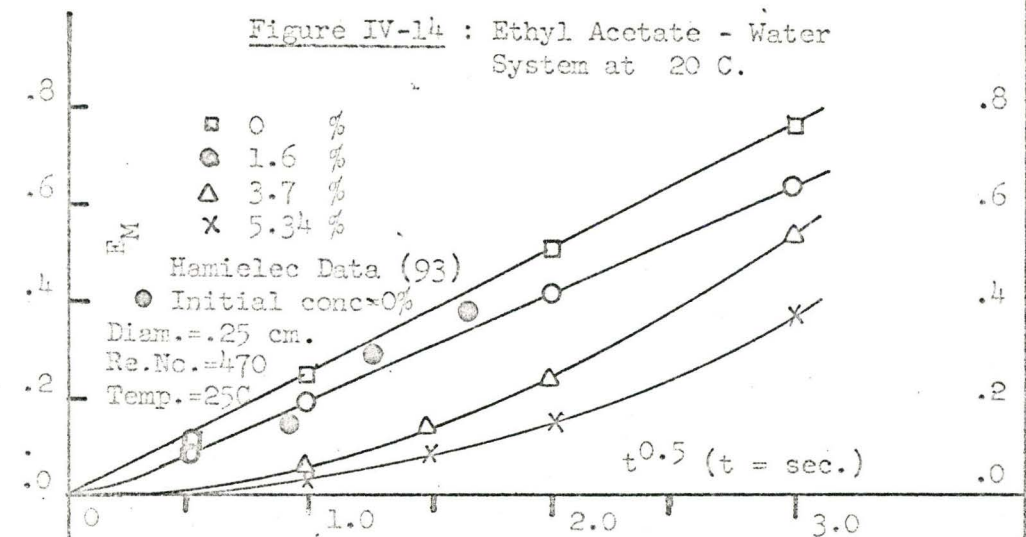

Figure IV-15 : Cyclohexanol - Water System at 30 C.

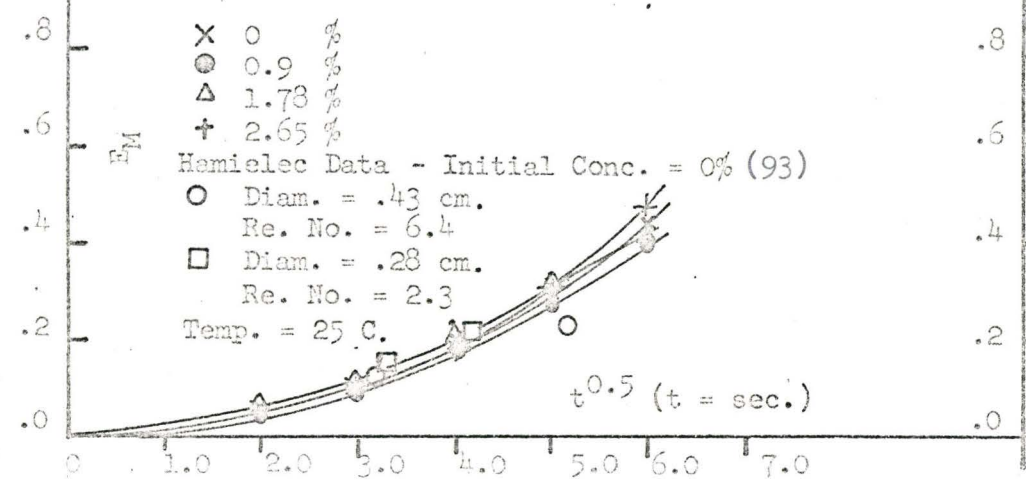

Figure IV-16 : Butyl Lactate - Water System at 20 C.

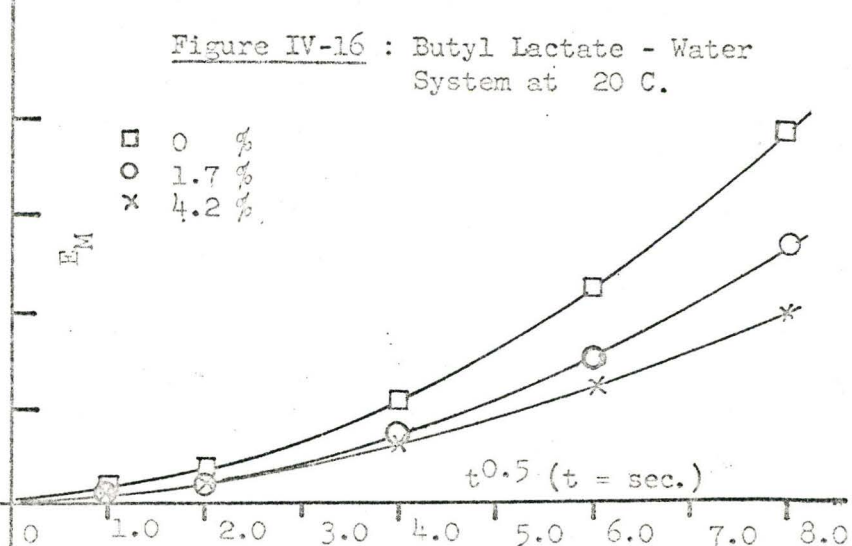

Figure IV-17 : Paraldehyde - Water System at 20 C.

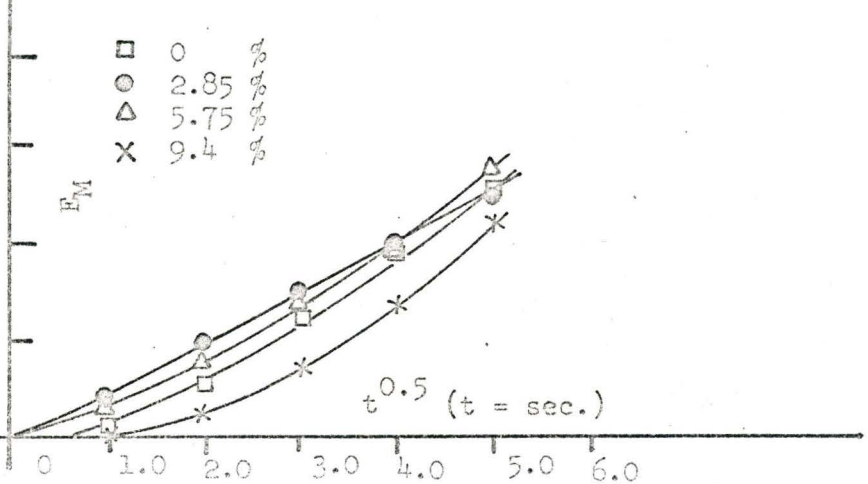

calculate E_F values from regressed data extrapolated to zero drop height. This had been done to find an order of magnitude for E_F.

Since the intercept method of Equation IV-5 was shown to be invalid, the E_F value for each system was set equal to extraction efficiency at the minimum experimental drop height (7 cm). This value represented the maximum end effect value possible. Drop times were calculated relative to the time for the minimum drop height. The calculated relative E_M and t values are tabulated in Appendix IX-10. The E_M values were then correlated against $t^{\frac{1}{2}}$ values by multiple regression analysis, and the regression equations are tabulated in Table IX-11. The values from these regressions are plotted in Figures IV-14 to IV-17. This was done in order to find the values of the dimensionless correlating factor $\dot{R}$, which had been defined as:-

$$\dot{R} = \frac{\text{effective diffusivity}}{\text{molecular diffusivity}} \qquad \text{(IV-21)}$$

from the slopes of the E_M versus $t^{\frac{1}{2}}$ curves, as given in Equation IV-4. These slopes were calculated by differentiating the regression equations for the data. Plots of $\dot{R}$ versus $t^{\frac{1}{2}}$ are shown in Figure IV-23, for each system, from values tabulated in Appendix IX-12.

The variations of $\dot{R}$ with dimensionless, initial concentration forces were shown more clearly in Figure IV-25, at a given drop time. This driving force was defined as:-

$$\Delta C = \frac{C_\phi - C_i}{C_\phi} \qquad \text{(IV-22)}$$

Curves for Equation IV-7 : $\ln(1 - E_T) = \frac{-3 K_L}{a} t$

Figure IV-18 : Ethyl Acetate - Water System at 20 C.

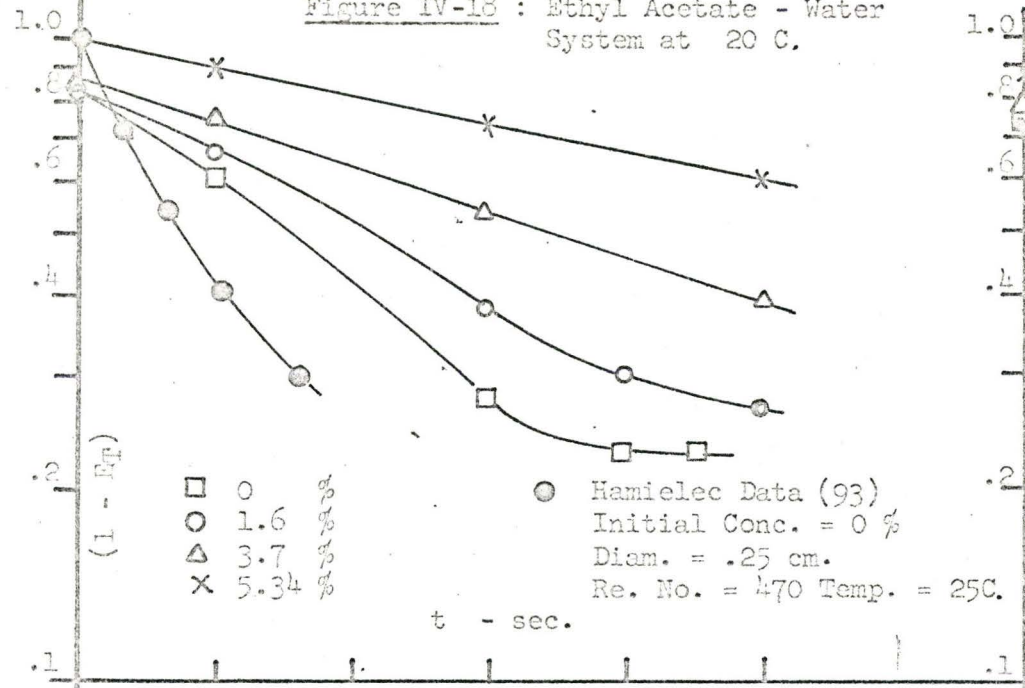

Figure IV-20 : Paraldehyde - Water System at 20 C.

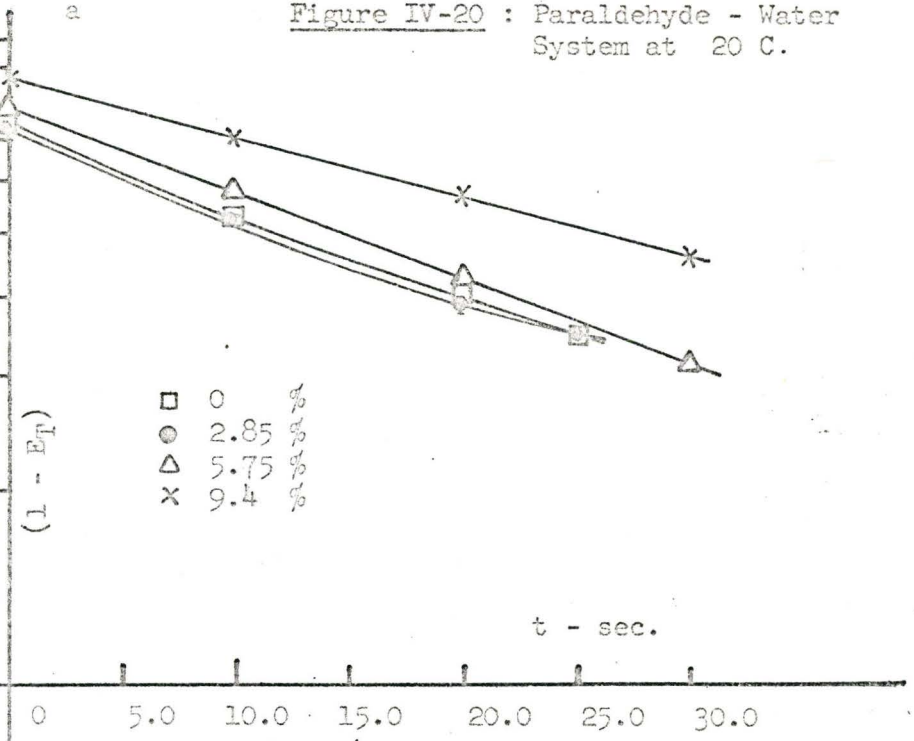

Figure IV-19 : Cyclohexanol - Water System at 30 C.

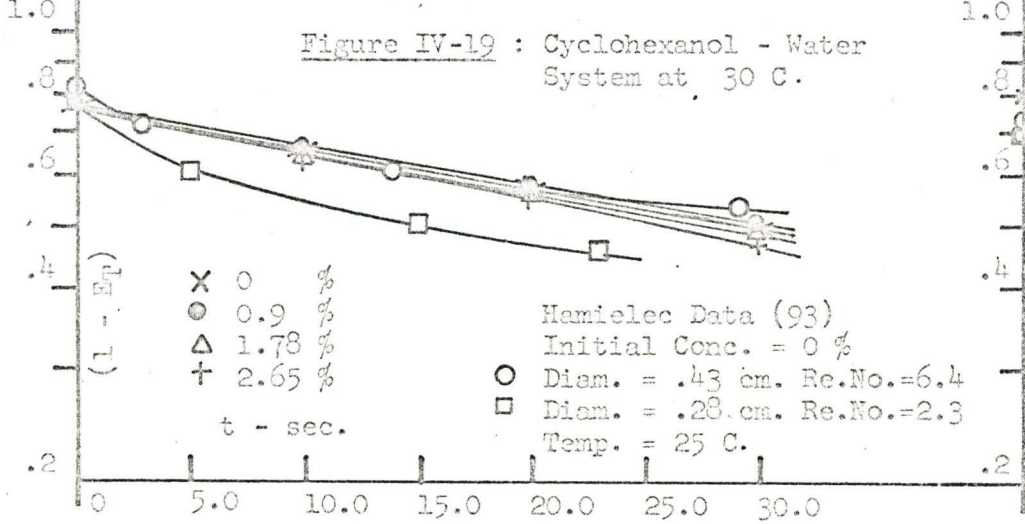

Figure IV-21 : Butyl Lactate - Water System at 20 C.

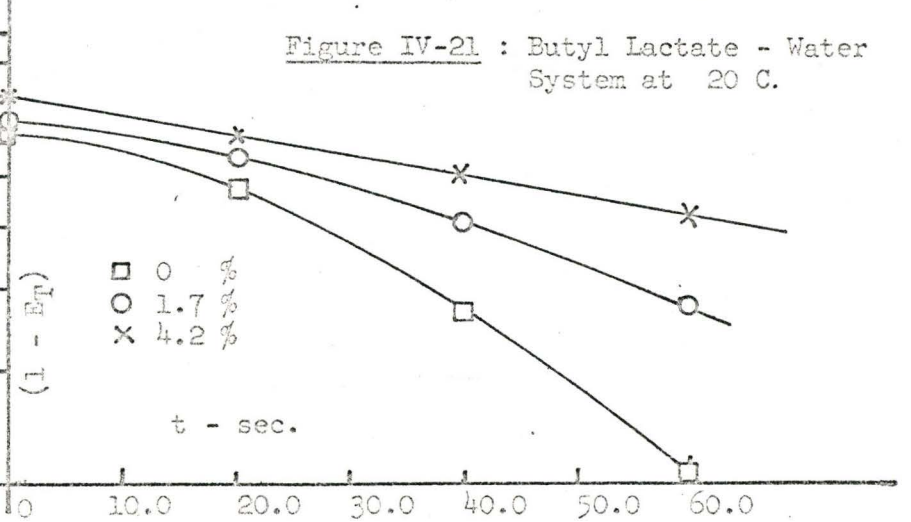

Figure IV-22 : Variations of Mass Transfer Coefficient K_L with Drop Time t

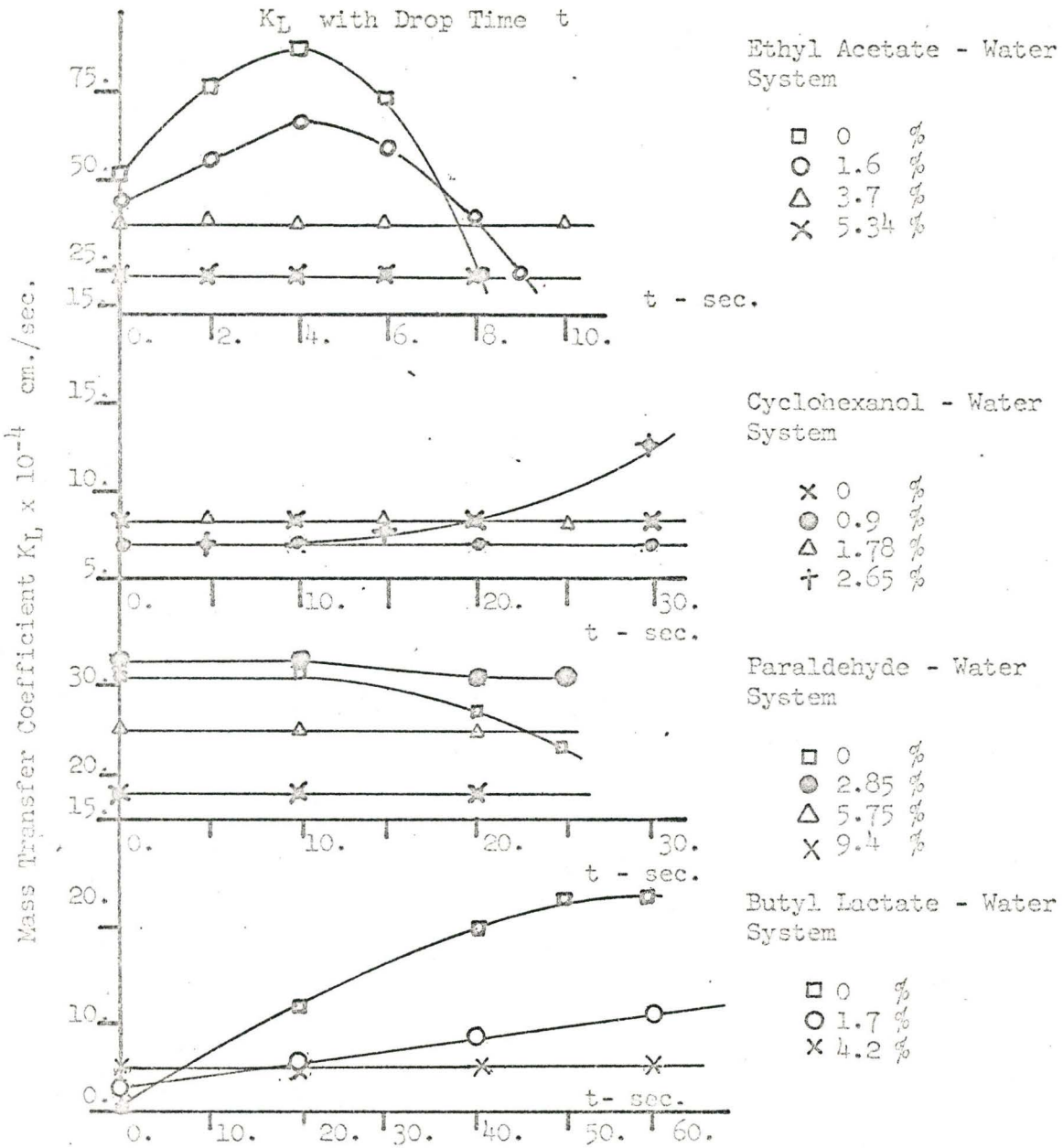

Figure IV-23 : Variations of Effective Diffusivity Factor $\dot{R}$ with $(\text{Drop Time})^{0.5}$

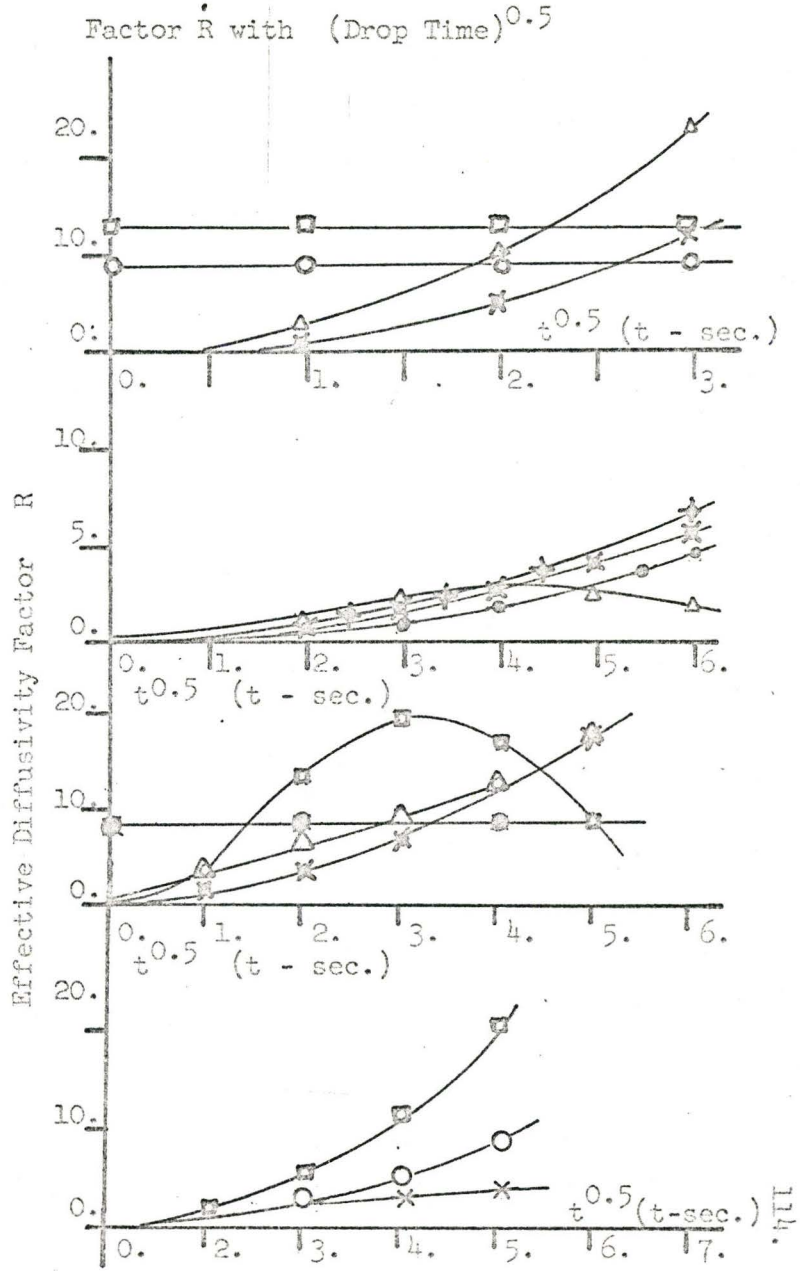

Figure IV-24 : Variations of Mass Transfer Coefficient K_L with Dimensionless Initial Concentration Driving Force ΔC

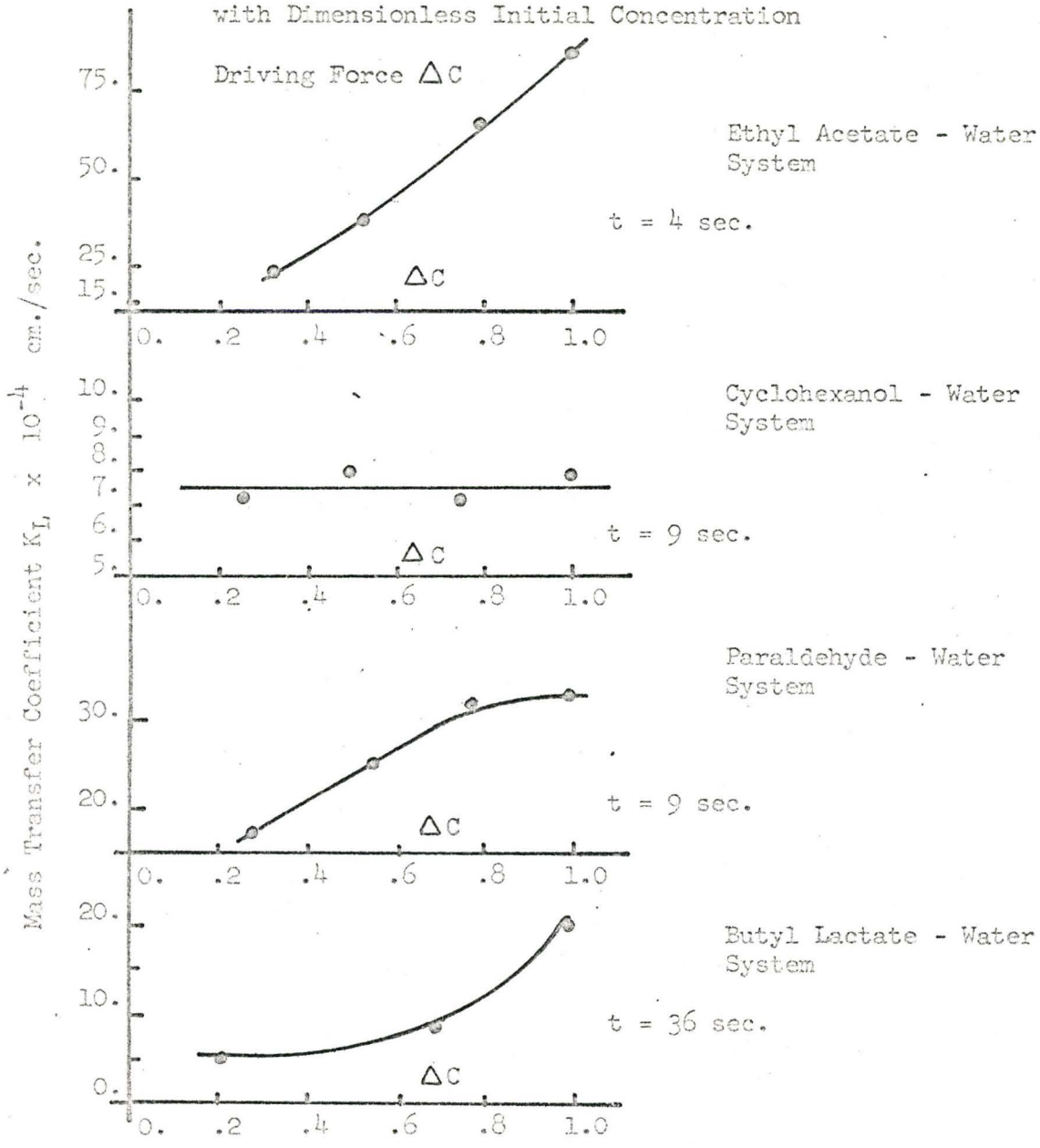

Figure IV-25 : Variations of Effective Diffusivity Factor $\dot{R}$ with Dimensionless Initial Concentration Driving Force ΔC

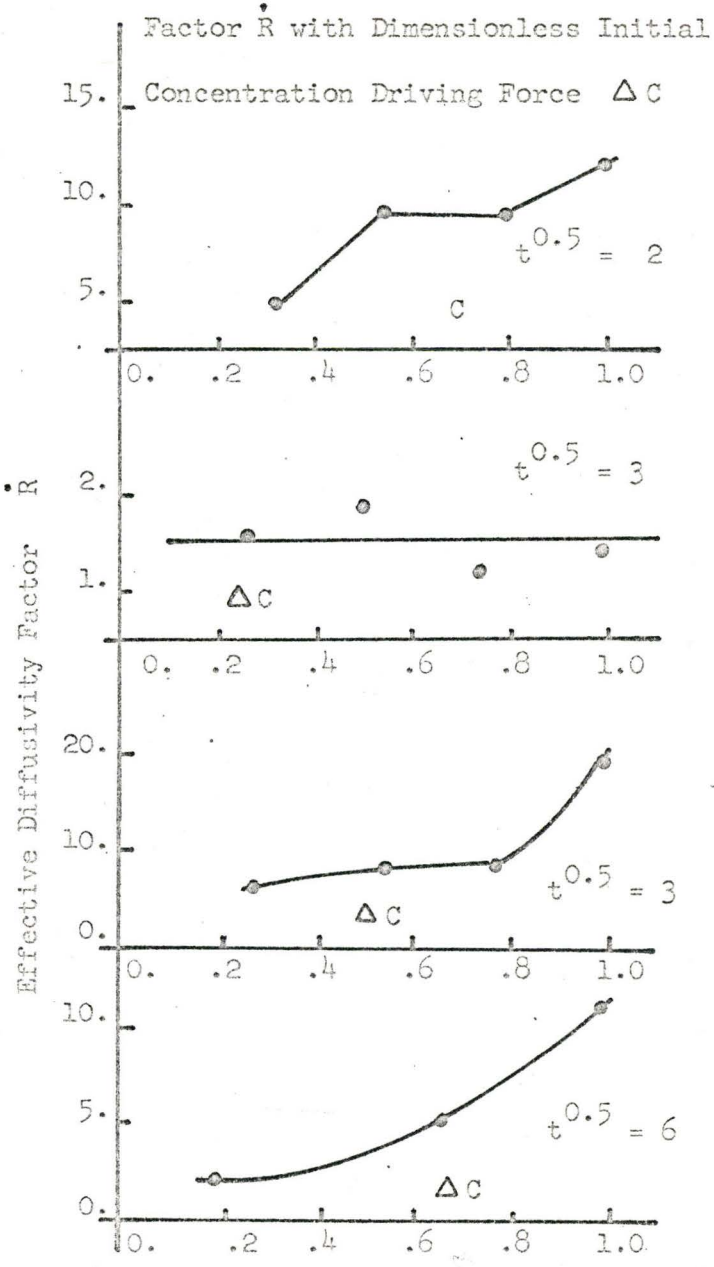

IV-J-2 Mass Transfer into Well-Mixed Drops

The effects of initial drop concentrations on the mass transfer coefficients K_L, were calculated from the slopes of curves of ln $(1 - E_T)$ versus t, as given by Equation IV-7. E_T values were calculated directly from experimental data and values of ln $(1 - E_T)$ were correlated against drop time by multiple regression analysis. The regression equations are listed in Appendix IX-13 and the regressed values of ln $(1 - E_T)$ are plotted against t in Figures IV-18 to IV-21. K_L values were calculated from the slopes of the curves, found by differentiating the regression equations. The K_L values are plotted against t in Figures IV-22 and tabulated in Appendix IX-14. Cross-plots of K_L versus dimensionless initial concentration driving force, at a given drop time, are shown in Figure IV-24.

IV-J-3 Comparison With Hamielec's Data

Experimental data found by Hamielec (7,93) for mass transfer from water saturated ethyl acetate and cyclohexanol systems into water drops are tabulated in Appendix IX-15 and compared with experimental data found in this study.

In Table IV-7, the experimental conditions for which the data were compared, are shown. In all cases the dispersed phase was pure water.

Table IV-7

Experimental Conditions for Comparative Mass Transfer Data

System	Hamielec Data			Experimental Data		
	Temp deg C	Drop Diam. cm	Re No	Temp deg C	Drop Diam. cm	Re No
Ethyl Acetate H_2O	25	.258	472	20	.268	473
Cyclohexanol H_2O	25	.434 .282	6.4 2.3	30	.310	5.94

E_T data by Hamielec for ethyl acetate are plotted in Figure IV-18. The plot showed a higher rate of mass transfer than found in this study. The drop Reynolds Numbers in both studies were in the transition zone between steady fall and drop oscillation. Due to lower interfacial tension at the higher solution temperature, the drops in Hamielec's case were probably oscillating, accounting for the higher transfer rate.

For cyclohexanol, E_T data from Hamielec plotted in Figure IV-19, were in fairly close agreement with the experimental results for the case where the drop Reynold Numbers were similar. Due to longer residence times, drops falling at Reynolds Number = 2.3 show higher extraction efficiency.

When E_M values found by assuming E_F as the extraction efficiency at the minimum drop height were used, agreement between the two sets of data were surprisingly good as shown in Figures IV-14 and IV-15. However, this was probably fortuitous. Again, due to the difficulty in finding E_F values, comparison between E_T values are probably more significant.

IV-J-4 Discussion of Model Study Results

Values of both the effective diffusivity factors $\dot{R}$ and the mass transfer coefficients K_L increased with rising initial concentration driving forces for ethyl acetate, butyl lactate and paraldehyde-water systems. Concentration effects were negligible for the cyclohexanol-water system. These observations were emphasized in the cross-plots of $\dot{R}$ and K_L against dimensionless, initial concentration driving forces at a given time.

Results for mass transfer coefficients are more accurate than for effective diffusivity factors. K_L values are functions of E_T values which are calculated directly from experimental data. $\dot{R}$ values are functions of E_M values which must be calculated from E_T values and an estimated E_F value for that system. If the E_F estimate was incorrect, the E_M values and hence the $\dot{R}$ values were also incorrect. This estimation is difficult to make if concentration driving forces affect the mass transfer rates. Under these conditions, the E_F values may no longer be constant for a system, and may vary with the drop height.

IV-J-5 Explanations for Concentration Effects on the Mass Transfer Rates

As described in the literature survey, earlier studies have shown that for three component systems, the mass transfer coefficients increased with concentration driving forces for the solute. This increase in transfer rates was caused by interfacial turbulence produced by random areas of high solute concentrations at the interface (71,72), unbalancing

the local interfacial tension forces. Thus, at least three components were required to produce interfacial turbulence. This turbulence disappeared as the concentration driving forces diminished.

Thus, no interfacial turbulence was formed in binary systems. However, if a third component which is soluble in either or both phases, was formed by any reaction, interfacial turbulence may result and transfer rates may be affected by concentration driving forces.

When saturated with water, esters formed an equilibrium with their components as shown:-

$$EtAc + H_2O \rightleftharpoons EtOH + AcOH \qquad (IV-23)$$

It was shown by Seto (26) that the alcohol caused interfacial turbulence in ester-water systems. Similarily paraldehyde decomposed to form small quantities of acetaldehyde. As little as 0.01% acetaldehyde in freshly distilled paraldehyde was enough to cause interfacial turbulence. This was observed when paraldehyde was poured on water. This effect was intensified when paraldehyde containing more acetaldehyde was poured on water.

Since cyclohexanol was inert in water, it formed a true binary system. Thus, there were no interfacial turbulence and concentration driving forces had no effect on the mass transfer rates.

As this thesis was being written, this phenomenon was confirmed by Schlieren photographs recently published Sawistowski et al (64), for many binary systems. No explanations were given by him for this phenomenon.

When interfacial turbulence is present, the assumption of a

constant E_F for any drop height for any given system may not necessarily be true. As mentioned in the literature survey (82), E_F is a function of the formation end effect E_{f1}, and of the coalescence end effect E_{f2}, as shown:-

$$E_F = E_{f1} + E_{f2} - E_{f1} \times E_{f2} \qquad \text{(IV-24)}$$

The formation end effect for any given system is constant for any drop height, since the initial concentration gradient at the interface was the same. At short drop heights, solute transfer into the drop may be small enough to permit interfacial turbulence to persist until the drop coalesced at the bottom of the column. Hence the coalescence end effects may be large, increasing the overall end effects. As the drop height is increased, solute transfer into the drop may become large enough to stop interfacial turbulence. Hence the coalescence end effect and also the overall end effect may tend towards a minimum as the drop height is increased.

IV-K Presentation of Data for Mass Transfer with Simultaneous Chemical Reaction in Drops

Experimental data are tabulated in Appendix X-2 for systems

a) Butyl lactate - sodium hydroxide-water

b) Ethyl acetate - sodium hydroxide-water

and are plotted in Figures IV-26 and IV-29. The words acid and alkali were used to indicate the method used to determine the mass transferred.

These data were correlated against drop heights by multiple regression analysis and are tabulated in Appendix X-3. Correlations

Figure IV-26 : Mass Transferred Versus Drop Height for Butyl Lactate - NaOH - H_2O System at 20 C.

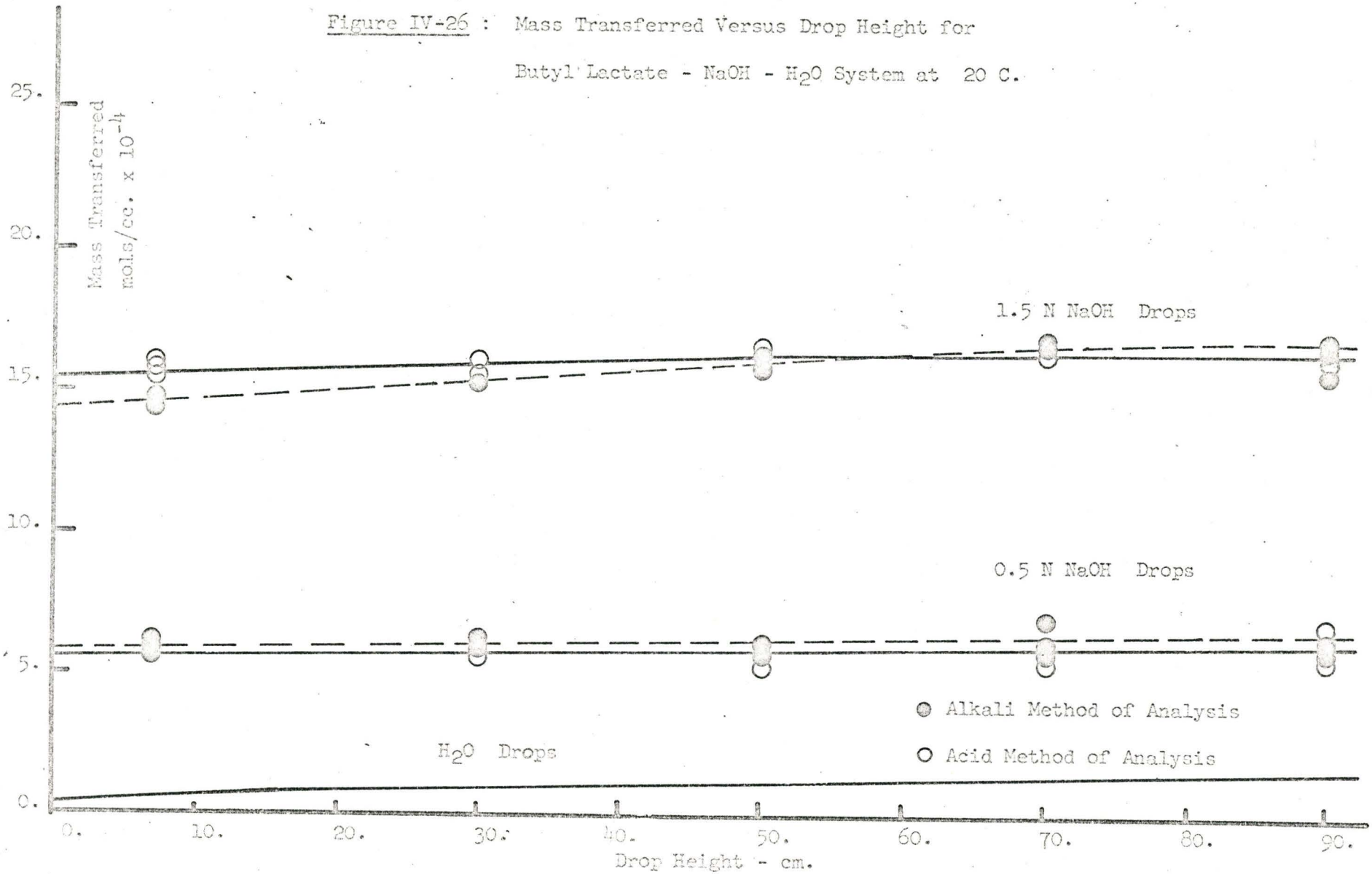

against drop times are tabulated only for the ethyl acetate system in Appendix X-4.

Statistical analyses of the data are shown in Appendix X-5. Variance of replication of data and 95% probability range of these data are also shown.

Results of the analysis of variance of the variables for each system are shown in Appendix X-6.

IV-L Discussion of Results for Butyl Lactate-Sodium Hydroxide-Water System

Experimental data are shown in Figure IV-26. Analysis of variance were carried out on the following variables:-

1) Initial sodium hydroxide concentration in the dispersed phase.
2) Drop height.
3) Interaction of drop heights and initial sodium hydroxide concentrations.

Analysis of variance showed that the alkali concentration effects were very large but the drop heights had only a small effect on mass transfer rates. The interaction effects were very small.

Thus, correlations for experimental data for the initial sodium hydroxide concentrations were widely separated, but had slopes which were almost zero.

Analysis of variance was also used to determine the difference in mass transfer data obtained by the two analytical methods described in experimental procedures. The results showed that due to the fairly

Figure IV-27 : Aqueous NaOH Drop Falling in Butyl Lactate

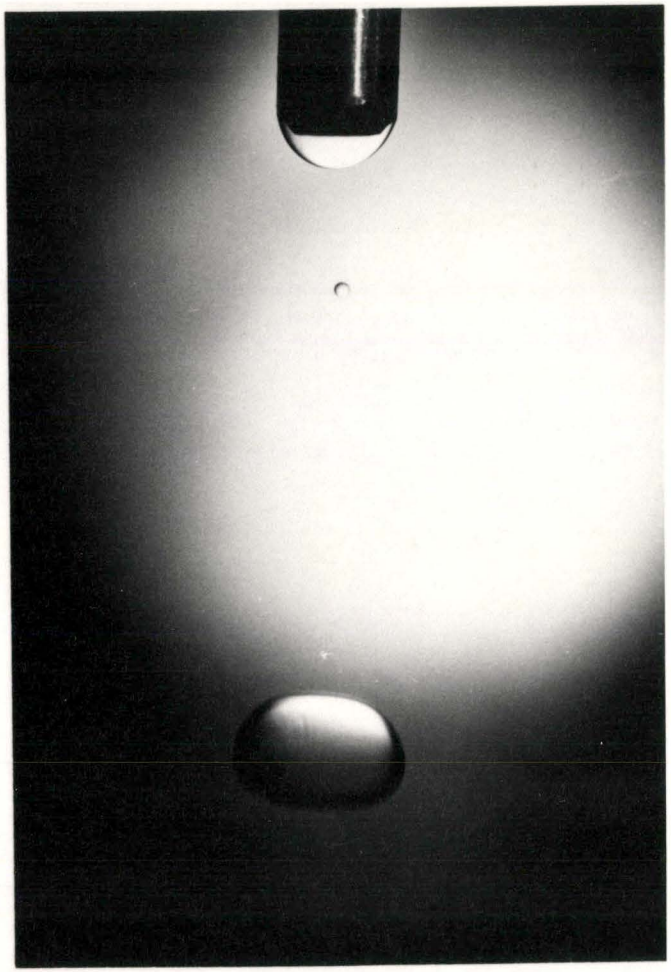

Figure IV-28 : Aqueous NaOH Drop Falling in Ethyl Acetate

large variances on the replication of data, either analytical method was applicable.

As a further check, analyses of variance were made on the two sets of data found by the two analytical methods. The results of these analyses were similar.

Since the slopes of the experimental correlations were almost zero, mass transfer for these systems occurred mainly during drop formation. This was confirmed by observation, as shown photographically in Figure IV-27, along with the contrasting picture of a quiescent drop of sodium hydroxide solution falling in the ethyl acetate continuous phase. Interfacial turbulence was so vigorous for the butyl lactate system during drop formation, that tiny water droplets were expelled and obscured the nozzle. This phenomenon vanished as the drop fell from the nozzle. The vigorous interfacial turbulence caused large mass transfer rates at drop formation. Since by contrast, there was very little mass transfer as the drop fell, no further analysis was done on this system.

IV-M Discussion of Results for Ethyl Acetate-Sodium Hydroxide-Water System

Experimental data are shown in Figure IV-29.

IV-M-1 Measurement of Mass Transferred

The acid method described in section IV-G-2 was used to measure mass transferred for 1N and 2N sodium hydroxide drop concentrations.

The alkali method described in section IV-G-1 was used for

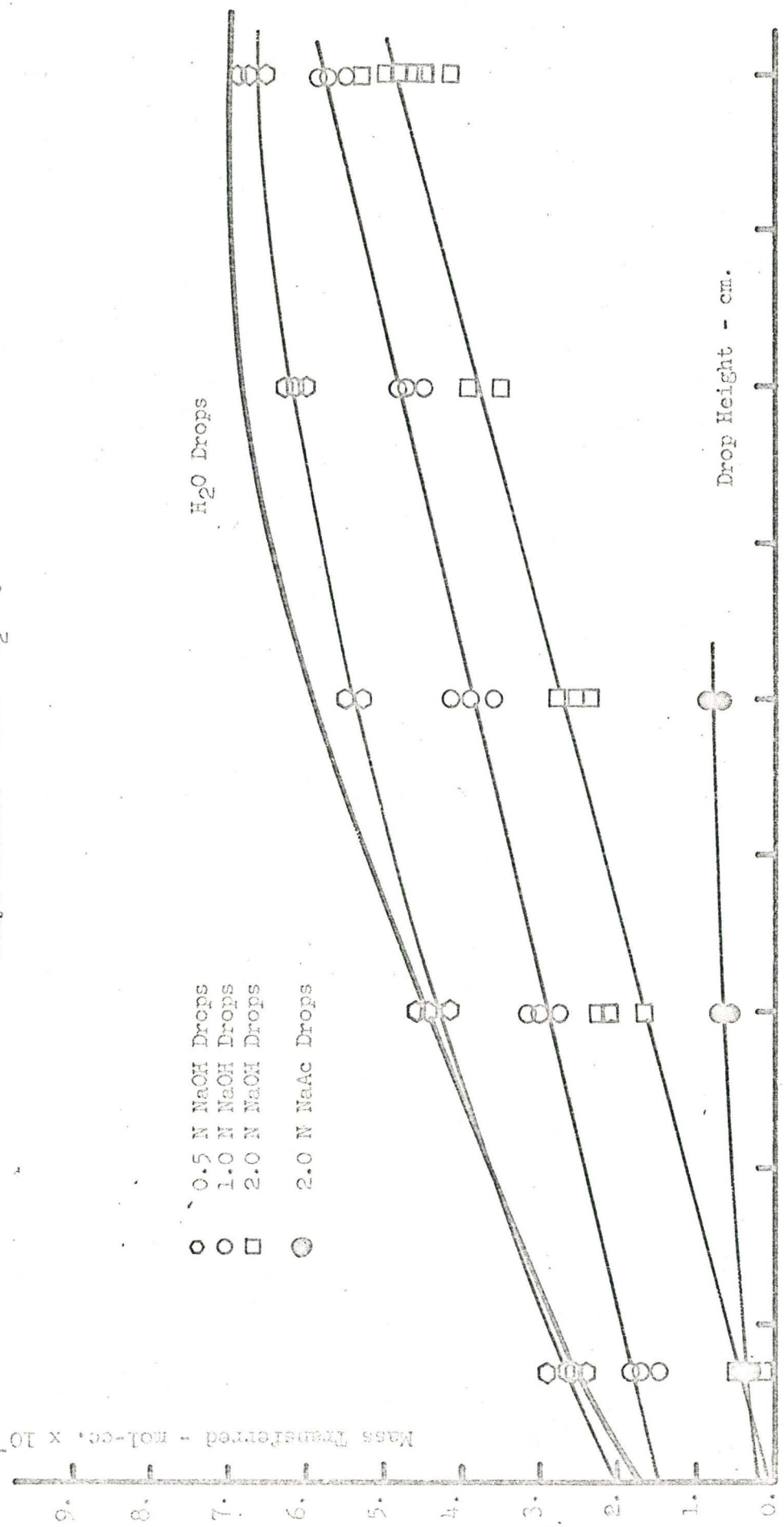

Figure IV-29 : Mass Transferred versus Drop Height for Ethyl Acetate - NaOH - H_2O System at 20 C.

the 0.5N sodium hydroxide drop concentration, since all the sodium hydroxide in the samples had been fully reacted.

When the initial sodium hydroxide concentration was greater than the ester transferred, the two analytical methods gave comparable results. This was due to the relatively long residence time of the reactants in the collecting funnel at the bottom of the column.

This was shown by assuming that the funnel acted as a plug flow reactor.

The saponification reaction is:-

$$NaOH + Ester \longrightarrow Na\ Salt + Alcohol \qquad \text{(IV-24)}$$

$$\text{Rate of reaction} = K_R\, C_{N_a}\, C_{E_t}$$

$$t = \frac{1}{K_R(C_{E_t} - C_{N_a})} \ln\left\{\frac{C_{E_t} - C_{N_a}X_o}{C_{E_t}(1-X_o)}\right\} \qquad \text{(IV-25)}$$

where t = residence time, minute

K_R = reaction constant, cc/mol min

C_{E_t} = initial ester concentration, cc/mol

C_{N_a} = initial NaOH concentration, cc/mol

X_o = fraction of NaOH reacted

for 1N NaOH - EtAc - H_2O system

$$t = 4.28 \text{ min}$$

$$K_R = 5{,}500 \text{ cc/mol min}$$

$$C_{E_t} = 6.41 \times 10^{-4} \text{ mol/cc}$$

$$C_{N_a} = 10 \times 10^{-4} \text{ mol/cc}$$

Substituting into Equation IV-25,

$$X_o = 0.64$$

$\therefore$ amount of NaOH reacted = 6.4×10^{-4} mol/cc.

IV-M-2 Analysis of Data

Analysis of variance of data showed that their correlating equations were unique with different slopes for each sodium hydroxide drop concentration.

Replicate standard deviations for data were smaller for this system, than for the butyl lactate-sodium hydroxide-water system. The alkali drops fell smoothly with no large turbulence effects, as observed in the butyl lactate system. Thus, the ethyl acetate-sodium hydroxide-water system was more suitable for mathematical analysis and experimentation.

IV-M-3 Salt Effect on Rate of Mass Transfer

Plots of mass transferred versus drop height, given in Figure IV-29, appeared to indicate that mass transfer rates decreased, with increasing concentration of sodium hydroxide in the dispersed phase. This apparent retardation was due either to the change in the transfer coefficient, or the concentration gradient $(C_{\phi} - C_i)$ or both of them, as described by Seto (26).

The factors for the change in mass transfer coefficients were all speculative, and were not proven. These factors were:-

1) Modification of hydrodynamic conditions near the interface.

2) Presence of an additional resistance, due to slow chemical reaction.

However, the decrease in concentration gradient was due to changes in ethyl acetate solubility, by the salt effect of sodium acetate and sodium hydroxide present at the interface. This decrease in

solubility produced by an electrolyte was given by the simple empirical relation (89):-

$$\ln \frac{S_o}{S} = K_S C_I \qquad \text{(IV-26)}$$

where C_I = ion concentration in the solution, mols/litre

S_o = solubility in pure water, mols/litre

S = solubility in the elctrolyte solution, mols/litre

K_S = salting coefficient

= 0.222 litres/mols for ethyl acetate in sodium hydroxide solutions

Salt effect of sodium acetate on ethyl acetate was easily evaluated by a few simple experiments. The salt effect of sodium hydroxide on ethyl acetate could not be measured experimentally since they reacted with each other. However, experimental data on salt effects (90,91) indicated that the salting coefficients for both sodium hydroxide and sodium acetate on ethyl acetate were the same.

Thus the variations of ethyl acetate solubility in sodium hydroxide solutions at twenty degrees centigrades are as shown in Table IV-8.

Table IV-8

Solubility of Ethyl Acetate in Aqueous Sodium Hydroxide Solutions

Sodium Hydroxide, Normality	1.975	0.998	0.506	0.0
Ethyl Acetate concentration, mols/litre	0.374	0.580	0.716	0.898

Thus, as the alkali normality increased to 2.0, the ester solubility dropped to 42 percent of the value in pure water. The salt

Table IV-9

Comparison of Spherical Drag Coefficients for Systems Used in Mass Transfer with Reaction Studies

Continuous System (Sat'd with Water)	Initial NaOH Conc in Drop Normality	Temp deg C	Drop Rad cm	Drop Re No	Drag Coefficients C_D Actual	C_D Solid Sphere
Butyl Lactate	0.0	20	0.234	11.15	2.55	4.35
	0.506		0.162	16.7	4.76	3.32
	1.545		0.109	8.9	2.14	4.85
Ethyl Acetate	0.0	20	0.134	473	0.32	0.465
	0.506		0.134	436	0.48	0.468
	0.998		0.128	428	0.52	0.474
	1.975		0.124	590	0.49	0.391

Figure IV-30 : Predictions of Danckwerts' Modified Equations Including Salt Effects for

Reacting System - Ethyl Acetate - 0.5 N NaOH

Reaction Constant = 91.8 cc./mol sec.
Diffusion Coefficient = 1 x 10^{-5} cm^2/sec.

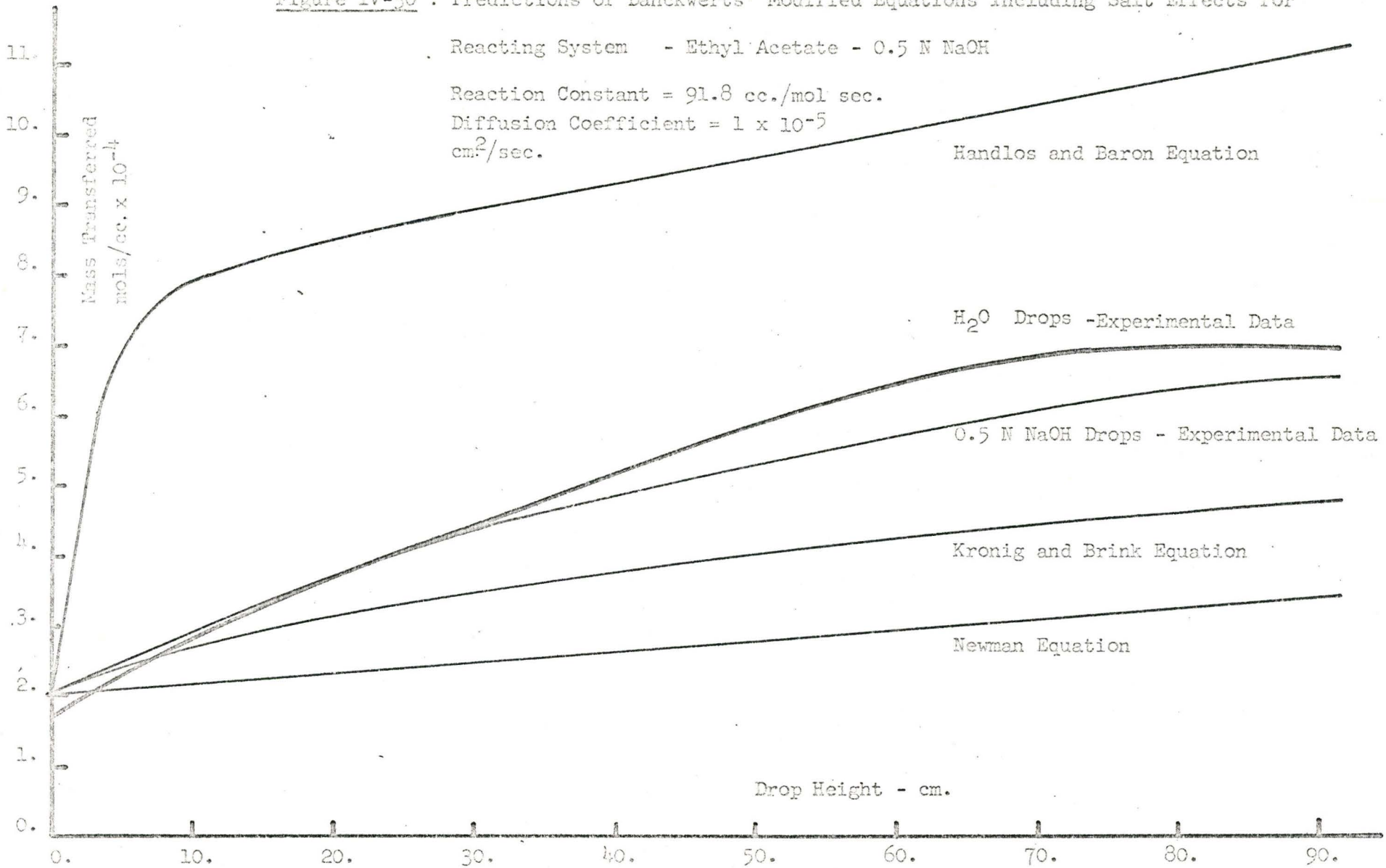

Figure IV-31 : Predictions of Danckwerts' Modified Equations Including Salt Effects for

Reacting System - Ethyl Acetate - 1.0 N NaOH

Reaction Constant = 91.8 cc./mol sec.
Diffusion Coefficient = 1 x 10^{-5} cm.^{2}/sec.

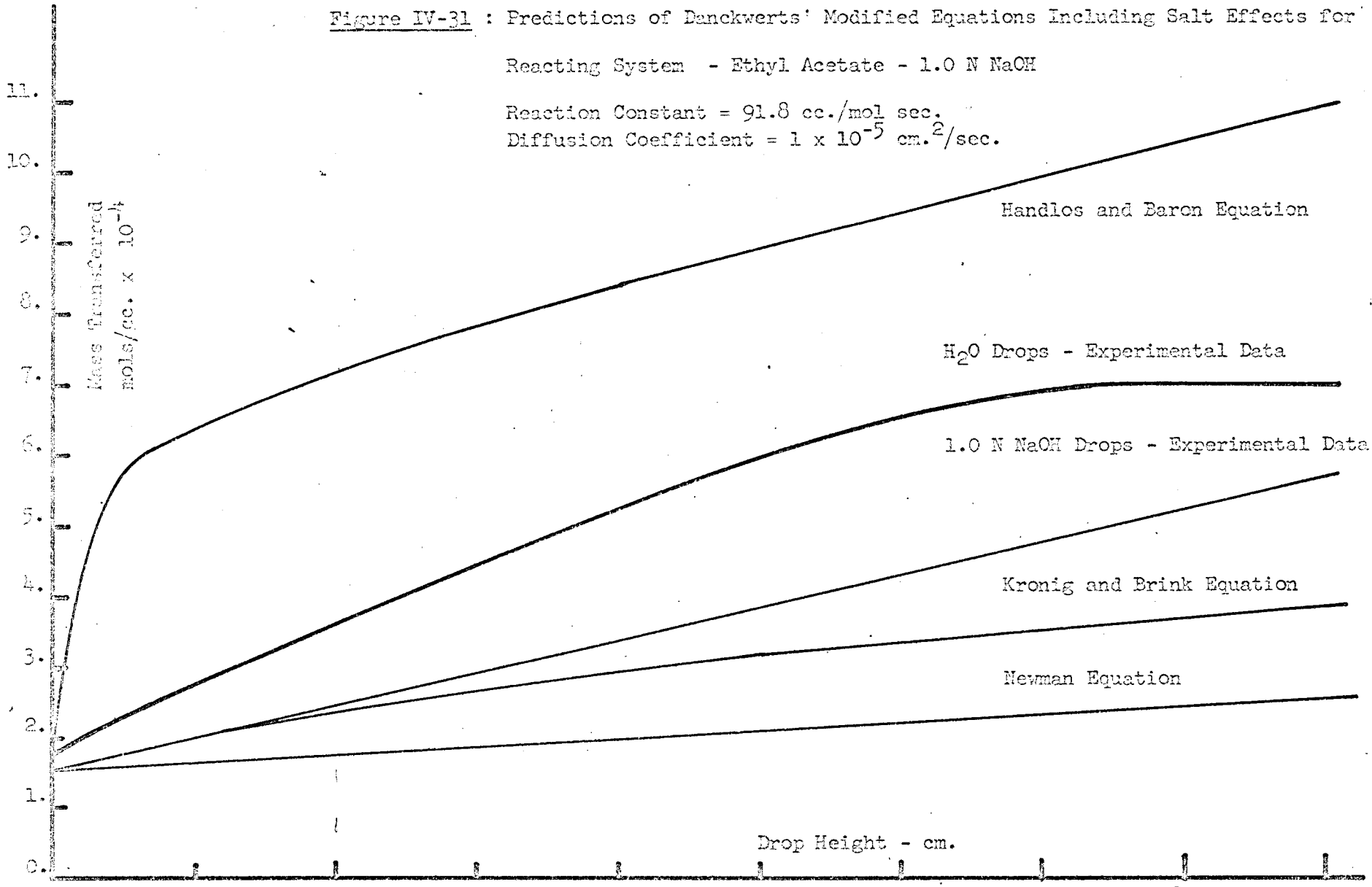

Figure IV-32 : Predictions of Danckwerts' Modified Equations Including Salt Effects for Reacting Systems - Ethyl Acetate - 2.0 N NaOH

Reaction Constant = 91.8 cc./mol sec.
Diffusion Coefficient = 1 x 10^{-5} cm.^{2}/sec.

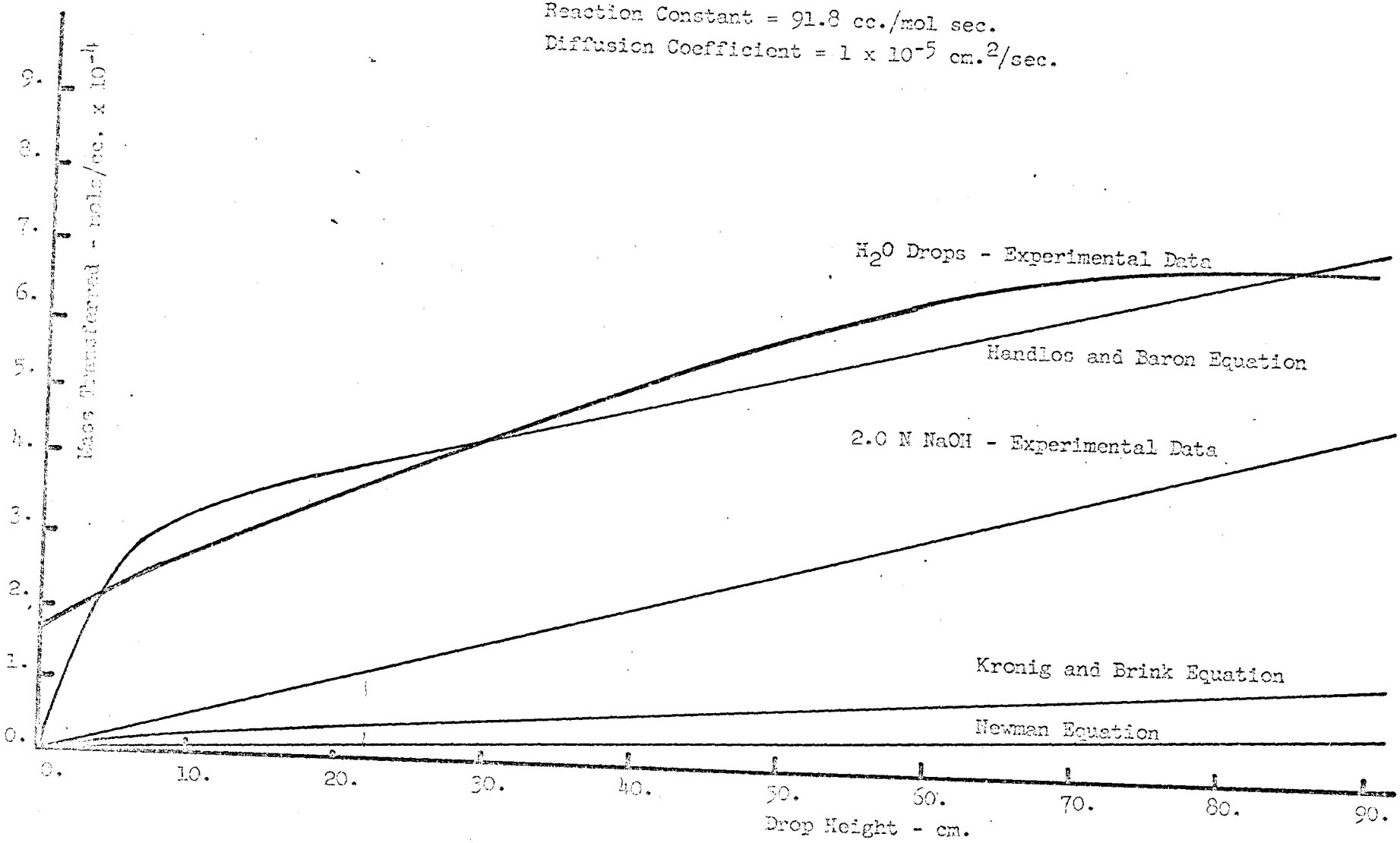

effect on mass transfer into drops was found by comparing the data for physical mass transfer into 2 N sodium acetate drops, with those for mass transfer with chemical reactions into 2 N sodium hydroxide drops. This comparison showed that the rate of mass transfer was enhanced by chemical reaction.

IV-M-4 Comparison of Experimental and Predicted Mass Transfer Data

As a first approximation, the experimental data were analyzed by assuming pseudo-first order reaction rates for the saponification of ethyl acetate by sodium hydroxide.

Experimental data were compared with those predicted by mass transfer equations generalized to include first order reactions as listed in Table IV-2.

These equations were:-

1) Newman Equation IV-12, for transfer into circulating drops.
2) Kronig and Brink Equation IV-13, for transfer into circulating drops.
3) Handlos and Baron Equation IV-14, for transfer into turbulent drops.

Comparison between predicted and experimental data for sodium hydroxide-ethyl acetate system are shown in Figures IV-30 to IV-32. For comparison purposes, the predicted results are given the same end effects as for the experimental results and tabulated in Appendix X-7.

Calculation of drag coefficients as shown in Table IV-9, indicated that the sodium hydroxide drops were stagnant. However, the model studies showed that the results lay between those predicted by turbulent drop model and fully circulating drop model.

Figure IV-33 : Variations of Effective Diffusivity with Time for Reacting System - Ethyl Acetate - 0.5 N NaOH

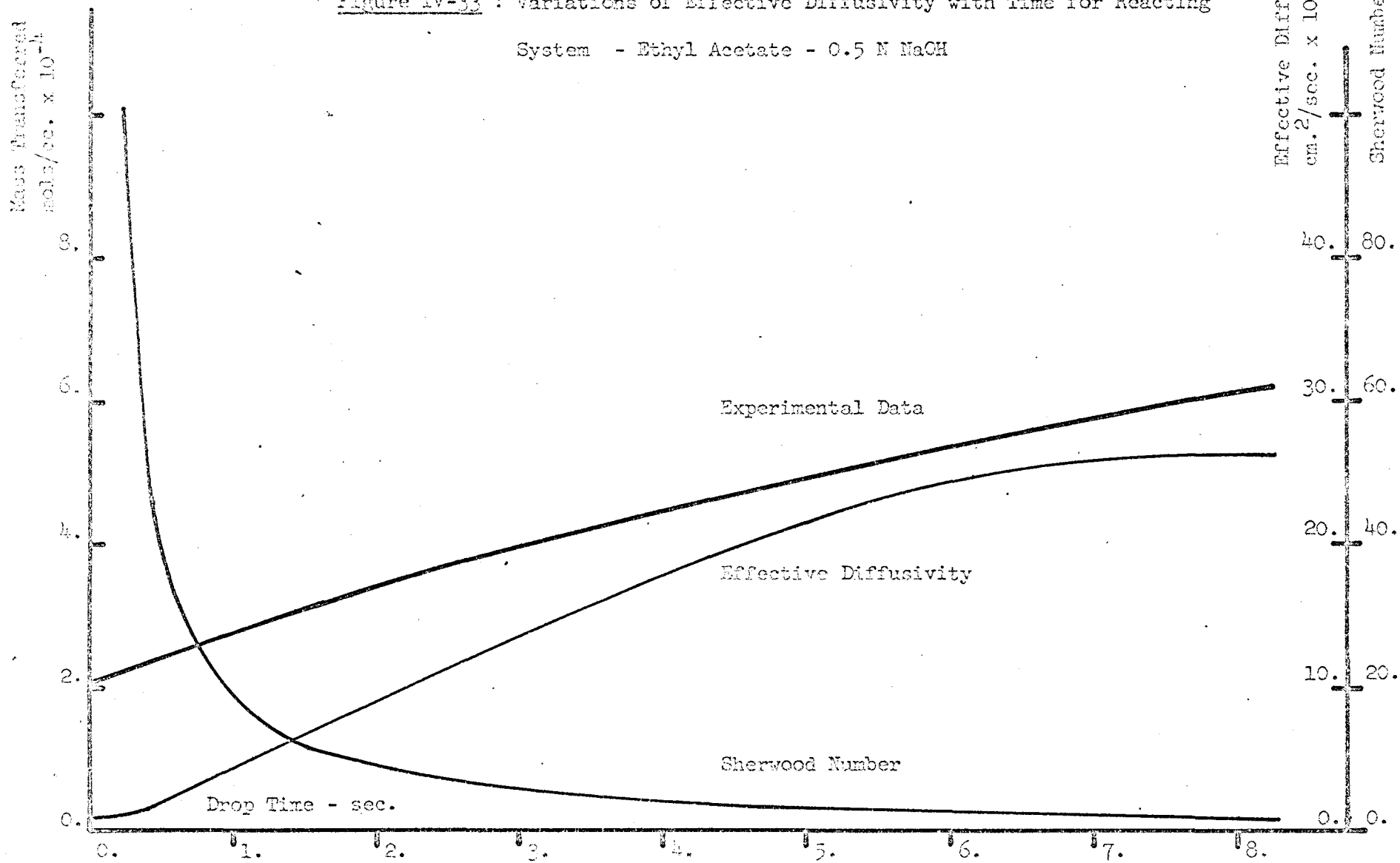

Figure IV-34 : Variations of Effective Diffusivity with Time for Reacting System - Ethyl Acetate - 1.0 N NaOH

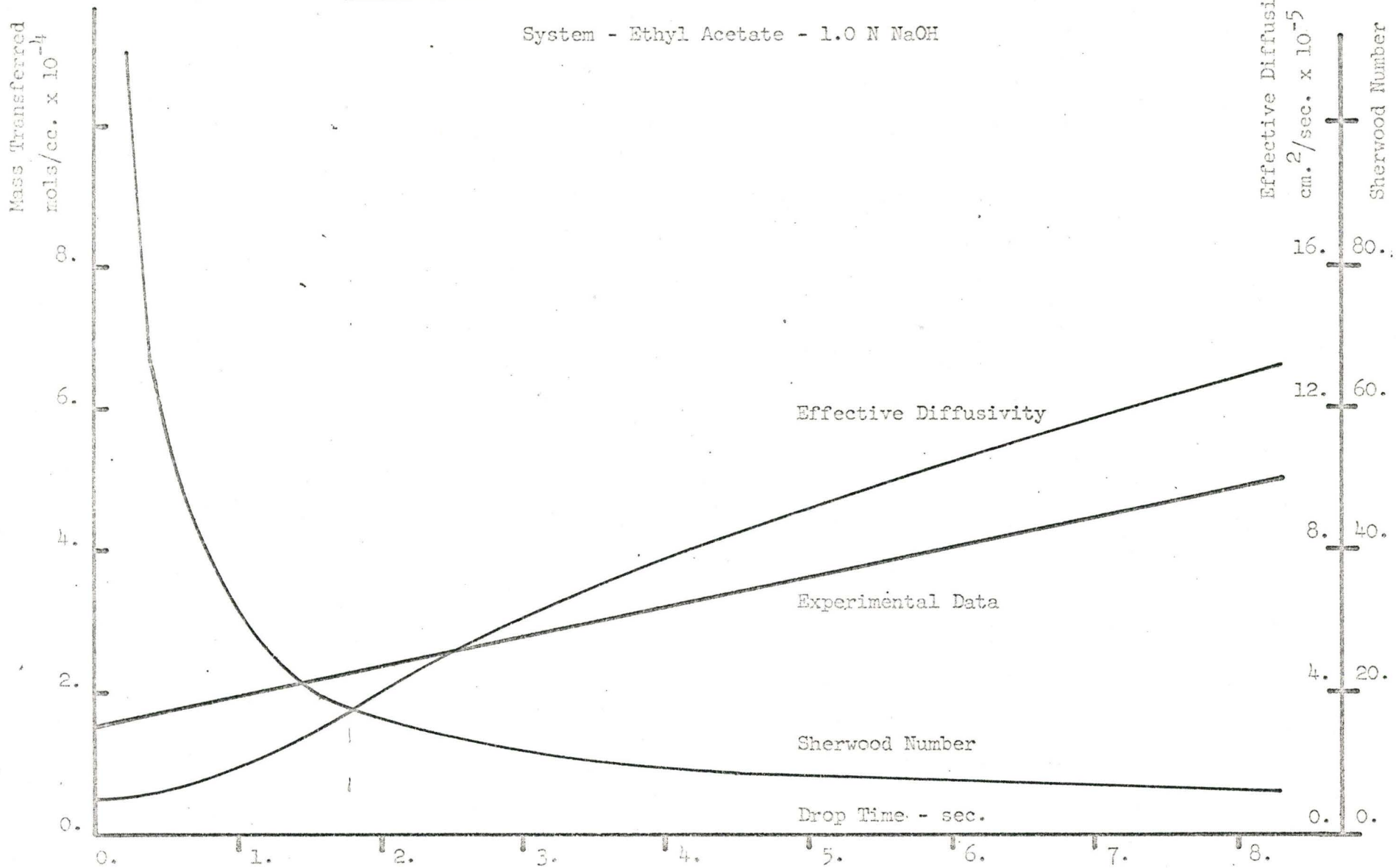

Figure IV-35 : Variations of Effective Diffusivity with Time for Reacting System - Ethyl Acetate - 2.0 N NaOH

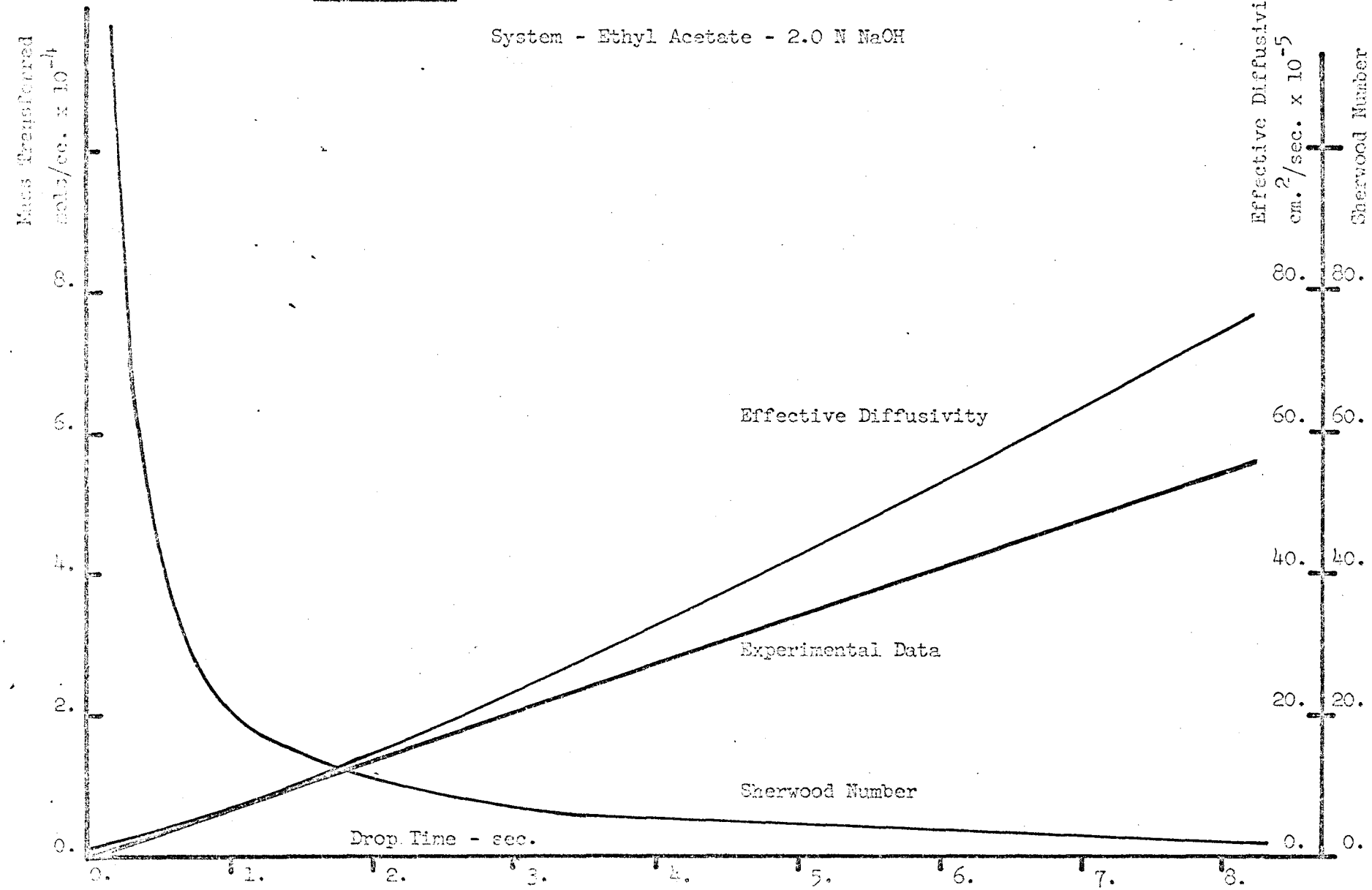

During the saponification of ester, alcohol was formed, as shown in Equation IV-24 . As described previously for physical mass transfer, interfacial turbulence was caused by the alcohol. This was shown in some current work by Seto (92). Comparison with predicted results showed that the resultant effective diffusivities D_e for this system lay between the value for turbulent drops and circulating drops and vary with time.

Studies were made on the prediction of mass transfer with simultaneous reaction into stagnant drops using a model where D_e was made time or concentration dependent. Details of the computer study are given in Appendix X-8. The method consisted of increasing the transfer rate into a stagnant drop by increasing the diffusion coefficient, until the predicted mass equaled the experimental result.

Experimental results have shown that the saponification of ethyl acetate by 2N and 1N sodium hydroxide solutions could be treated as pseudo-first order since the consumption of the alkali increased linearly with time. However, since all the alkali was used up for the 0.5 N system, it was treated as a second-order system. Results of this study are shown in Figures IV-33 to IV-35 and tabulated in Appendix X-9. Variations of effective diffusivity and Sherwood Number with time are also shown.

The Sherwood Number, which is a dimensionless mass transfer coefficient, dropped sharply with time for all sodium hydroxide systems. This predicted Sherwood Number Sh, was based on the effective diffusivity D_e, as shown:-

$$Sh = \frac{K_L d}{D_e} \qquad \text{(IV-27)}$$

Figure IV-36 : Comparisons of Experimental and Calculated Sherwood Numbers for Ethyl Acetate - NaOH - H_2O System

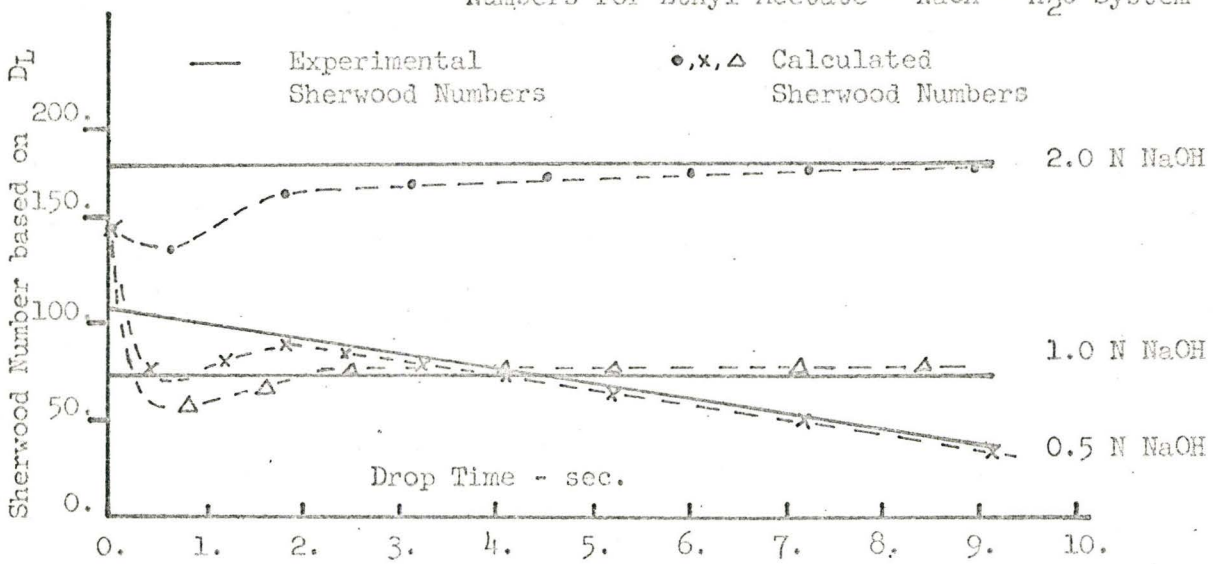

Figure IV-37 : Variations of Effective Diffusivity with Time for Ethyl Acetate - NaOH - H_2O System

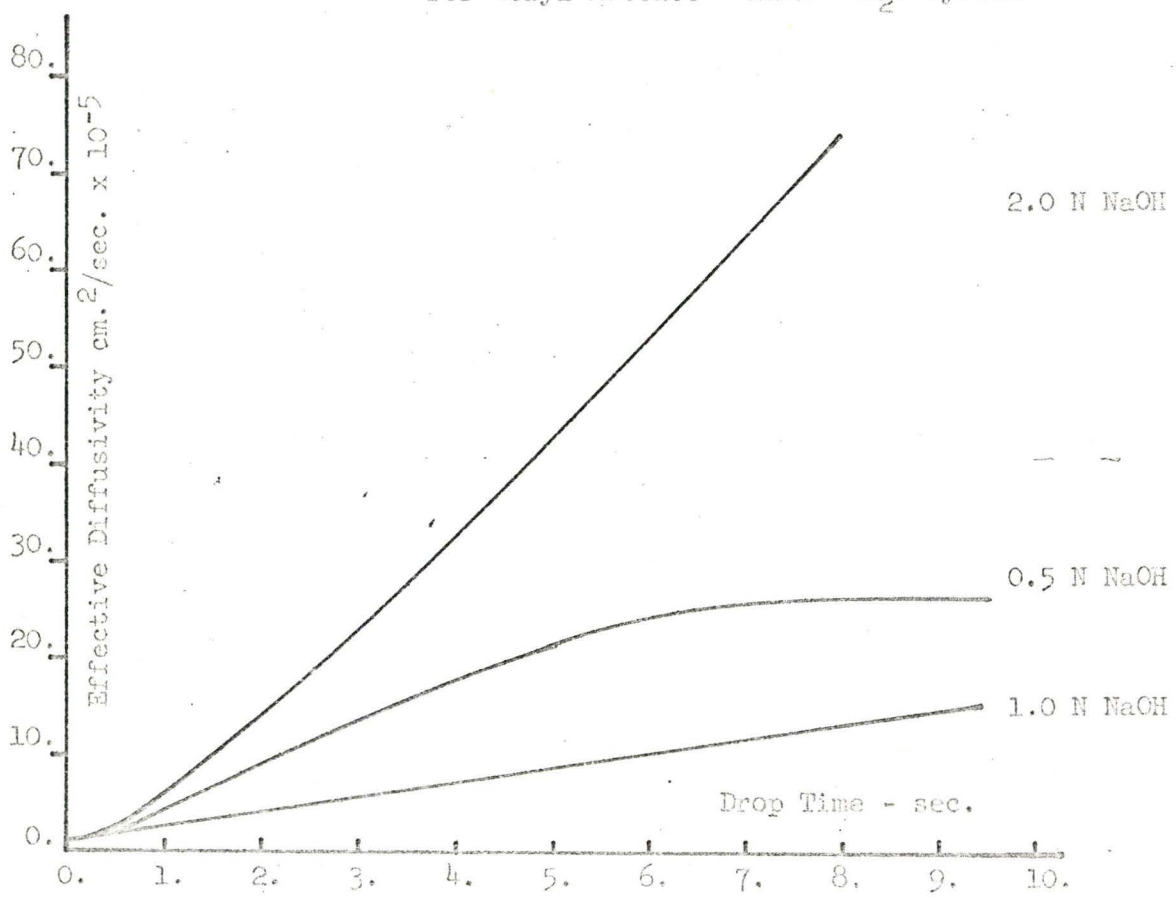

However, experimental Sherwood Numbers were based on molecular diffusivity. Thus, the predicted Sherwood Numbers were compared with experimental results in Figure IV-36, by replacing the D_e with molecular diffusion coefficients. Although initial agreement between the two Sherwood Numbers was poor, the two values approached each other as time increased.

Sherwood Number is a function of the dimensionless concentration gradient $\frac{\partial C}{\partial R}$, at the surface of the drop

$$Sh = -2 \left.\frac{\partial C}{\partial R}\right]_{R=1} \qquad \text{(IV-28)}$$

Thus, the initial poor agreement between experimental and predicted Sherwood Numbers, was due to errors in calculating the very steep concentration gradient at the start, with the mesh size used in the numerical solutions of the mass transfer model. This was true especially for the 2N sodium hydroxide drops.

The ester solubility was so low that this concentration gradient remained steep for a long time. This fact was learned by studying the effect of mesh sizes on the accuracy of results.

Another cause for the poor initial agreement in Sherwood Numbers arose from errors in the experimental data. When D_e is affected by interfacial turbulence effects, the overall end effects cannot be found accurately by interpolating experimental data to zero drop time. Hence experimental Sherwood Numbers are also inaccurate at short times.

As shown in Figure IV-37, D_e increased with time for all sodium hydroxide drop concentrations. As the reactants were consumed, D_e tended to level off and fall towards molecular diffusivity. For 2N sodium

hydroxide drops, the ester solubility was so low that the reaction effect surpassed the diffusion effect, causing a large increase in D_e.

IV-N Conclusions and Contributions

In this section, the conclusions and contributions from each area of experimental study are given.

IV-N-1 Physical Mass Transfer into Drops

Initial concentration driving forces have no effect on physical mass transfer rates for two component systems, since an equilibrium is established at the interface. This was demonstrated quantitatively with the cyclohexanol-water system.

However if a third component is formed by side reactions in a two component system, mass transfer rates may be enhanced with increasing initial concentration driving forces.

This increase in transfer rate may occur if interfacial turbulence is formed by the third component.

This enhancement has been shown quantitatively for the following systems:-

1) Ethyl acetate - water
2) Butyl lactate - water
3) Paraldehyde - water

IV-N-2 Mass Transfer with Simultaneous Chemical Reaction

Experimental study was concluded on the following systems:-

1) Butyl lactate - sodium hydroxide - water

2) Ethyl acetate - sodium hydroxide - water

These are the only known data currently available, which involve resistance to transfer solely in the dispersed phase for reacting systems.

The rate of mass transfer of ethyl acetate into aqueous sodium hydroxide drops was apparently reduced as the concentration of the alkali increased. This was shown to be due to the salt effects of the alkali which reduced the solubility of the ethyl acetate in the aqueous drop. Hence it was shown that the rate of mass transfer was enhanced by chemical reaction.

For both systems, the rate of mass transfer was greatly increased by interfacial turbulence formed by reaction products.

IV-N-3 Model Studies

No model currently available was able to accurately predict mass transfer with chemical reaction into dispersed phase. This includes the model developed in this thesis, since they all consider only constant convection effects upon the transfer rates.

This work has shown that in many cases, interfacial turbulences may occur, enhancing the mass transfer coefficients. It has been demonstrated that the intensity of the interfacial turbulence is a variable with time and system.

IV-N-4 General Conclusions

All mass transfer studies have stressed that clean, inert apparatus and pure systems must be used to prevent surfactants from decreasing the mass transfer rates. This work has shown that physical mass transfer studies must be carried out with system which are inert under the experimental conditions. Otherwise, transfer rates may be enhanced by interfacial turbulences caused by decomposition products.

All results for mass transfer with chemical reactions should be examined for effects of interfacial turbulence caused by reaction products.

Currently, there are no useful hydrodynamic explanations for interfacial turbulence since there are no equations of motion for the interface. Thus, before an accurate model predicting transfer with interfacial turbulence can be made, a phenomenological equation describing this motion is required.

IV-O Recommendations

This work has shown the need for more study to determine formation and coalescence end effects. Work has been done in formation end effects only for physical mass transfer systems. Nothing has been done on the effects of interfacial turbulence or chemical reactions on formation end effects. As far as is known, very little work has been done on coalescence end effects.

A wider range of reaction constants may be studied if a solute soluble in both phases was transferred from a continuous phase to a

reactant in the dispersed phase. By a judicious choice of systems, interfacial turbulence may be avoided.

More experimental data are required to characterize the occurrence of interfacial turbulence.

Finally, more experimental data are required for mass transfer with and without chemical reactions into oscillating drops. Above a certain oscillation frequency, interfacial turbulence effects should have no influence upon the mass transfer rates.

IV-P Nomenclature

a = drop radius, cm

A_D = surface area of drop, cm^2

C_A^l = concentration of solute A, gm/cc

C_A = C_A^l / C_ϕ

= dimensionless concentration

C_1 = initial concentration in the dispersed phase, gm/cc

C_D = drag coefficient

C_I = ion concentration, mols/cc

C_ϕ = equilibrium concentration in the dispersed phase, gm/cc

ΔC^l = $C_1 - C_\phi$

= concentration driving force across dispersed phase interface, gm/cc

ΔC = $\Delta C^l / C_\phi$

= dimensionless concentration driving forces

d = drop diameter, cm

D_L = molecular diffusivity, cm^2/sec

D_e = effective diffusivity, cm^2/sec

Ef_1 = formation end effect

Ef_2 = coalescence end effect

E_F = overall end effect

E_M = extraction efficiency during free fall or rise of drop

E_T = overall extraction efficiency

g = acceleration due to gravity, cm/sec^2

K_L = dispersed phase mass transfer coefficient, cm/sec

K_R = reaction constant, cc/mol min

K_S = salt effect coefficient, cc/mol

M = mass transferred, mols

RK^1 = chemical reaction rate constant, sec^{-1}

$RK = \frac{RK^1 a^2}{D_L}$

= dimensionless chemical reaction rate constant

$Pe = \frac{dV_D}{D_L}$

= Peclet Number

$R = \frac{D_e}{D_L}$

= enhancement factor

$Re = \frac{dV_D \rho_o}{\mu_o}$

= drop Reynolds Number

r = drop radius, cm

$R = \frac{r}{a}$

= dimensionless drop radius

S_o = saturation concentration in water, mol/cc

S = saturation concentration in salt solution, mol/cc

t = time, sec

V_R, V_θ = velocity components of streamlines in the radial and angular directions respectively, cm/sec

V = drop volume, cm^3

V_D = drop velocity, cm/sec

$V_D' = \frac{V_D}{1+X}$

= modified drop velocity, cm/sec

X_o = fraction reacted

$X = \frac{\mu_i}{\mu_o}$

= viscosity ratio

Greek Letters

μ = viscosity, centipoise

ρ = density, gm/cc

θ = polar angle, spherical co-ordinate

Coefficients in Series Solution

n = n'th term in series

A_n, λ_n = coefficients for Kronig and Brink equation by Heertjes et al (18)

B_n, γ_n = coefficients for Handlos and Baron equation by Wellek et at (77)

Subscript

i = dispersed phase

o = continuous phase

Statistical Terms

$S(x)$ = estimated standard deviation of the population

$S(\bar{x})$ = estimated standard deviation of the means of samples of size n

x = sample

$\bar{x}$ = sample mean

μ = true mean of population

t = values from t-test tables

V Summary of Contributions

The principal contribution of Section III was the extension of the Johns and Beckmann model (86) for predicting mass transfer into circulating drops, to account for simultaneous chemical reaction. Numerical solutions were obtained for the model, using polar co-ordinates (R,θ). This permitted easy substitution of various velocity profiles inside the drop, to account for effects of Reynolds Numbers up to 80 at viscosity ratios from 0 to infinity on the mass transfer rates. Solutions were also found for dimensionless reaction rate constants of 0, 10 and 200. It was also shown that the lower and upper limits of the model were defined by the Newman equation (54) for transfer into stagnant drops and the Kronig and Brink equation (58) for transfer into fully circulating drops, respectively. These models had been modified by Danckwerts' method (59) to account for chemical reaction.

The principal contributions of Section IV were the presentation of experimental data for mass transfer into dispersed phase. The effects of initial concentration driving forces on physical mass transfer rates for binary systems were shown. For true binary systems, there were no concentration effects on the mass transfer rates. However, if a third component was produced by a side reaction, interfacial turbulence may occur, enhancing the mass transfer rate. Interfacial turbulence effects were further demonstrated by studies of mass transfer with simultaneous chemical reaction into dispersed phases.

These experimental studies have shown that current models

describing mass transfer into drops were inaccurate when interfacial turbulence occurred. The variations in the diffusion coefficients with time due to interfacial turbulence during mass transfer with chemical reactions were also shown by a computer study of the transfer process.

VI References

1. Whitman, W.G., Long, L. and Wang, H.W., Ind. Eng. Chem., 18, 363, (1926).

2. Sherwood, T.K., Evans, J.E. and Longcor, J.V.A., Trans. Amer. Inst. Chem. Eng., 35, 597, (1939).

3. Licht, W. and Conway, J.B., Ind. Eng. Chem., 42, 1151, (1950).

4. Dixon, B.E. and Russell, A.A.W., J. Soc. Chem. Ind. Lond., 69, 284, (1950).

5. Licht, W. and Pansing, W.F., Ind. Eng. Chem., 45, 1885, (1953).

6. Dixon, B.E. and Swallow, J.E.L., J. Appl. Chem., 4, 86, (1954).

7. Johnson, A.I. and Hamielec, A.E., A.I.Ch.E.J., 6, 145, (1960).

8. Johnson, A.I., Hamielec, A.E., Ward, D.M. and Golding, A., Can. J. of Chem. Eng. 36, 221, (1958).

9. Johnson, H.F. and Bliss, H., Trans. A.I. Ch.E., 42, 231, (1946).

10. West, F.B., Robinson, P.A., Morgenthaler Jr., A.C., Beck, T.R. and McGregor, D.K., Ind. Eng. Chem. 43, 234, (1951).

11. Bird, R.B., Stewart, W.E., Lightfoot, E.N., Transport Phenomena, John Wiley and Sons, Inc., (1962).

12. Baird, M.H.I., Chem Eng. Sci., 9, p.268, (1958).

13. Ilkovic, D., Coll. Czech. Chem. Commun., 6, 498, (1934).

14. MacGillovry, D. and Redeal, E.K., Rec. Tarv. Chem., 56, 1013 p.137.

15. Popovich, A.T., Jervis, R.E., and Trass, O., Chem. Eng. Sci., 19, 357, (1964).

16. Coulson, J.M. and Skinner, S.J., Chem. Eng. Sci. 1, 197, (1952).

17. Groothius, H. and Kramers, H., Chem. Eng. Sci., 4, 17, (1955).

18. Heertjes, P.M., Holve, W.A. and Talsma, H., Chem. Eng. Sci., 3, 122, (1954).

19. Higbie, R.W., Trans. A.I.Ch.E., 6, 498, (1935)

20. Groothius, H., Zuiderweg, F.J., Chem. Eng. Sci., 12, 288, (1960).

21. Smith, A.R., Caswell, J.E., Larson, P.P. and Covers, S.D., Can. J. Chem. Eng., 41, 150, (1964).

22. Skelland, A.H.P. and Wellek, R.M., A.I.Ch.E.J., 10, 491, (1964).

23. Sherwood, T.K. and Wei, J.C., Ind. Eng. Chem., 49, 1030, (1957).

24. Lewis, J.B., Trans. Inst. Chem. Engrs. (London), 31, 323, (1953).

25. Lewis, J.B. and Pratt, H.C.R., Nature, 171, 1155, (1953).

26. Seto, P., M.Eng. Thesis, McMaster University, Hamilton, (1963).

27. Wei, J.C., Ph.D. Thesis, Mass. Inst. of Tech., Cambridge, Mass.,(1955)

28. Sternling, C.V. and Scriven, L.E., A.I.Ch.E.J., 5, 514, (1959).

29. Orell, A. and Westwater, J.W., A.I.Ch.E.J., 8, 350, (1960).

30. Sawistowski, H. and Goltz, G.E., Trans. Inst. Chem. Engrs., 41, 174, (1963).

31. MacKay, G. and Mason, S.G., Can. J. of Chem. Eng., 41, 203, (1963).

32. Goltz, G.E., J. Imp. Coll. Chem. Eng. Soc., 12, 40, (1958-9).

33. Ruckenstein, E. and Berbente, C., Chem. Eng. Sci, 19, 329, (1964).

34. Ruckenstein, E., Chem. Eng. Sci., 19, 505, (1964).

35. Grassman, P. and Anderes, G., Chem. Ing. Tech., 31, 154, (1959).

36. Anderes, G., Ibid., 34, 597, (1962).

37. Hadamard, J.C.R., Acad. Sci. Paris, 152, 1735, (1911).

38. Rybczynski, W., Bull. Acad. Sci. Cracovie, A, 40, (1911).

39. Levich, V.G., Physicochemical Hydrodynamics, Prentice-Hall, (1955).

40. Treybal, R., Ind. Eng. Chem., 52, 445, (1960).

41. Boye-Christensen, G. and Terjesen, S.G., Chem. Eng. Sci., 7, 222, (1958).

42. Boye-Christensen, G. and Terjesen, S.G., Chem. Eng. Sci., 9, 225, (1959).

43. Holme, A. and Terjesen, S.G., Chem. Eng. Sci., 4, 265, (1955).

44. Lindland, K.P. and Terjesen, S.G., Chem. Eng. Sci., 5, 1, (1956).

45. Thorsen, G. and Terjesen, S.G., Chem. Eng. Sci., 17, 137, (1962).

46. Calderbank, P.H., and Korchinski, I.J.O., Chem. Eng. Sci., 6, 65, (1956).

47. Elzinga, E.R. and Banchero, J.T., Chem. Eng. Prog. Symp., Series 55, 29, (1959).

48. Harriott, P., Can. J. Chem. Eng., 40, 60, (1962).

49. Garner, F.H. and Skelland, A.H.P., Chem. Eng. Sci., 4, 149, (1955).

50. Linton, M. and Sutherland, K.L., 2nd Intl. Congress of Surface Activity, Vol. 1, p.494, Butterworths Scientific Publications, (1957).

51. Sideman, S. and Shabtai, H., Can. J. Chem. Eng., 42, 107, (1964).

52. Wellek, R.M., Ph.D. Thesis, Illinois Institute of Technology, (1963).

53. Wellek, R.M. and Skelland, A.H.P., A.I.Ch.E.J., 10, 491, (1964).

54. Newman, A.B., Trans. A.I.Ch.E., 28, 310, (1931).

55. Groeber, H., Zeit. Ver. Deut. Ing., 69, 705, (1925).

56. Jakob, M., Heat Transfer, John Wiley and Sons Inc., N. Y., Vol. 1, (1949).

57. Vermeulen, T., Ind. Eng. Chem., 45, 1664, (1953).

58. Kronig, R. and Brink, J.C., Appl. Sci. Res., A-2, 142, (1950).

59. Danckwerts, P.V., Trans. Farad. Soc., 47, 1014, (1951).

60. Handlos, A.E. and Baron, T., A.I.Ch.E.J., 3, No. 1, 127, (1957).

61. Fujinawa, K., Nakaike, Y., Kagaku Kogaku, 25, 274, (1961).

62. Lightfoot, E.N., A.I.Ch.E.J., 10, 278, (1964).

63. Olander, D.R., A.I.Ch.E.J., 12, 1018, (1966).

64. Austin, L.J., Ying, W.E. and Sawistowski, H., Chem. Eng. Sci., 21, 1109, (1966).

65. Brian, P.L.T., Vivian, J.E. and Matiatos, D.C., A.I.Ch.E.J., 13, 28, (1967).

66. Olander, D.R. and Reddy, L.B., Chem. Eng. Sci., 19, 67, (1964).

67. Blokker, P.C., 2nd Int. Cong. of Surface Activity, Vol. I, 503, Butterworths Scientific Publications, (1957).

68. Bakker, C.A.P., Van Buytenen, P.M. and Beek, W.J., Chem. Eng. Sci., 21, 1039, (1966).

69. Marsh, B.D. and Heidiger, W.J., A.I.Ch.E.J., 4, 129, (1965).

70. Heertjes, P.M. and de Nie, L.H., Chem. Eng. Sci., 21, 755, (1966).

71. Davies, J.T., Advances in Chemical Engineering, 4, 3, Academic Press, (1963).

72. Davies, J.T. and Haydon, D.A., 2nd Int. Cong. of Surface Activity, Vol. I, 417, Butterworths Scientific Publications, (1957).

73. Rose, P.M. and Kintner, R.C., A.I.Ch.E.J., 12, 530, (1966).

74. Kintner, R.C., Advances in Chemical Engineering, 4, 52, Academic Press, (1963).

75. Treybal, R.E., Liquid Extraction, 2nd Edition, McGraw-Hill Publishing Co., (1963).

76. Olander, D.R., A.I.Ch.E.J., 12, 1018, (1966).

77. Wellek, R.M. and Skelland, A.H.P., A.I.Ch.E.J., 11, 557, (1965).

78. Patel, J.M. and Wellek, R.M., A.I.Ch.E.J., 13, 384, (1967).

79. Angelo, J.B., Lightfoot, E.N. and Howard, D.W., A.I.Ch.E.J., 12, 751, (1966).

80. Schlichting, H., Boundary Layer Theory, McGraw-Hill Publishing Co., 4th Edition, (1960).

81. Satapathy, R. and Smith, W., J. Fluid Mech., 10, 561, (1961).

82. Hamielec, A.E. and Johnson, A.I., Can. J. Chem. Eng., 40, 41, (1962).

83. Hamielec, A.E., Ph.D. Thesis, U. of Toronto, (1961).

84. Nakano, Y. and ChiTien, Can. J. Chem. Eng., 45, 135, (1967).

85. Kintner, R.C., Horton, T.J., Grauman, R.E. and Amberkar, S., Can. J. Chem. Eng., 39, 235, (1961).

86. Johns, L.E. Jr. and Beckmann, R.B., A.I.Ch.E.J., 12, 10, (1966).

87. Volk, W., Applied Statistic for Engineers, McGraw-Hill Publishing Co., (1958).

88. Crow, E.L., Davis, F.A. and Maxfield, M.W., Statistics Manual, Dover Publications, No. S599.

89. Perry, J.H., Chemical Engineers' Handbook, 3rd Edition, McGraw-Hill Publishing Co., (1949).

90. Harned, H.W. and Owen, B.P., Physical Chemistry of Electrolytic Solutions, Monograph Series #137, Reinhold Publishing Corp., (1958).

91. Long, F.A. and McDevit, W.F., Chem. Revs., 158, 119, (1946).

92. Seto, P., Private Communications.

93. Hamielec, A.E., M.A.Sc. Thesis, Mass Transfer to Falling Drops, U. of Toronto, 1958.

94. Lapidus, L., Digital Computation for Chemical Engineers, McGraw-Hill Publishing Co., 1962.

95. U.S. Patent, 2830080, April 8, 1958.

VII Acknowledgement

The efforts of many people are represented in the completion of any thesis. This work is no exception. I would like to thank in particular the following individuals:-

Dr. A.I. Johnson, my research supervisor, for his guidance, inspiration and especially his patience;

Dr. A.E. Hamielec, my associate research supervisor, for his many suggestions and aid, particularly in the theoretical study of mass transfer;

Jack Whorwood, technician in the Photographic Department, for his help in solving photographic problems;

Bob Dunn, technician in the Chemical Engineering Department, for his help in the construction of the equipment;

Mrs. Sally Tanaka, typist, for her skillful and conscientious work;

and finally, but by no means least, my parents, Mr. and Mrs. Matsujiro Watada, for their quiet encouragement and understanding throughout my study.

VIII Appendices for Theoretical Section III

Appendix VIII-1

Computer Program to Solve the General Model for Mass Transfer with Reaction into Circulating Drops

A general model was developed, as shown in Equation III-3 to describe mass transfer with simultaneous chemical reaction into circulating drops. The model was solved by a finite difference approximation as given in Equation III-19.

A program was written to calculate the mass transferred, the Sherwood Number, and the drop concentration, by the method of solution outlined in Section III . However, the concentration gradients required to calculate the local Sherwood Numbers, were found by differentiating the Lagrangian interpolation of the concentrations at mesh points near the surface of the drop.

The method followed, as given by Lapidus (94), expressed the concentration gradient as:-

$$\left.\frac{dC}{dR}\right|_{R_1} = \frac{3R_1^2 - 2R_1(R_2+R_3+R_4) + (R_2R_3+R_2R_4+R_3R_4)}{(R_1-R_2)(R_1-R_3)(R_1-R_4)} C_1$$

$$+ \frac{3R_1^2 - 2R_1(R_1+R_3+R_4) + (R_1R_3+R_1R_4+R_3R_4)}{(R_2-R_1)(R_2-R_3)(R_2-R_4)} C_2$$

$$+ \frac{3R_1^2 - 2R_1(R_1+R_2+R_4) + (R_1R_2+R_1R_4+R_2R_4)}{(R_3-R_1)(R_3-R_2)(R_3-R_4)} C_3$$

$$+ \frac{3R_1^2 - 2R_1(R_1+R_2+R_3) + (R_1R_2+R_1R_3+R_2R_3)}{(R_4-R_1)(R_4-R_2)(R_4-R_3)} C_4 \qquad \text{(VIII-1)}$$

where C_1, C_2, C_3 and C_4 were the concentrations at a sequence of radial mesh points, beginning with point R_1 at the surface of the drop and going inside to point R_4.

The program listing and sample output are included at the rear of this section. The input data are defined below, in the order of their appearance:-

JCONT This is a switch to determine the initial concentration profile in the drop.

If JCONT = 1, the initial concentration profile inside the drop equals zero.

If JCONT $\neq$ 1, the initial concentration profile inside the drop is read in from a set of binary input data cards.

Thus, if the calculations were interrupted at any time, a set of binary data cards may be punched out along with the final output data. When the calculations were resumed later, these binary data cards may be used as input to redefine the initial concentration profile. The program as given shows only the provisions for binary data deck input. If required, the statements to produce binary deck outputs can be easily entered at the end of the program.

KRUN = program number

NRINC = number of radial increments

NAINC = number of angular increments

PE = Peclet Number

RK = dimensionless reaction rate constant

VR = $\frac{\text{viscosity of dispersed phase}}{\text{viscosity of continuous phase}}$

DT = dimensionless time step

NPRINT = number of printouts

NINT = number of iterations per printout

The velocity profile may be readily changed by replacing the functions for:-

VTH = dimensionless angular velocity component

VRAD = dimensionless radial velocity component

in the section titled C COEFF FOR MARCHING CALCN

The program listing is as shown in the following pages.

VIII-1-a Program Listing

```
C      PROGRAM FOR STUDYING CONCENTRATION CHANGE IN CIRCULATING DROPS
C      WITH FIRST ORDER REACTION.
C
C      PE IS PECLET NO ,RK IS REACTION CONSTANT,VR IS VISCOSITY RATIO
C      NRINC IS NO OF RADIAL MESH POINTS,NAINC IS NO ANGULAR MESH POINTS
C  TCOEFF = COEFF FOR CALCN OF MASS TRANSFERRED
C PAMAS = MASS TRANSFERRED DURING TIME DT
C  TMAS = TOTAL MASS TRANSFERRED UP TO TIME T
C DT IS TIME INCREMENT,          NPRINT IS NO. OF PRINTOUTS
C NINT IS NO. OF ITERATIONS
C
      DIMENSION C(45,31,2),A1(45),R(45),SHLO(45),WSIN(31),WCOS(31),
     1  COTAN(31),A2(45,31),A3(45,31),A4(45,31),A5(45,31)
C
      READ (5,100) JCONT
      READ(5,100) KRUN,NRINC,NAINC
      READ(5,102) PE,RK,VR
      READ(5,104) DT,NPRINT,NINT
      WRITE(6,101) KRUN,NRINC,NAINC
      WRITE(6,103) PE,RK,VR
      WRITE(6,105) DT,NPRINT,NINT
C     CALCULATE RADIAL AND ANGULAR INCREMENTS
      LR=NRINC-1
      LR2 = NRINC - 2
      LR3 = NRINC - 3
      LA=NAINC-1
      DR=1./FLOAT(LR)
      DA=3.1416/FLOAT(LA)
      TCOEF  = DT*DA*3.1415926/4.
C  CALCULATION OF SIN, COS, COTAN, AND RADII IN ARRAY
      DO 212 J = 1,NAINC
      ANG = DA*FLOAT(J-1)
      WSIN(J) = SIN(ANG)
      WCOS(J) = COS(ANG)
  212 COTAN(J) = WCOS(J)/WSIN(J)
      DO 213 I = 1,NRINC
      R(I) = DR*FLOAT(I-1)
213   CONTINUE
      AREA = 0.0
      DO 26 J = 2,NAINC
      AREA = AREA +.3.1415926*(WSIN(J) + WSIN(J-1))*DA
26    CONTINUE
      WRITE (6,233) AREA
C COEFF FOR MARCHING CALCN
      X1 = DT/DR
      X2 = X1/DR
      X3 = PE*X1/4.
      X5 = DT/DA
      X6 = X5/DA
      X7 = X5/2.
      X8 = PE*X5/4.
      V1 = 2.*(VR+1.)
      DO 1 J = 2,NAINC
      DO 1 I = 2,NRINC
      V1R = -(1. - 2.*R(I)*R(I))*WSIN(J)/V1
      VRAD = (1. - R(I)*R(I))*WCOS(J)/V1
```

```
   22 A1(J) = 1. - 2.*X2 - 2.*X6/(R(I)*R(I)) - RK*DT
      A2(I,J) = X2 + X1/R(I) - VRAD*X3
      A3(I,J) = X2 - X1/R(I) + VRAD*X3
      A4(I,J) =  COTAN(J)*X7/(R(I)*R(I)) + X6/(R(I)*R(I)) - VTH*X8/R(I)
     1 A5(I,J) = -COTAN(J)*X7/(R(I)*R(I)) + X6/(R(I)*R(I)) + VTH*X8/R(I)
C  COEFF FOR CALC OF LOCAL SH NO
      R1 = DR*FLOAT(NRINC - 2)
      R2 = DR*FLOAT(NRINC - 3)
      R3 = DR*FLOAT(NRINC - 4)
      R4 = R1*R2
      R5 = R1*R3
      R6 = R2*R3
      ANUM1 = 3. - 2.*(R1 + R2 + R3) + (R4 + R5 + R6)
      ANUM2 = 3. - 2.*(1. + R2 + R3) + (R2 + R3 + R6)
      ANUM3 = 3. - 2.*(1. + R1 + R3) + (R1 + R3 + R5)
      ANUM4 = 3. - 2.*(1. + R1 + R2)+ (R1 + R2 + R4)
      DEN1 = (1. - R1)*(1. - R2)*(1. - R3)
      DEN2 = (R1 - 1.)*(R1 - R2)*(R1 - R3)
      DEN3 = (R2 - 1.)*(R2 - R1)*(R2 - R3)
      DEN4 = (R3 - 1.)*(R3 - R1)*(R3 - R2)
      F1 = ANUM1/DEN1
      F2 = ANUM2/DEN2
      F3 = ANUM3/DEN3
      F4 = ANUM4/DEN4
C READING IN OF THE BINARY DECK
      IF (JCONT.EQ.1) GO TO 20
      READ (5) ((C(I,J,1), I = 1,NRINC), J = 1,NAINC)
      READ (5) TIME, TMAS
      GO TO 21
C     SET BOUNDARY CONDITIONS AND INITIAL CONDITIONS
   20 DO 2 I = 1,NRINC
      DO 2 J=1,NAINC
      IF (I.EQ.NRINC) GO TO 11
      C(I,J,1) = 0.0
      GO TO 2
   11 C(I,J,1) = 1.
    2 CONTINUE
      TIME=0.
      TMAS = 0.0
      PAMAS = 0.0
      IF (JCONT.EQ.1) GO TO 90
   21 WRITE (6,111) TIME, ((C(I,J,1), I=1,NRINC,4), J = 1,NAINC)
      WRITE (6,232) PAMAS, TMAS
C     START MARCHING CALCULATIONS
   91 JCONT = 5
      DO 4 K=1,NPRINT
      DO 7 KK=1,NINT
      TIME=TIME+DT
      DO 5 I=2,LR
      DO 5 J=2,LA
      C(I,J,2) = C(I,J,1)*A1(I) + C(I+1,J,1)*A2(I,J) + C(I-1,J,1)*A3(I,J
     1)  + C(I,J+1,1)*A4(I,J) + C(I,J-1,1)*A5(I,J)
5     CONTINUE
      DO 600 I=2,LR
      C(I,1,2)=C(I,2,2)
  600 C(I,NAINC,2) = C(I,LA,2)
      DO 201 J=1,NAINC
      C(1,J,2) = (C(2,1,2) + C(2,NAINC,2))/2.
```

```
201     CONTINUE
        DO 6 I=1,LR
        DO 6 J = 1,NAINC
        C(I,J,1)=C(I,J,2)
6       CONTINUE
C CALC OF LOCAL SHERWOOD NO BY DIFFERENTIAL OF LAGRANGE INTERPOLATION
   90   DO 210 J = 1,NAINC
        GRAD = F1 + F2*C(LR,J,1) + F3*C(LR2,J,1) + F4*C(LR3,J,1)
  210   SHLO(J) =  2.*GRAD
C   CALCN OF MASS TRANSFERRED
        PAMAS = 0.0
        DO 25 J = 2,NAINC
        PAMAS = PAMAS + TCOEF*(SHLO(J) + SHLO(J-1))*(WSIN(J) + WSIN(J-1))
25      CONTINUE
        TMAS = TMAS + PAMAS
    7   CONTINUE
C DROP CONCENTRATION BASED ON RESULTS OBTAINED FROM INTEGRATION OF LOCAL SH NO
C AND INCRECREMENTAL SURFACE AREAS. TOTAL MASS TRANSFERRED/4.188790132 = CONC
        CONC = TMAS/4.188790132
C CALCULATION OF OVERALL SHERWOOD NO BY TRAPEZOIDAL INTEGRATION OF LOC SH NO
        SHAV = 0.0
        DO 211 J = 2,NAINC
        SHAV = SHAV + DA*(SHLO(J)*WSIN(J) + SHLO(J-1)*WSIN(J-1))/4.
211     CONTINUE
        WRITE (6,111) TIME, ((C(I,J,1), I=1,NRINC,4), J = 1,NAINC)
        WRITE (6,230)
        WRITE (6,231) (SHLO(J), J = 1,NAINC)
        WRITE (6,202) SHAV
C CALCULATION OF THE AVG CONCENTRATION IN THE DROP
        VOL=0.
        TAMR1 = 0.0
        DO 15 I=2,NRINC
        DO 15 J=2,NAINC
        DVOL = 6.2832*R(I)*R(I)*WSIN(J)*DR*DA
        VOL=VOL+DVOL
        PCONC = (C(I,J,1) + C(I-1,J,1) + C(I,J-1,1) + C(I-1,J-1,1))*DVOL/4
       1.
        TAMR1 = PCONC + TAMR1
   15   CONTINUE
        WRITE(6,113) VOL
        AVCON2 = TAMR1/VOL
        CONJ = 1.0 - AVCON2
        SHJON = SHAV/CONJ
        WRITE (6,240) CONC
        WRITE (6,242) AVCON2
        WRITE (6,243) SHJON, CONJ
    4   WRITE (6,232) PAMAS, TMAS
        IF (JCONT.EQ.1) GO TO 91
C PRINTOUT OF BINARY DECK, WHERE JCONT IS COUNTER FOR READING IN THE DECK
        STOP
  100   FORMAT(3I5)
  101   FORMAT(7H RUN NO,I5,3HFOR,I5,21HRADIAL INCREMENTS AND,I5,
       1)HANGULAR INCREMENTS)
  102   FORMAT(3F10.2)
  103   FORMAT(10H PECLET NO,F10.2,17HREACTION CONSTANT,F10.2,15HVISCOSITY
       . 1 RATIO,F10.5)
  104   FORMAT (F20.15, 2I5)
  105   FORMAT(15H TIME INCREMENT,F15.10, 15HNO OF PRINTOUTS, I5, 23HINCRE
```

```
     1MENTS PER PRINTOUT, I5)
  106 FORMAT (3F15.7)
  107 FORMAT (1H0, 2X, 2HA1, F8.4, 2X, 2HB1, F10.5, 2X, 5HRE NO, F10.5)
  111 FORMAT (1X, 7HTIME IS, F10.5,/(2X, 11F6.3))
  113 FORMAT(2X,9HVOLUME IS,F10.5)
  202 FORMAT (1H0, 2X, 12HAVG SH NO IS,  F15.8)
  230 FORMAT (1H0, 2X, 30HLOCAL SH NO BY LAGRANGE INTERP)
  231 FORMAT (2X, 10F12.4)
  232 FORMAT (1H0, 2X, 16HMASS TRANS IN DT, F10.6, 4X, 22HTOTAL MASS TRA
     1NSFERRED, F10.6)
  233 FORMAT (1H0, 2X, 23HSURFACE AREA OF DROP IS, 2X, F10.5)
  240 FORMAT (1H0, 2X, 36HDROP CONC FROM INTEG OF LOC SH NO = , 2X,
     1 F10.6)
  242 FORMAT (1H0, 2X, 20HCORRECTED AVG CONC =, F15.6)
  243 FORMAT (/2X, 13HSH NO JOHNS =, F15.8, 2X, 16HAVG CONC-JOHNS =,
     1 F15.6/)
      END
```

VIII-1-b Sample Output

In the output, most of the terms are self-explanatory. The concentration profile in the drop form a large part of the output.

With physical mass transfer, the term titled, "CORRECTED AVG CONC", represents the mass transferred, as well as the average solute concentration in the drop. However, the mass transferred with simultaneous chemical reaction in a drop, is given as "TOTAL MASS TRANSFERRED". The term titled, "SH NO JOHNS", represents the modified Sherwood Number as given by Equation III The term titled, "AVG CONC-JOHNS", which equals (1.0 - Average Drop Concentration), was required to calculate the modified Sherwood Number.

The sample output is as shown:-

Sample Output

```
RUN NO     1FOR   41RADIAL INCREMENTS AND   31ANGULAR INCREMENTS
PECLET NO        0.00REACTION CONSTANT      10.00VISCOSITY RATIO    0.00000
TIME INCREMENT     .000002500NO OF PRINTOUTS   50INCREMENTS PER PRINTOUT

  SURFACE AREA OF DROP IS      12.55488
TIME IS    0.00000
  0.000 0.000 0.000 0.000 0.000 0.000 0.000 0.000 0.000 0.000 1.000
  0.000 0.000 0.000 0.000 0.000 0.000 0.000 0.000 0.000 0.000 1.000
  0.000 0.000 0.000 0.000 0.000 0.000 0.000 0.000 0.000 0.000 1.000
  0.000 0.000 0.000 0.000 0.000 0.000 0.000 0.000 0.000 0.000 1.000
  0.000 0.000 0.000 0.000 0.000 0.000 0.000 0.000 0.000 0.000 1.000
  0.000 0.000 0.000 0.000 0.000 0.000 0.000 0.000 0.000 0.000 1.000
  0.000 0.000 0.000 0.000 0.000 0.000 0.000 0.000 0.000 0.000 1.000
  0.000 0.000 0.000 0.000 0.000 0.000 0.000 0.000 0.000 0.000 1.000
  0.000 0.000 0.000 0.000 0.000 0.000 0.000 0.000 0.000 0.000 1.000
  0.000 0.000 0.000 0.000 0.000 0.000 0.000 0.000 0.000 0.000 1.000
  0.000 0.000 0.000 0.000 0.000 0.000 0.000 0.000 0.000 0.000 1.000
  0.000 0.000 0.000 0.000 0.000 0.000 0.000 0.000 0.000 0.000 1.000
  0.000 0.000 0.000 0.000 0.000 0.000 0.000 0.000 0.000 0.000 1.000
  0.000 0.000 0.000 0.000 0.000 0.000 0.000 0.000 0.000 0.000 1.000
  0.000 0.000 0.000 0.000 0.000 0.000 0.000 0.000 0.000 0.000 1.000
  0.000 0.000 0.000 0.000 0.000 0.000 0.000 0.000 0.000 0.000 1.000
  0.000 0.000 0.000 0.000 0.000 0.000 0.000 0.000 0.000 0.000 1.000
  0.000 0.000 0.000 0.000 0.000 0.000 0.000 0.000 0.000 0.000 1.000
  0.000 0.000 0.000 0.000 0.000 0.000 0.000 0.000 0.000 0.000 1.000
  0.000 0.000 0.000 0.000 0.000 0.000 0.000 0.000 0.000 0.000 1.000
  0.000 0.000 0.000 0.000 0.000 0.000 0.000 0.000 0.000 0.000 1.000
  0.000 0.000 0.000 0.000 0.000 0.000 0.000 0.000 0.000 0.000 1.000
  0.000 0.000 0.000 0.000 0.000 0.000 0.000 0.000 0.000 0.000 1.000
  0.000 0.000 0.000 0.000 0.000 0.000 0.000 0.000 0.000 0.000 1.000
  0.000 0.000 0.000 0.000 0.000 0.000 0.000 0.000 0.000 0.000 1.000
  0.000 0.000 0.000 0.000 0.000 0.000 0.000 0.000 0.000 0.000 1.000
  0.000 0.000 0.000 0.000 0.000 0.000 0.000 0.000 0.000 0.000 1.000
  0.000 0.000 0.000 0.000 0.000 0.000 0.000 0.000 0.000 0.000 1.000
  0.000 0.000 0.000 0.000 0.000 0.000 0.000 0.000 0.000 0.000 1.000
  0.000 0.000 0.000 0.000 0.000 0.000 0.000 0.000 0.000 0.000 1.000
  0.000 0.000 0.000 0.000 0.000 0.000 0.000 0.000 0.000 0.000 1.000

  LOCAL SH NO BY LAGRANGE INTERP
      146.6667    146.6667    146.6667    146.6667    146.6667    146.6667
      146.6667    146.6667    146.6667    146.6667    146.6667    146.6667
      146.6667    146.6667    146.6667    146.6667    146.6667    146.6667
      146.6667

  AVG SH NO IS    146.53260987
 VOLUME IS    4.34321

  DROP CONC FROM INTEG OF LOC SH NO =        .000549

  CORRECTED AVG CONC =          .036134

 SH NO JOHNS =    152.02586610  AVG CONC-JOHNS =         .96386631

  MASS TRANS IN DT    .002302    TOTAL MASS TRANSFERRED    .002302
```

Appendix VIII-2

Program to Solve the Danckwerts' Modification of the Kronig and Brink Equation for Mass Transfer with Chemical Reaction in Circulating Drops

The Kronig and Brink equation was modified by Danckwerts to account for mass transfer with chemical reaction in circulating drops, as shown in Equation III-33. A program was written to calculate the mass transferred, the Sherwood Number and the drop concentration, by the methods given in Section III-I-2.

The program listing and sample output are included at the end of this section.

The input data are defined below, in the order of their appearance:-

DT = dimensionless time increment

CHEM(L) = dimensionless chemical reaction rate constant

L = number of different reaction rate constants analyzed

A(I), U(I) = functions for the Kronig and Brink equation as given by Heertjes et al (18) in Table II-1

I = number of functions in the series solution

In the output, the title "SH NO JOHNS" is used to represent the modified Sherwood Number as given by Equation III-40. The term titled, "CONC-JOHNS", equals (1.0 - average drop concentration).

VIII-2-a Program Listing

```
C
C      DANCKWERTS METHOD FOR K AND B USING ANALYTICAL METHOD FOR SH NO
C
       DIMENSION CHEM(5), TIME(50), CONC(50), CMAS(50), SHNO(50),
      1 RATE(50), CONJ(50), SHJON(50), TMAS(50), A(7), U(7)
       READ (5,101) DT
       L4 = 1
       READ (5,101) (CHEM(L), L = 1,L4)
       READ (5,101) (A(I), I = 1,7)
       READ (5,101) (U(I), I = 1,7)
       VOL = 4.0*3.1415926/3.0
       WRITE (6,105) (A(I), I = 1,7)
       WRITE (6,106) (U(I), I = 1,7)
       DO 10 L = 1,L4
       WRITE (6,107)
       WRITE (6,102) CHEM(L), DT
       DO 2 K = 1,41
       TIME(K) = DT*FLOAT(K-1)
       DUM1 = 0.0
       DUM2 = 0.0
       DUM3 = 0.0
       DO 4 I = 1,7
       ANUM = A(I)*A(I)
       X = 16.0*U(I)
       REACT = CHEM(L) + X
       FUNC = X/EXP(TIME(K)*REACT)
       FUNC2 = (CHEM(L) + FUNC)*ANUM/REACT
       DUM1 = DUM1 + FUNC2*U(I)
       DUM2 = DUM2 + ANUM*U(I)*(CHEM(L)*TIME(K)*REACT - FUNC + X)/(REACT
      1 *REACT)
       DUM3 = DUM3 + FUNC2
     4 CONTINUE
C
       SHNO(K) = 4.0*DUM1
       CMAS(K) = 6.0*DUM2
       CONC(K) = 1.0 - 0.375*DUM3
       RATE(K) = 1.5*SHNO(K)
       TMAS(K) = VOL*CMAS(K)
C
C      CONVERSION TO JOHNS NOTATION
       CONJ(K) = 1.0 - CONC(K)
       SHJON(K) = SHNO(K)/CONJ(K)
     2 CONTINUE
C
       WRITE (6,103)
       WRITE (6,104) (TIME(K), RATE(K), SHNO(K), CONC(K), TMAS(K),
      1CMAS(K), CONJ(K), SHJON(K), K = 1,41)
    10 CONTINUE
C
   101 FORMAT (7F10.3)
   102 FORMAT (2X, 15HREACTION RATE =, F15.3, 2X, 4HDT =, F15.6/)
   103 FORMAT (6X, 4HTIME, 10X, 4HRATE, 10X, 4HSHNO, 10X, 4HCONC, 2X,
      1 10HTOTAL MASS, 4X, 8HMASS/VOL, 4X, 10HCONC-JOHNS, 4X,
      2 10HSHNO-JOHNS//)
   104 FORMAT (2X, F8.5, 3F14.6, 2F12.6, 2F14.6)
   105 FORMAT (/2X, 4HA(I)/ 2X, 7F10.4//)
   106 FORMAT (/2X, 4HU(I)/ 2X, 7F10.4//)
   107 FORMAT (///)

       END
```

VIII-2-b Sample Output

A(I)

1.3300 0.6000 0.3600 0.3500 0.2800 0.2200 0.1600

U(I)

1.6780 8.4800 21.1000 38.5000 63.0000 89.9000 123.8000

REACTION RATE = 100.000 DT = 0.001000

TIME	RATE	SHNO	CONC	TOTAL MASS	MASS/VOL	CONC-JOHNS	SHNO-JOHNS
0.0	155.588470	103.725647	0.049977	0.0	0.0	0.950023	109.182190
0.00100	82.923294	55.282196	0.155755	0.468060	0.111741	0.844245	65.481247
0.00200	59.742615	39.828415	0.211611	0.759018	0.181202	0.788389	50.518707
0.00300	50.069885	33.379929	0.247831	0.986488	0.235507	0.752169	44.378220
0.00400	45.140457	30.093643	0.274036	1.184882	0.282870	0.725964	41.453339
0.00500	42.258957	28.172638	0.294168	1.367449	0.326455	0.705832	39.914062
0.00600	40.409180	26.939453	0.310190	1.540328	0.367726	0.689810	39.053436
0.00700	39.141312	26.094208	0.323234	1.706782	0.407464	0.676766	38.557205
0.00800	38.230515	25.487015	0.334014	1.868731	0.446127	0.665986	38.269577
0.00900	37.553238	25.035492	0.343024	2.027384	0.484002	0.656976	38.107132
0.01000	37.036346	24.690903	0.350613	2.183557	0.521286	0.649387	38.021820
0.01100	36.633957	24.422638	0.357046	2.337817	0.558113	0.642954	37.985031
0.01200	36.315765	24.210510	0.362527	2.490579	0.594582	0.637473	37.978851
0.01300	36.061020	24.040680	0.367215	2.642143	0.630765	0.632785	37.991837
0.01400	35.854950	23.903305	0.371239	2.792750	0.666720	0.628761	38.016541
0.01500	35.686844	23.791229	0.374704	2.942573	0.702488	0.625296	38.047928

Appendix VIII-3

Program to Solve the Danckwerts' Modification of the Newman Equation for Mass Transfer with Chemical Reaction in Stagnant Drops

The Newman equation was modified by Danckwerts to account for mass transfer with chemical reaction in stagnant drops, as shown in Equation III-29. A program was written to calculate the mass transferred, the Sherwood Number and the drop concentrations, by the methods given in Section III-I-1.

The program listings and sample outputs are included at the end of this section.

The input data are defined below, in the order of their appearance:-

DT = dimensionless time increment

CHEM(L) = dimensionless chemical reaction rate constant

L = number of different reaction rate constants analysed

In the output, the title "SH NO JOHNS", is used to represent the modified Sherwood Number as given by Equation III-40. The term entitled, "CONC - JOHNS", equals (1.0 - average drop concentration). The program listing is as shown in the following page.

VIII-3-a Program Listing

```
C
C       DANCKWERTS MODIFICATION OF THE NEWMAN EQUATION
C
        DIMENSION CHEM(5), TIME(45), CONC(5,45), CMAS(5,45), SHNO(5,45),
       1 RATE(5,45), CONJ(5,45), SHJON(5,45), TMAS(5,45)
        L4 = 1
        READ (5,101) DT, (CHEM(L), L = 1,L4)
        DUM4 = 6.0/(3.1415926**2)
        VOL = 4.0*3.1415926/3.0
C
        DO 10 L = 1,L4
        WRITE (6,102) CHEM(L), DT
         DO 2  K = 1,41
        TIME(K) = DT*FLOAT(K-1)
        DUM1 = 0.0
        DUM2 = 0.0
        DUM3 = 0.0
        DO 4 I = 1,10
        X = FLOAT(I)
        Y = (X*3.1415926)**2
        REACT = CHEM(L) + Y
        FUNC = EXP(TIME(K)*REACT)
        FUNC2 = (CHEM(L) + Y/FUNC)/REACT
        DUM1 = DUM1 + FUNC2
        DUM3 = DUM3 + FUNC2/(X*X)
        DUM2 = DUM2 + (REACT*CHEM(L)*TIME(K) + Y - Y/FUNC)/REACT**2
      4 CONTINUE
        SHNO(L,K) = 4.0*DUM1
        RATE(L,K) = 1.5*SHNO(L,K)
        CMAS(L,K) = 6.0*DUM2
        TMAS(L,K) = VOL*CMAS(L,K)
        CONC(L,K) = 1.0 - DUM4*DUM3
C
C       CONVERSION TO JOHNS NOTATION
        CONJ(L,K) = 1.0 - CONC(L,K)
        SHJON(L,K) = SHNO(L,K)/CONJ(L,K)
      2 CONTINUE
        WRITE (6,103)
        WRITE (6,104) (TIME(K), RATE(L,K), SHNO(L,K), CONC(L,K),
       1 TMAS(L,K), CMAS(L,K), CONJ(L,K), SHJON(L,K), K = 1,41)
     10 CONTINUE
        STOP
    101 FORMAT (8F10.2)
    102 FORMAT (2X, 15HREACTION RATE =, F15.3, 2X, 4HDT =, F15.6/)
    103 FORMAT (6X, 4HTIME, 10X, 4HRATE, 10X, 4HSHNO, 10X, 4HCONC, 2X,
       1 10HTOTAL MASS, 4X, 8HMASS/VOL, 4X, 10HCONC-JOHNS, 4X,
       2 10HSHNO-JOHNS//)
    104 FORMAT (2X, F8.5, 3F14.6, 2F12.6, 2F14.6)
        END
```

VIII-3-b Sample Output

The sample output is as shown in the next page.

Sample Output

EACTION RATE = 100.000 DT = 0.001000

TIME	RATE	SHNO	CONC	TOTAL MASS	MASS/VOL	CONC-JOHNS	SHNO-JOHNS
0.0	60.000000	40.000000	0.057856	0.0	0.0	0.942144	42.456329
0.00100	43.778229	29.185486	0.106203	0.213360	0.050936	0.893797	32.653351
0.00200	35.493622	23.662415	0.138846	0.377585	0.090142	0.861154	27.477554
0.00300	30.895172	20.596786	0.162493	0.515757	0.123128	0.837507	24.592972
0.00400	28.137009	18.758011	0.180498	0.638938	0.152535	0.819502	22.889511
0.00500	26.368484	17.578995	0.194689	0.752840	0.179727	0.805311	21.828827
0.00600	25.171326	16.780884	0.206148	0.860632	0.205461	0.793852	21.138550
0.00700	24.325470	16.216980	0.215558	0.964201	0.230186	0.784442	20.673279
0.00800	23.707596	15.805073	0.223386	1.064736	0.254187	0.776614	20.351257
0.00900	23.244308	15.496212	0.229961	1.163028	0.277653	0.770039	20.123917
0.01000	22.889648	15.259769	0.235524	1.259619	0.300712	0.764476	19.961090
0.01100	22.613586	15.075733	0.240261	1.354897	0.323458	0.759739	19.843292
0.01200	22.395721	14.930481	0.244314	1.449147	0.345959	0.755686	19.757507
0.01300	22.221817	14.814545	0.247795	1.542581	0.368264	0.752205	19.694809
0.01400	22.081619	14.721085	0.250796	1.635358	0.390413	0.749204	19.648956
0.01500	21.967697	14.645138	0.253393	1.727606	0.412436	0.746607	19.615570
0.01600	21.874435	14.582966	0.255643	1.819422	0.434355	0.744357	19.591354
0.01700	21.797638	14.531761	0.257598	1.910882	0.456190	0.742402	19.573975
0.01800	21.733994	14.489338	0.259302	2.002049	0.477954	0.740698	19.561737
0.01900	21.681030	14.454029	0.260788	2.092974	0.499661	0.739212	19.553284
0.02000	21.636749	14.424507	0.262088	2.183696	0.521319	0.737912	19.547729
0.02100	21.599594	14.399731	0.263224	2.274248	0.542937	0.736776	19.544250
0.02200	21.568268	14.378849	0.264220	2.364655	0.564520	0.735780	19.542328
0.02300	21.541809	14.361210	0.265094	2.454947	0.586076	0.734906	19.541550
0.02400	21.519379	14.346256	0.265861	2.545130	0.607605	0.734139	19.541611
0.02500	21.500305	14.333542	0.266536	2.635228	0.629115	0.733464	19.542252
0.02600	21.484055	14.322712	0.267129	2.725254	0.650607	0.732871	19.543289
0.02700	21.470184	14.313461	0.267653	2.815218	0.672084	0.732347	19.544632
0.02800	21.458313	14.305550	0.268113	2.905124	0.693547	0.731887	19.546127
0.02900	21.448120	14.298756	0.268520	2.994987	0.715001	0.731480	19.547714

Appendix VIII-4

The Effect of Mesh Size on Computed Results for Physical Mass Transfer into Drops

Computed mass transfer results are compared for physical mass transfer into drops with Hadamard-Rybczynski velocity profile and modified Peclet Number Pe_J = 250.

	Dimensionless Concentrations		
Dimensionless Time	Kronig and Brink Model	Mesh Size (81,31)	Mesh Size (41,31)
.0005	.108	.073	.078
.001	.160	.102	.105
.002	.225	.143	.145
.003	.270	.175	.178
.004	.305	.203	.205
.005	.340	.230	.230
.008	.425		.305
.011	.475		.360
.014	.523		.470
.016	.550		.520
.018	.585		.560
.020	.610		.590

Appendix VIII-5

The Effect of Wall Proximity on Physical Mass Transfer into Drops

The effect of wall proximity increasing the Hadamard-Rybczynski velocity profile on mass transfer is shown for 1.5, 4 and 8 times the velocity rate at viscosity ratio $\frac{\mu_i}{\mu_o} = 0$

Dimensionless Concentrations

Dimensionless Time	Kronig and Brink Model	Matrix (81,31) 8 x Had.Vel.	Matrix (41,31) 1.5 x Had.Vel.	Matrix (41,31) 4 x Had.Vel.
.0005	.108	.073	.078	.078
.0010	.160	.113	.105	.105
.0015	.190	.150	.128	.130
.0020	.225	.198	.145	.155
.0025	.250	.240	.163	.185
.0030	.270	.270	.177	.215
.0040	.305	.305	.208	.277
.0050	.340	.338	.240	.330
.0060	.368	.365	.275	.365
.0070	.392		.310	.387
.0080	.425		.345	.405
.0090	.437		.380	.428
.0100	.455		.418	.455
.0110	.475		.448	.470
.0120	.490		.476	.490
.0140	.523		.515	
.0160	.550		.545	

Appendix VIII-6

Variations of Modified Sherwood Number Sh_J with Time for Physical Mass Transfer into Drops at Various Modified Peclet Numbers Pe_J

Pe	Pe_J	X	RK	t	$\bar{C}$	Sh	Sh_J
0	0	0	0	0	.036	146.53	152.5
				.00125	.118	31.55	35.9
				.0025	.162	20.90	25.0
				.00375	.195	16.55	20.6
				.005	.223	14.02	18.05
				.0075	.269	11.05	15.1
				.0100	.306	9.29	13.4
				.0125	.338	8.09	12.2
				.0150	.366	7.21	11.4
				.0175	.392	6.53	10.75
				.0200	.415	5.98	10.20
				.0250	.456	5.13	9.43
				.0300	.492	4.51	8.9
				.0350	.524	4.03	8.45
				.0400	.553	3.64	8.15
				.0450	.579	3.32	7.88
				.0500	.603	3.04	7.65
80	20	0	0	0	.036	146.53	152.5
				.00125	.117	31.55	35.8
				.0025	.161	20.92	24.9
				.00375	.195	16.58	20.6
				.005	.222	14.06	18.1
				.0075	.268	11.12	15.2
				.010	.305	9.39	13.5
				.0125	.337	8.22	12.4
				.015	.365	7.38	11.6
				.0175	.390	6.72	11.0
				.0200	.414	6.21	10.6
				.0250	.456	5.43	9.98
				.0300	.493	4.87	9.60
				.0350	.527	4.45	9.43
				.0400	.559	4.12	9.35

Appendix VIII-6 (cont'd)

Pe	Pe_J	X	RK	t	$\bar{C}$	Sh	Sh_J
320	80	0	0	0	.036	146.53	152.5
				.00125	.117	31.69	35.9
				.0025	.161	21.19	25.3
				.00375	.194	17.00	21.1
				.005	.222	14.66	18.9
				.0075	.268	12.09	16.5
				.010	.308	10.75	15.55
				.0125	.344	9.96	15.2
				.015	.378	9.47	15.2
				.0175	.411	9.14	15.5
				.020	.444	8.93	16.0
				.0250	.510	8.65	17.6
				.030	.576	8.39	19.8
				.035	.640	7.85	21.8
				.040	.698	6.89	22.8
400	100	0	0	0	.036	146.53	152.5
				.00125	.117	31.77	36.1
				.0025	.161	21.35	25.5
				.00375	.194	17.26	21.4
				.005	.247	13.59	18.1
				.0075	.269	12.64	17.3
				.010	.311	11.48	16.7
				.0125	.349	10.85	16.7
				.0150	.387	10.49	17.2
				.0175	.426	10.27	17.9
				.020	.464	10.13	18.9
				.025	.541	9.89	21.6
				.030	.616	9.19	23.9
				.035	.682	7.72	24.3
				.040	.735	6.00	22.7

Appendix VIII-6 (cont'd)

Pe	Pe_J	X	RK	t	$\bar{C}$	Sh	Sh_J
1000	250	0	0	.0005	.078	57.5	62.5
				.001	.105	37.5	41.9
				.002	.145	26.0	30.4
				.003	.178	22.5	27.4
				.005	.228	19.41	25.1
				.007	.280	18.68	26.0
				.010	.360	18.44	28.8
				.012	.419	18.32	31.5
				.015	.500	16.41	32.8
				.0175	.554	12.62	28.2
				.020	.590	9.00	21.9
				.025	.646	6.21	17.6
				.030	.699	5.68	18.9
				.035	.730	5.29	19.6
				.040	.767	4.34	18.6
				.0445	.794	3.60	17.5
8000	1000	1	0	0	.036	146.53	152.5
				.00125	.119	50.92	57.8
				.0025	.185	49.37	60.6
				.00375	.263	49.17	66.8
				.005	.370	36.16	50.75
				.0075	.398	15.70	26.1
				.010	.454	14.99	27.5
				.0125	.499	11.11	22.2
				.0150	.538	10.55	22.8
				.0175	.572	8.76	20.5
				.020	.603	8.27	20.8
				.025	.657	6.804	19.8
				.030	.702	5.74	19.3
				.035	.740	4.91	18.9
				.040	.773	4.24	18.7

Appendix VIII-6 (cont'd)

	RK	t	$\bar{C}$	Sh	Sh_J
Newman Equation	0	.001	.109	28.69	32.19
		.002	.146	22.31	26.13
		.003	.177	18.39	22.33
		.005	.224	13.94	17.98
		.007	.262	11.49	15.57
		.010	.309	9.28	13.43
		.015	.370	7.21	11.44
		.020	.419	5.98	10.29
		.025	.460	5.14	9.52
		.030	.496	4.51	8.96
		.035	.528	4.03	8.55
		.040	.557	3.64	8.22
Kronig and Brink Equation	0.0	.001	.161	53.30	63.49
		.002	.225	35.49	45.80
		.003	.272	27.25	37.41
		.005	.340	19.61	29.72
		.007	.393	15.86	26.13
		.010	.456	12.64	23.24
		.015	.539	9.60	21.17
		.020	.603	7.76	19.57
		.025	.656	6.48	18.86
		.030	.701	5.51	18.46
		.035	.740	4.75	18.22
		.040	.773	4.11	18.09

Appendix VIII-7

Effect of Viscosity Ratio on Circulation Time T for Hadamard Streamlines ψ_i.

It was shown in Equation III-17, that the dimensionless circulation time, $T = \frac{8(1+X)\,q(\xi)}{Pe}$ according to Kronig and Brink (58):

where $q(\xi) = 3.26$ for $\xi = 0.1$ at Peclet Number = 1000.

The Kronig and Brink co-ordinate $\xi = 0.1$ is equivalent to the streamline $\psi_i = -\frac{.0061}{1+X}$

at $\theta = 90^\circ$, this streamline cuts the radius

at R = 0.16 and 0.985

Viscosity Ratio = $\frac{\mu_i}{\mu_o}$	Multiples of Hadamard Velocity	Circulation Time (dimensionless)
0	1	.0261
	1.5	.0175
	4	.0065
	8	.0033
2	1	.0783
	1.5	.0525
	4	.0195
	8	.0099

Appendix VIII-8

Physical Mass Transfer into Drops with Hamielec Velocity Profiles at Viscosity Ratios of 0 and 2 at Reynold Number = 60

Pe	X	RK	t	$\overline{C}$	Sh	Sh_J
1000	0	0.0	0	.036	146.53	152.5
			.0005	.078	59.53	64.5
			.001	.106	42.10	47.2
			.002	.149	34.20	40.2
			.003	.187	32.57	40.2
			.005	.262	31.99	43.5
			.007	.346	31.63	48.5
			.010	.416	19.02	32.6
			.0125	.500	11.50	23.0
			.0150	.543	10.24	22.4
1000	2	0.0	0	.036	146.53	152.5
			.0005	.078	58.80	63.8
			.001	.106	40.64	45.5
			.002	.149	31.59	37.2
			.003	.187	29.11	35.9
			.005	.257	27.56	37.1
			.007	.327	27.02	40.6
			.010	.423	22.56	39.1
			.0125	.490	16.47	32.3
			.0150	.538	13.33	28.8

Appendix VIII-9

Variations of Sherwood Number with Peclet Number for Mass Transfer with Simultaneous Chemical Reaction

Pe	Pe$_J$	X	RK	t	$\bar{C}$	Sh	Sh$_J$
0	0	0	10.0	.00	.036	146.53	152.03
				.00125	.117	31.90	36.13
				.0025	.161	21.44	25.54
				.0050	.220	14.80	18.96
				.0075	.262	12.01	16.28
				.0100	.297	10.39	14.78
				.015	.350	8.56	13.17
				.020	.391	7.52	12.34
				.025	.424	6.84	11.88
				.030	.451	6.37	11.61
				.035	.474	6.02	11.46
				.040	.494	5.75	11.37
400	100	0	10.0	0	.036	146.53	152.03
				.00125	.117	32.13	36.37
				.0025	.159	21.89	26.04
				.005	.218	15.76	20.17
				.0075	.263	13.54	18.36
				.01	.301	12.47	17.84
				.0125	.336	11.91	17.92
				.0150	.369	11.59	18.36
				.0175	.401	11.41	19.05
				.020	.433	11.29	19.91
				.025	.495	11.10	21.96
				.030	.552	10.57	23.57
				.035	.599	9.51	23.74
				.040	.636	8.33	22.85
				.0438	.656	7.59	22.07

Appendix VIII-9 (cont'd)

	RK	t	$\bar{C}$	Sh	Sh_J
Danckwerts' Modification of the Newman Equation	10.0	.001	.108	28.74	32.23
		.002	.146	22.45	26.27
		.003	.175	18.62	22.58
		.005	.221	14.35	18.42
		.007	.257	12.03	16.19
		.010	.299	10.01	14.28
		.015	.353	8.18	12.64
		.020	.394	7.14	11.79
		.025	.428	6.47	11.37
		.030	.455	5.99	11.00
		.035	.478	5.64	10.81
		.040	.498	5.37	10.70
Danckwerts' Modification of the Kronig and Brink Equation	10.0	.001	.160	53.51	63.70
		.002	.224	35.94	46.30
		.003	.269	27.91	38.18
		.005	.335	20.55	30.90
		.007	.385	17.02	27.66
		.010	.443	14.05	25.23
		.015	.516	11.37	23.47
		.020	.570	9.82	22.84
		.025	.612	8.80	22.70
		.030	.647	8.06	22.81
		.035	.674	7.51	23.04
		.040	.697	7.07	23.33

Appendix VIII-9 (cont'd)

Pe	Pe_J	X	RK	t	$\bar{C}$	Sh	Sh_J
2000	500	0	10.0	0	.036	146.53	152.03
				.00125	.116	37.29	42.19
				.00250	.164	31.08	37.16
				.0050	.255	29.91	40.15
				.0075	.354	29.15	45.15
				.01	.430	19.25	33.79
				.0125	.472	12.95	24.52
				.0150	.503	12.03	24.21
				.0175	.533	11.90	25.50
				.020	.562	11.10	25.32
				.025	.604	9.44	23.80
				.030	.639	8.90	24.67
				.035	.666	8.16	24.47
				.040	.690	7.79	25.12
				.0438	.704	7.44	25.15
4000	1000	0	10.0	.00	.036	146.53	152.03
				.00125	.119	51.17	58.05
				.0025	.184	49.64	60.81
				.0050	.324	37.02	54.77
				.0075	.387	17.69	28.87
				.010	.439	17.04	30.35
				.0125	.478	13.57	26.02
				.0150	.513	13.08	26.86
				.0175	.542	11.56	25.24
				.020	.568	11.16	25.80
				.025	.610	9.98	25.59
				.030	.644	9.16	25.76
				.035	.672	8.57	26.11
				.040	.695	8.10	26.54

Appendix VIII-10

Variations of Sherwood Number with Peclet Number for Mass Transfer with Simultaneous Chemical Reaction

Pe	Pe_J	X	RK	t	$\bar{C}$	Sh	Sh_J
0	0	10,000	200	0	.036	146.53	152.5
				.00125	.110	38.33	43.1
				.0025	.140	30.82	35.9
				.00375	.158	28.46	33.9
				.005	.170	27.39	33.0
				.0075	.183	26.51	32.4
				.010	.190	26.20	32.4
				.0125	.193	26.07	32.4
				.0150	.195	26.00	32.4
				.0175	.196	25.98	32.4
				.0200	.197	25.97	32.4
				.0250	.197	25.96	32.4
				.0265	.197	25.96	32.40
320	80	0	200	0	.036	146.53	152.5
				.00125	.109	38.46	43.2
				.0025	.140	31.05	36.1
				.00375	.157	28.77	34.2
				.005	.169	27.78	33.5
				.0075	.183	27.02	33.1
				.010	.190	26.78	33.1
				.0125	.193	26.69	33.1
				.0150	.196	26.66	33.3
				.0175	.197	26.65	33.3
				.0200	.198	26.64	33.3
				.0250	.198	26.64	33.3
				.0300	.199	26.64	33.3
				.0350	.199	26.64	33.3
				.0400	.199	26.64	33.3
				.0425	.199	26.64	33.3
1000	250	0	200	0	.036	146.53	152.0
				.0005	.076	60.37	65.5
				.001	.10	43.14	48.0
				.002	.129	34.47	39.6
				.003	.148	32.08	37.7
				.005	.172	30.82	37.2
				.007	.188	30.59	37.7
				.01	.203	30.54	38.3
				.015	.214	30.41	38.7

Appendix VIII-10 (cont'd)

Pe	PeJ	X	RK	t	$\bar{C}$	Sh	ShJ
1000	375	0	200	0	.036	146.53	152.0
				.0005	.076	61.03	66.0
(1.5 x Hadamard Velocity)				.001	.10	44.40	49.4
				.002	.130	36.61	42.1
				.003	.150	34.84	41.0
				.005	.178	34.19	41.6
				.007	.199	34.13	42.6
				.01	.219	33.93	43.4
				.015	.229	32.83	42.5
1000	1000	0	200	0	.036	146.53	152.0
				.0005	.076	68.08	73.8
(4 x Hadamard Velocity)				.001	.100	57.04	63.5
				.002	.138	54.54	63.3
				.003	.174	54.45	66.0
				.004	.205	54.14	68.0
				.005	.227	49.14	63.5
				.007	.244	42.67	56.5
				.01	.256	42.44	57.0
				.015	.264	41.98	57.0
Danckwerts'			200	.001	.098	38.75	42.93
Modification of				.002	.129	30.84	35.39
the Newman Equation:				.003	.147	28.00	32.85
(43 terms in the				.005	.169	25.85	31.12
series solution)				.007	.181	25.09	30.63
				.009	.187	24.76	30.47
				.010	.190	24.67	30.44
Danckwerts'			200	.001	.098	37.95	42.06
Modification of				.002	.129	30.06	34.50
the Kronig and				.003	.148	27.22	31.93
Brink Equation				.005	.169	25.07	30.18
				.007	.181	24.31	29.68
				.010	.190	23.89	29.48
				.015	.195	23.70	29.44
				.020	.197	23.66	29.45
				.025	.197	23.65	29.45
				.030	.197	23.65	29.46
				.035	.197	23.65	29.46
				.040	.197	23.65	29.46

IX Appendices for Experimental Section IV for Studies of Physical Mass Transfer into Drops

Appendix IX-1 Measurement of Terminal Velocity of Dispersed Phase

The terminal velocity of falling drops was measured photographically by an open flash technique, using a Strobotac. The Strobotac is a strobelight with a variable flash rate, normally used to measure rotational speeds. The accuracy is $\pm$ 1%.

The apparatus is shown schematically in Figure IX-1. The Strobotac was placed to the rear and above the nozzle. The camera was focused in front of the apparatus and the shutters were held open. The drops were photographed with the room lights off and with the Strobotac providing the only source of light.

Hence, a picture showing a series of images of a single drop falling in front of the camera was made. An example is shown in Figure IX-2. Knowing the flash rate and the magnification factor, the drop velocity was found by measuring the distances between the images of the drop.

Figure IX-1 : Apparatus for Taking Stroboscopic Photographs of Falling Drops

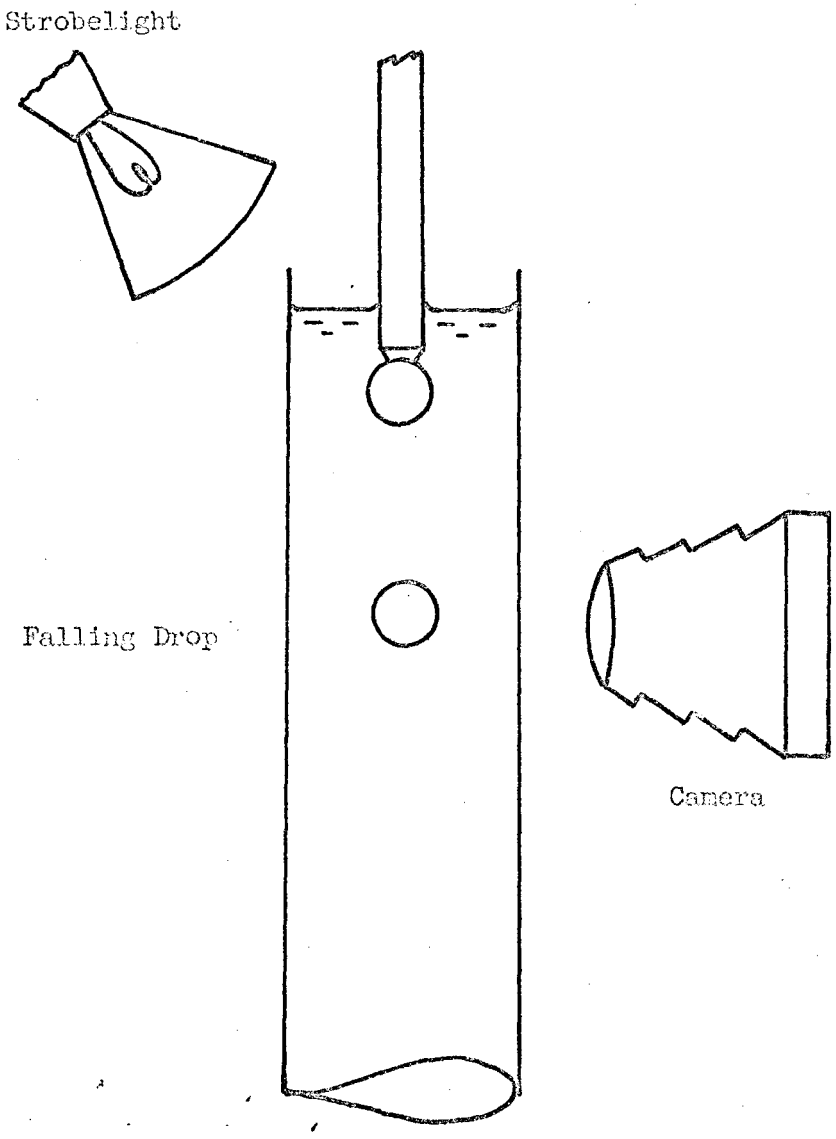

Figure IX-2 : Stroboscopic Picture of a Water Drop Falling in Paraldehyde

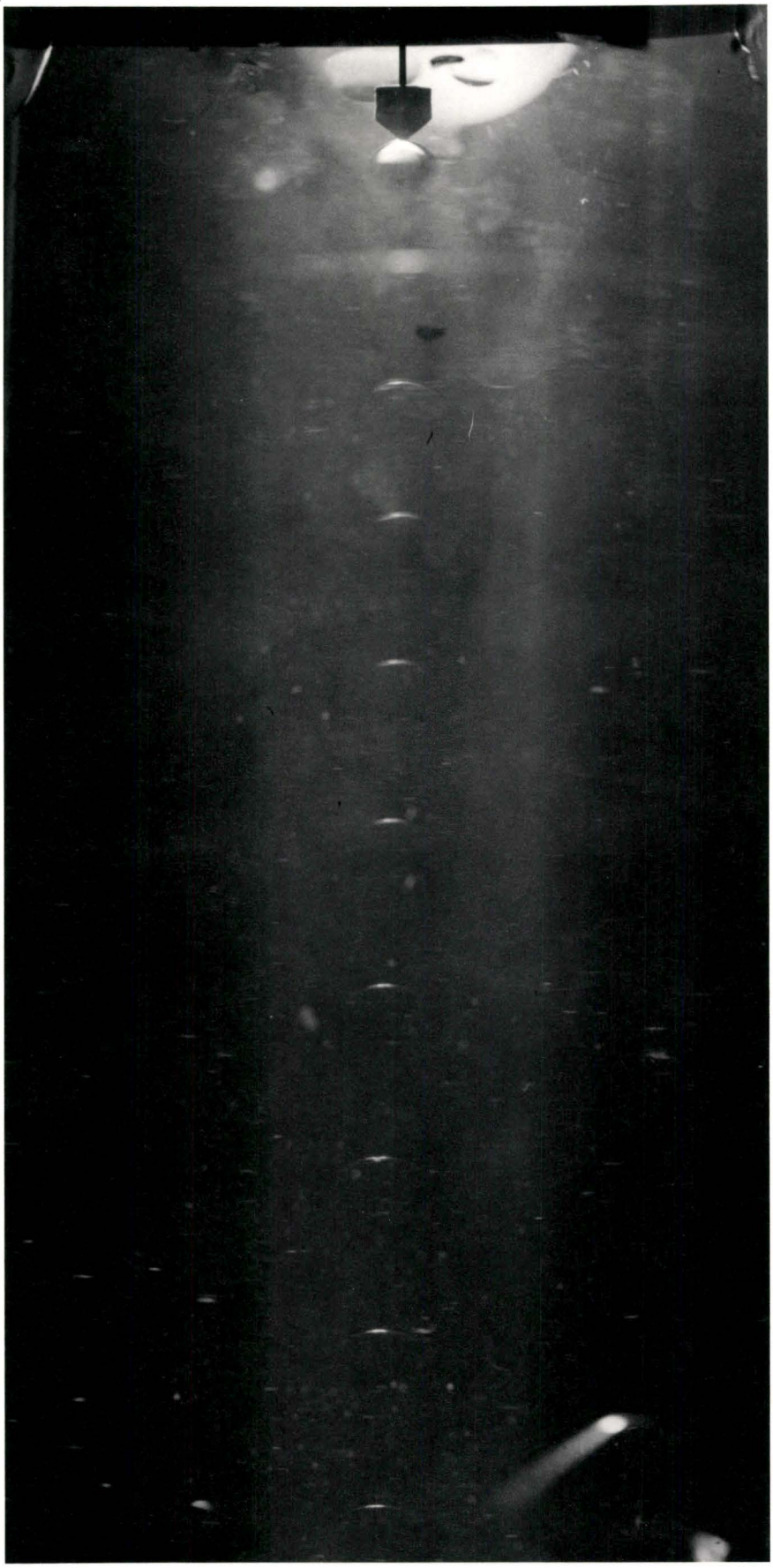

Appendix IX-2

Determination of Acetaldehyde by Titration Method

Tomoda's method (95) was used to determine the acetaldehyde control. The compound was allowed to go through a series of reaction, as represented by the following equation:-

$$CH_3CHO + NaHSO_3 \longrightarrow CH_3CH(OH)SO_3Na \xrightarrow{\frac{1}{2}\ NaHSO_3}$$

$$Na_2SO_3 + CO_2 + H_2O + CH_3CHO$$

Finally, the sodium sulfite formed, was titrated with iodine solution and the equivalent amount of acetaldehyde was then estimated.

IX Procedure

1) Place the sample in a 250-ml Erlenmeyer flask, containing cold water and 5 mls of 2% sodium bisulfite solution.
2) Let stand for ten minutes.
3) Titrate with .02N iodine solution.
4) After the blue end point is reached, add an excess of sodium bicarbonate, and continue titration to second end point.

IX Calculation

$$\% \text{ Acetaldehyde by wt} = \frac{\text{Iodine titre} \times 22.0 \times 100.0}{1000 \times \text{Sample Volume}}$$

Appendix IX-3 Calibration Curves for Refractometer

Calibration curves were made for Bausch and Lomb Dipping Refractometer, using Prism A. An initial curve was made for refractive index versus weight percent concentration of solute in aqueous solutions. Saturation concentration of the solute was found by first measuring the refractive index of the saturated solution. Then the solution was diluted until the refractive index fell within the indices for known solution. Finally, the calibration curve was extrapolated to the saturation concentration.

The calibration curves were plotted in Figure IX-3 as percent by weight concentration versus scale reading on the Refractometer. Charts are available to convert these readings to refractive indices if desired.

Figure IX-3 : Calibration Curves for Bausch and Lomb Dipping Refractometer with Prism A

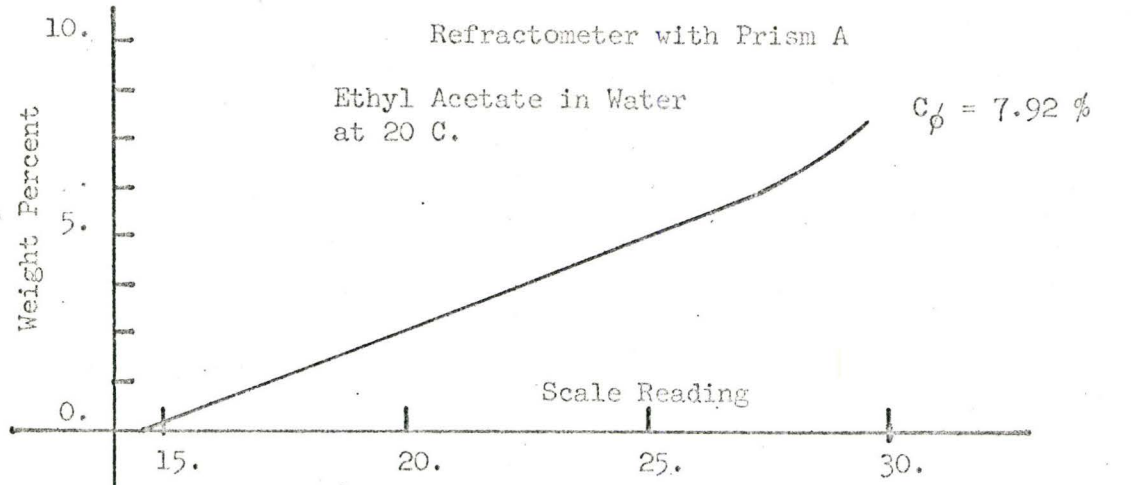

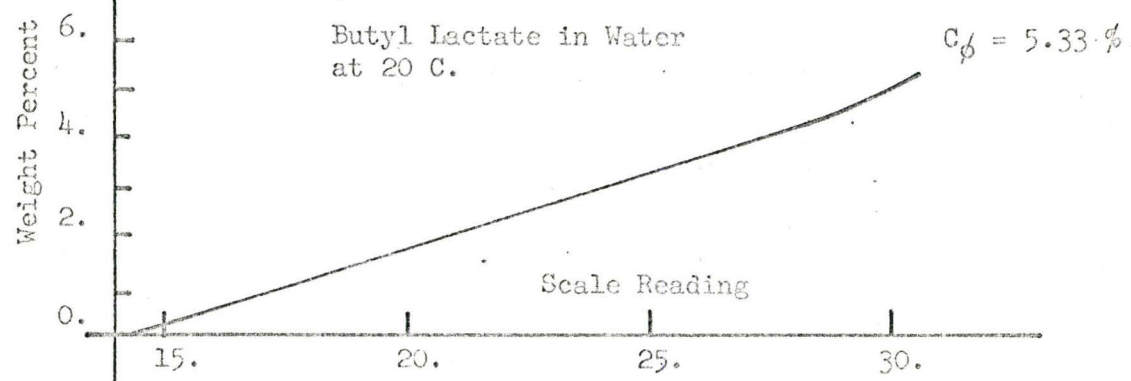

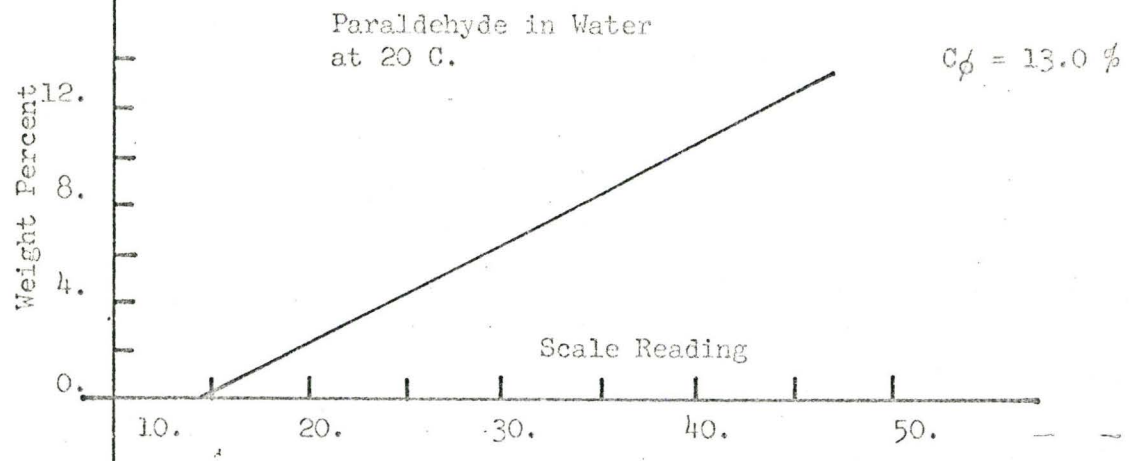

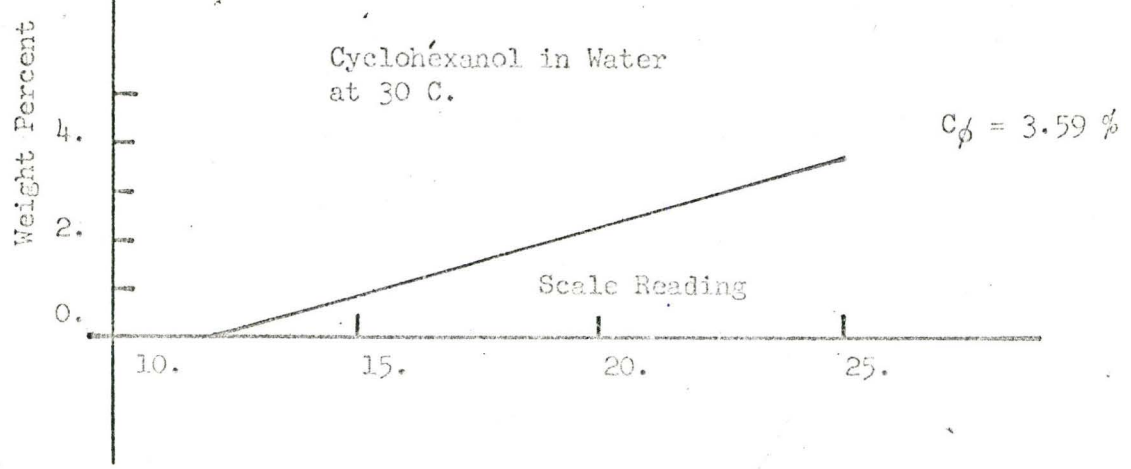

Appendix IX-4

Physical Properties of Systems Studied for Mass Transfer

Continuous System (Saturated with Water)	ρ gm/cc.	μ poise	Initial Drop Solute Conc. % by Wt.	ρ gm/cc.	Temp. deg. C.	Saturation Conc. Solute in Water % by Wt.
Ethyl Acetate	0.9070	0.0053	0.0	0.9982	20	7.92
			1.6	0.9990		
			3.7	0.9988		
			5.4	0.9968		
Butyl Lactate	0.9926	0.0483	0.0	0.9982	20	5.35
			1.7	1.0014		
			4.2	1.0021		
Paraldehyde	0.9960	0.1425	0.0	0.9982	20	13.0
			2.85	1.0096		
			5.75	1.0126		
			9.4	1.0149		
Cyclohexanol	0.9510	0.128	0.0	0.9957	30	3.59
			0.9	0.9998		
			1.78	0.9997		
			2.65	0.9995		

Appendix IX-5

Physical Mass Transfer Data

System	Initial Drop Conc. % by Wt.	Drop Ht. cm.	Drop Time-Sec. Avg.	$\pm t_{.05} S(\bar{x})$	Exit Conc. % by Wt.		Efficiencies for Regressed Data E_T	E_M	Drop Rad-cm. Avg.	$\pm t_{.05} S(\bar{x})$
Ethyl Acetate $-H_2O$	0	94.631	9.50	0.026	5.95	6.20	0.757	0.701	0.134	0.0009
					5.90	6.00				
					5.90	5.85				
					6.20	6.20				
		75.582	7.61	0.025	6.10	5.90	0.768	0.714		
					5.90	5.80				
					6.00	6.00				
					6.00	6.00				
		53.143	5.35	0.014	5.40	5.60	0.674	0.599		
					5.60	5.60				
					5.60	5.55				
					5.50	5.55				
		30.457	3.09	0.016	3.60	3.70	0.495	0.379		
					3.60	3.80				
					3.80	3.70				
					3.90	3.70				
		7.231	0.78	0.016	2.15	2.05	0.263	0.094		
					2.30	2.20				
					2.20	2.10				
					2.05	2.15				
		0.0	0.0	0.0			0.187	0.0		
	1.6	94.631	9.57	0.028	6.20	6.20	0.724	0.668	0.135	0.0011
					6.20	6.20				

Appendix IX-5 (cont'd) Physical Mass Transfer Data

System	Initial Drop Conc. % by Wt.	Drop Ht. cm.	Drop Time-Sec. Avg.	$\pm t_{.05} S(\bar{x})$	Exit Conc. % by Wt.		Efficiencies for Regressed Data E_T	E_M	Drop Rad-cm. Avg.	$\pm t_{.05} S(\bar{x})$
Ethyl Acetate $-H_2O$	1.6	75.582	7.61	0.018	5.90	5.90	0.686	0.622		
					5.90	5.90				
		53.143	5.37	0.021	5.30	5.40	0.578	0.492		
					5.40	5.40				
		30.457	3.04	0.013	4.00	4.20	0.421	0.303		
					4.20	4.35				
					4.10	4.10				
					4.35	4.35				
		7.231	0.73	0.015	3.10	3.00	0.231	0.074		
					3.15	3.15				
		0.0	0.0	0.0			0.169	0.0		
	3.7	94.631	9.50	0.022	6.20	6.20	0.588	0.498	0.136	0.0012
					6.10	6.25				
		75.582	7.53	0.021	5.90	6.00	0.546	0.447		
					6.00	6.05				
		53.143	5.28	0.023	5.45	5.60	0.428	0.304		
					5.50	5.60				
		30.457	3.10	0.014	4.80	4.95	0.297	0.144		
					4.85	4.95				
					5.05	5.05				

Appendix IX-5 (cont'd) Physical Mass Transfer Data

System	Initial Drop. Conc. % by Wt.	Drop Ht. cm.	Drop Time-Sec. Avg.	$\pm t_{.05} S(\bar{x})$	Exit Conc. % by Wt.		Efficiencies for Regressed Data E_T	E_M	Drop Rad-cm. Avg.	$\pm t_{.05} S(\bar{x})$
Ethyl Acetate $-H_2O$	3.7	7.231	0.73	0.013	4.65	4.65	0.199	0.024		
					4.45	4.55				
					4.45	4.50				
		0.0	0.0	0.0			0.179	0.0		
	5.34	94.631	9.54	0.027	6.20	6.30	0.404	0.388	0.134	0.0011
					6.50	6.40				
		75.582	7.64	0.019	6.20	6.20	0.328	0.310		
					6.25	6.10				
		53.143	5.37	0.017	6.00	6.00	0.239	0.218		
					6.00	5.90				
		30.457	3.13	0.015	5.80	5.80	0.148	0.125		
					5.80	5.75				
		7.231	0.79	0.015	5.45	5.50	0.056	0.030		
					5.35	5.40				
		0.0	0.0	0.0			0.027	0.0		
Cyclohexanol $-H_2O$	0.0	94.631	34.22	0.156	1.95	2.00	0.552	0.415	0.156	0.0020
					2.05	1.90				
					1.90	1.95				
					2.08	2.10				
		75.582	26.70	0.212	1.70	1.70	0.488	0.331		
					1.60	1.55				
					1.70	1.75				

Appendix IX-5 (cont'd)

Physical Mass Transfer Data

System	Initial Drop Conc. % by Wt.	Drop Ht. cm.	Drop Time-Sec. Avg.	$\pm t_{.05} S(\bar{x})$	Exit Conc. % by Wt.		Efficiencies for Regressed Data E_T	E_M	Drop Rad-cm. Avg.	$\pm t_{.05} S(\bar{x})$
Cyclohexanol $-H_2O$	0.0	53.143	19.41	0.184	1.55	1.50	0.412	0.233		
					1.53	1.45				
					1.60	1.65				
		30.457	10.75	0.100	1.25	1.30	0.336	0.133		
					1.20	1.20				
					1.30	1.38				
		7.231	2.34	0.013	0.95	0.90	0.258	0.032		
					0.75	0.80				
					0.90	0.90				
		0.0	0.0	0.0			0.23	0.0		
	0.9	94.631	33.66	0.122	2.38	2.35	0.531	0.375	0.153	0.0016
					2.30	2.23				
					2.35	2.35				
					2.35	2.30				
		75.582	27.38	0.081	2.16	2.16	0.474	0.299		
					2.14	2.20				
					2.08	2.03				
		53.143	20.24	0.111	1.93	1.97	0.407	0.211		
					2.05	2.15				
					2.10	2.05				
		30.457	11.36	0.056	1.72	1.78	0.340	0.121		
					1.95	1.90				
					1.95	1.93				

Appendix IX-5 (cont'd) Physical Mass Transfer Data

System	Initial Drop Conc. % by Wt.	Drop Ht. cm.	Drop Time-Sec Avg.	$\pm t_{.05} S(\bar{x})$	Exit Conc. % by Wt.		Efficiencies for Regressed Data E_T	E_M	Drop Rad-cm. Avg.	$\pm t_{.05} S(\bar{x})$
Cyclohexanol $-H_2O$	0.9	7.231	2.38	0.018	1.52 1.58 1.65	1.52 1.55 1.63	0.271	0.029		
		0.0	0.0	0.0			0.249	0.0		
	1.78	94.631	33.73	0.042	2.75 2.75	2.75 2.70	0.531	0.410	0.158	.0017
		75.582	26.58	0.085	2.70 2.65	2.70 2.65	0.486	0.353		
		53.143	18.88	0.040	2.50 2.50	2.50 2.55	0.420	0.269		
		30.457	10.59	0.057	2.40 2.40	2.40 2.45	0.338	0.167		
		7.231	2.34	0.019	2.20 2.20	2.20 2.23	0.239	0.043		
		0.0	0.0	0.0			0.206	0.0		
	2.67	94.631	33.60	0.076	3.18 3.23	3.18 3.23	0.531	0.439	0.156	.0009
		75.582	26.69	0.048	3.10 3.13	3.15 3.13	0.486	0.351		
		53.143	18.93	0.041	3.05 3.05	3.05 3.10	0.420	0.247		

Appendix IX-5 (cont'd) Physical Mass Transfer Data

System	Initial Drop Conc. % by Wt.	Drop Ht. cm.	Drop Time-Sec. Avg.	$\pm t_{.05} S(\bar{x})$	Exit Conc. % by Wt.		Efficiencies for Regressed Data E_T	E_M	Drop Rad- cm. Avg.	$\pm t_{.05} S(\bar{x})$
Cyclohexanol $-H_2O$	2.67	30.457	10.82	0.053	3.00	3.00	0.338	0.141		
					3.00	3.00				
		7.231	2.37	0.020	2.95	2.90	0.239	0.34		
					2.90	2.90				
		0.0	0.0	0.0			0.206	0.0		
Paraldehyde $-H_2O$	0.0	94.631	24.22	0.536	8.45	8.35	0.644	0.508	0.300	0.0059
					8.35	8.30				
		75.582	19.51	0.282	7.95	7.95	0.601	0.449		
					7.80	7.70				
		53.143	14.89	0.138	6.90	6.90	0.541	0.366		
					7.10	7.05				
		30.457	9.45	0.159	5.90	5.95	0.456	0.249		
					6.00	6.00				
		7.231	2.42	0.058	4.25	4.25	0.328	0.071		
					4.20	4.30				
		0.0	0.0	0.0			0.276	0.0		
	2.85	94.631	22.61	0.187	9.30	9.30	0.632	0.507	0.265	0.0077
					9.25	9.25				
		75.582	18.56	0.113	9.05	9.00	0.603	0.469		
					8.90	8.85				

Appendix IX-5 (cont'd)

Physical Mass Transfer Data

System	Initial Drop Conc. % by Wt.	Drop Ht. cm.	Drop Time-Sec. Avg.	$\pm t_{.05} S(\bar{x})$	Exit Conc. % by Wt.		Efficiencies for Regressed Data E_T	E_M	Drop Rad- Avg.	cm. $\pm t_{.05} S(\bar{x})$
Paraldehyde $-H_2O$	2.85	53.143	13.95	0.150	8.30 8.30	8.30 8.35	0.539	0.382		
		30.457	8.61	0.105	7.30 7.25	7.35 7.45	0.440	0.250		
		7.231	2.27	0.074	6.05 5.75	6.05 5.80	0.303	0.067		
		0.0	0.0	0.0			0.253	0.0		
	5.75	94.631	22.18	0.320	10.05 10.20	10.05 10.15	0.604	0.507	0.243	0.0080
		75.582	17.80	0.115	9.70 9.80	9.70 9.65	0.541	0.469		
		53.143	13.24	0.138	9.15 9.15	9.15 9.25	0.481	0.382		
		30.457	7.98	0.052	8.70 8.60	8.75 8.60	0.397	0.250		
		7.231	2.05	0.059	7.50 7.45	7.55 7.60	0.246	0.067		
		0.0	0.0	0.0			0.179	0.0		
	9.4	94.631	21.04	0.192	10.95 11.00	10.90 11.15	0.452	0.365	0.230	0.0055

Appendix IX-5 (cont'd) Physical Mass Transfer Data

System	Initial Drop Conc. % by Wt.	Drop Ht. cm.	Drop Time-Sec. Avg.	$\pm t_{.05} S(\bar{x})$	Exit Conc. % by Wt.		Efficiencies for Regressed Data E_T	E_M	Drop Rad- cm. Avg.	$\pm t_{.05} S(\bar{x})$
Paraldehyde $-H_2O$	9.4	75.582	17.12	0.238	10.85 10.70	10.80 10.75	0.388	0.292		
		53.143	12.70	0.415	10.65 10.65	10.65 10.55	0.313	0.205		
		30.457	7.10	0.120	10.25 10.25	10.25 10.20	0.238	0.118		
		7.231	1.79	0.059	9.95 9.90	9.95 10.00	0.160	0.028		
		0.0	0.0	0.0			0.136	**0.0**		
Butyl Lactate $-H_2O$	0.0	90.0	74.44	0.610	4.60 4.60	4.60 4.60	0.865	0.819	0.234	0.0047
		70.0	61.35	0.590	4.25 4.30	4.27 4.30	0.799	0.730		
		50.0	45.75	0.355	3.68 3.60	3.65 3.50	0.671	0.558		
		30.0	27.18	0.269	2.73 2.60	2.76 2.50	0.513	0.345		
		7.0	5.88	0.086	1.80 1.60	1.85 1.65	0.316	0.081		
		0.0	0.0	0.0			0.256	0.0		
	1.7	90.0	83.55	0.384	4.45 4.45	4.40 4.50	0.763	0.684	0.208	.0025

Appendix IX-5 (cont'd)

Physical Mass Transfer Data

System	Initial Drop Conc. % by Wt.	Drop Ht. cm.	Drop Time-Sec Avg.	$\pm t_{.05} S(\bar{x})$	Exit Conc. % by Wt.		Efficiencies for Regressed Data E_T	E_M	Drop Rad-cm. Avg.	$\pm t_{.05} S(\bar{x})$
Butyl Lactate $-H_2O$	1.7	70.0	67.25	0.325	4.10 4.00	4.15 4.10	0.649	0.532		
		50.0	47.21	0.462	3.65 3.70	3.60 3.60	0.535	0.380		
		30.0	28.39	0.062	3.10 3.25	3.15 3.30	0.421	0.228		
		7.0	5.84	0.055	2.75 2.85	2.60 2.85	0.290	0.053		
		0.0	0.0	0.0			0.250	0.0		
	4.2	90.0	78.60	0.555	4.85 4.85	4.85 4.80	0.556	0.456	0.203	.0039
		70.0	63.13	0.995	4.75 4.75	4.75 4.75	0.504	0.392		
		50.0	43.11	0.140	4.65 4.75	4.65 4.75	0.435	0.307		
		30.0	25.38	0.096	4.60 4.60	4.60 4.60	0.348	0.200		
		7.0	5.34	0.049	4.45 4.45	4.45 4.45	0.226	0.051		
		0.0	0.0	0.0			0.184	0.0		

Appendix IX-6

Correlation of Physical Mass Transfer Data
for Percent Transferred vs Drop Ht. by MLTRG Analysis

System	Drop Conc. % by Wt.	Correlation	Standard Error Estimate	Degrees Freedom
Ethyl Acetate, H_2O	0	$y = 1.479 + 0.084x - 0.405 \times 10^{-5}x^3$	0.18556	37
	1.6	$y = 2.668 + 0.054x - 0.189 \times 10^{-5}x^3$	0.10743	21
	3.7	$y = 4.456 + 0.0096x + 0.238 \times 10^{-3}x^2 - 0.164 \times 10^{-7}x^4$	0.08399	20
	5.34	$y = 5.409 + 0.0103x$	0.08167	18
Cyclo-hexanol, H_2O	0	$y = 0.840 + 0.01205x$	0.09419	30
	0.9	$y = 1.571 + 0.008x$	0.08041	30
	1.78	$y = 2.152 + 0.00865x - 0.256 \times 10^{-4}x^2$	0.02927	17
	2.67	$y = 2.892 + 0.0032 4x$	0.02164	18
Paralde-hyde, H_2O	0	$y = 3.591 + .0976x - .7699 \times 10^{-3}x^2 + 0.2877 \times 10^{-5}x^3$	0.08662	16
	2.85	$y = 5.418 + 0.0724x - 0.336 \times 10^{-3}x^2$	0.08878	17
	5.75	$y = 7.048 + 0.0729x - 0.8172 \times 10^{-3}x^2 + 0.4129 \times 10^{-5}x^3$	0.07591	16
	9.4	$y = 9.89 + 0.0120x$	0.07761	18
Butyl Lactate, H_2O	0	$y = 1.363 + 0.046x - 0.1358 \times 10^{-7}x^4$	0.09312	17
	1.7	$y = 2.606 + 0.0207x$	0.07445	18
	4.2	$y = 4.408 + 0.0069x - 0.248 \times 10^{-4}x^2$	0.02909	17

Note: MLTRG = Multiple Regression

Appendix IX-7

Correlation of Physical Mass Transfer Data
for Percent Transferred vs Drop Time by MLTRG Analysis

System	Drop Conc. % by Wt.	Correlation	Standard Error Estimate	Degrees Freedom
Ethyl Acetate, H_2O	0	$y = 1.429 + 0.8464t - 0.00405t^3$	0.1866	37
	1.6	$y = 2.671 + 0.5382t - 0.00186t^3$	0.1040	21
	3.7	$y = 4.462 + 0.08461t + 0.02614t^2 - 0.177 \times 10^{-3}t^4$	0.08502	20
	5.34	$y = 5.325 + 0.149t - 0.0045t^2$	0.0744	17
Cyclo-hexanol, H_2O	0	$y = 0.8464 + 0.0333t$	0.0899	30
	0.9	$y = 1.561 + 0.0225t$	0.0769	30
	1.78	$y = 2.158 + 0.0242t - 0.2039 \times 10^{-3}t^2$	0.0303	17
	2.67	$y = 2.894 + 0.00909t$	0.0215	18
Paralde-hyde, H_2O	0	$y = 3.664 + 0.247t - 0.896 \times 10^{-4}t^3$	0.0858	17
	2.85	$y = 5.389 + 0.234t - 9.121 \times 10^{-3}t^3$	0.0872	17
	5.75	$y = 6.998 + 0.284t - 0.012t^2 + 0.25 \times 10^{-3}t^3$	0.0773	16
	9.4	$y = 9.865 + 0.0546t$	0.0685	18
Butyl Lactate, H_2O	0	$y = 1.523 + 0.0318t + 0.401 \times 10^{-3}t^2 - 0.493 \times 10^{-7}t^4$	0.0817	16
	1.7	$y = 2.61 + 0.0219t$	0.0737	18
	4.2	$y = 4.415 + 0.00776t - 0.325 \times 10^{-4}t^2$	0.0307	17

Note: MLTRG = Multiple Regression.

Appendix IX-8

95% Probability Range for Normal Distribution
$\pm$ 1.96S(x) for Physical Mass Transfer

System	Drop Conc. % by Wt.	Drop Ht. cm.	Avg. Exit Conc. % by Wt.	Degrees Freedom	Replicate Standard Deviation S(x)	Conc. 95% Probability Range $\pm$ 1.96S(x)
Ethyl Acetate - H_2O	0	94.631	6.025	7	0.151	0.287
		75.582	5.963	7	0.092	0.175
		53.143	5.314	7	0.088	0.167
		30.457	3.715	7	0.104	0.217
		7.231	2.163	7	0.085	0.162
	1.6	94.631	6.20	3	0.001	0.0019
		75.582	5.90	3	0.001	0.0019
		53.143	5.375	3	0.050	0.095
		30.457	4.206	7	0.135	0.257
		7.231	3.10	3	0.071	0.135
	3.7	94.631	6.188	3	0.063	0.120
		75.582	5.988	3	0.063	0.120
		53.143	5.538	3	0.075	0.143
		30.457	4.942	5	0.102	0.194
		7.231	4.542	5	0.092	0.175
	5.34	94.631	6.35	3	0.129	0.245
		75.582	6.188	3	0.063	0.120
		53.143	5.975	3	0.050	0.095
		30.457	5.788	3	0.020	0.038
		7.231	5.425	3	0.065	0.1235

Appendix IX-8 (cont'd)

95% Probability Range for Normal Distribution
$\pm$ 1.96S(x) for Physical Mass Transfer

System	Drop Conc. % by Wt.	Drop Ht. cm.	Avg. Exit Conc. % by Wt.	Degrees Freedom	Replicate Standard Deviation S(x)	Conc. 95% Probability Range $\pm$ 1.96S(x)
Cyclohexanol - H_2O	0	94.631	1.99	7	0.0786	0.1495
		75.582	1.667	5	0.0753	0.1430
		53.143	1.547	5	0.0712	0.1355
		30.457	1.272	5	0.0694	0.132
		7.231	0.85	5	0.0753	0.143
	0.9	94.631	2.326	7	0.0475	0.0903
		75.582	2.128	5	0.0621	0.118
		53.143	1.042	5	0.0811	0.154
		30.457	1.872	5	0.0979	0.186
		7.231	1.575	5	0.0554	0.1055
	1.78	94.631	2.738	3	0.025	0.0475
		75.582	2.675	3	0.0289	0.055
		53.143	2.513	3	0.0250	0.0475
		30.457	2.413	3	0.025	0.0475
		7.231	2.208	3	0.015	0.0285
	2.67	94.631	3.205	3	0.0289	0.055
		75.582	2.128	3	0.0206	0.0391
		53.143	3.063	3	0.0250	0.0475
		30.457	3.00	3	0.000	0.0
		7.231	2.913	3	0.025	0.0475

Appendix IX-8 (cont'd)

95% Probability Range for Normal Distribution
$\pm$ 1.96S(x) for Physical Mass Transfer

System	Drop Conc. % by Wt.	Drop Ht. cm.	Avg Exit Conc. % by Wt.	Degrees Freedom	Replicate Standard Deviation S(x)	Conc. 95% Probability Range $\pm$ 1.96S(x)
Paraldehyde - H_2O	0.0	94.631	8.363	3	0.0629	0.120
		75.582	7.85	3	0.1225	0.233
		53.143	6.699	3	0.1031	0.196
		30.457	5.963	3	0.0479	0.091
		7.231	4.625	3	0.0408	0.0775
	2.85	94.631	9.275	3	0.0289	0.055
		75.582	8.95	3	0.0913	0.173
		53.143	8.313	3	0.0250	0.0475
		30.457	7.338	3	0.0854	0.162
		7.231	5.913	3	0.1601	0.304
	5.75	94.631	10.113	3	0.075	0.1425
		75.582	9.713	3	0.0629	0.120
		53.143	9.175	3	0.0500	0.095
		30.457	8.663	3	0.0750	0.143
		7.231	7.525	3	0.0646	0.124
	9.4	94.631	11.00	3	0.1080	0.206
		75.582	10.775	3	0.0646	0.124
		53.143	10.625	3	0.0500	0.095
		30.457	10.238	3	0.0250	0.0475
		7.231	9.95	3	0.0409	0.078

Appendix IX-8 (cont'd)

95% Probability Range for Normal Distribution
$\pm$ 1.96S(x) for Physical Mass Transfer

System	Drop Conc. % by Wt.	Drop Ht. cm.	Avg. Exit Conc. % by Wt.	Degrees Freedom	Replicate Standard Deviation S(x)	Conc. 95% Probability Range $\pm$ 1.96S(x)
Butyl Lactate - H_2O	0	90.0	4.60	3	0.0006	0.0014
		70.0	4.28	3	0.0245	0.0465
		50.0	3.608	3	0.0789	0.150
		30.0	2.648	3	0.1204	0.229
		7.0	1.725	3	0.1190	0.226
	1.7	90.0	4.475	3	0.0408	0.0775
		70.0	4.088	3	0.0629	0.120
		50.0	3.638	3	0.0479	0.0913
		30.0	3.20	3	0.0913	0.135
		7.0	2.75	3	0.1181	0.224
	4.2	90.0	4.838	3	0.0250	0.0475
		70.0	4.75	3	0.00	0.00
		50.0	4.70	3	0.0577	0.110
		30.0	4.60	3	0.0006	0.00114
		7.0	4.45	3	0.0008	0.00152

Appendix IX-9 Analysis of Variance for Mass Transfer Data

	Source	Degrees Freedom	Variance $S^2(x)$	Calc'd F	Tabulated F.05	Total number Data
System: Ethyl Acetate, H_2O	Initial Conc	3	8.03	922.75	2.71	108
Variables						
(1) Initial Drop Conc 0%, 1.6%, 3.7%, 5.34%	Drop Ht	4	26.34	3,026.8	2.47	
(2) Drop Ht - cm 94.631, 75.582, 53.143, 30.457, 7.231	Interaction	12	2.24	257.71	1.87	
	Error	88	0.009			
System: Cyclohexanol, H_2O	Initial Conc	3	11.097	3,139.81	2.72	104
Variables						
(1) Initial Drop Conc 0%, 0.9%, 1.8%, 2.65%	Drop Ht	4	1.440	407.50	2.48	
(2) Drop Ht - cm 94.631, 75.582, 53.143, 30.457, 7.231	Interaction	12	0.1777	50.28	1.88	
	Error	84	0.0035			

Appendix IX-9 (cont'd)

Analysis of Variance for Mass Transfer Data

	Source	Degrees Freedom	Variance $S^2(x)$	Calc'd F	Tabulated F.05	Total number Data
System: Paraldehyde, H_2O	Initial Conc	3	52.982	8,919.973	2.76	80
Variables						
(1) Initial Drop Conc 0%, 2.85%, 5.75%, 9.4%	Drop Ht	4	19.528	3,287.685	2.52	
(2) Drop Ht - cm 94.631, 75.582, 53.143, 30.457, 7.231	Interaction	12	1.123	189.053	1.92	
	Error	60	0.0059			
System: Butyl Lactate, H_2O	Initial Conc	2	9.417	2,028.03	3.20	60
Variables						
(1) Initial Drop Conc 0%, 1.7%, 4.2%	Drop Ht	4	5.350	1,152.07	2.57	
(2) Drop Ht - cm 90.0, 70.0, 50.0, 30.0, 7.0	Interaction	8	1.092	235.11	2.14	
	Error	45	0.0046			

Appendix IX-10

E_M Data Calculated Relative to E_M at 7 cm Drop Height. Drop Time t Calculated Relative to Drop Time for 7 cm Drop Height

System	Initial Drop Conc. % by Wt.	Relative Drop Time Sec.	$t^{0.5}$	Relative E_M	System	Initial Drop Conc. % by Wt.	Relative Drop Time Sec.	$t^{0.5}$	Relative E_M
Ethyl Acetate, H_2O	0.0	8.72	2.95	0.67	Cyclohexanol, H_2O	0.0	31.88	5.65	0.396
		6.83	2.61	0.685			24.36	4.93	0.309
		4.57	2.14	0.557			17.07	4.14	0.208
		2.21	1.49	0.315			8.41	2.90	0.105
		0.0	0.0	0.0			0.0	0.0	0.0
	1.6	8.84	2.97	0.641		0.9	31.28	5.60	0.357
		6.88	2.63	0.591			25.00	5.00	0.279
		4.64	2.15	0.452			17.86	4.24	0.187
		2.31	1.52	0.247			8.98	3.00	0.95
		0.0	0.0	0.0			0.0	0.0	0.0
	3.7	8.77	2.97	0.486		1.78	31.39	5.60	0.384
		6.80	2.61	0.434			24.24	4.93	0.324
		4.55	2.14	0.287			16.54	4.06	0.237
		2.37	1.54	0.123			8.25	2.87	0.130
		0.0	0.0	0.0			0.0	0.0	0.0
	5.34	8.75	2.96	0.369		2.67	31.23	5.6	0.420
		6.85	2.62	0.289			24.32	4.93	0.328
		4.58	2.14	0.194			16.56	4.07	0.221
		2.34	1.53	0.098			8.45	2.91	0.111
		0.0	0.0	0.0			0.0	0.0	0.0

Appendix IX-10 (cont'd)

E_M Data Calculated Relative to E_M at 7 cm Drop Height. Drop Time t Calculated Relative to Drop Time for 7 cm Drop Height

System	Initial Drop Conc. % by Wt.	Relative Drop Time Sec.	$t^{0.5}$	Relative E_M	System	Initial Drop Conc. % by Wt.	Relative Drop Time Sec.	$t^{0.5}$	Relative E_M
Paraldehyde,	0.0	21.80	4.67	0.470	Butyl	0.0	68.56	8.29	0.803
		17.09	4.14	0.407	Lactate,		55.47	7.45	0.706
H_2O		12.47	3.54	0.318			39.87	6.31	0.519
		7.03	2.65	0.191	H_2O		21.30	4.61	0.287
		0.0	0.0	0.0			0.0	0.0	0.0
	2.85	20.34	4.50	0.472		1.7	67.71	8.24	0.666
		16.29	4.04	0.431			61.41	7.84	0.506
		11.68	3.42	0.338			41.37	6.43	0.345
		6.35	2.52	0.196			22.55	4.76	0.185
		0.0	0.0	0.0			0.0	0.0	0.0
	5.75	20.13	4.50	0.474		4.2	72.26	8.5	0.426
		15.75	3.97	0.391			57.79	7.6	0.359
		11.19	3.34	0.311			37.77	6.15	0.270
		5.94	2.44	0.200			20.04	4.48	0.158
		0.0	0.0	0.0			0.0	0.0	0.0
	9.4	19.25	4.40	0.347					
		15.33	3.91	0.271					
		10.91	3.30	0.182					
		5.31	2.31	0.092					
		0.0	0.0	0.0					

Appendix IX-11 Correlation of Regressed Physical Transfer Data into the Form E_M vs $t^{\frac{1}{2}}$, by MLTRG Analysis Using Relative E_M Data

System	Drop Conc. % by Wt.	Correlation	Standard Error Estimate	Degrees Freedom
Ethyl Acetate, H_2O	0	$y = -0.0227 + 0.2628x$	0.0505	2
	1.6	$y = -0.0277 + 0.2232x$	0.0451	3
	3.7	$y = 0.0021 + 0.0586x^2$	0.0291	3
	5.34	$y = -0.210 \times 10^{-3} + 0.0422x^2$	0.7343×10^{-3}	3
Cyclo-hexanol, H_2O	0	$y = -0.876 \times 10^{-3} + 0.0125x^2$	0.4717×10^{-2}	3
	0.9	$y = -0.567 \times 10^{-2} + 0.0114x^2$	0.7925×10^{-2}	3
	1.78	$y = -0.1814 \times 10^{-2} + 0.0214x^2 - .1621 \times 10^{-2}x^3$	0.6094×10^{-2}	3
	2.67	$y = -0.126 \times 10^{-2} + 0.0135x^2$	0.1787×10^{-2}	3
Paraldehyde, H_2O	0	$y = 0.1325 \times 10^{-4} - .0369x + .0561x^2 - 0.5692 \times 10^{-2}x^3$	0.1726×10^{-2}	3
	2.85	$y = -0.0215 + 0.1066x$	0.9903×10^{-2}	3
	5.75	$y = 0.8397 \times 10^{-5} + 0.0545x + 0.0113x^2$	0.1948×10^{-2}	3
	9.4	$y = -0.3945 \times 10^{-2} + 0.01795x^2$	0.6628×10^{-2}	3
Butyl Lactate, H_2O	0	$y = 0.0221 + 0.0119x^2$	0.0313	3
	1.7	$y = -0.4417 \times 10^{-2} + 0.848 \times 10^{-2}x^2$	0.9786×10^{-2}	3
	4.2	$y = -0.975 \times 10^{-4} + 0.0102x^2 - 0.5172 \times 10^{-3}x^3$	0.4317×10^{-2}	3

Note: MLTRG = Multiple Regression

Appendix IX-12

$\dot{R}$ Data Calculated from $E_M = \sqrt{\frac{\dot{R}\pi^2 D_L t}{a^2}}$

System	Drop Conc. % by Wt.	0.5	1.0	1.5	2.0	2.5	3.0	$t^{0.5}$
Ethyl Acetate, H_2O	0	12.60	12.60	12.60	12.60	12.60	12.60	
	1.6	9.20	9.20	9.20	9.20	9.20	9.20	
	3.7	0.645	2.58	5.78	10.30	16.10	23.20	
	5.3	0.324	1.29	2.93	5.8	8.10	11.60	
		1	2	3	4	5	6	$t^{0.5}$
Cyclohexanol, H_2O	0	0.154	0.615	1.39	2.47	3.85	5.55	
	0.9	0.124	0.493	1.11	1.98	3.09	4.44	
	1.78	0.365	1.11	1.82	2.21	2.16	1.69	
	2.67	0.180	0.72	1.62	2.88	4.50	6.45	
		1	2	3	4	5	6	$t^{0.5}$
Paraldehyde, H_2O	0	3.10	13.00	19.50	17.30	8.75	4.15	
	2.85	8.10	8.10	8.10	8.10	8.10	8.10	
	5.75	3.56	5.95	8.95	12.60	16.80	21.40	
	9.4	0.69	2.76	6.20	12.40	17.30	24.80	
		1	2	3	4	6	8	$t^{0.5}$
Butyl Lactate, H_2O	0	0.314	1.250	2.820	5.02	11.30	20.20	
	1.7	0.126	0.504	1.140	2.01	4.54	8.10	
	4.2	0.149	0.525	0.930	1.35	1.85	1.71	

Appendix IX-13

Correlation of Physical Mass Transfer Data into the form ln (1 - Et) vs Time by MLTRG Analysis

System	Drop Conc. % by Wt.	Correlation	Standard Error Estimate	Degrees Freedom
Ethyl Acetate, H_2O	0	$y = -0.2025 - 0.1156t - 0.01539t^2 + 0.156 \times 10^{-3}t^4$	0.07016	36
	1.6	$y = -0.1933 - 0.09075t - 0.008718t^2 + 0.673 \times 10^{-4}t^4$	0.03099	20
	3.7	$y = -0.1416 - 0.08031t$	0.0421	22
	5.34	$y = -0.00673 - 0.05179t$	0.04174	18
Cyclo-hexanol, H_2O	0	$y = -0.2470 - 0.01589t$	0.04398	30
	0.9	$y = -0.2662 - 0.01404t$	0.04748	30
	1.78	$y = -0.2452 - 0.0155t$	0.02988	18
	2.67	$y = -0.2813 - 0.0138t - 0.976 \times 10^{-7}t^4$	0.04569	17
Paraldehyde, H_2O	0	$y = -0.3173 - 0.03159t + 0.136 \times 10^{-6}t^4$	0.01605	17
	2.85	$y = -0.2721 - 0.03707t + 0.4029 \times 10^{-6}t^4$	0.01604	17
	5.75	$y = -0.235 - 0.03117t$	0.02391	18
	9.4	$y = -0.1216 - 0.0303$	0.0303	18
Butyl Lactate, H_2O	0	$y = -0.3844 - 0.408 \times 10^{-3}t^2 + 0.213 \times 10^{-7}t^4$	0.03365	17
	1.7	$y = -0.3207 - 0.00439t - 0.1037 \times 10^{-3}t^2$	0.0413	17
	4.2	$y = -0.2293 - 0.00754t$	0.0505	17

Appendix IX-14

$K_L \times 10^{-4}$ Calculated from $\ln (1 - E_T) = \frac{-3K_L t}{a}$

System	Drop Conc. % by Wt.	0	2	4	6	8	9	t sec.
Ethyl Acetate, H_2O	0	51.6	76.8	88.8	73.8	19.8	27.4	
	1.6	40.9	55.6	64.5	61.9	41.6	23.3	
	3.7	36.4	36.4	36.4	36.4	36.4	36.4	
	5.3	23.1	23.1	23.1	23.1	23.1	23.1	
		0	5	10	20	30	35	t sec.
Cyclohexanol, H_2O	0	8.26	8.26	8.26	8.26	8.26	8.26	
	0.9	7.16	7.16	7.16	7.16	7.16	7.16	
	1.78	8.16	8.16	8.16	8.16	8.16	8.16	
	2.67	7.17	7.17	7.38	8.78	12.60	15.85	
		0	5	10	15	20	25	t sec.
Paraldehyde, H_2O	0	31.60	31.52	31.05	29.77	27.24	23.09	
	2.85	32.80	32.60	32.60	32.30	31.60	31.40	
	5.75	25.30	25.30	25.30	25.30	25.30	25.30	
	9.4	17.75	17.75	17.75	17.75	17.75	17.75	
		0	5	10	20	40	60	t sec.
Butyl Lactate, H_2O	0	0	3.17	6.29	12.20	21.30	23.80	— —
	1.7	3.04	3.76	4.48	5.91	8.76	11.65	
	4.2	5.10	5.10	5.10	5.10	5.10	5.10	

Appendix IX-15

Physical Mass Transfer Study Data by Hamielec (93)
for Transfer into Water Drops from Water-Saturated Continuous Phase

System	Temp. deg. C.	Drop Re. No.	Drop Diam cm.	Saturation Conc. % by Wt.	E_T	E_M	Relative E_M	Drop Time Sec.	Relative Drop Time Sec.
Ethyl Acetate,	25.0	470.0	.258	8.73	0.0			0	
					0.298	0.298		0.6	
H_2O					0.448	0.449	0.151	1.4	0.8
					0.594	0.595	0.297	2.2	1.6
					0.685	0.686	0.388	3.3	2.7
Cyclohexanol,	25.0	2.3	.282	4.15	0.245			0	
					0.395	0.20		5.2	
H_2O					0.505	0.34	0.14	16.0	10.8
					0.561	0.42	0.22	22.0	16.8
	25.0	6.4	.434	4.15	0.20			0	
					0.295	0.119		3.0	
					0.403	0.254	0.135	13.5	10.5
					0.493	0.366	0.247	29.0	26.0

X Appendices for Experimental Section IV for Studies of Mass Transfer with Simultaneous Chemical Reaction in Drops

Appendix X-1

Physical Properties of Systems Studied for Mass Transfer with Chemical Reaction

Continuous System (Sat'd with Water)	Continuous Phase ρ gm/cc	Continuous Phase μ poise	Initial NaOH Normality	Dispersed Phase ρ gm/cc.	Dispersed Phase μ poise	Avg Drop Radius cm.	Terminal Velocity cm/sec. ($\pm$ 1%)
Butyl Lactate	0.9926	0.0483	0.506	1.0623	.9150	.162 $\pm$.004	2.50
			1.545	1.0219		.109 $\pm$.003	1.98
Ethyl Acetate	0.9070	0.0053	0.506	1.0219	.0150	.134 $\pm$.002	9.54
			0.998	1.0433	.0129	.128 $\pm$.002	9.77
			1.975	1.1756	.0150	.124 $\pm$.002	13.90

K = 91.8 cc/mol sec for reaction rate constant for Ethyl Acetate - NaOH system

Appendix X-2

Mass Transfer with Simultaneous Chemical Reaction Data

System	Initial NaOH Drop Conc. Normality	Drop Ht cm.	Drop Time-Sec. Avg.	$\pm t_{.05} S(\bar{x})$	Mass Transferred X 10^{-4} mol/cc		Drop Rad-cm. Avg.	$\pm t_{.05} S(\bar{x})$
Ethyl Acetate, NaOH, H_2O	0.506	90.0	10.84	0.036	6.45 6.73	6.62 6.88	0.134	0.0020
		70.0	8.33	0.044	5.98 6.18	5.98 6.23		
		50.0	5.99	0.054	5.28 5.49	5.22 5.47		
		30.0	3.57	0.024	4.08 4.38	4.40 4.60		
		7.00	0.81	0.013	2.49 2.93	2.38 2.67		
	0.998	90.0	10.00	0.035	5.72 5.73	5.53 5.90	0.128	0.0016
		70.0	7.97	0.033	4.84 4.47	4.71 4.90		
		50.0	5.61	0.042	3.70 4.01	3.90 4.15		
		30.0	3.25	0.029	2.73 3.02	3.06 3.20		
		7.0	0.83	0.021	1.79 1.72 1.51	1.95 1.90		

Appendix X-2 Mass Transfer with Simultaneous Chemical Reaction Data

System	Initial NaOH Drop Conc.	Drop Ht cm.	Drop Time-Sec. Avg.	$\pm t_{.05} S(\bar{x})$	Mass Transferred X 10^{-4} mol/cc Acid Quench		Complete Reaction		Drop Rad- cm. Avg.	$\pm t_{.05} S(\bar{x})$
	Normality								Acid Quench	
Butyl Lactate, NaOH, H_2O	0.5	90.0	42.60	0.333	5.88	5.75	6.97	7.08	0.162	0.0039
					6.18	7.53	6.63	6.62		
									Complete Reaction	
		70.0	35.38	0.239	5.35	5.64	7.06	6.57	0.161	0.0046
					5.87	5.51	6.06	6.20		
		50.0	25.39	0.353	5.88	5.78	6.32	6.31		
					5.53	5.39	6.16	6.39		
		30.0	15.27	0.162	5.77	6.30	5.86	6.18		
					5.57	5.87	6.12	6.13		
		7.0	2.84	0.064	5.54	5.88	5.88	5.52		
					5.64	5.66	5.77	6.23		
	1.5	90.0	48.83	0.976	15.72	16.49	16.88	17.17		
					16.60	16.67	15.76	16.61		
									Acid Quench	
									0.109	0.0034
		70.0	36.60	1.025	16.25	16.93	16.94	16.87		
					16.31	16.60	16.58	16.46		
									Complete Reaction	
									0.113	0.0051
		50.0	28.81	0.362	16.65	16.31	16.29	15.76		
					16.43	16.55	15.79	15.71		
		30.0	16.56	0.353	16.22	15.47	15.51	15.53		
					16.22	16.08	15.42	15.47		
		7.0	3.07	0.053	15.59	15.96	14.60	14.88		
					15.56	15.76	14.42	14.75		

Appendix X-2

Mass Transfer with Simultaneous Chemical Reaction Data

System	Initial NaOH Drop Conc.	Drop Ht cm.	Drop Time-Sec. Avg.	$\pm t_{.05}S(\bar{x})$	Mass Transferred X 10^{-4} mol/cc		Drop Rad-cm. Avg.	$\pm t_{.05}S(\bar{x})$
	Normality							
Ethyl Acetate, NaOH, H_2O	1.975	90.0	7.18	0.045	5.41	4.83	0.124	0.0019
					4.10	3.98		
					4.44	4.85		
						4.61		
		70.0	5.58	0.043	4.94	3.53		
					3.91	3.94		
		50.0	3.97	0.045	2.73	2.44		
					2.76	2.35		
		30.0	2.34	0.029	2.31	1.68		
					2.22	1.67		
		7.0	0.65	0.011	0.30	0.0		
					0.33	0.0		
Sodium Acetate, + H_2O	2N	50.0	3.93	0.022	0.75	0.74	0.123	0.0027
					0.77	0.83		
		30.0	2.34	0.048	0.66	0.58		
					0.65	0.75		
		7.0	0.61	0.039	0.31	0.34		
					0.37	0.43		

Appendix X-3

Multiple Regression Analysis for Correlation of Mass Transfer
With Reaction Data for mol/cc x 10^{-4} Transferred vs Drop Height-cm

System	Drop Conc.	Correlation	Standard Error Estimate x 10^{-4}	Degrees Freedom
		x 10^{-4}		
NaOH Soln in Butyl Lactate	0.5N NaOH (Acid)	$y = 5.657 + 0.8759 \times 10^{-8}x^4$	0.42152	18
	0.5N NaOH (Alkali)	$y = 5.739 + 0.0114x$	0.25197	18
	1.5N NaOH (Acid)	$y = 15.548 + 0.0187x - 0.1321 \times 10^{-7}x^4$	0.29643	17
	1.5N NaOH (Alkali)	$y = 14.394 + 0.0354x - 0.1415 \times 10^{-7}x^4$	0.33425	17
NaOH Soln in Ethyl Acetate	0.5N NaOH (Alkali)	$y = 2.074 + 0.0853x - 0.385 \times 10^{-3}x^2$	0.1835	17
	1N NaOH (Acid)	$y = 1.512 + 0.0469x$	0.18057	19
	2N NaOH (Acid)	$y = 0.040 + 0.0532x$	0.4724	22
Na Acetate Soln in Ethyl Acetate	2N NaAc	$y = 0.256 + 0.0154x - 0.2016 \times 10^{-5}x^3$	0.05520	9

Note:
1) Term Alkali refers to system where addition NaOH soln added to effluent.
2) Term Acid refers to system where effluent quenched in acid solution.
3) y x 10^{-4} to obtain mol/cc transferred.

Appendix X-4

Multiple Regression Analysis for Correlation of Mass Transfer
With Reaction Data for mol/cc x 10^{-4} Transferred vs Drop Time-sec

System	Drop Conc.	Correlation	Standard Error Estimate x 10^{-4}	Degrees Freedom
		x 10^{-4}		
NaOH Soln in Ethyl Acetate	0.5N NaOH (Alkali)	$y = 2.093 + 0.7093x - 0.0267x^2$	0.18325	17
	1N NaOH (Acid)	$y = 1.512 + 0.4187x$	0.19295	19
	2N NaOH (Acid)	$y = .0135 + 0.6773x$	0.4864	22

N.B. Terms Acid and Alkali - to indicate method of analysis.

Appendix X-5 95% Probability Range for Normal Distribution $\{\pm 1.96S(x)\}$ for Mass Transfer with Reaction

System	Initial NaOH Drop Conc. Normality	Drop Ht cm.	Avg Exit Conc Ester x 10^{-4} mol/cc (Acid)	(Alkali)	Degrees Freedom	Replicate Standard Deviations S(x) x 10^{-4} mol/cc (Acid)	(Alkali)	Conc-95% Probability Range ($\pm 1.96S(x)$) x 10^{-4} mol/cc (Acid)	(Alkali)
Butyl Lactate,	0.5	90.0	6.335	6.825	3	0.817	0.236	1.55	0.449
		70.0	5.593	6.473	3	0.220	0.444	0.418	0.845
NaOH,		50.0	5.645	6.295	3	0.226	0.099	0.429	0.188
		30.0	5.878	6.073	3	0.308	0.142	0.585	0.270
H_2O		7.0	5.68	5.60	3	0.143	0.293	0.272	0.556
	1.5	90.0	16.37	16.605	3	0.437	0.608	0.830	1.155
		70.0	16.523	16.713	3	0.314	0.230	0.596	0.438
		50.0	16.485	15.888	3	0.149	0.269	0.283	0.512
		30.0	15.998	15.483	3	0.357	0.049	0.678	0.0931
		7.0	15.718	14.663	3	0.181	0.199	0.344	0.378
Sodium Acetate,	2N	50.0	0.773		3		0.1382		0.2620
		30.0	0.66		3		0.0698		0.1325
H_2O		7.0	0.363		3		0.0512		0.0974

N.B. Terms Acid and Alkali - to indicate method of analysis.

Appendix X-5 (Cont'd)

95% Probability Range for Normal Distribution $\{\pm 1.96S(x)\}$ for Mass Transfer with Reaction

System	Initial NaOH Drop Conc. Normality	Drop Ht cm.	Avg Exit Conc Ester x 10^{-4} mol/cc	Degrees Freedom	Replicate Standard Deviations S(x) x 10^{-4} mol/cc	Conc-95% Probability Range ($\pm 1.96S(x)$) x 10^{-4} mol/cc
Ethyl Acetate,	0.5 (Alkali)	90.0	6.67	3	0.043	0.081
		70.0	6.093	3	0.093	0.177
NaOH,		50.0	5.365	3	0.102	0.194
		30.0	4.365	3	0.123	0.234
H_2O		7.0	2.618	3	0.165	0.313
	1.0 (Acid)	90.0	5.72	3	0.150	0.285
		70.0	4.705	3	0.190	0.361
		50.0	3.940	3	0.190	0.361
		30.0	3.003	3	0.201	0.382
		7.0	1.774	4	0.174	0.330
	2.0 (Acid)	90.0	4.603	6	0.526	1.000
		70.0	4.08	3	0.602	1.145
		50.0	2.57	3	0.206	0.392
		30.0	1.97	3	0.345	0.655
		7.0	0.158	3	0.185	0.351

N.B. Terms Acid and Alkali - to indicate method of analysis.

Appendix X-6 Analysis of Variance for Mass Transfer with Reaction Data

System: Butyl Lactate, NaOH, H_2O	Source	Degrees Freedom	$S^2(x)$ Variance x 10^{-8}	Calc'd F	Tabulated $F_{0.05}$	Total Number Data
Variables	Conc	3	665.06	5,882.52	2.76	80
(1) Drop Ht. - cm. 90, 70, 50, 30, 7	Drop Ht	4	2.70	23.87	2.52	
(2) Initial Drop Conc. 0.5N (Acid) 0.5N (Alkali) 1.5N (Acid) 1.5N (Alkali)	Interaction	12	0.53	4.64	1.92	
	Error	60	0.113			
Variables	Analysis	1	2.278	18.186	4.17	40
(1) Drop Ht. - cm. 90, 70, 50, 30, 7	Drop Ht	4	0.750	5.987	2.69	
(2) Analysis Method for Initial Conc 0.5N (Acid) 0.5N (Alkali)	Interaction	4	0.185	1.477	2.69	
	Error	30	0.125			
Variables	Analysis	1	1.224	12.134	4.17	40
(1) Drop Ht. - cm. 90, 70, 50, 30, 7	Drop Ht	4	2.730	27,067	2.69	
(2) Analysis Method for Initial Conc. 1.5N (Acid) 1.5N (Alkali)	Interaction	4	0.609	6.038	2.69	
	Error	30	0.101			

N.B. Terms Acid and Alkali - to indicate method of analysis.

Appendix X-6 (Cont'd)

Analysis of Variance for Mass Transfer with Reaction Data

System: Butyl Lactate, NaOH, H_2O	Source	Degrees Freedom	$S^2(x)$ Variance x 10^{-8}	Calc'd F	Tabulated $F_{0.05}$	Total Number Data
Variables	Conc	1	1,080.09	7,963.7	4.17	40
(1) Drop Ht. - cm. 90, 70, 50, 30, 7	Drop Ht	4	0.446	3.289	2.69	
(2) Initial NaOH Drop Conc. - Acid Method 0.5N 1.5N	Interaction	4	0.410	3.026	2.69	
	Error	30	0.1356			
Variables	Conc	1	915.02	10,112.43	4.17	40
(1) Drop Ht. - cm. 90, 70, 50, 30, 7	Drop Ht	4	2.87	31.772	2.69	
(2) Initial NaOH drop Conc. - Alkali 0.5N 1.5N Method	Interaction	4	0.54	5.994	2.69	
	Error	30	0.09			

N.B. Terms Acid and Alkali - to indicate method of analysis.

Appendix X-6 (Cont'd)

Analysis of Variance for Mass Transfer with Reaction Data

System: Ethyl Acetate, NaOH, H_2O	Source	Degrees Freedom	$S^2(x)$ Variance x 10^{-8}	Calc'd F	Tabulated $F_{0.05}$	Total Number Data
Variables	Conc	2	4.297	49.707	3.18	65
(1) Drop Ht - cm. 90, 70, 50, 30, 7	Drop Ht	4	26.595	307.62	2.56	
(2) Initial NaOH Drop Conc. 0.5N (Alkali) 1N (Acid) 2N (Acid)	Interaction	8	2.067	23.913	2.13	
	Error	50	0.0865			

Definitions

Alkali
Excess NaOH added to sample
Ester transfer found by back-titration

Acid
Sample added to acid soln
Ester transfer found by back-titration

Appendix X-7

Mass Transfer of Ethyl Acetate with Simultaneous Chemical Reaction into Aqueous Sodium Hydroxide Drops Predicted by Various Models Modified by Danckwerts' Method.

Initial NaOH Drop Concentration Normality	Drop Height cm.	Mass Transferred - mols/cc x 10^{-4} Newman Equation	Kronig and Brink Equation	Handlos and Baron Equation
2.0	90	0.7	1.3	7.3
	70	0.6	1.1	6.3
	50	0.4	0.9	5.3
	30	0.3	0.6	4.4
	7	0.1	0.2	3.1
	0	0.01	0.01	0.01
1.0	90	2.6	3.9	11.0
	70	2.3	3.5	10.0
	50	2.1	3.1	9.0
	30	1.9	2.7	7.8
	7	1.6	1.9	6.1
	0	1.5	1.5	1.5
0.5	90	3.5	4.8	11.2
	70	3.1	4.4	10.5
	50	2.8	4.0	9.8
	30	2.5	3.5	8.9
	7	2.1	2.6	7.5
	0	2.0	2.0	2.0

Appendix X-8

Computer Program to Study the Variations of Diffusion Coefficients with Time During Mass Transfer with Chemical Reaction into Drops.

X-8-A Introduction

In the Experimental Section IV, existing models were found unable to accurately predict the mass transferred into drops, when the transfer process was accompanied by simultaneous chemical reactions. This was due to interfacial turbulence which enhanced the transfer rate.

Since the interfacial turbulence varied in intensity with time and system, the resultant effective diffusion coefficients could not be measured directly. Instead, the changes in the diffusion coefficients were studied with a mass transfer model, using a computer.

X-8-B Theory

The ethyl acetate-sodium hydroxide-water system was chosen for the study. Since the drops of aqueous sodium hydroxide were found to be stagnant, the model described mass transfer with simultaneous chemical reaction into stagnant drops. The diffusion coefficient was varied in magnitude until the predicted mass transferred equaled the experimental amount, over a short period of time. This was continued until the variations of the diffusion coefficients over the entire drop time was found.

This study was based on the following assumptions:-

1) Spherical drop.

2) Resistance to mass transfer was confined inside the drop.

3) All physical properties except the diffusion coefficient, were constant.

4) The concentration profile showed axial and polar symmetry.

X-8-C Model for Mass Transfer with First-Order Reaction

Mass transfer with simultaneous first-order reaction into stagnant drops is described by:-

$$\frac{\partial C'}{\partial t} = \frac{1}{r^2} \frac{\partial}{\partial r} \left\{ D_e \, r^2 \frac{\partial C'}{\partial r} \right\} - RK'.C' \qquad (X\text{-}1)$$

where the effective diffusivity D_e, is defined as:-

$$D_e = D_L \, (1 + B) \qquad (X\text{-}2)$$

The coefficient B is used to vary the value of the molecular diffusion coefficient D_L

Equation X-1 is made dimensionless as shown:-

$$\frac{\partial C}{\partial T} = \frac{\partial^2 C}{\partial R^2} + \frac{2}{R} \frac{\partial C}{\partial R} - RK.C \qquad (X\text{-}3)$$

where $R = \frac{r}{a}$ = dimensionless radius (X-3a)

$C = \frac{C'}{C_\phi}$ = dimensionless concentration (X-3b)

$RK = \frac{RK' a^2}{D_e}$ = dimensionless reaction constant (X-3c)

$T = \frac{D_e t}{a^2}$ = dimensionless time

with boundary and initial conditions

$$R = 1 \qquad C = 1 \qquad T \geqslant 0 \qquad \text{(X-4)}$$

$$0 \leqslant R \leqslant 1 \qquad C = 0 \qquad T = 0 \qquad \text{(X-5)}$$

The dimensionless mass transfer coefficients or Sherwood Numbers are calculated from the concentration gradient at the surface as shown:-

$$Sh = \frac{2K_L a}{D_e} = -2 \left.\frac{\partial C}{\partial R}\right|_{R=1} \qquad \text{(X-6)}$$

The dimensionless mass transferred M is

$$M = \frac{A}{2} Sh \int_{T=0}^{T} dT \qquad \text{(X-7)}$$

where $$M = \frac{M'}{C_\phi a^3} \qquad \text{(X-8)}$$

and A = dimensionless surface area of the drop.

The experimental Sherwood Number Sh_E is calculated from:-

$$Sh_E = \frac{2K_L a}{D_L} = \frac{2a^2}{3C_\phi D_L} \frac{dC'}{dt} \qquad \text{(X-8)}$$

where $\frac{dC'}{dt}$ is the slope of the curve relating mass transferred per unit drop volume, against drop time.

The accuracy of the calculated Sherwood Numbers are examined by comparison with experimental Sherwood Numbers. The calculated Sherwood Numbers were multiplied by $\frac{D_e}{D_L}$ so that both numbers are based on the molecular diffusion coefficient as shown:-

$$Sh_E = Sh \frac{D_e}{D_L} \qquad \text{(X-9)}$$

X-8-C-1 Method of Solution

Equation X-2 is solved by an explicit finite difference method as shown:-

$$\text{CONC (I, 2)} = \text{CONC (I+1, 1)}\left\{\frac{\Delta T}{\Delta R^2} + \frac{\Delta T}{R\Delta R}\right\} + \text{CONC (I, 1)}\left\{1 - \frac{2\Delta T}{\Delta R^2} - RK.\Delta T\right\} + \text{CONC (I-1, 1)}\left\{\frac{\Delta T}{\Delta R^2} - \frac{\Delta T}{R\Delta R}\right\} \qquad \text{(X-10)}$$

where CONC (I,1) is the concentration at point I, along a radius at time (T) and CONC (I,2) is the concentration at time (T + ΔT).

The concentration gradients required to calculate the Sherwood Numbers are found by differentiating the Lagrange interpolution of the concentrations near the surface, as shown in Appendix VIII-1.

X-8-D Model for Mass Transfer with Second-Order Reaction

Experimental results have suggested that reaction during mass transfer of ethyl acetate into 2N and 1N sodium hydroxide may be represented by first-order reaction expressions. However, the reaction between 0.5N sodium hydroxide and ethyl acetate was of second order.

The dimensionless equation describing mass transfer with simultaneous second-order reaction into stagnant drops is:-

$$\frac{\partial C_A}{\partial T} = \frac{\partial^2 C_A}{\partial R^2} + \frac{2}{R}\frac{\partial C_A}{\partial R} - RK_A C_A C_B$$

$$\frac{\partial C_B}{\partial T} = \frac{\partial^2 C_B}{\partial R^2} + \frac{2}{R}\frac{\partial C_B}{\partial R} - RK_B C_A C_B \qquad \text{(X-11)}$$

where $RK_A = \dfrac{RK\ a^2 C_{B\phi}}{D_{L_A}}$ (X-11a)

$RK_B = \dfrac{RK\ a^2 C_{A\phi}}{D_{L_B}}$ (X-11b)

D_{L_A} and D_{L_B} are diffusion coefficients for C_A and C_B, respectively and

$C_{A\phi}$ = initial concentration of reactant A

$C_{B\phi}$ = saturation concentration of B

The initial and boundary conditions are

$R = 1 \qquad C_B = 1 \qquad T \geqslant 0$ (X-12)

$0 \leqslant R \leqslant 1 \qquad C_B = 0 \qquad T = 0$ (X-13)

$C_A = 1$

These equations are solved by a method similar to that used for solving mass transfer with first-order reaction in the previous Section X-8-C.

X-8-E Program Listing

This program studies the variations in effective diffusivity with time during mass transfer of ethyl acetate into aqueous sodium hydroxide drops with simultaneous first order reaction.

The input data are defined below, in the order of their appearance:-

JCONT This is a switch to determine the initial concentration profile in the drop.

If JCONT = 1, the initial drop concentration profile is calculated from estimated end effect.

If JCONT $\neq$ 1, the initial drop concentration profile is read in from a set of binary input data cards.

These data cards are punched out at the termination of the program, so that calculating may be continued later.

NPRINT = number of printouts

NINT = number of iterations before printout of results

NRINC = radial increments

B = factor to increase value of diffusion coefficient

DELB = incremental change in B

A1, A2, A3 = coefficients from correlations for experimental mass transfer data with time

DTIME = incremental change in dimensionless time

CNAOH = initial concentration of sodium hydroxide in the dispersed phase, mols/cc

RAD = drop radius, cm

CSAT = solubility of ethyl acetate in water, adjusted for salt effects, mols/cc

DENS = initial density of the dispersed phase

DIFF = molecular diffusion coefficient, cm^2/sec

REAC = second order reaction rate constant, cc/mol sec

WMOL = mol cot, gm/gm mol

CHECK = tolerance on calculated mass transfer with respect to experimental data, mols/cc

The listing is as shown in the following pages.

```
3118 H WATADA     MLTRG 2N                    FØRTRAN SØURCE LIST
      ISN         SØURCE STATEMENT

     0 $IBFTC
       C  SØLUTIØN ØF MASS TRANSFER WITH FIRST ØRDER REACTIØN INTØ DRØP WITH E
       C  DIFFUSIVITY, CHANGING WITH RADII
       C
       C
       C  REPEAT ØF WØRK WITH 2 N NAØH, USING SMALLER DTIME
       C
       C  DE = 1  + B IS USED TØ DESCRIDE THE VALUE ØF EFFECTIVE DIFFUSIVITY
       C
     1         DIMENSIØN C(42,2), R(42), XX(200), DE(42), BCØN(42), DE2(42),
              1 DEB(42), DEB2(42), CB(42,2), CNA(42)
     2         READ (5,101) JCØNT
     4         READ (5,101) NPRINT, NINT, NRINC
    10         READ (5,102) B, DELB
    11         READ (5,102) A1, A2, A3
    12         READ (5,102) DTIME
    13         READ (5,102) CNAØH, RAD, CSAT, DENS
    14         READ (5,102) DIFF, REAC, WMØL, CHECK
    15         WRITE (6,108) NPRINT, NINT, NRINC, JCØNT
    16         WRITE (6,109) B, DELB, A1, A2, A3
    17         WRITE (6,110) DTIME, CNAØH, RAD, CSAT, DENS
    20         WRITE (6,111) DIFF, REAC, WMØL, CHECK
       C
       C   DEND = INITIAL MASS IN DRØP - FRØM END EFFECT
       C
       C  SET TEST TIME TØ 40 SEC
    21         CALL TIMSET(40)
       C  INITAL MASS = DEND
    22         DEND = A1
    23         CSTART = DEND/CSAT
    24         WRITE (6,121) DEND
       C
    25         N1 = 1
    26         N2 = N1 + 1
    27         N3 = N1 -1
       C  CØEFFICIENTS
    30         LR = NRINC - 1
    31         LR2 = NRINC - 2
    32         LR3 = NRINC - 3
    33         LR4 = NRINC - 4
    34         DRAD = 1.0/FLØAT(LR)
       C  RADII IN DRØP
    35         DØ 12 I = 2,NRINC
    36      12 R(I) = DRAD*FLØAT(I-1)
    40         WRITE (6,116) (DRAD, DTIME, CHEM)
       C  CØEFFICIENTS FØR CALC ØF LØCAL SH NØ.
    45         R1 = DRAD*FLØAT(LR2)
    46         R2 = DRAD*FLØAT(LR3)
    47         R3 = DRAD*FLØAT(LR4)
    50         B4 = R1*R2
    51         B5 = R1*R3
    52         B6 = R2*R3
    53         ANUM1 = 3. - 2.*(R1 + R2 + R3) + (B4 + B5 + B6)
    54         ANUM2 = 3. - 2.*(1. + R2 + R3) + (R2 + R3 + B6)
    55         ANUM3 = 3. - 2.*(1. + R1 + R3) + (R1 + R3 + B5)
```

```
)3118 H WATADA     NLTRG 2N                    FØRTRAN SØURCE LIST
      ISN        SØURCE STATEMENT

        56         ANUM4 = 3. - 2.*(1. + R1 + R2) + (R1 + R2 + 84)
        57         DEN1 = (1. - R1)*(1. - R2)*(1. - R3)
        60         DEN2 = (R1 - 1.)*(R1 - R2)*(R1 - R3)
        61         DEN3 = (R2 - 1.)*(R2 - R1)*(R2 - R3)
        62         DEN4 = (R3 - 1.)*(R3 - R1)*(R3 - R2)
        63         F1 = ANUM1/DEN1
        64         F2 = ANUM2/DEN2
        65         F3 = ANUM3/DEN3
        66         F4 = ANUM4/DEN4
             C
             C BINARY DECK INPUT DATA
        67         IF (JCØNT.EQ.1) GØ TØ 20
        72         READ (5) (C(I,1), I = 1,NRINC)
        77         READ (5)(TMAS, B, TIME, CØNC, SHNØ, DELB)
       104         GØ TØ 21
             C
             C INITIAL CØNDITIØN
       105        20 DØ 10 LT = 1,2
       106           DØ 11 I = 1,LR
       107        11 C(I,1) = CSTART
       111        10 C(NRINC,LT) = 1.0
       113           TINT = 0.0
       114           TIME = 0.0
       115           TMAS = 0.0
       116           CØNC = 0.0
       117           GØ TØ 22
             C     LØC 2
       120        21 WRITE (6,105) (TIME, (C(I,1), I = 1,NRINC))
       131           DØ 51 I = 2,NRINC
       132        51 DE(I) = (1. + B)*DIFF
       134           DE(1) = DE(2)
       135           WRITE (6,110) (DE(I), I = 1,NRINC)
       142           WRITE (6,106) (SHNØ, CØNC, B, TMAS)
       147           WRITE (6,120) DELB
       150           WRITE (6,113)
       151        23 JCØNT = 5
             C
             C    CALCULATIØN
       152           PERC = 0.0
       153           DØ 1 KK = 1,NPRINT
       154           TIME = DTIME*FLØAT(NINT)+ TIME
       155           CØMP = A1 + A2*TIME + A3*TIME*TIME
       156           FUNC1 = CØMP + CØMP*CHECK
       157           FUNC2 = CØMP - CØMP*CHECK
       160           DB = DELB
       161           EMAS = TMAS
       162           LOW = 0
       163           KHIGH = 0
       164           ITER = 0
       165           NSKIP = 1
       166           DØ 40 I = N1,NRINC
       167        40 BCØN(I) = C(I,1)
             C
       171         7 CØNTINUE
       172           CALL TINTST(I)
```

```
5118 H WATADA      MLTRG 2N                    FØRTRAN SØURCE LIST
     ISN          SØURCE STATEMENT

     173          IF (I.LT.0) GØ TØ 91
     176          DØ 2 K = 1,NTNT
     177          ØLDSH = SHNØ
     200          DØ 24 I = N2,NRINC
     201       24 DE(I) = (1. + B)*DIFF
     203          DE(N1) = DE(N2)
     204          DE(1) = DE(2)
     205          DT = DE(NRINC)*DTIME/(RAD*RAD)
     206          CHEM = REAC*CNAØH*RAD*RAD/DE(NRINC)
     207          W4 = CHEM*DT
     210          DUM1 = DT/(DE(NRINC)*DRAD**2)
     211          DUM2 = DT/(DE(NRINC)*DRAD)
          C
     212          DØ 3 I = N2,LR
     213          W1 = DE(I)*DUM1
     214          W2 = (DE(I+1) - DE(I-1))*DUM1/4.
     215          W3 = DE(I)*DUM2/R(I)
     216        3 C(I,2) = C(I+1,1)*(W1 + W2 + W3) + C(I,1)*(1. - 2.*W1 - W4) +
                 1 C(I-1,1)*(W1 - W2 - W3)
          C
          C CØNC AT CENTRE
     220          C(N1,2) = C(N2,2)
     221          C(NRINC,2) = 1.0
          C
     222          DØ 9 I = N1,NRINC
     223        9 C(I,1) = C(I,2)
     225       22 CØNTINUE
          C
          C   LØCAL SH NØ
     226          GRAD = F1 + F2*C(LR,1) + F3*C(LR2,1) + F4*C(LR3,1)
     227          SHNØ =     2.*GRAD
     230          IF (JCØNT.EQ.1) GØ TØ 21
          C
          C
          C   CALC ØF MASS TRANSFERRED , FRØM SH NØ
          C   DRØP SURFACE AREA = 4*3.14159 = 12.5663704
          C   DRØP VØL = 4*3.14159/3 = 4.188790132
     233        2 TMAS = TMAS + DT*3.1415926*(ØLDSH + SHNØ)
     235          CØNC = TMAS*CSAT/4.188790132 + DEND
          C
          C    CØMPARISØN WITH EXP DATA
          C
     236          ITER = ITER + 1
     237          IF (NSKIP.EQ.1) GØ TØ 60
     242          IF (CØNC.GT.FUNC1.AND.CØNC2.LT.FUNC2) GØ TØ 32
     245          IF (CØNC.LT.FUNC2.AND.CØNC2.GT.FUNC1) GØ TØ 33
     250       60 NSKIP = 2
     251          IF (CØNC.GT.FUNC1) GØ TØ 5
     254          IF (GØNC.LT.FUNC2) GØ TØ 6
     257          GØ TØ 8
          C   DECCELERATIØN ØF DB FACTØR
     260       33 DB = DB/2.0
     261          GØ TØ 6
     262       32 DB = DB/2.0
          C
```

```
18 H WATADA     NLTRG 2N                    FØRTRAN SØURCE LIST
    ISN         SØURCE STATEMENT

       C    CHANGE IN B FACTØR
   263       5 B = B - DB
   264         CØNC2 = CØNC
   265         KHIGH = KHIGH + 1
   266         TMAS = EMAS
   267         DØ 41 I = N1,NRINC
   270      41 C(I,1) = BCØN(I)
   272         GØ TØ 7
   273       6 B = B + DB
   274         CØNC2 = CØNC
   275         LØW = LØW + 1
   276         TMAS = EMAS
   277         DØ 42 I = N1,NRINC
   300      42 C(I,1) = BCØN(I)
   302         GØ TØ 7
   303       8 ITEM = KHIGH + LØW
       C
   304         DØ 50 I = N2,NRINC
   305      50 DE2(I) = (1. + B)*DIFF
   307         DE2(N1) = DE2(N2)
       C   LØC 3
   310         WRITE (6,117) ITER, DT, DTIME
   311         WRITE (6,104) (KHIGH, LØW, ITEM)
   316         WRITE (6,105) (TIME, (C(I,1), I = 1,NRINC))
   327         WRITE (6,107) (SHNØ, CØNC, CØMP, PERC)
   334         WRITE (6,119) (FUNC1, FUNC2, B, TMAS, EMAS)
   341         WRITE (6,120) DB
   342         WRITE (6,123)
   343         WRITE (6,118) (DE(I), I = 1,NRINC)
   350         WRITE (6,122) (DE2(I), I = 1,NRINC)
   355         DELB = DELB + 0.1
   356       1 CØNTINUE
   360         GØ TØ 31
   361      91 TIME = TIME - DTIME*FLØAT(NINT)
   362         PERC = 0.0
   363         CØMP = A1 + A2*TIME + A3*TIME*TIME
   364         FUNC1 = CØMP + CØNP*CHECK
   365         FUNC2 = CØMP  - CØMP*CHECK
   366         SHNØ = ØLDSH
   367         CØNC = EMAS*CSAT/4.188790132 + DEND
   370         WRITE (6,130) KK
   371         WRITE (6,104) (KHIGH, LØW, ITEM, TIME)
   376         WRITE (6,107) (SHNØ, CØNC, CØMP, PERC)
   403         WRITE (6,119) (FUNC1, FUNC2, B, TMAS, EMAS)
   410         WRITE (6,120) DB
   411      31 WRITE (7) (C(I,1), I = 1,NRINC)
   416         WRITE (7) (TMAS, B, TIME, CØNC, SHNØ, DELB)
   423         STØP
   424     101 FØRMAT (3I5)
   425     102 FØRMAT (4F15.8)
   426     104 FØRMAT (1H0, 2X, 16HHIGH ITERATIØN =, I10, 2X, 15HLØW ITERATIØN =,
             1 I10, 2X, 7HITØTAL =, I10)
   427     105 FØRMAT (1H0, 2X, 12HCØNC ØF ETAC, 5X, 7HTIME IS, F10.5//(21F6.3))
   430     106 FØRMAT (1H0, 2X, 7HSH NØ =, F20.8, 2X, 19HMASS TRANS MØL/CC =,
             1 F20.15, 2X, 9HCØEFF B =, F10.4, 2X, 6HTMAS =, F10.7)
```

```
18 H WATADA      MLTRG 2N                    FØRTRAN SØURCE LIST
    ISN          SØURCE STATEMENT
     431    107 FØRMAT (1HO, 2X, 7HSH NØ =, F10.5, 2X, 18HCALC MASS MØL/CC =,
               1 F20.15, 2X, 17HEXP MASS MØL/CC =, F20.15, 2X, 9HPERCENT =, F15.8)
     432    119 FØRMAT (1HO, 2X, 11HTØP LIMIT =, F20.15, 2X, 11HLØW LIMIT =,
               1   F20.15, 2X, 3HB =, F15.8, 2X, 6HTMAS =, F10.7, 2X, 6HEMAS =,
               2 F10.7)
     433    108 FØRMAT (1HO, 2X, 8HNPRINT =, I7, 2X, 6HNINT =, I7, 2X, 7HNRINC =,
               1 I7, 5X, 7HJCØNT =, I7)
     434    109 FØRMAT (1HO, 2X, 3HB =, F9.4, 2X, 9HDELTA B =, F12.8, 2X,
               1 12HLIRA CØEFF =, 3F12.8)
     435    110 FØRMAT (1HO, 2X, 4HDT =, F12.9, 2X, 11HCØNC NAØH =, F12.9, 2X,
               110HDRØP RAD =, F12.9, 2X, 6HCSAT =, F12.9, 2X, 9HDENSITY =, F10.7)
     436    111 FØRMAT (1HO, 2X, 6HDIFF =, F12.9, 2X, 7HREACT =, F12.9, 2X, 13HET/
               1C MØL WT =, F8.4, 2X, 27HTØLERANCE ØN CALC RESULTS =, F12.9)
     437    112 FØRMAT (1HO, 2X, 4HLØC1)
     440    113 FØRMAT (1HO, 2X, 4HLØC2)
     441    115 FØRMAT (10X, 20F6.2)
     442    116 FØRMAT (1HO, 2X, 6HDRAD =, F10.5, 2X, 7HDTIME =, F10.5, 2X,
               1 17HCHEM (NØ DIMEN) =, F10.5)
     443    117 FØRMAT (1HO, 2X, 4HLØC3, 4X, 6HITER =, I10, 2X, 4HDT =, F12.8,
               1 2X, 12HDTIME(SEC) =, F12.8)
     444    118 FØRMAT (1HO, 2X, 8HEFF DIFF//(2X, 10F11.7))
     445    120 FØRMAT (1HO, 2X, 4HDB =, F10.5)
     446    121 FØRMAT (1HO, 2X, 12HEND EFFECT =, F15.8)
     447    122 FØRMAT (1HO, 2X, 32HEFF DIFF FØR NEXT DTIME TRANSFER//(2X,
               1 10F11.7))
     450    123 FØRMAT (1HO, 2X, 40HEFF DIFF FRØM DTIME BEFØRE USED FØR CALC)
     451    124 FØRMAT (1HO, 2X, 5HNØ1 =, I10, 2X, 5HNØ2 =, I10, 2X, 5HNØ3 =, I10)
     452    125 FØRMAT (1HO, 2X, 6HTIME =, F10.5, 2X, 6HCØMP =, F15.8, 2X,
               1   7HFUNC1 =, F15.8, 2X, 7HFUNC2 =, F15.8)
     453    126 FØRMAT (1HO, 2X, 6HCØNC =, F15.8, 2X, 7HKHIGH =, I10, 2X, 5HLØW =,
               1 I10, 2X, 6HITER =, I10, 2X, 3HB =, F15.9)
     454    130 FØRMAT (1HO, 2X, 16HTIMIST LT TINSET, 4X, 4HKK =, I10//(4X,
               1 23HREPEAT ØF PREVIØUS DATA))
     455         END
C00900=
C00900=
```

X-8-F Sample Output

A sample output is given as follows:-

```
 NPRINT =    10  NINT =    200  NRINC =     4   JCØNT =     2
 B =   0.0000  DELTA B =  2.00000000  LIRA CØEFF =  0.00000135  0.00006773  0.00000000
 DT =  0.00300000  CØNC NAØH =  0.00197500  DRØP RAD =  0.12225000  CSAT =  0.00028100  DENSITY = 1.1755053
 DIFF =  0.00001000  REACT = 91.80000019  ETAC MØL WT = 88.1000  TØLERANCE ØN CALC RESULTS =  0.00100000
 END EFFECT =     0.00000135
 DRAD =   0.02439  DTIME =   0.00300  CHEM (NØ DIMEN) =   0.00000
 CØNC ØF ETAC     TIME IS   0.60000
0.004 0.004 0.004 0.004 0.004 0.004 0.004 0.004 0.004 0.004 0.004 0.004 0.004 0.004 0.004 0.004 0.004 0.004
0.004 0.004 0.004 0.004 0.004 0.004 0.004 0.004 0.004 0.004 0.005 0.005 0.007 0.014 0.029 0.063 0.131 0.252
 EFF DIFF
  0.0001329  0.0001329  0.0001329  0.0001329  0.0001329  0.0001329  0.0001329  0.0001329  0.0001329  0.0001
  0.0001329  0.0001329  0.0001329  0.0001329  0.0001329  0.0001329  0.0001329  0.0001329  0.0001329  0.0001
  0.0001329  0.0001329  0.0001329  0.0001329  0.0001329  0.0001329  0.0001329  0.0001329  0.0001329  0.0001
  0.0001329  0.0001329  0.0001329  0.0001329  0.0001329  0.0001329  0.0001329  0.0001329  0.0001329  0.0001
  0.0001329  0.0001329
 SH NØ =          13.31130517  MASS TRANS MØL/CC =          0.00004199  CØEFF B =   12.2875  TMAS = 0.60582
 DB =   0.30000
 LØC2
 LØC3    ITER =          6  DT =  0.00002878  DTIME(SEC) =  0.00300000
 HIGH ITERATIØN =          1  LØW ITERATIØN =          4  TØTAL =          5
 CØNC ØF ETAC     TIME IS   1.20000
0.004 0.004 0.004 0.004 0.004 0.004 0.004 0.004 0.004 0.004 0.004 0.004 0.004 0.004 0.004 0.004 0.004 0.004
0.004 0.004 0.005 0.005 0.007 0.009 0.012 0.018 0.027 0.042 0.063 0.093 0.134 0.189 0.259 0.346 0.449 0.569
 SH NØ =  12.69265  CALC MASS MØL/CC =          0.00008264  EXP MASS MØL/CC =          0.00008263  PERCENT
 TØP LIMIT =          0.00008271  LØW LIMIT =          0.00008254  B =    13.33749807  TMAS = 1.2117597  E
 DB =   0.15000
 EFF DIFF FRØM DTIME BEFØRE USED FØR CALC
 EFF DIFF
  0.0001434  0.0001434  0.0001434  0.0001434  0.0001434  0.0001434  0.0001434  0.0001434  0.0001434  0.0001
  0.0001434  0.0001434  0.0001434  0.0001434  0.0001434  0.0001434  0.0001434  0.0001434  0.0001434  0.0001
  0.0001434  0.0001434  0.0001434  0.0001434  0.0001434  0.0001434  0.0001434  0.0001434  0.0001434  0.0001
  0.0001434  0.0001434  0.0001434  0.0001434  0.0001434  0.0001434  0.0001434  0.0001434  0.0001434  0.0001
  0.0001434  0.0001434
 EFF DIFF FØR NEXT DTIME TRANSFER
```

X-8-G Nomenclature

a = drop radius, cm

B = coefficient used in calculating D_e

C_A, C_B = concentrations of A and B respectively, mols/cc

C_{A_o}, C_{B_o} = initial concentrations of A and B respectively, mols/cc

C^l = concentration, mols/cc

C_ϕ = equilibrium concentration, mols/cc

C = dimensionless concentration

$$= \frac{C^l}{C_\phi}$$

D_e = effective diffusion coefficient, cm^2/sec

D_L = molecular diffusion coefficient, cm^2/sec

D_{L_A}, D_{L_B} = molecular diffusion coefficient for A and B respectively, cm^2/sec

K_L = mass transfer coefficient, cm/sec

M = mass transferred, mols

$$M = \frac{M^l}{C_\phi a^3}$$

= dimensionless mass transferred

RK = reaction rate constant, cc/mol sec

$$RK_A = \frac{RK\, a^2 C_{B_o}}{D_{L_A}}$$

= dimensionless rate constant for A

$$RK_B = \frac{RK\, a^2 C_{A_o}}{D_{L_B}}$$

= dimensionless rate constant for B

r = radial distance, cm

$$R = \frac{r}{a}$$

$= \frac{r}{a}$ = dimensionless radial distance

$Sh = \frac{2aK_L}{D_e}$

= Sherwood Number

$Sh_E = \frac{2aK_L}{D_L}$

= experimental Sherwood Number

t = time, sec

$T = \frac{D_e t}{a^2}$

= dimensionless time

Appendix X-9

Predicted Variations of Effective Diffusivity with Time for Mass Transfer of Ethyl Acetate with Simultaneous Reaction into Aqueous Sodium Hydroxide Drops.

NaOH Concentration Normality	Drop Time sec.	Effective Diffusivity $cm^2/sec \times 10^{-5}$	Sherwood Number Based on Effective Diffusivity	Sherwood Number Based on Molecular Diffusivity
2.0	0.0	1.0	150.3	150.3
	0.6	3.8	35.9	136.5
	1.2	9.0	17.7	160.0
	1.8	14.1	11.8	166.0
	2.4	19.0	8.9	169.0
	3.0	24.2	7.1	172.5
	3.6	29.1	5.9	172.5
	4.5	37.0	4.7	174.5
	5.1	42.9	4.1	176.5
	6.0	51.3	3.4	177.0
	7.2	65.5	2.7	178.0
	8.1	74.9	2.3	175.0
	9.0	90.7	2.0	178.5
1.0	0.0	1.0	150.3	150.3
	0.4	0.9	65.9	57.4
	0.8	1.5	39.1	58.6
	1.2	2.3	26.5	61.5
	1.6	3.2	20.3	64.9
	2.4	4.9	14.1	69.0
	3.2	6.2	11.2	69.4
	4.0	7.7	9.3	71.8
	5.2	9.6	7.6	73.4
	6.0	10.5	6.9	72.2
	7.2	11.5	6.1	70.5
	8.4	13.8	5.4	75.0
	9.2	13.8	5.2	71.5

Appendix X-9 (cont'd)

NaOH Concentration Normality	Drop Time sec.	Effective Diffusivity $cm^2/sec \times 10^{-5}$	Sherwood Number Based on Effective Diffusivity	Sherwood Number Based on Molecular Diffusivity
0.5	0.0	1.0	150.3	150.3
	0.4	1.5	48.8	70.6
	0.8	3.1	24.0	74.4
	1.2	5.1	15.5	79.0
	1.6	7.4	11.3	83.0
	2.4	10.9	7.3	79.0
	3.2	14.3	5.3	75.0
	4.0	17.4	4.0	70.0
	5.2	21.2	2.9	61.0
	6.0	24.3	2.4	57.5
	7.2	26.2	1.8	48.2
	8.4	26.2	1.5	38.2
	9.2	26.2	1.3	33.3

Appendix X-10

Variations of Experimental Sherwood Number with Time for Mass Transfer of Ethyl Acetate with Simultaneous Chemical Reaction into Aqueous Sodium Hydroxide Drops.

NaOH Concentration Normality	Drop Time sec.	Sherwood Number
2.0	-	181.0
1.0	-	73.3
0.5	0.	104.0
	0.5	100.5
	1.0	96.5
	2.0	88.6
	4.0	73.0
	6.0	57.1
	8.0	41.5
	10.0	25.7